Universidad Pública de Navarra

Departamento de Producción Agraria

Instituto de Agrobiotecnología

Regulation of the response of plants to volatile compounds emitted by fungal phytopathogens

Tesis Doctoral para optar al grado de Doctor, presentada por:

Pablo García Gómez

Director: Dr. Javier Pozueta Romero
Codirector: Dr. Abdellatif Bahaji Nazih
Tutor: Dra. Inmaculada Farrán Blanch

Pamplona, 2020

upna
Universidad Pública de Navarra
Nafarroako Unibertsitate Publikoa

El Dr. **Javier Pozueta Romero**, Profesor de Investigación del Consejo Superior de Investigaciones Científicas y el Dr. **Abdellatif Bahaji Nazih**, Investigador Distinguido del Consejo Superior de Investigaciones Científicas,

CERTIFICAN:

Que el trabajo titulado "*Regulation of the response of plants to volatile compounds emitted by fungal phytopathogens*" recogido en la presente memoria, ha sido realizado por Pablo García Gómez en el Instituto de Agrobiotecnología (CSIC/Gobierno de Navarra) y cumple las condiciones exigidas por la legislación vigente para optar al grado de Doctor. Pablo García Gómez ha disfrutado de una beca predoctoral FPI (referencia **BES-2014-068741**) del Ministerio de Ciencia, Innovación y Universidades. Este trabajo ha sido financiado por los proyectos **BIO2013-49125-C2-1-P** y **BIO2016-78747-P** de la Comisión Interministerial de Ciencia y Tecnología.

Y para que así conste, firman la presente en Pamplona, a X de X de 2020.

Fdo. Javier Pozueta Romero

Fdo. Abdellatif Bahaji Nazih

upna
Universidad Pública de Navarra
Nafarroako Unibertsitate Publikoa

CONTENIDOS

RESUMEN

upna
Universidad Pública de Navarra
Nafarroako Unibertsitate Publikoa

upna
Universidad Pública de Navarra
Nafarroako Unibertsitate Publikoa

El crecimiento y el desarrollo de las plantas están afectados por microorganismos presentes en la filosfera, la rizosfera y/o la endosfera. En la fase de precolonización, antes de que se establezca un contacto físico con la planta, bacterias y hongos beneficiosos sintetizan una gran cantidad de sustancias que fomentan el crecimiento de la planta. Tales sustancias fomentan además la formación de raíces laterales y el crecimiento de pelos radiculares, mejorando así la capacidad exploratoria de las raíces para obtener agua y minerales del suelo y aumentando la superficie de la raíz y, por tanto, su predisposición para ser colonizada e infectada. Estos microorganismos también emiten un gran número de compuestos volátiles (VCs), con masa molecular inferior a 300 Da y alta presión de vapor, que promueven el crecimiento de la planta y la fotosíntesis y modulan la arquitectura de la raíz. Recientemente, el grupo de investigación en el que he realizado mis investigaciones demostró que esta capacidad no está restringida a microorganismos beneficiosos, sino que también se extiende a patógenos. Este trabajo se ha llevado a cabo con la doble intención de identificar la naturaleza de los VCs microbianos con propiedades bioestimulantes y profundizar en el conocimiento de los mecanismos implicados en la respuesta de las raíces a los VCs emitidos por microorganismos patógenos.

Mediante el uso de un sistema de co-cultivo "box-in box" en el que las plantas crecen en la proximidad de cultivos microbianos cubiertos con filtros de carbón activado que adsorben VCs con masas moleculares superiores a 45 Da, en el **capítulo 1** investigué hasta qué punto señales aéreas emitidas por diferentes microorganismos son capaces de producir distintas respuestas en las plantas. Además, evalué la contribución y modo de acción de compuestos volátiles orgánicos e inorgánicos (VOCs and VICs, respectivamente) de origen microbiano en estas respuestas. Para ello expuse plantas de Arabidopsis a VCs emitidos por cultivos adyacentes de *Alternaria alternata* y *Penicillium aurantiogriseum* cubiertos o no con filtros de carbón activado. Estudios por cromatografía de gases-masas no detectaron VOCs en el aire de las cámaras en las que estaban incluidos los cultivos de hongos cubiertos con filtro. Sin embargo, el aire de estas cámaras presentaba una concentración mayor de CO_2, CO y NO. Independientemente de la filtración por carbón activado, VCs emitidos por los dos fitopatógenos utilizados en este estudio promovieron el crecimiento e indujeron cambios distintos en el desarrollo. Plantas cultivadas en concentraciones de CO_2 existentes en las cámaras de crecimiento de los cultivos microbianos eran similares a las cultivadas en condiciones

de CO_2 ambiental. Plantas expuestas a VCs filtrados o no por carbón activado o a altos niveles de CO_2 mostraron cambios transcriptómicos similares a los inducidos por alta irradiación lumínica. La información obtenida indica que (a) VICs fúngicos diferentes al CO_2 y/o VOCs no detectados por nuestros sistemas analíticos influyen fuertemente en la respuesta de la planta a VCs, (b) diferentes microorganismos liberan VCs con diferente potencial bioactivo, (c) cambios transcriptómicos en plantas expuestas a VCs se deben principalmente a una señalización del incremento de la fotosíntesis, y (d) la respuesta de la planta a VCs está regulada, al menos parcialmente, a nivel post-transcripcional.

En el **capítulo 2**, usando el mismo sistema "box-in-box" del capítulo 1, caracterice la respuesta a nivel proteómico, hormonómico y metabólico de raíces de Arabidopsis a VCs emitidos por *P. aurantiogriseum*. El análisis proteómicos reveló que los VCs fúngicos reprimen la expresión de acuaporinas inducibles por auxinas así como la expresión del transportador de hierro IRT1 sensible a citoquininas (CKs) y enzimas reguladoras de la acumulación de especies reactivas de oxigeno (ROS). Los VCs fúngicos también aumentaban la expresión de proteínas que controlan la producción de isoprenoides derivados de mevalonato (MVA) y de enzimas inducibles por CKs y etileno involucradas en la conversión de metionina en etileno y en la eliminación de cianuro. Estos cambios están asociados con un incremento de la eficiencia del uso del agua, una reducción del contenido de hierro y un incremento de la producción de ROS, etileno y CKs derivadas de MVA. Los patrones de expresión de marcadores hormonales y la caracterización de la respuesta de mutantes aportaron evidencias sobre la implicación de la eliminación del cianuro y la señalización de auxinas, CKs, etileno y ROS en los cambios de la arquitectura radicular inducidos por la exposición a VCs. En conjunto, los datos presentados en este capítulo muestran que los VCs emitidos por fitopatógenos fúngicos modulan la arquitectura y el metabolismo de la raíz a través de complejos mecanismos en los que la eliminación de cianuro y una reprogramación del proteoma inducida por hormonas y ROS juegan un papel importante. Algunos de estos mecanismos difieren de los que intervienen en la respuesta de la planta a VCs emitidos por microorganismos beneficiosos.

SUMMARY

upna
Universidad Pública de Navarra
Nafarroako Unibertsitate Publikoa

upna
Universidad Pública de Navarra
Nafarroako Unibertsitate Publikoa

Plants' growth and development are influenced by microorganisms occurring either aboveground in the phyllosphere, underground in the rhizosphere and/or in the endosphere inside the vascular transport system and apoplastic space. In the precolonization phase, before direct contact with plants occurs, beneficial bacteria and fungi synthesize a multitude of substances that promote growth and cause massive lateral root formation and enhanced root hair growth, thus improving the root´s exploratory capacity for water and minerals and predisposing plants for microbial colonization and infection. These microorganisms also emit a large number of volatile compounds (VCs) with molecular masses of less than 300 Da and high vapour pressure that promote growth and photosynthesis, and modulate root system architecture in both host and non-host plants. We have recently demonstrated that this capacity is not restricted to beneficial microbes, but also extends to phytopathogens. This thesis has been focused on investigating the nature of VCs involved in plant´s response, and deepen in the knowledge of the mechanisms responsible for that response in roots.

Using a "box-in-box" co-cultivation system in which plants are grown in the vicinity of microbial cultures covered with organic VC-adsorbing charcoal filters, in **chapter 1** I addressed the question of whether airborne signals from different microorganisms can promote distinct responses in plants. In addition, I evaluated the contribution and mode of action of microbial volatile organic and inorganic compounds (VOCs and VICs, respectively) in these responses. Towards this end Arabidopsis plants were exposed to VCs emitted by adjacent *Alternaria alternata* and *Penicillium aurantiogriseum* cultures, with and without charcoal filtration. No VOCs were detected by gas chromatography combined with mass spectrometric detection in the headspace of growth chambers containing fungal cultures with charcoal filters. However, these growth chambers exhibited higher CO_2 and bioactive CO and NO headspace concentrations. Independently of charcoal filtration, VCs from both fungal phytopathogens promoted growth and distinct developmental changes. Plants cultured at CO_2 levels observed in growth boxes containing fungal cultures were identical to those cultured at ambient CO_2. Plants exposed to charcoal-filtered fungal VCs, non-filtered VCs, or super-elevated CO_2 levels exhibited transcriptional changes resembling those induced by increased irradiance. Thus, I concluded that, in the "box-in-box" system, (a) fungal VICs other than CO_2 and/or VOCs not detected by our analytical systems strongly influence the plants´ responses to fungal VCs, (b) different microorganisms release VCs with distinct

action potentials, (c) transcriptional changes in VC-exposed plants are mainly due to enhanced photosynthesis signaling, and (d) regulation of some plant responses to fungal VCs is primarily post-transcriptional.

In **chapter 2**, using the same "box-in-box" co-cultivation system of chapter 1, I characterized the response of *Arabidopsis thaliana* roots to VCs emitted by *P. aurantiogriseum*. High-throughput, isobaric labeling-based proteomic analyses revealed that fungal VCs down-regulated the expression of auxin-responsive aquaporins and the cytokinin (CK)-responsive iron carrier IRT1, and of enzymes that regulate accumulation of reactive oxygen species (ROS). Fungal VCs also increased expression of proteins controlling the production of mevalonate (MVA)-derived isoprenoids, and ethylene- and CK-responsive enzymes involved in converting methionine to ethylene, and in cyanide scavenging. These changes were associated with enhanced intrinsic photosynthetic water use efficiency, reduced iron content, and stimulation of ROS, ethylene, cyanide and MVA-derived CKs production. Expression patterns of hormone reporters and developmental responses of mutants provided strong evidence for the involvement of cyanide scavenging and auxin, ethylene, CK and ROS- mediated proteome resetting in the fungal VC-promoted changes in root architecture. Some of the mechanisms involved in the root response to *P. aurantiogriseum* VCs differ from those involved in the response to VCs emitted by beneficial microorganisms.

INTRODUCCIÓN

upna
Universidad Pública de Navarra
Nafarroako Unibertsitate Publikoa

upna
Universidad Pública de Navarra
Nafarroako Unibertsitate Publikoa

Tanto la demanda creciente de alimentos surgida como consecuencia del incremento de la población mundial, como la progresiva reducción de las superficies cultivables han generado la necesidad de identificar nuevos tratamientos que permitan incrementar el rendimiento de los cultivos. La "revolución verde" permitió incrementar la producción de cereales desde 820 millones de toneladas en 1960 a 2400 millones de toneladas en 2015 (http://iofacturo.mx/ecologia/que-es-la-revolucion-verde). Sin embargo, esto ha sido posible en gran medida gracias a la aplicación intensiva de fertilizantes elaborados a partir de recursos limitados de nitrógeno y fósforo y a la sobre-explotación de recursos hídricos. La "nueva agricultura" capaz de hacer frente a los futuros desafíos y demandas de la humanidad tendrá que reunir condiciones de sostenibilidad y respeto al medio ambiente. Previsiblemente, gran parte de las medidas que se adopten en este sentido estarán basadas en el empleo de bioestimulantes de origen microbiano (Bhattacharyya and Jha, 2012; Farrar et al., 2014) definidos como cualquier microorganismo o sustancia procedente de un microorganismo que, aplicado sobre una planta, incremente su eficiencia de captación de nutrientes, su tolerancia a estrés abiótico, su rendimiento y/o calidad independientemente de su contenido en nutrientes (du Jardin, 2015).

1. LOS MICROORGANISMOS PRODUCEN COMPUESTOS VOLÁTILES BIOESTIMULANTES

1.1. Compuestos volátiles producidos por algunos microorganismos beneficiosos fomentan el crecimiento e inducen cambios en la fisiología y el desarrollo de las plantas

Bacterias y hongos microscópicos existentes en la filosfera, la rizosfera y la endosfera sintetizan sustancias tales como carbohidratos, proteínas, lípidos, aminoácidos, hormonas, etc. que actúan directa o indirectamente sobre la planta regulando su crecimiento, desarrollo y/o metabolismo (De-la-Peña y Loyola-Vargas, 2014). En la fase de pre-colonización (antes de que tenga lugar un contacto físico entre la planta y el microorganismo) los microorganismos beneficiosos producen compuestos que actúan como "semi-" o "info-químicos" que participan en innumerables procesos de comunicación e interacción entre las plantas y los microorganismos. Entre otros compuestos, estos microorganismos sintetizan y emiten una amplia gama de compuestos volátiles (VCs) de bajo peso molecular y punto de ebullición que son capaces de difundir a través del aire, el suelo y superficies porosas (Schulz y Dickschat, 2007; Lemfack

et al., 2014). Dependiendo de las condiciones de cultivo, mezclas de VCs emitidos por algunos aislados de bacterias y de hongos beneficiosos existentes en la rizosfera promueven el crecimiento y cambios en la arquitectura radicular de las plantas que facilitan la captación de nutrientes y agua (Ryu et al., 2003; Zhang et al., 2007; Splivallo et al., 2009; Zhang et al., 2009; Gutiérrez-Luna et al., 2010; Blom et al., 2011; Meldau et al., 2013; Naznin et al., 2013; Hung et al., 2014; Delaplace et al., 2015; Ditengou et al., 2015; Garnica-Vergara et al., 2016; Cordovez et al., 2018). VCs emitidos por *Bacillus subtilis* GB03 incrementan la eficiencia fotosintética y el contenido de clorofila en las hojas (Zhang et al., 2008). Además, estos compuestos facilitan la captación de hierro mediante la estimulación de la maquinaria implicada en la solubilización y transporte de este nutriente (Zhang et al., 2009). Estudios de mutantes de Arabidopsis con alteraciones en la producción y señalización de hormonas expuestos a la acción de VCs emitidos por algunos aislados de *B. subtilis* han aportado evidencia sobre la implicación del ácido abscísico (ABA) y las auxinas en el fomento del crecimiento por mezclas de VCs microbianos (Zhang et al., 2008).

1.2. VCs emitidos por microorganismos patógenos también fomentan el crecimiento e inducen cambios en el metabolismo y el desarrollo de las plantas

Investigaciones llevadas a cabo en el laboratorio del Instituto de Agrobiotecnología en el que he realizado mi trabajo de tesis doctoral demostraron que una amplia gama de microorganismos filogenéticamente diversos (tanto bacterias como hongos, incluyendo patógenos y microorganismos que normalmente no interactúan de manera mutualista con las plantas) son capaces de emitir VCs que fomentan el crecimiento de las plantas, el desarrollo radicular y la floración (**Figura 1**) (Sánchez-López et al., 2016b). La exposición a VCs emitidos por fitopatógenos también conlleva un notable incremento de la capacidad fotosintética y del contenido de pigmentos fotosintéticos, azúcares solubles y almidón foliar (Ezquer et al., 2010; Li et al., 2011; Sánchez-López et al., 2016b). Contra todo pronóstico, Sánchez-López et al. (2016a) demostraron que VCs emitidos por el fitopatógeno oportunista *Alternaria alternata* promueven la acumulación de niveles excepcionalmente elevados de almidón en mutantes *pgi1-2* carentes de fosfoglucoisomerasa plastidial (pPGI). Estas observaciones aportaron evidencias sobre la existencia de importantes rutas de biosíntesis de almidón alternativas a la ruta "clásica" según la cual pPGI juega un papel fundamental en la conexión del ciclo de

Calvin-Benson (CBC) con las reacciones directamente implicadas en la biosíntesis de almidón (Bahaji et al., 2014a; Bahaji et al., 2014b).

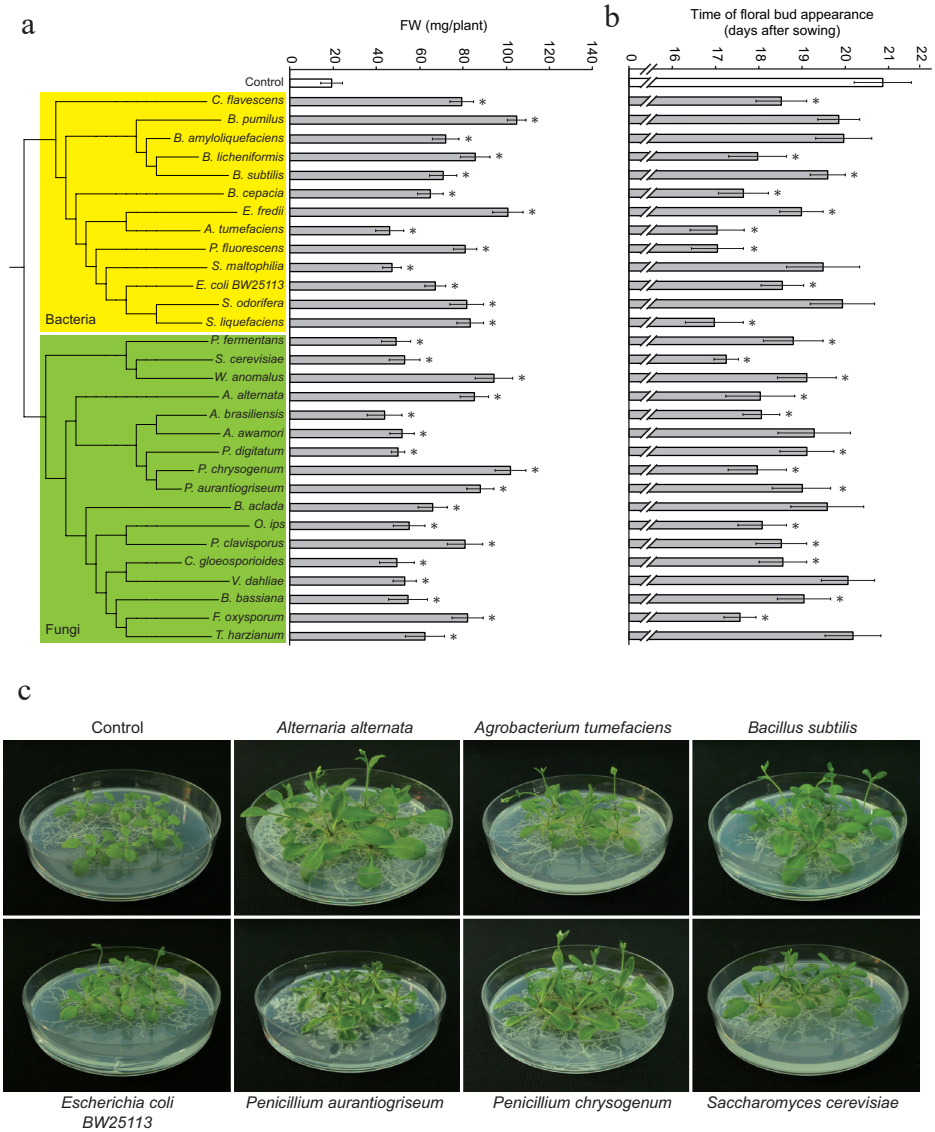

Figura 1: VCs emitidos por microorganismos filogenéticamente diversos fomentan el crecimiento y la floración en plantas de Arabidopsis cultivadas *in vitro.* (a) Peso fresco de roseta, (b) tiempo de aparición del botón floral y (c) fenotipo externo de plantas de Arabidopsis cultivadas en ausencia o presencia durante una semana de cultivos adyacentes de los microorganismos que se indican en la figura. El árbol filogenético fue construido usando PhyloT phylogenetic (www.phyloT.biobyte.de) (Sánchez-López et al., 2016b).

Aún a pesar de las grandes diferencias existentes entre los volatilomas de hongos y bacterias (Schulz y Dickschat, 2007; Lemfack et al., 2014), estudios comparativos de los cambios que ocurren en el transcriptoma de plantas de Arabidopsis expuestas a mezclas de VCs emitidos por la bacteria beneficiosa *B. subtillis* y por el hongo fitopatógeno *A. alternata* evidenciaron la existencia de mecanismos moleculares altamente conservados de respuesta de la planta a diferentes mezclas de VCs microbianos (Sánchez-López et al., 2016b). Entre las alteraciones observadas en los transcriptomas de estas plantas cabe destacar el incremento de la expresión de funciones reguladas por citoquininas (CKs) y por la luz, implicadas en la producción de pigmentos fotosintéticos, la asimilación del azufre (conversión de SO_4^{2-} en SO_3^{2-} y producción de sulfolípidos), la protección contra el estrés oxidativo, la síntesis de componentes de la pared celular, el metabolismo de aminoácidos y la síntesis y degradación de almidón (Sánchez-López et al., 2016b).

Plantas de Arabidopsis tratadas con VCs de *A. alternata* experimentan una reducción del contenido de ABA y un notable incremento del contenido de CKs activas (Sánchez-López et al., 2016a; Sánchez-López et al., 2016b). El efecto ejercido por los VCs de *A. alternata* en el crecimiento, desarrollo y metabolismo de plantas de Arabidopsis es reducido en mutantes de producción y señalización de CKs (Sánchez-López et al., 2016b). Globalmente, la información disponible al inicio de mis investigaciones indicaba que la respuesta de las plantas a VCs microbianos está fundamentalmente regulada a nivel transcripcional a través de mecanismos en los que la luz, el ABA y las CKs juegan un papel importante (**Figura 2**) (Sánchez-López et al., 2016b). Sin embargo, hay que destacar que investigaciones llevadas a cabo recientemente en nuestro laboratorio han demostrado que la respuesta de la planta a VCs microbianos está altamente regulada a nivel post-traduccional. Ameztoy et al. (2019) mostraron que la exposición de las plantas a VCs emitidos por *A. alternata* conlleva una reducción global del thiol redox proteoma, especialmente de proteínas relacionadas con la fotosíntesis. Los mismos autores mostraron que el tratamiento con VCs fúngicos sobre plantas *ntrc* carentes de una tiorredoxina plastidial NADP-dependiente (NTRC) que regula el estado redox del cloroplasto (Pérez-Ruiz et al., 2017) (a) oxida el redox-proteoma de este mutante y (b) ejerce un efecto reducido sobre la acumulación de almidón, el crecimiento, el desarrollo radicular y la floración en este mutante. Todo ello indicaría que cambios en el redox-proteoma de la planta mediados por NTRC juegan un papel importante en su respuesta a VCs microbianos (Li et al., 2011; Ameztoy et al., 2019).

Estudios realizados por Sánchez-López et al. (2016b) basados en el empleo de

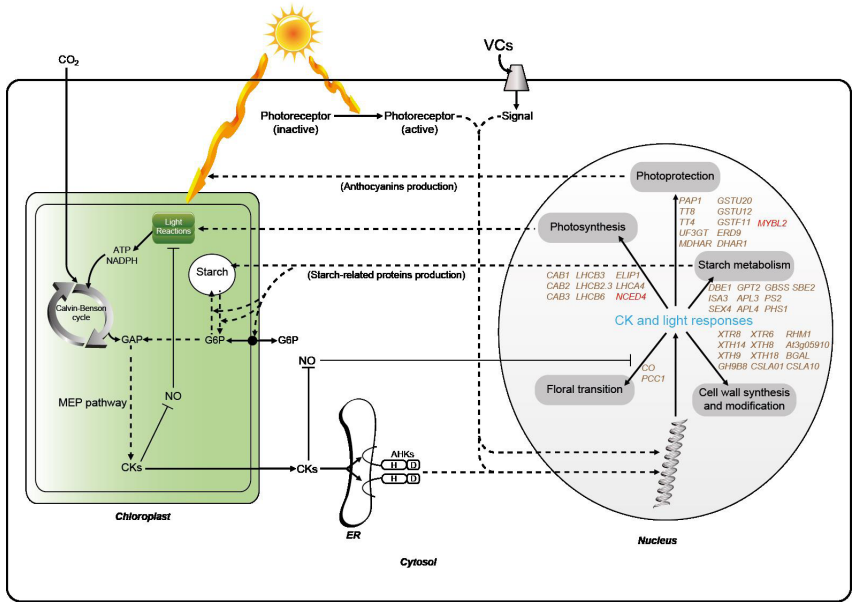

Figura 2: Modelo integrativo de los mecanismos que regulan transcripcionalmente la respuesta de la planta a VCs emitidos por *A. alternata*. La descripción detallada de este modelo aparece en la sección "hipótesis de trabajo" de esta memoria (Sánchez-López et al., 2016b).

una amplia colección de microorganismos filogenéticamente diversos mostraron que VCs emitidos por el hongo filamentoso *Penicillium aurantiogriseum* ejercen un efecto peculiar sobre el desarrollo radicular de la planta, distinto al ejercido por VCs de otros microorganismos. Plantas sometidas a la acción de VCs emitidos por este fitopatógeno desarrollan un sistema radicular muy profuso con numerosas raíces secundarias y pelos radiculares muy abundantes y largos (**Figura 3**) dando lugar a un incremento de la superficie de contacto de la planta con el medio, y por tanto, de su capacidad de adquirir nutrientes y agua. Esta peculiaridad de *P. aurantiogriseum* convierte a este hongo en un atractivo modelo tanto para investigar los mecanismos que fomentan el crecimiento y el desarrollo en plantas sometidas a VCs microbianos como para llevar a cabo estudios de bioprospección de nuevos compuestos que incrementen el rendimiento de los cultivos de manera sostenible y económica.

1.3. Naturaleza de los VCs microbianos que fomentan el crecimiento y producen

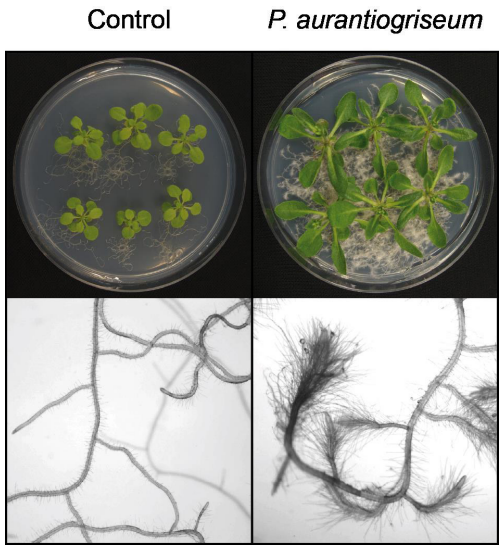

Figura 3: VCs emitidos por el hongo fitopatógeno *P. aurantiogriseum* fomentan el crecimiento de la parte aérea y la formación y desarrollo de pelos radiculares en plantas de Arabidopsis. La fotografía muestra raíces de plantas de Arabidopsis en ausencia (control) o presencia durante 7 días de cultivos adyacentes de *P. aurantiogriseum*.

cambios en el desarrollo de las plantas

Todas las investigaciones realizadas hasta el momento sobre el efecto estimulante de VCs microbianos en el crecimiento y desarrollo de las plantas han girado en torno a compuestos de naturaleza orgánica comúnmente designados como VOCs (de "volatile organic compounds") (Kanchiswamy et al., 2015). De los 2000 VOCs microbianos identificados hasta el momento (Lemfack et al., 2018) muy pocos se han descrito como promotores del crecimiento. El trabajo pionero en esta temática (Ryu et al., 2003) identificó 2 compuestos (3-hydroxybutan-2-ona (acetoína) y 2,3-butanediol), como los principales VOCs emitidos por *B. subtilis* causantes del fomento del crecimiento de la planta. Recientemente, se han identificado otros VOCs microbianos que fomentan el crecimiento de la planta tales como el dimetildisulfuro (Meldau et al., 2013), algunos sesquiterpenos tales como el thujopseno y el β-cariofileno (Ditengou et al., 2015) o la 6-pentil-2H-piran-2-ona (Garnica-Vergara et al., 2016). No obstante, el efecto estimulante de estos compuestos aplicados en estado puro sobre el crecimiento de la planta es muy inferior al observado en plantas expuestas a mezclas de VCs microbianos.

Además de VOCs, los microorganismos son capaces de producir algunos VCs de carácter inorgánico (VICs), tales como el ácido sulfídrico (H_2S), el hidrógeno

molecular (H_2), el óxido nítrico (NO), el dióxido de nitrógeno (NO_2), el óxido nitroso (N_2O), el monóxido de carbono (CO), el dióxido de carbono (CO_2), el amoníaco (NH_3) y el ácido cianhídrico (HCN) (Engel et al., 1972; Wharton and Weintraub, 1980; Siegel and Siegel, 1987; Nandi and Sengupta, 1998; Conrath et al., 2004; Blom et al., 2011; Shatalin et al., 2011; Schreiber et al., 2012; Weise et al., 2013). Aplicados en elevadas concentraciones, estos compuestos pueden resultar nocivos para la planta. Sin embargo, algunos de estos compuestos (e.g. H_2S, CO, NO, NO_2, N_2O o H_2) pueden ejercer un efecto beneficioso cuando se aplican en bajas concentraciones (Dong et al., 2003; He et al., 2004; Guo et al., 2009; Jin et al., 2009; Kong et al., 2010; Xu et al., 2010; Chen et al., 2011; Dooley et al., 2013; Jin et al., 2013; Lisjak et al., 2013; Zeng et al., 2013; Lin et al., 2014; Takahashi et al., 2014; Wang and Liao, 2016; Kuruthukulangarakoola et al., 2017). VICs emitidos por algunas bacterias que fomentan el crecimiento son determinantes importantes de la arquitectura radicular de la planta (Creus et al., 2005; Molina-Favero et al., 2008).

1.4. Limitaciones de los sistemas empleados para el estudio de la respuesta de las plantas a VCs microbianos

Todos los estudios sobre la respuesta de las plantas a VCs microbianos se han llevado a cabo haciendo uso de sistemas de co-cultivo sellados en los que no existe contacto físico entre las plantas y los microorganismos y en los que el intercambio de gases con el exterior es muy limitado. El sistema de co-cultivo más simple y ampliamente utilizado está basado en la utilización de placas de Petri septadas y selladas con Parafilm. Tales placas poseen dos compartimentos conectados entre sí a través de una ranura que permite el intercambio de gases entre ambos compartimentos (Kai et al., 2016). En uno de los compartimentos se cultivan las plantas, mientras que en el otro se cultivan los microorganismo emisores de VCs (**Figura 4a**). Otro sistema de co-cultivo sellado utilizado para el estudio de las relaciones planta-microorganismo consiste en un mini-invernadero que consta de un recipiente cerrado donde se cultivan las plantas, conectado a un matraz donde se cultivan los microorganismos cuyos VCs son impulsados al mini-invernadero mediante una bomba (**Figura 4b**) (Kai et al., 2016).

Todos los microorganismos productores de VCs promotores del crecimiento y de cambios del desarrollo de la planta descritos hasta el momento son heterótrofos. En condiciones aeróbicas estos microorganismos consumen O_2 y emiten CO_2. Los

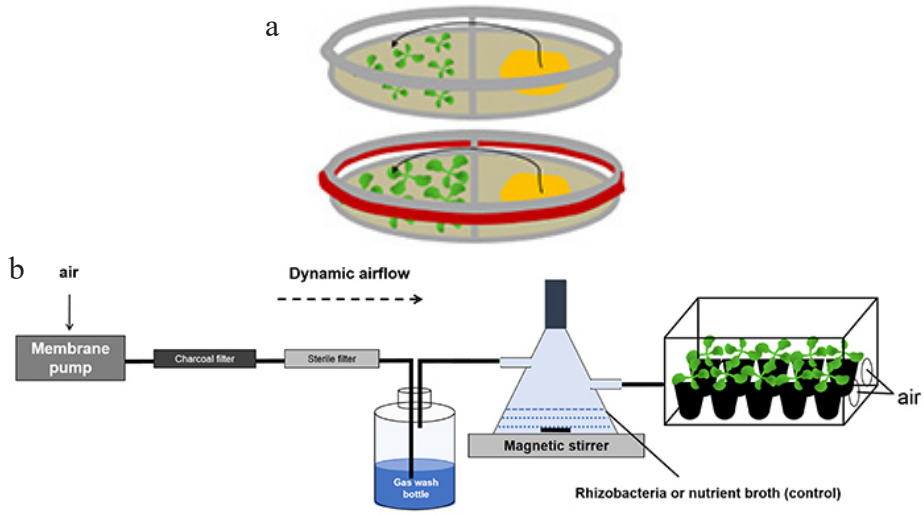

Figura 4: Sistemas de co-cultivo utilizados en el estudio de los VCs microbianos. (a) Sistema de co-cultivo basado en el uso de placas Petri septadas (arriba placa abierta; abajo placa sellada con Parafilm) y (b) esquema del sistema de mini-invernadero (Kai et al., 2016).

sistemas de co-cultivo anteriormente descritos acumulan altos niveles de CO_2 como consecuencia de la respiración microbiana (Kai and Piechulla, 2009). Concentraciones elevadas de CO_2 y niveles reducidos de O_2 potencian la fijación fotosintética de CO_2, reducen la fotorrespiración y promueven el crecimiento, la floración, la acumulación de almidón y cambios en la arquitectura radicular de la planta (Quebedeaux and Hardy, 1975; Makino and Mae, 1999; Ramonell et al., 2001; Ainsworth and Rogers, 2007; Song et al., 2009; Niu et al., 2011; Hachiya et al., 2014; Thompson et al., 2017). Por ello, algunos investigadores han propuesto que el efecto estimulante de los VCs emitidos por microorganismos en los sistemas de co-cultivo arriba descritos podría ser debido en gran parte a la exposición de las plantas a elevadas concentraciones de CO_2 y han cuestionado la implicación de otro tipo de VCs en este fenómeno (Kai and Piechulla, 2009; Casarrubia et al., 2016; Kai et al., 2016). Como consecuencia de la controversia generada, se ha propuesto que los sistemas de co-cultivo sellados para el estudio de la respuesta de las plantas a VCs microbianos deben incluir sistemas de monitorización del CO_2 (Piechulla, 2017).

2. FACTORES QUE AFECTAN A LA ARQUITECTURA RADICULAR

Las raíces cumplen funciones tan esenciales para la supervivencia de la planta como la toma de agua y nutrientes, la fijación al suelo o el establecimiento de interacciones con el entorno, ya sean con microorganismos o con otras plantas. En algunas especies, las raíces son almacenadoras de sustancias de reserva. Todas estas funciones dependen en gran medida de la arquitectura de la raíz que, a su vez depende de la longitud de la raíz primaria (PR) y del número y longitud de bifurcaciones surgidas de la PR denominadas raíces laterales (LR). Tanto la PR como las LRs están revestidas de pelos radiculares, que son células especializadas en la captura de agua y minerales. Según su origen y desarrollo se distinguen dos tipos de sistemas radicales (**Figura 5**). Las gimnospermas y las dicotiledóneas poseen un sistema radicular alorrizo, caracterizado por poseer una PR dominante sobre las LRs. Las monocotiledóneas y las pteridófitas poseen un sistema radical homorrizo que está formado por un conjunto de raíces adventicias y que se halla profusamente ramificado. En ambos casos la arquitectura de la raíz está determinada por factores endógenos y exógenos.

2.1. Factores endógenos

Auxinas

Las auxinas están involucradas prácticamente en todos los procesos de desarrollo de las plantas. A concentraciones fisiológicas, promueven la división de las células vegetales, aunque en altas concentraciones pueden inducir o inhibir la elongación celular (Perrot-Rechenmman and Napier, 2005). El ácido indolacético (IAA) es la auxina más estudiada y se presenta en forma libre o conjugada con otros compuestos. Existen varias rutas de síntesis del IAA en plantas que se agrupan en: rutas dependientes e independientes de la metabolización del triptófano **(Figura 6)**.

En general las zonas más importantes de síntesis del IAA son los tejidos jóvenes (yemas, hojas, frutos y semillas inmaduras). El transporte y la distribución de las auxinas a las restantes partes de la planta juegan un papel importante para el desarrollo de la misma. El transporte acropétalo de las auxinas se produce desde los tejidos aéreos jóvenes hacia las raíces a través de rutas de larga y corta distancia (Ljung et al., 2005; Teale et al., 2006). En la ruta de larga distancia, las auxinas se transportan a través del floema maduro mientras que en la ruta de corta distancia el transporte de las auxinas tiene lugar de célula a célula y está mediado por transportadores específicos de entrada y salida de auxinas (Vieten et al., 2007; Vanneste and Friml, 2009). En *Arabidopsis*

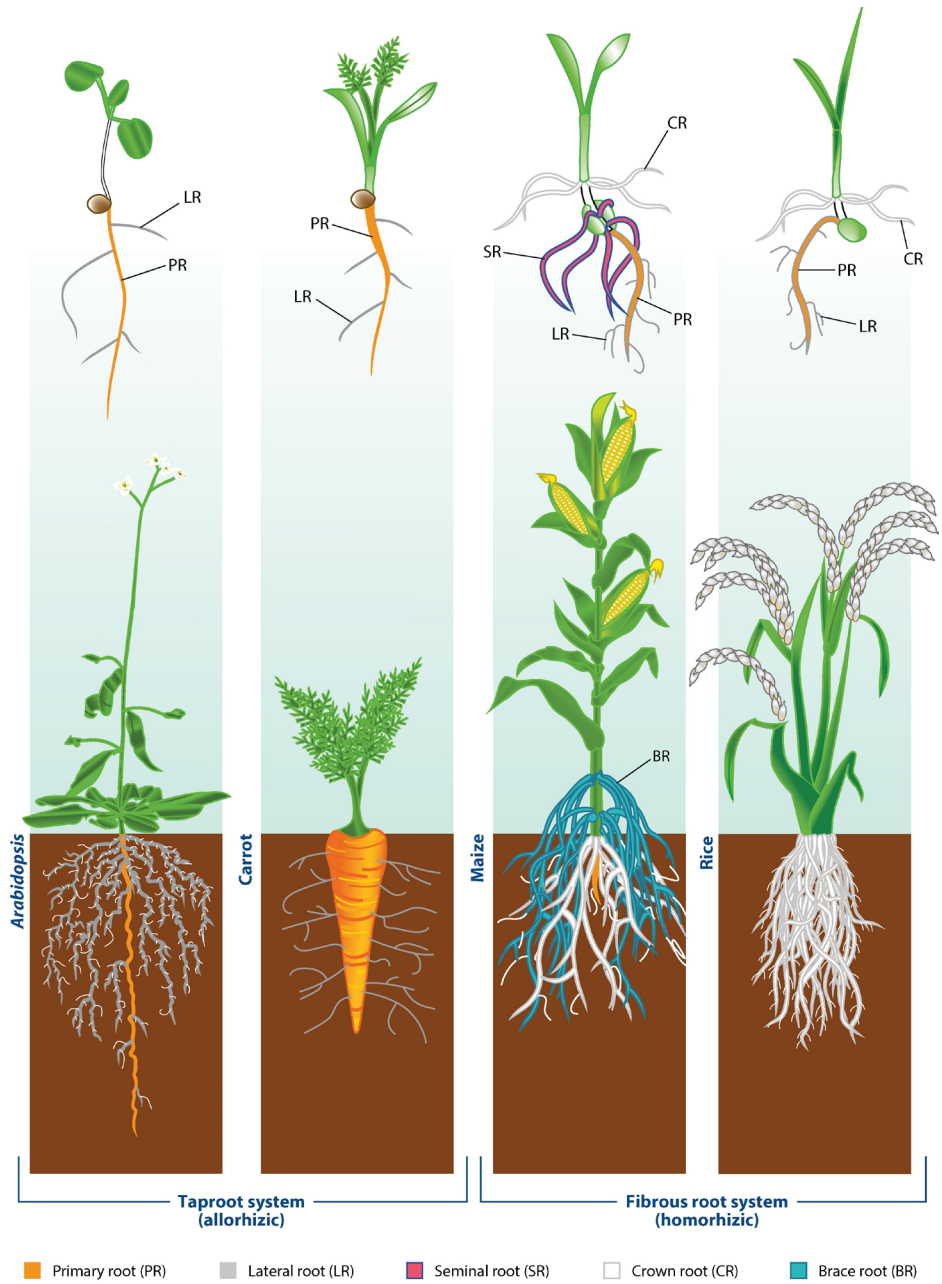

Figura 5: Representación esquemática de los distintos tipos de sistemas radiculares (Bellini et al., 2014).

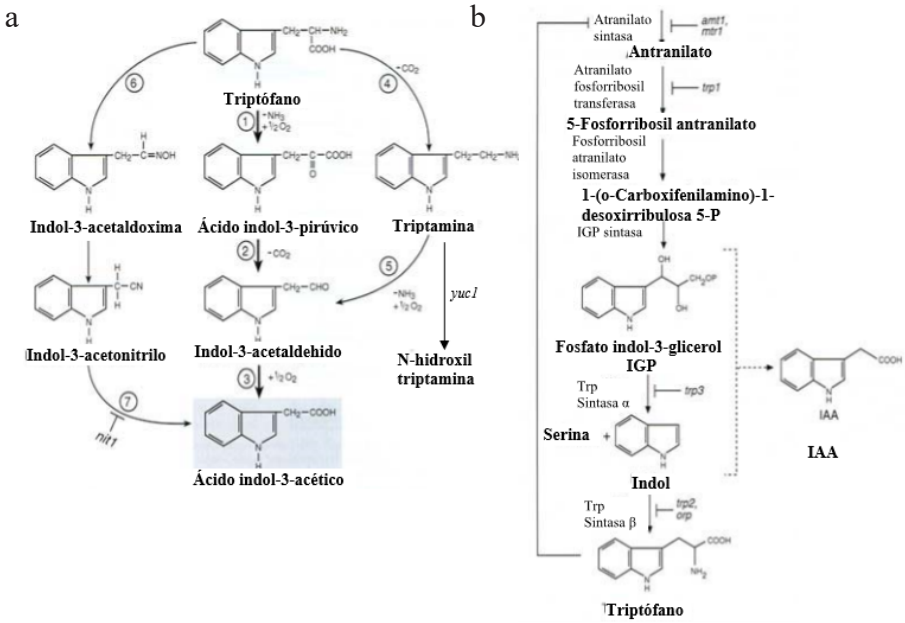

Figura 6: Rutas de síntesis de IAA. (a) Rutas triptófano-dependientes. El triptófano puede convertirse en IAA a través de reacciones acopladas de desaminación (que dan lugar a ácido indol-3-pirúvico), descarboxilación (que dan lugar al indol-3-acetaldehido, que también puede obtenerse por la desaminación de la triptamina) y oxidación (dando lugar al IAA). Rutas alternativas de producción de IAA a partir del triptófano incluyen (i) la producción de indol-3-acetaldehído vía triptamina, o (ii) la producción de indol-3-acetaldoxima, que una vez convertida en indol-3-acetonitrilo, puede dar lugar a IAA (Srivastava, 2002). (b) Ruta independiente de triptófano. Esta ruta surge a partir del producto final de la ruta del shikimato (corismato), que es convertido en antranilato, 5-fosforribosilantranilato, dioxirribulosa, fosfato indol-3glicerol (IGP) e indol mediante la acción acoplada de las enzimas antranilato sintasa, fosforribosil antranilato transferasa, fosforribosil antranilato isomerasa, IGP sintasa y triptófano sintasa. El IAA puede sintetizarse a partir de indol o IGP (Srivastava, 2002).

thaliana, se han descrito tres familias de proteínas transportadoras de auxinas: las AUX1 y similares (AUX1/LAX), las PIN y las p-glicoproteínas (PGP) de tipo ABC (Zazímalová et al., 2010). Las proteínas de la familia PIN exportan auxinas (Blilou et al., 2005; Geisler and Murphy, 2006) mientras que las de la familia AUX1/LAX las importan (Bennett et al., 1996; Swarup et al., 2001). Las PGP actúan indistintamente tanto como importadoras como exportadoras (Geisler and Murphy, 2006). El flujo de auxinas por estos transportadores juega un papel importante en la distribución de estas en la raíz y, por tanto, en la arquitectura radicular. Mutantes deficientes en AUX1 son agravitrópicos y presentan alteraciones en la distancia entre LRs y en la aparición y desarrollo de pelos radiculares (Vanneste and Friml, 2009). Por otro lado, las mutaciones

de proteínas PIN alteran el desarrollo de los meristemos de la raíz, la organogénesis, la diferenciación del tejido vascular y la respuesta gravitrópica, lo que sugiere que estas proteínas juegan un papel crítico en estos procesos (Blilou et al., 2005; Zhao et al., 2015).

Una vez en el interior de la célula, las auxinas se unen a la proteína receptora TIR1 y son señalizadas según se ilustra en la **Figura 7**.

Citoquininas

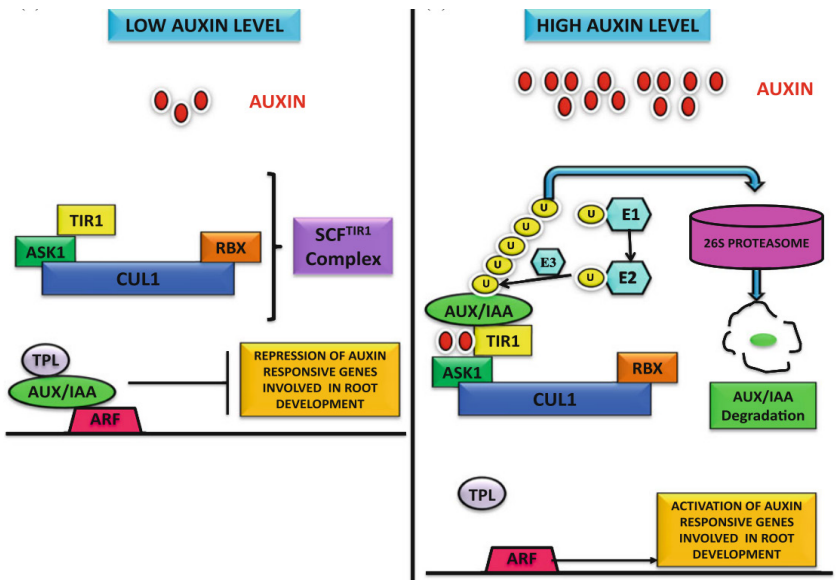

Figura 7: Modelo de señalización de auxinas. Con niveles bajos de auxinas, el correpresor TPL reprime la transcripción regulada por auxina mediante la unión de las proteínas AUX/IAA a los ARFs. Con niveles altos, el complejo SCF^{TIR1} se une a la auxina y se dirige a las proteínas AUX/IAA para su degradación a través de la vía ubiquitina-proteasoma. La ubiquitina se conjuga covalentemente a las AUX/IAA por la actividad secuencial de tres enzimas: las enzimas activadoras de ubiquitina (E1), las enzimas conjugadoras de ubiquitina (E2) y las proteínas ligasas de ubiquitina (E3). Esto permite a las proteínas AUX/IAA ser reconocidas por el proteasoma y degradarlas, liberando los ARF y activando los genes involucrados en la respuesta a auxinas (Saini et al., 2013).

Las CKs estimulan la división celular de las plantas, controlan la diferenciación del meristemo de la raíz, promueven la formación de pelos radiculares e inhiben la formación de LRs y el alargamiento de la PR (Riefler et al., 2006; Bishopp et al., 2009; Ramireddy et al., 2014). Mutantes deficientes en producción o señalización de CKs se caracterizan por poseer una PR más larga y un mayor número de LRs que las plantas silvestres (Bishopp et al., 2009; Ramireddy et al., 2014). Las CKs son derivados de

adenina que poseen una cadena lateral en la posición N6, que es la que determina su actividad biológica en plantas. La cadena lateral puede ser de naturaleza isoprenoide o aromática. Entre las CKs isoprenoides se encuentran la cis-zeatina (cZ), la trans-zeatina (tZ), la isopenteniladenina (iP) y la dihidrozeatina (DZ), con sus respectivos derivados glicosilados (Sakakibara, 2006). Entre las CKs aromáticas se incluyen la benciladenina, la kinetina y la metahidroxibenziladenina. La síntesis de CKs isoprenoides en las plantas se produce a través de dos rutas metabólicas: la ruta del metileritritol fosfato (MEP) y la ruta del mevalonato (MVA) (**Figura 8**) (Sakakibara, 2006).

Históricamente se asumía que las CKs solo eran sintetizadas en las raíces de las plantas y de ahí se transportaban hacia el tallo y las hojas (Beck and Wagner, 1994). Sin embargo, las CKs también pueden sintetizarse en la parte aérea de las plantas (Hirose et al., 2008). Dependiendo de su naturaleza química, el movimiento de las CKs en la planta puede ser tanto hacia las raíces como hacia las hojas. Por ejemplo la tZ es transportada hacia el ápice de la planta a través del xilema, mientras que la iP se transporta fundamentalmente a través del floema (Hirose et al., 2008; Kudo et al., 2010). Se conoce la existencia de un transporte de CKs entre células a través de dos familias de transportadores: permeasas de purinas y transportadores de nucleósidos (Kang et al., 2017). El mecanismo principal de señalización de las CKs está basado en el sistema de doble componente de transferencia de grupos fosfato que se ilustra en la **Figura 9**.

Etileno

El etileno es un VOC que juega un papel fundamental en la formación y el crecimiento de las LRs e inhibe el alargamiento de la raíz y el transporte de auxina. Mutantes con elevada síntesis o señalización de etileno poseen un reducido número de LRs, mientras que mutantes insensibles al etileno muestran una gran proliferación de LRs (Negi et al., 2008). El etileno también es clave para el desarrollo de los pelos radiculares. Mutantes insensibles a la acción del etileno muestran pelos radiculares más cortos, mientras que mutantes sobreproductores de etileno poseen pelos radiculares más largos (Pitts et al., 1998; Rahman et al., 2002). En las plantas el etileno se produce a partir de la S-adenosil metionina mediante la acción acoplada de la 1-aminociclopropano-1-carboxilato sintasa y la aminociclopropano-1-carboxilato oxidasa (**Figura 10**). Los mecanismos de señalización del etileno se ilustran en la **Figura 11.**

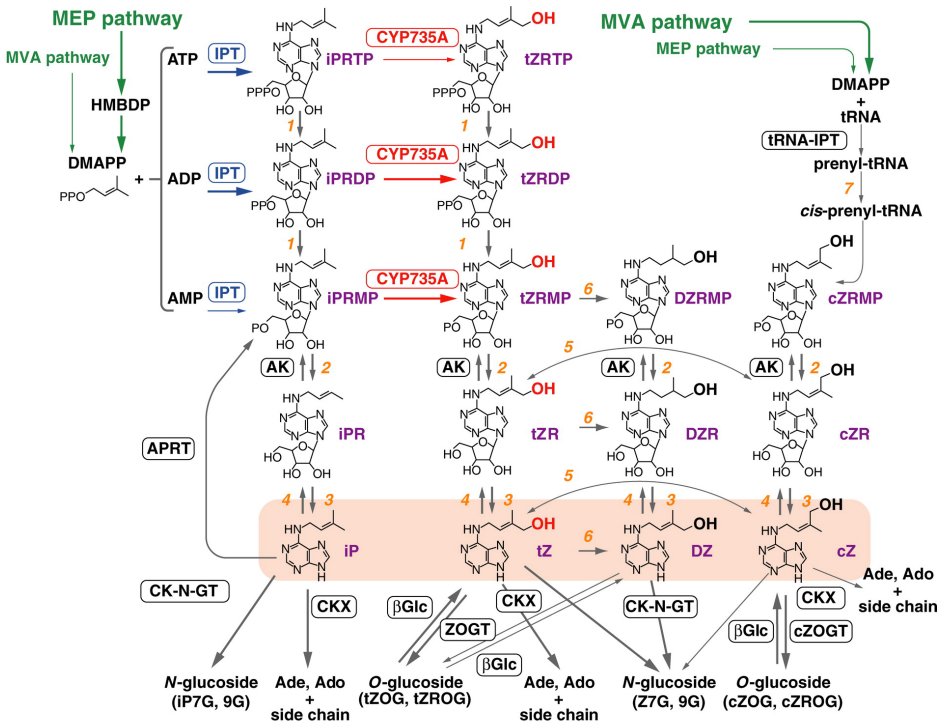

Figura 8: Rutas implicadas en la biosíntesis de CKs en Arabidopsis. Según este modelo, las cadenas laterales isoprenoides de isopenteniladenina (iP), trans-zeatina (tZ) y dihidrozeatina (DZ) provienen mayoritariamente de la ruta del metileritritol fosfato (MEP), mientras que la cadena lateral de la cis-zeatina (cZ) proviene de la ruta del ácido mevalónico (MVA). Las enzimas isopenteniltransferasas (IPT) son las encargadas de sintetizar iPRTP, iPRDP e iPRMP, a partir de ATP, ADP y AMP, respectivamente. iPRTP, iPRDP e iPRMP pueden convertirse en sus respectivas formas de tZ (tZRTP, tZRDP y tZRMP) gracias a la enzima CYP735A. La formación de iPRMP a partir de iPRTP e iPRDP es catalizada por fosfatasas. Ambas formas iPRMP y tZRMP (junto con DZRMP y cZRMP) se metabolizan en los nucleosidos iPR, tZR, DZR y cZR respectivamente por la acción de la adenosina quinasa (AK), los cuales pueden transformarse en las respectivas CKs activas por la adenosin nucleosidasa (Sakakibara, 2006).

Óxido nítrico

El NO es un determinante importante del desarrollo de PRs y LRs. Comparadas con plantas silvestres, plantas deficientes en NO poseen una raíz primaria larga y un reducido número de LRs, mientras que plantas expuestas a sustancias donadoras de NO o que acumulan altos niveles de este VIC presentan un elevado número de LRs (Correa-Aragunde et al., 2004). El NO también está implicado en el desarrollo de los pelos radiculares. Un incremento de los niveles de NO endógeno fomenta el desarrollo de estas estructuras, mientras que un descenso del NO endógeno inhibe su formación y desarrollo (Lombardo et al., 2006). El NO se produce en numerosos orgánulos

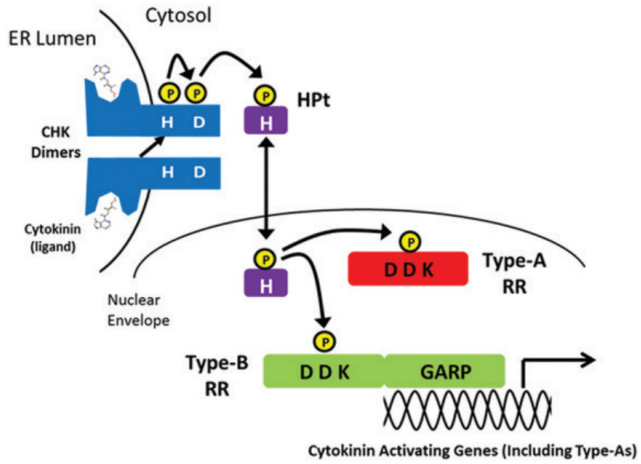

Figura 9: Mecanismo de señalización de CKs de doble componente de transferencia de grupos fosfato. Según este modelo, la CK se une en la luz del retículo endoplasmático (ER) al receptor dimerizado CHK, situado en la membrana del ER, comenzando así la vía de señalización. El receptor se autofosforila en un residuo de histidina conservado, que luego se transmite a un residuo de ácido aspártico conservado. La señal se desplaza a través del citosol a una proteína de fosfotransferencia de histidina (HPt), que luego se mueve al núcleo, transfiriendo el fosfato a un residuo de ácido aspártico conservado en los reguladores de respuesta a CKs (RR), clasificados en dos grandes grupos: tipo A (type-A RR) y tipo B (type-B RR). Ambos RR conservan un motivo de aminoácidos concreto (DDK). Los de tipo B además contiene un dominio de factor de transcripción GARP, que les permite activar genes regulados por citoquinina, mientras que los de tipo A, al no poseer este dominio, funcionan como represores de la respuesta a CKs (Keshisian and Rashote, 2015).

(mitocondrias, cloroplastos y peroxisomas) mediante reacciones enzimáticas en las que intervienen peroxidasas, nitrato sintasas y enzimas similares a la NO sintasa. El NO también puede producirse de forma no-enzimática en ciertas condiciones, como en el caso de una bajada del pH que puede provocar la formación de NO a partir de nitrato (Wilson et al., 2008; del Río, 2011; Hancock, 2012; Mur et al., 2012; del Río et al., 2014). Independientemente de su origen, el NO es una especie reactiva del nitrógeno que puede modular la función de las proteínas a través de la nitrosilación de los grupos tioles de cisteínas o reaccionar con ROS, para generar peroxinitrito, que a su vez puede dar lugar a la nitración de las tirosinas de las proteínas**.**

Especies reactivas de oxígeno

Los ROS (H_2O_2 y O_2^-) son determinantes importantes de la arquitectura de la raíz (Tsukagoshi et al., 2010). Los productores más importantes de H_2O_2 en plantas son la glicolato oxidasa y la acil-CoA oxidasa peroxisomales implicadas en las vías de

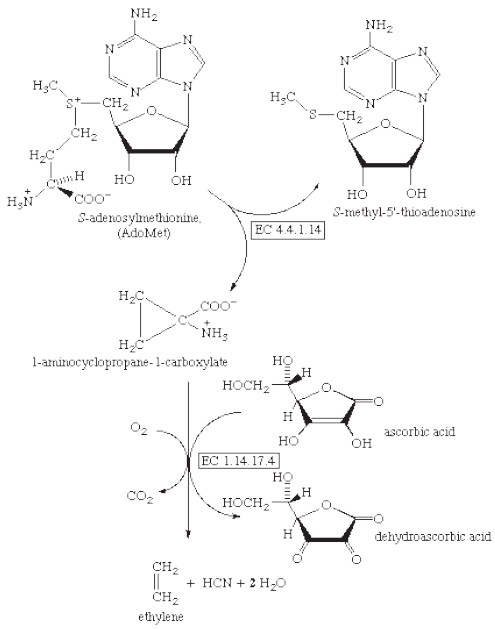

Figura 10: Ruta de síntesis del etileno. Las plantas utilizan como precursor del etileno la S-adenosilmetionina, la cual es transformada por la 1-aminociclopropano-1-carboxilato sintasa (EC 4.4.1.14), obteniendose 1-amino-ciclopropano-1-carboxilato y liberándose S-metil-5-tioadenosina, y posteriormente la aminociclopropano-1-carboxilato oxidasa (EC 1.14.17.4), mediante el uso de ácido ascórbico como cofactor, transforma el 1-amino-ciclopropilcarboxilato en etileno, generándose además ácido cianhídrico (HCN) y CO_2. https://www.qmul.ac.uk/sbcs/iubmb/enzyme/reaction/misc/ethene.html

fotorrespiración y de la β-oxidación de ácidos grasos, respectivamente. Las peroxidasas unidas a la pared celular también son importantes productores de H_2O_2 (Bolwell and Daudi, 2009; O'Brien et al., 2012). Una fuente importante de O_2^- es la NADPH oxidasa localizada en la membrana plasmática (Suzuki et al., 2011; Marino et al., 2012; Baxter et al., 2014). Otras fuentes importantes de O_2^- y H_2O_2 son los cloroplastos y las mitocondrias donde tiene lugar diferentes reacciones oxidativas y de transporte de electrones (Asada, 2006; del Río et al., 2006; Rhoads et al., 2006; Halliwell and Gutteridge, 2007; del Río and Puppo, 2009; del Río, 2013). Plantas silvestres tratadas con inhibidores de la actividad de la NADPH oxidasa o mutantes *rhd2* que no expresan una NADPH oxidasa no poseen pelos radiculares y desarrollan raíces cortas (Foreman et al., 2003).

Existen diferentes mecanismos de regulación génica por ROS. Está ampliamente aceptado que la detección de ROS externos e internos por sensores de membrana conlleva la inducción de cascadas de reacciones en las que MAP quinasas (MAPKs) transfieren grupos fosfato a factores de transcripción (**Figura 12**) (Apel and

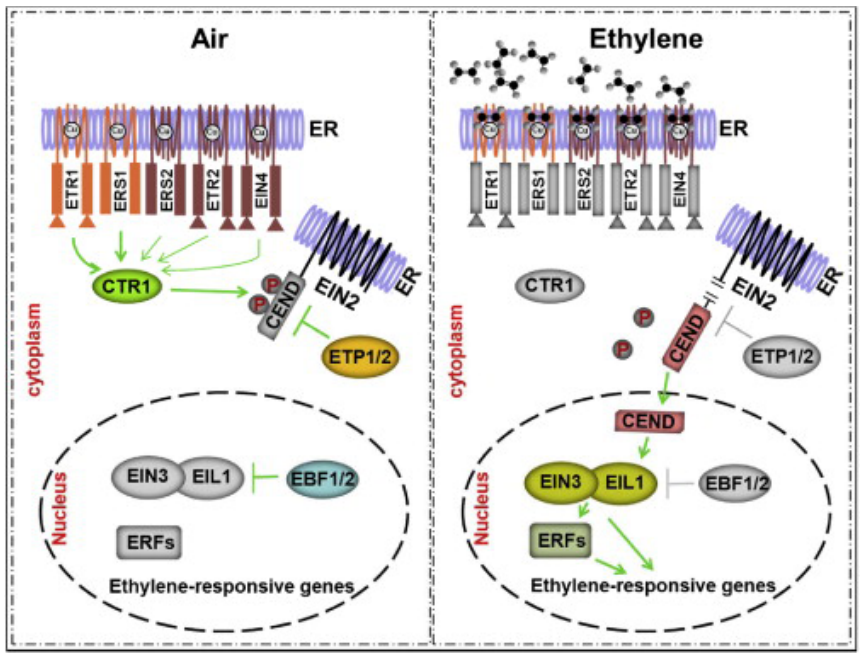

Figura 11: Modelo propuesto de la señalización de etileno en Arabidopsis. El etileno es percibido en la membrana del ER por una familia de receptores (ETR1, ERS1, ETR2, EIN4 y ERS2). En ausencia de etileno (Air), los receptores activos interactúan con la región N-terminal del regulador negativo CTR1 (Kieber et al., 1993) para fosforilar directamente el dominio C-terminal del regulador positivo de las respuestas de etileno EIN2 (Alonso et al., 1999), impidiendo la separación del dominio CEND de EIN2 por las proteínas F-box EPT1/2 y reprimiendo la transducción de señalización. En el núcleo, las proteínas implicadas en la señalización de etileno EIN3/EIL1 se degradan a través del ubiquitina-proteasoma mediado por las proteínas F-box EBF1/2. En presencia de etileno tiene lugar una inactivación de sus receptores y CTR1, lo que resulta en la desfosforilación de EIN2 y, por lo tanto, la escisión del dominio CEND. Este dominio CEND se transporta al núcleo y participa en la estabilización y acumulación de EIN3/EIL1 y, en consecuencia, induce la transcripción de factores de respuesta a etileno (ERFs) y otros genes sensibles al etileno (Yang et al., 2015).

Hirt, 2004). La señalización de ROS internos también puede producirse mediante la inactivación de una proteína fosfatasa que defosforila a las MAPKs (**Figura 12**). Los ROS también pueden modular la expresión génica modificando la actividad de los factores de transcripción (Apel and Hirt, 2004) (**Figura 12**).

2.2. Factores exógenos que afectan a la arquitectura radicular

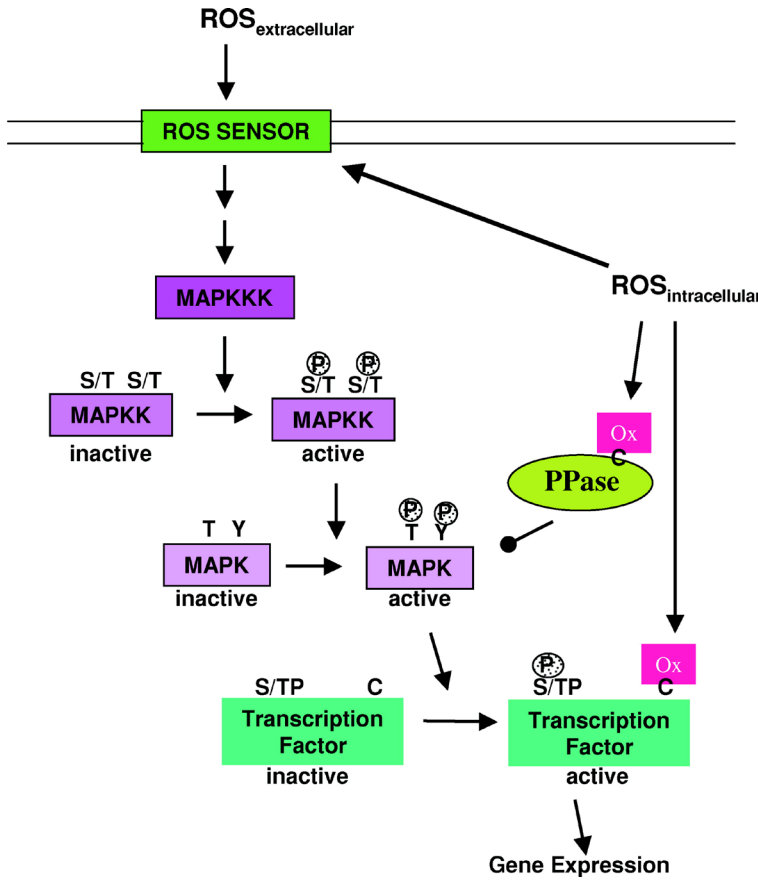

Figura 12: Esquema propuesto para la detección y señalización de ROS en plantas. Los ROS de origen tanto intracelular como extracelular son detectados por sensores de ROS, constituidos por proteínas histidin-quinasas de membrana, las cuales activan una cascada de fosforilacion de proteínas MAP quinasas (MAPKKK, MAPKK y MAPK), que inducen la activación de factores de transcripción mediante la fosforilacion de los mismos mediante la MAPK activa. Los ROS intracelulares pueden mantener activa la MAPK gracias a la inhibición por oxidación de una fosfatasa (PPase) o actuar directamente sobre la activación de los factores de transcripción a través de la oxidación de residuos de cisteínas. (Apel and Hirt, 2004)

Factores abióticos

La arquitectura radicular está fuertemente determinada por factores exógenos de carácter abiótico, tales como la disponibilidad de agua y de macronutrientes (fósforo, azufre, potasio, calcio y nitrógeno) y micronutrientes esenciales (hierro, boro, molibdeno, manganeso, cobre, níquel y zinc). En función de la disponibilidad de agua, las plantas responden fomentando el crecimiento de sus raíces laterales en las zonas con mayor grado de humedad o reprimiendo el crecimiento en zonas con escasa humedad (Bao et

al., 2014; Orman-Ligueza et al., 2018; Robbins and Dinneny, 2018). La disponibilidad de nutrientes puede alterar el número, la longitud, el ángulo y el diámetro de las raíces y los pelos radiculares (Forde and Lorenzo, 2001; López-Bucio et al., 2003; Malamy, 2005). Las plantas responden a concentraciones crecientes de nitrato inhibiendo el crecimiento de la raíz primaria y de las raíces laterales (Lopez-Bucio et al., 2005). Plantas crecidas en suelos pobres en fosfato reducen drásticamente el crecimiento de la raíz primaria (Sánchez-Calderón et al., 2005) y desarrollan más raíces laterales y pelos radiculares que plantas crecidas con altas concentraciones de fosfatos (Williamson et al., 2001; Lopez-Bucio et al., 2002; Jiang et al., 2007). Una deficiencia leve de hierro fomenta el alargamiento de las raíces primaria y laterales, mientras que una deficiencia severa causa retraso en el crecimiento de las raíces (Gruber et al., 2013). La deficiencia de zinc conlleva el desarrollo de un sistema radicular altamente ramificado (Gruber et al., 2013).

Factores bióticos

Los microorganismos existentes en la rizosfera también modifican la arquitectura radicular de las plantas. Estos microorganismos pueden mejorar el desarrollo y el crecimiento de las raíces mediante la producción y liberación al exterior de fitohormonas tales como auxinas, CKs y etileno (Thuler et al., 2003; Perrig et al., 2007; Cassán et al., 2009; Moubayidin et al., 2009; Stepanova and Alonso, 2009; Dodd et al., 2010; Overvoorde et al., 2010) o mediante la liberación de enzimas que interfieren en el metabolismo de fitohormonas. La enzima más estudiada es la 1-aminociclopropano-1-carboxilato deaminasa, que modula la producción de etileno en la planta (Penrose et al., 2001; Glick 2005; Contesto et al., 2008). Muchos microorganismos pueden fomentar el crecimiento y desarrollo de las LRs (Combes-Meynet et al., 2011; Chamam et al., 2013) y de los pelos radiculares (Dobbelaere et al., 1999; Contesto et al., 2008), fomentando así la capacidad exploratoria de nutrientes de la planta y, por tanto, el crecimiento.

3. HIPÓTESIS DE TRABAJO

El estudio de la respuesta de las plantas a VCs emitidos por microbios fitopatógenos constituye un modelo ideal tanto para investigar los mecanismos reguladores del metabolismo, crecimiento y desarrollo de la planta y su interacción con los microorganismos, como para diseñar estrategias biotecnológicas que permitan incrementar la productividad de los cultivos. Las hipótesis planteadas al inicio de mi

trabajo de tesis doctoral pueden incluirse en dos grandes bloques cuyos fundamentos y razonamientos se detallan a continuación:

3.1. Hipótesis relacionadas con la naturaleza de los VCs bioestimulantes de origen microbiano

Todos los microorganismos productores de VCs que fomentan el crecimiento y cambios del desarrollo de la planta descritos hasta el momento (tanto los patógenos utilizados por el grupo de investigación en el que he realizado mi trabajo como los beneficiosos utilizados por otros grupos de investigación) son heterótrofos. En condiciones aeróbicas estos microorganismos consumen O_2 y emiten CO_2. Los sistemas sellados de co-cultivo clásicamente empleados para el estudio de las relaciones planta-microorganismo mediadas por VCs acumulan altos niveles de CO_2 como consecuencia de la respiración microbiana (Kai and Piechulla, 2009). Concentraciones elevadas de CO_2 y niveles reducidos de O_2 potencian la fijación fotosintética de CO_2 y promueven el crecimiento, la floración, la acumulación de almidón y cambios en la arquitectura radicular de la planta (Quebedeaux and Hardy, 1975; Makino and Mae, 1999; Ramonell et al., 2001; Ainsworth and Rogers, 2007; Song et al., 2009; Niu et al., 2011; Hachiya et al., 2014; Thompson et al., 2017). El sistema "box-in-box" utilizado por mi grupo de investigación para realizar estudios de la respuesta de la planta a VCs microbianos es un sistema "semi-sellado" en el que el intercambio de gases con el exterior está mediado por una fina lámina de plástico semipermeable a VCs de pequeño tamaño molecular. Consecuentemente, una hipótesis de trabajo contemplada al inicio de mi trabajo proponía que una parte considerable de la respuesta de la planta a los VCs emitidos por microorganismos patógenos descritos por mi grupo de investigación son debidos a la exposición de las plantas a elevadas concentraciones de CO_2.

Todas las investigaciones realizadas hasta el momento sobre el efecto bioestimulante de los VCs microbianos han girado en torno a VOCs (Kanchiswamy et al., 2015). Sin embargo, además de VOCs, los microorganismos son capaces de producir VICs que, aplicados en bajas concentraciones pueden ejercer un efecto beneficioso para la planta (Dong et al., 2003; He et al., 2004; Guo et al., 2009; Jin et al., 2009; Kong et al., 2010; Xu et al., 2010; Chen et al., 2011; Dooley et al., 2013; Jin et al., 2013, Lisjak et al., 2013; Zeng et al., 2013; Lin et al., 2014; Takahashi et al., 2014; Wang and Liao, 2016; Kuruthukulangarakoola et al., 2017). Es más, VICs emitidos por algunas

bacterias que fomentan el crecimiento son determinantes importantes de la arquitectura radicular de la planta (Creus et al., 2005; Molina-Favero et al., 2008). Por lo tanto, otra hipótesis de trabajo planteada al inicio de mis investigaciones proponía que algunos VICs (incluyendo los emitidos por hongos fitopatógenos) juegan un papel importante en la respuesta de la planta a VCs microbianos.

3.2. Hipótesis relacionadas con la regulación de la respuesta de las raíces a VCs microbianos

Investigaciones llevadas a cabo antes de mi incorporación al laboratorio en el que he realizado mi trabajo de investigación permitieron elaborar un esquema integrativo de los procesos bioquímicos y moleculares que operan en las plantas expuestas a la acción de los VCs emitidos por microorganismos patógenos (**Figura 2**). La hipótesis de trabajo planteada al inicio de mi investigación contemplaba que los VCs emitidos por fitopatógenos fúngicos son percibidos por receptores localizados en la membrana plasmática de células foliares que producen señales promotoras de la expresión de funciones relacionadas con la fotosíntesis. El incremento de la actividad fotosintética resultante conlleva incrementos en la producción de gliceraldehido-3-P, un intermediario del CBC que actúa como precursor de la síntesis de compuestos isoprenoides plastidiales tales como clorofilas, carotenoides y hormonas, entre las que destacan las giberelinas y CKs. Estas últimas inician una cascada de reacciones que derivan en la producción de proteínas relacionadas con la captación de luz, la fotoprotección, la síntesis de componentes de pared celular, la iniciación de la floración y el desarrollo radicular, la defensa contra el estrés oxidativo, el metabolismo de aminoácidos y la captación de hexosas citosólicas precursoras de la biosíntesis de almidón. Según este modelo, la regulación de la respuesta de la planta a VCs microbianos está altamente regulada a nivel transcripcional (Sánchez-López et al., 2016b). Sin embargo, existen indicios de que esto no es del todo correcto. Así, trabajos realizados en nuestro laboratorio han mostrado que la acumulación de niveles excepcionalmente elevados de almidón foliar promovida por los VCs fúngicos depende en gran medida de la activación redox de enzimas del metabolismo del almidón (Li et al., 2011). Además, la mayoría de los cambios observados en el proteoma de plantas expuestas a VCs microbianos no están asociados con cambios en el transcriptoma (Sánchez-López et al., 2016a). Es más, parece que los mecanismos de regulación post-transcripcional juegan un papel importante en

la adaptación de las plantas (especialmente las raíces) a cambios del entorno (Floris et al., 2009; Lan et al., 2012). Por lo tanto, otra hipótesis de trabajo planteada al inicio de mis investigaciones contemplaba que la respuesta de las plantas (especialmente de las raíces) a VCs microbianos está regulada post-transcripcionalmente.

En la fase de pre-colonización los microorganismos beneficiosos producen VCs que promueven cambios en la arquitectura radicular de las plantas que facilitan la captación de nutrientes y agua. Estas adaptaciones son el resultado de procesos en los que (a) la señalización de hormonas (especialmente auxinas, etileno y CKs) y ROS juegan un papel destacado y (b) determinadas rutas metabólicas actúan como fuente de energía y de moléculas-señal. Sin embargo, hasta el momento no se han realizado estudios de los cambios que ocurren en el metaboloma, el proteoma y el hormonoma de raíces de plantas expuestas a VCs emitidos por fitopatógenos. Otra hipótesis de trabajo planteada al inicio de mis investigaciones proponía que los microorganismos patógenos emiten VCs que fomentan el crecimiento y cambios en el desarrollo radicular a través de cambios en la señalización de hormonas y ROS que a su vez dan lugar a cambios en el proteoma y metaboloma de la planta.

OBJETIVOS

upna
Universidad Pública de Navarra
Nafarroako Unibertsitate Publikoa

El objetivo general de esta tesis es profundizar en el conocimiento de los mecanismos que regulan la interacción entre las plantas y los microorganismos fitopatógenos durante la fase de pre-colonización. Para ello se plantean los siguientes objetivos específicos:

1) Identificar la naturaleza de los VCs emitidos por dos hongos fitopatógenos (*A. alternata* y *P. aurantiogriseum*) que fomentan el crecimiento y promueven cambios en el metabolismo y el desarrollo de Arabidopsis.

2) Estudiar los mecanismos bioquímicos y moleculares implicados en la respuesta de las raíces a los VCs emitidos por *P. aurantiogriseum.*

upna
Universidad Pública de Navarra
Nafarroako Unibertsitate Publikoa

CAPÍTULO 1

Volatile compounds other than CO_2 emitted by different microorganisms promote distinct post-transcriptionally regulated responses in plants

upna
Universidad Pública de Navarra
Nafarroako Unibertsitate Publikoa

1. INTRODUCTION

The metabolic activity of microorganisms results in the emission of complex mixtures of volatile compounds (VCs). It is well known that beneficial bacteria and fungi can produce volatiles that promote plant growth as well as developmental and metabolic changes (Ryu et al., 2003; Hung et al., 2013; Kanchiswamy et al., 2015). We have recently shown that this capacity is not restricted to beneficial microorganisms, but also extends to phytopathogens (Sánchez-López et al., 2016b). When Arabidopsis plants were exposed to airborne signals released by the saprophytic fungus *Alternaria alternata,* growth promotion was accompanied by enhanced photosynthetic electron transport and CO_2 assimilation rates, accelerated flowering, changes in the redox status of enzymes involved in starch metabolism, and starch over-accumulation resulting from the activation of non-canonical starch biosynthetic pathway(s) (Ezquer et al., 2010; Li et al., 2011; Sánchez-López et al., 2016a; Sánchez-López et al., 2016b). Short exposure to VCs emitted by *A. alternata* and plant growth-promoting bacteria induced similar transcriptomic changes, indicating that plants react to microbial VCs through highly conserved regulatory mechanisms (Sánchez-López et al., 2016b). These findings expanded our knowledge of the diversity and complexity of the mechanisms involved in modulating plant physiology and growth when plants interact with microorganisms, and raised questions about the evolution of the involved processes and their ecological significance.

Growth promotion by microbial VCs has frequently been associated with lipophilic carbon-based compounds with molecular masses less than 300 Da and high vapour pressure, which are known as volatile organic compounds (VOCs) (Kanchiswamy et al., 2015). Nearly 2000 microbial VOCs emitted by 1000 microorganisms are presently registered in the microbial VOC database (Lemfack et al., 2018). Over 50 of these VOCs have been shown to induce changes in the plant´s growth, physiology and/or defence responses (Piechulla et al., 2017). In many cases, exposure of plants to discrete (individual) VOCs or VOC mixtures either failed to reproduce or only partially reproduced the effects induced by the complex blends of VCs emitted by plant growth promoting microorganisms (Groenhagen et al., 2013; Naznin et al., 2013; Cordovez et al., 2017). This indicates that VOCs not detected by the analytical methods used in these studies may be partly responsible for the growth-promoting effects of microbial VCs. In addition to VOCs, microorganisms also release a limited number of volatile

inorganic compounds (VICs) with molecular masses less than 45 Da such as hydrogen sulfide (H_2S), molecular hydrogen (H_2), nitric oxide (NO), nitrogen dioxide (NO_2), nitrous oxide (N_2O), carbon monoxide (CO), carbon dioxide (CO_2), hydrogen cyanide (HCN) and ammonia (NH_3) (Engel et al., 1972; Wharton and Weintraub, 1980; Siegel and Siegel, 1987; Nandi and Sengupta, 1998; Conrath et al., 2004; Blom et al., 2011; Shatalin et al., 2011; Schreiber et al., 2012; Weise et al., 2013). These compounds can cross biological membranes. Some of them are very reactive with proteins and can act as signalling molecules that promote photosynthesis, growth and developmental changes in plants when exogenously applied in a discrete form and in low concentrations (Dong et al., 2003; He et al., 2004; Guo et al., 2009; Jin et al., 2009; Kong et al., 2010; Xu et al., 2010; Chen et al., 2011; Dooley et al., 2013; Jin et al., 2013; Lisjak et al., 2013; Zeng et al., 2013; Lin et al., 2014; Takahashi et al., 2014; Wang and Liao, 2016; Kuruthukulangarakoola et al., 2017). There is also evidence that emissions of some of these compounds from growth-promoting rhizobacteria are an important determinant of root development in their host plants (Boccara et al., 2005; Johnson et al., 2008; Molina-Favero et al., 2008).

A number of studies on plant´s responses to microbial VCs have largely relied on the use of sealed dual co-cultivation systems in which plants are exposed to complex mixtures of VICs and VOCs released by nearby microbial cultures (Ryu et al., 2003; Zhang et al., 2009; Ezquer et al., 2010; Blom et al., 2011; Ditengou et al., 2015; Casarrubia et al., 2016; Sánchez-López et al., 2016a; Sánchez-López et al., 2016b; Cordovez et al., 2017). All currently known microorganisms that produce plant growth-promoting volatiles are heterotrophic and thus emit respiratory CO_2 and consume O_2 when grown under aerobic conditions. In sealed co-cultivation systems, microbial respiratory CO_2 can accumulate to high levels in the headspace (Kai and Piechulla, 2009) while O_2 levels can fall below the atmospheric O_2 concentrations. Elevated CO_2 and strong reduction of O_2 levels enhance photosynthesis, reduce photorespiration, and promote plant growth, flowering, starch accumulation and changes in root architecture (Quebedeaux and Hardy, 1975; Makino and Mae, 1999; Ramonell et al., 2001; Ainsworth and Rogers, 2007; Song et al., 2009; Niu et al., 2011; Hachiya et al., 2014; Thompson et al., 2017). Therefore, several authors have argued that the responses of plants grown in closely proximity to microbial cultures in sealed containers could be largely due to accumulation of elevated levels of CO_2 from microbial respiration, which calls into

question past interpretations of results obtained using sealed co-cultivation systems (Kai and Piechulla, 2009; Casarrubia et al., 2016; Kai et al., 2016). Consequently, studies using sealed co-cultivation systems should include appropriate CO_2 controls and online monitoring of the levels of this gas in the growth containers. In addition, the design of the test system should be described in detail (Piechulla, 2017; Piechulla et al., 2017).

Our previous studies on plant responses to microbial volatiles were conducted using a "box-in-box" co-cultivation system in which the plant and microbial cultures were placed in a container sealed with a polyvinyl chloride (PVC) plastic wrap (cf. Supplemental Figure 2 in Ezquer et al., 2010, cf. Supplemental Figure 1 in Sánchez-López et al., 2016b). In studies using this and other sealed test systems, plants co-cultured with phylogenetically distant microbial species exhibited very similar transcriptomic changes, suggesting that all of the microorganisms emit the same bioactive VC(s) (Sánchez-López et al., 2016b). It is thus possible that our observations were due at least in part to elevated CO_2 resulting from microbial respiration. Using the same "box-in-box" test system, here we have conducted new studies to address the question of whether airborne signals from different microorganisms can promote distinct responses in plants. In addition, we evaluated the contribution and mode of action of microbial VOCs and VICs (including respiratory CO_2) in these responses by performing comparative analyses of plants´ developmental, biochemical and molecular responses to (i) CO_2, (ii) complex mixtures of VICs and VOCs, and (iii) VOCs-depleted (VICs-containing) volatile emissions from the fungal phytopathogens *A. alternata* and *P. aurantiogriseum*. Our results show that, in the test system used in this work and our previous studies, respiratory CO_2 plays only a minor role in plant responses to microbial VCs. Moreover, we present evidence that mixtures of VICs from different microorganisms can promote growth and distinct developmental changes in Arabidopsis. We also provide evidence that (a) the highly conserved transcriptional changes occurring in plants exposed to microbial VCs are indirectly due to enhanced photosynthesis, and (b) some plant responses to fungal VOCs-depleted VC mixtures are primarily regulated at the post-transcriptional level.

2. MATERIALS AND METHODS

Plant and microbial cultures, growth conditions and sampling

The work was carried out using *Arabidopsis thaliana* L. (Heynh) ecotype Columbia

(Col-0) and the fungal species *A. alternata* (CECT 20192) and *P. aurantiogriseum* (CECT 20226). Plants were cultured in Petri dishes (92x16mm, Ref. 82.1472.001, Sarstedt) containing sucrose-free solid half strength Murashige and Skoog (MS) (Phytotechlab M519) medium. *A. alternata* and *P. aurantiagriseum* were cultured in Petri dishes (35x10mm, Ref. 82.1135.500, Sarstedt) containing solid MS medium supplemented with 90 mM sucrose. To investigate the plants´ responses to fungal VCs, microbial cultures without lids (with or without filter of charcoal, SIGMA 05105) and plant cultures without lids were placed in sterile boxes without physical contact, and sealed with a PVC film. As negative controls, plant cultures were placed in sealed boxes together with Petri dishes containing sterile MS medium. The sealed boxes containing plants and fungal cultures were placed in CO_2-controlled growth cabinets (Conviron®, Manitoba, Canada) with a 16 h light (90 µmol photons sec^{-1} m^{-2})/8 h dark photoperiod (22ºC during the light period and 18ºC during the dark period). The growth cabinets were modified including a Vaisala CARBOCAP, Carbon Dioxide Module GMM112 to allow the cabinets to reach 10000 ppm CO_2. Microbial VCs and CO_2 treatments started at the 14th day after sowing. Unless otherwise indicated plants were grown on horizontal plates.

Root morphological analysis

The numbers and lengths of the plants´ roots and root hairs in plants grown on vertical plates were measured using a stereomicroscope Olympus MVX10 (Japan). Microphotographs were captured with a DP72 video camera (Olympus, Japan) and the Cell D software (Olympus, Japan).

Analytical procedures

Fully expanded source leaves of plants cultured in the absence or presence of VCs or exogenously supplied CO_2 were harvested at the end of the light period, freeze-clamped, and ground to a fine powder in liquid nitrogen with a pestle and mortar. Starch was measured using an amyloglucosydase–based test kit (Boehringer Mannheim, Germany). For measurement of sucrose, glucose and fructose levels, a 0.1 g aliquot of the frozen powder was resuspended in 1 ml of 90% ethanol, left at 70 ºC for 90 min, and centrifuged at 13,000 x g for 10 min. Sugar contents from supernatants were then determined by HPLC with pulsed amperometric detection on a ICS-3000 Dionex system.

Gas exchange determinations

Fully expanded apical leaves were enclosed in a LI-COR 6400 gas exchange portable photosynthesis system (LI-COR, Lincoln, Nebraska, USA). The gas exchange determinations were conducted at 25 ºC with a photosynthetic photon flux density of 350 µmol m^{-2} s^{-1}. Net rates of CO_2 assimilation (*An*) were calculated using equations developed by von Caemmerer and Farquhar (1981).

Headspace analysis of microbial VCs

The system to analyse the microbial VCs in the headspace of growth chambers containing fungal cultures is illustrated in **Figure 1**. The solid-phase microextraction (SPME) technique was selected for gas chromatography-mass spectrometry (GC-MS) analyses of VOCs. The PVC wrap of the sealed growth boxes was carefully drilled with a Divinylbenzene/Carboxen/Polydimethylsiloxane (DVB/CAR/PDMS) coated fiber, and VOCs were adsorbed at 22 ºC for 30 min. The fiber was injected into an Agilent 7890A gas chromatograph containing a 30 m x 0,25 mm fused silica HP-5MS column. The chromatographic conditions used were: inlet 250 ºC; column 40 ºC for 2 min followed by ramping at 5 ºC/min to 250 ºC. Mass spectral analyses were carried out with an Agilent 5975C instrument. The scan mass range extended from m/z 20 to 400. Mass spectra of VCs were compared to those obtained from the NIST library and identifications were confirmed using commercially available standard compounds. High purity chemicals (generally with purities above 99%) were purchased from Sigma-Aldrich to identify some compounds released by the fungi. Kovats retention indices were calculated according to generally accepted standards (van Den Dool and Dec Kratz, 1963), based on the chromatographic retention times of a saturated alkane mixture (C7 - C30; Sigma-Aldrich) and other alkanes (< C7) occurring in the chromatogram background.

For online monitoring of the CO_2 contents in sealed growth boxes with or without fungal cultures, the sealed growth boxes were connected to a Vaisala CARBOCAP® Carbon Dioxide Probe GMP343 combined with a Vaisala Handheld Measurement Indicator MI70. For O_2 and CO contents analyses, sealed growth boxes were connected to a MX4 portable headspace analyser (Industrial Scientific Corporation, Pennsylvania, United States). For NO analyses, sealed growth boxes were connected to a Ecotech Serinus 40 Oxides Nitrogen Analyser (Ecotech Pty Ltd., Knoxfield, VIC, Australia).

936/21221977/A), which includes enabling Kalman filter in measuring settings.

a

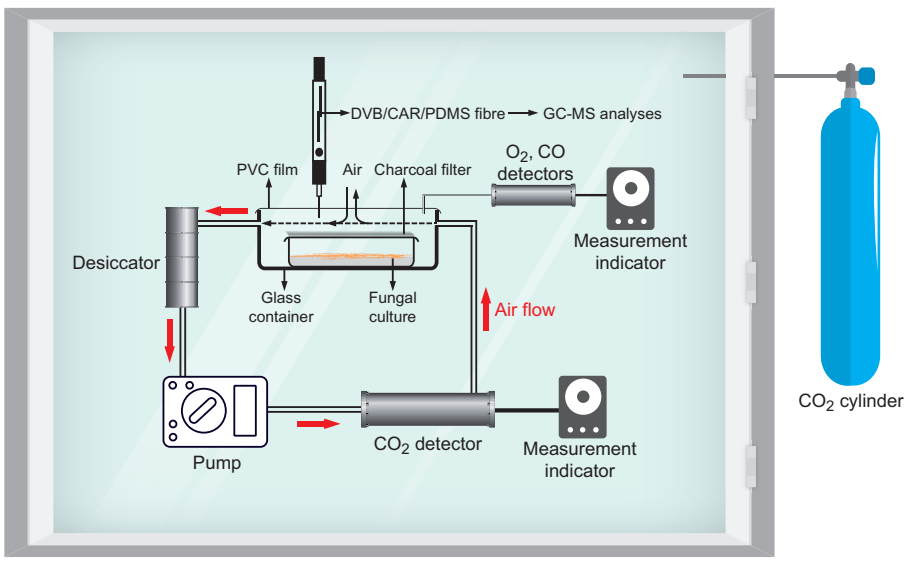

b

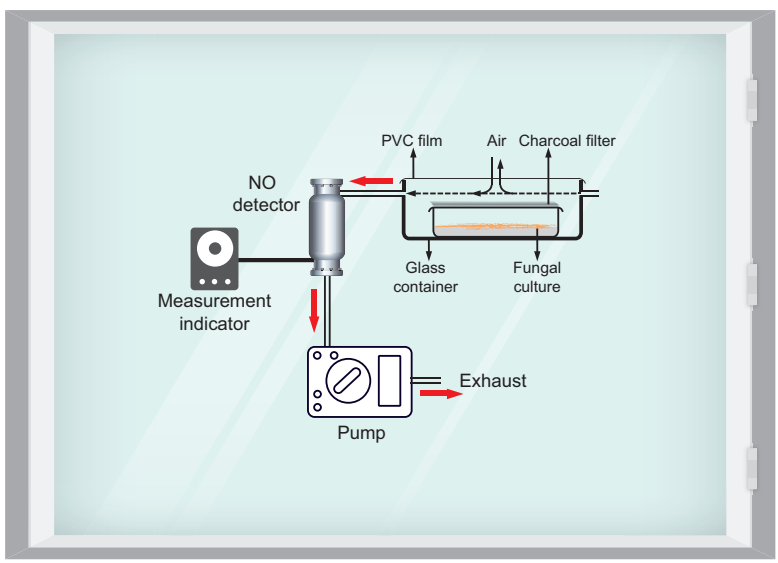

Figure 1: System to analyse (a) VOCs, CO_2, O_2 and CO; and (b) NO in the headspace of growth chambers containing fungal cultures.

The Analyser was used under the conditions needed to meet EN Type approval (TUV

Textural characterization of activated charcoal

Nitrogen adsorption at -196 ºC was measured using an ASAP 2020 volumetric adsorption analyser from Micromeritics (Norcross, Georgia, USA). Approximately 0.1532 g of sample was weighed in an elongated Pyrex glass tube. Before adsorption analysis, the sample was outgassed for at least 15 h at 573 K at the degassification port of the adsorption apparatus with a residual vacuum of 7 x 10^{-1} Pa. Specific surface areas were calculated from the N_2 adsorption data (molecular cross section 0.162 nm²) by the

$$\frac{1}{n^a(1-{}^{p}/_{p^0})} = \frac{1}{n^a_m} + \frac{1}{n^a_m C} \cdot \frac{1-{}^{p}/_{p^0}}{{}^{p}/_{p^0}}$$

Brunauer-Emmett-Teller method:

where n^a is the amount adsorbed, n^a_m is the monolayer capacity, p/p^o is the relative pressure, and C is a constant related to the heat of adsorption.

Micropore volume was estimated by applying the DR method to the N_2

$$\log V = logV^0 - Dlog^2 \frac{p^0}{p}$$

($V_{microDR}$) adsorption data:

where V is the volume adsorbed at a given relative pressure, V^o is the micropore volume and D is a constant characteristic of the adsorbent structure.

Mesopore volume (V_{meso}) values were obtained by subtracting the amount adsorbed at p/p^o 0.80 and 0.30. Macropore volume (V_{macro}) was obtained by difference between V_t and the amount adsorbed at p/p^o 0.80. Pore volumes were calculated using liquid-state density for adsorbate of N_2 at 0.808 g cms.1^{-3} (Garrido et al., 1987; Rodríguez-Reinoso et al., 1989).

Gene expression analyses

We proceeded essentially as described in Sánchez-López et al. (2016b). Briefly, total RNA was extracted from frozen Arabidopsis leaves of plants cultured in vitro using the Trizol method according to the manufacturer's procedure (Invitrogen), and then purified with the RNeasy kit (Qiagen). RNA amplification, labelling and statistical data analysis were performed basically as described by Adie et al. (2007). The Arabidopsis

Gene Expression Microarray 4 x 44K (G2519, Agilent Technologies) was used for hybridization. Three independent biological replicates were hybridized for leaves from microbe-treated plants and from controls. Images from Cy3 and Hyper5 channels were equilibrated to compensate for intensity differences and captured with a GenePix 4000B scanner (Axon). Spots were quantified using GenPix software (Axon) and normalized using the Lowess method. Means of the three replicates log-ratio intensities and their standard deviations were calculated, and the expression data were statistically analysed using the LIMMA package (Smyth and Speed, 2003). Functional characterization of the differentially expressed genes was done using the Mapman tool (http://gabi.rzpd.de/projects/MapMan/).

Non-reducing western blot analyses

Fifty mg of the homogenized frozen material (see above) was extracted in cold 16% (w/v) TCA in diethyl ether, mixed, and stored at –20 ºC for 2 h. The pellet was collected by centrifugation at 10,000 x g for 5 min at 4 ºC, washed 3 times with ice-cold acetone, dried briefly under vacuum, and resuspended in 1x Laemmli sample buffer containing no reductant. Proteins were separated on 10% SDS-PAGE under non-reducing conditions as described by Hendriks et al. (2003), transferred to nitrocellulose filters, and immunodecorated by using the antisera raised against the small subunit of maize AGP, and a goat anti-rabbit IgG alkaline phosphatase conjugate as the secondary antibody (Sigma).

Statistical analysis

The data presented are the means (± SE) from four independent experiments, with 3-5 biological replicates, each biological replicate being a pool of 12 plants. The significance of differences between control and treated was statistically evaluated by means of Student´s t-test using SPSS software. Differences were considered significant if $p<0.05$.

3. RESULTS

Volatile emissions of *A. alternata* and *P. aurantiogriseum* promote distinct developmental changes in Arabidopsis plants cultured in a "box-in-box" co-cultivation system

Volatiles emitted by *A. alternata* and *P. aurantiogriseum* cultures promoted rosette

growth and flowering in adjacent plants (**Figure 2**), in keeping with the results of Sánchez-López et al. (2016b). Furthermore, fungal VCs promoted root growth (**Figure 2**), root hair proliferation and elongation, and formation of first and second order lateral roots (LRs), thereby increasing the density of the root system (**Figure 3**).

Volatiles from both microorganisms promoted distinct developmental responses in vicinity plants. Leaves of plants exposed to VCs from *P. aurantiogriseum* were more wrinkled, thicker, and harder than those of plants exposed to VCs from *A. alternata* (**Figure 1a** and data not shown). Primary roots of plants exposed to *A. alternata* VCs were longer than those of control plants and *P. aurantiogriseum* VC-exposed plants (**Figure 3c**). Furthermore, whereas *A. alternata* VCs had no effect on the length of first order LRs, *P. aurantiogriseum* VCs inhibited the growth of this root type (**Figure 3c**). In addition, the root hairs of plants treated with *P. aurantiogriseum* VCs were substantially longer than those of plants treated with *A. alternata* VCs (**Figure 3b,c**). *P. aurantiogriseum* VCs also stimulated the formation of second-order LRs more strongly than *A. alternata* VCs (**Figure 3c**), leading to a higher density of second-order LRs in plants treated with *P. aurantiogriseum* compared to those treated with *A. alternata* VCs (**Figure 3a,c**). The strong proliferation and elongation of root hairs, combined with the shortening of the LRs induced by *P. aurantiogriseum* VCs led to the formation of peculiar brush-like structures that were not seen in roots of plants exposed to *A. alternata* VCs (**Figure 2, Figure 3a,b**).

Charcoal-filtered and non-filtered fungal volatile emissions promote similar responses in exposed plants

We next investigated the contribution of fungal VOCs and VICs in the plant responses in the "box-in-box" system used in this work and previous studies. So, we characterized Arabidopsis plants grown in the absence or presence for one week of adjacent *A. alternata* and *P. aurantiogriseum* cultures covered with a black, porous nylon mesh, with or without a top layer of VOC-adsorbing activated charcoal (**Figure 4**). According to the adsorption isotherm of N_2 at -196 ºC (**Supplemental Figure 1a**) and the porosity distribution (**Supplemental Figure 1b**), the type of charcoal used in this study was a micro-meso-porous carbon with specific surface area of 1109 m^2/g, micropores greater than 0.7 nm and mesoproses between 2 and 5 nm (**Supplemental Table 1**). Therefore, small molecules such as CO_2 (with a molecular cross section of 0.162 nm^2 and size of

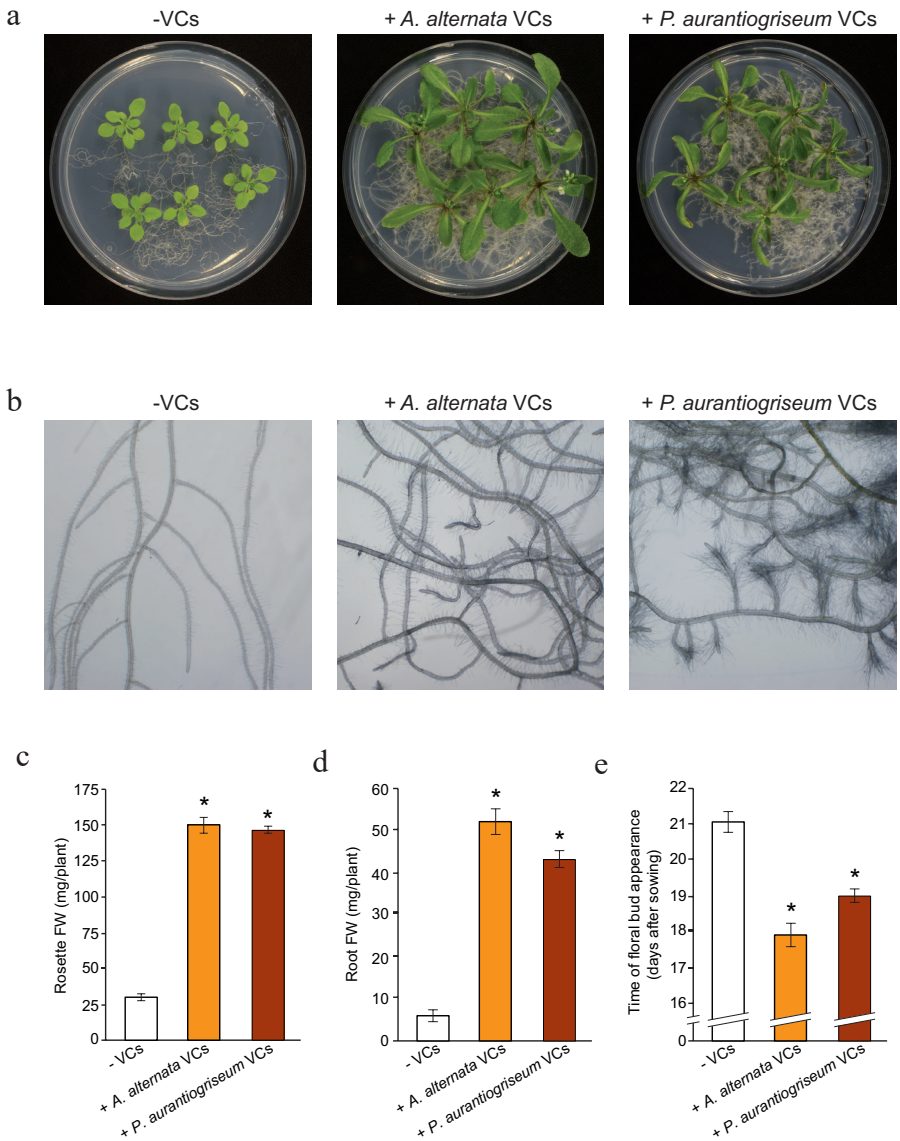

Figure 2: Volatile emissions of *A. alternata* and *P. aurantiogriseum* promote rosette and root growth and flowering in Arabidopsis plants cultured in a "box-in-box" co-cultivation system. (a) External phenotypes of plants and (b) roots, and (c) rosette FW, (d) root FW and (e) time of floral bud appearance of Arabidopsis plants grown in the absence or continuous presence for one week of adjacent cultures of *A. alternata* or *P. aurantiogriseum*. Values given in (c), (d) and (e) represent the means ± SE of 3 biological replicates obtained from 3 independent experiments, each biological replicate being a pool of 12 plants. Asterisks indicate significant differences relative to plants not cultured with adjacent fungal cultures based on Student´s t-test ($p<0.05$).

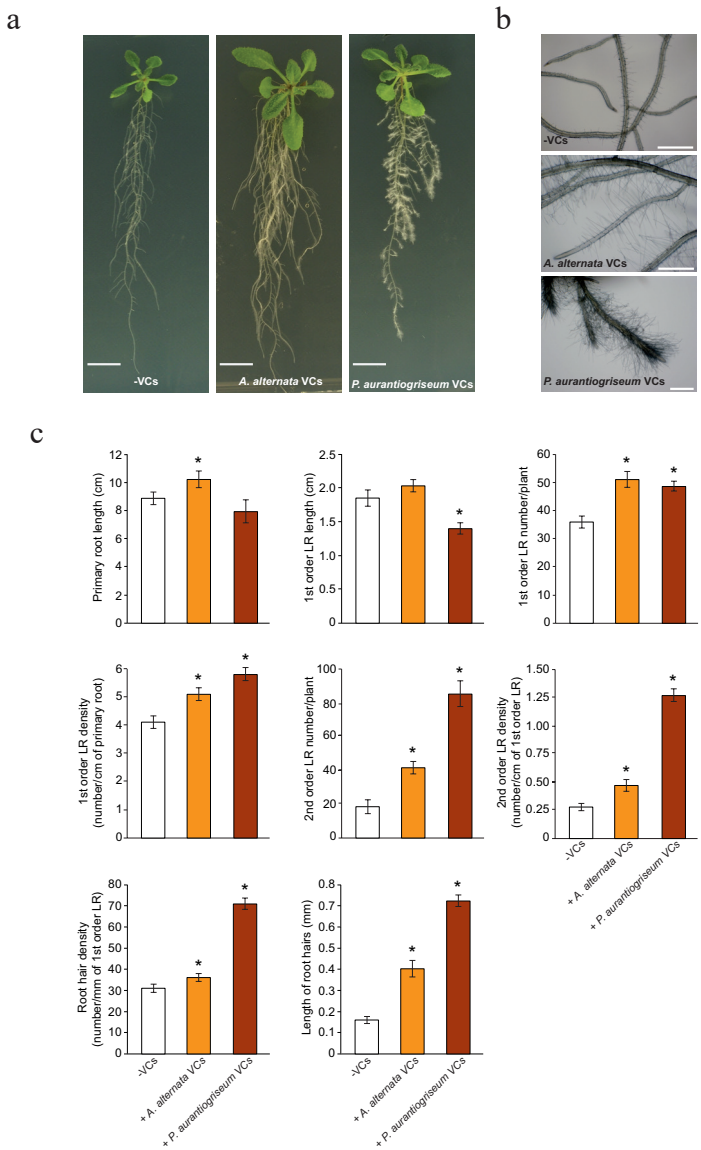

Figure 3: Volatile emissions of *A. alternata* and *P. aurantiogriseum* promote distinct responses in the root architecture of Arabidopsis plants cultured in a "box-in-box" co-cultivation system. (a) External phenotypes of plants and (b) roots, and (c) root architecture parameters of Arabidopsis plants grown on vertical plates in the absence or continuous presence for one week of adjacent cultures of *A. alternata* or *P. aurantiogriseum.* and b = 1 cm and 1 mm, respectively. Values given in (c) represent the means ± SE of three biological replicates obtained from three independent experiments, each biological replicate being a pool of 12 plants. Asterisks indicate significant differences relative to plants not cultured with adjacent fungal cultures based on Student´s t-test ($p<0.05$). Scale bars in a and b are 1 cm and 1 mm, respectively.

0.33x0.53x0.33 nm), CO, NO, O_2, etc. could cross the porosity of this carbon, especially in the presence of larger molecules that could cover the smallest microporosity. We reasoned that if the plant´s responses to microbial VCs were mainly due to VOCs, charcoal-filtered (VOCs-depleted, VICs-containing) fungal volatile emissions should trigger at most a weak response. Conversely, if the fungal cultures release VICs with high action potentials, charcoal-filtered microbial volatile emissions should still trigger

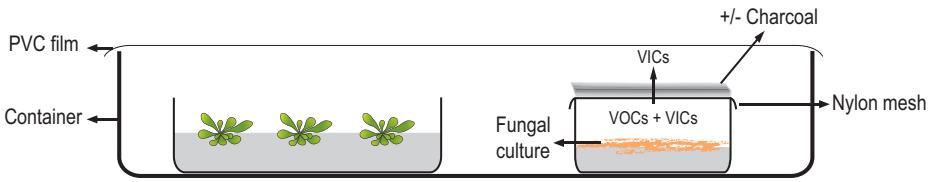

Figure 4: Schematic representation of the "box-in-box" co-cultivation system used in this work. Plant cultures were placed in boxes containing *A. alternata* or *P. aurantiogriseum* cultures covered with a porous nylon mesh with or without an upper charcoal filter.

strong responses in plants.

As a first step in these studies, we conducted compositional analyses of the VCs in the headspace of PVC film-sealed growth chambers containing *A. alternata* or *P. aurantiogriseum* cultures with and without charcoal filters. VOCs analyses were done using SPME coupled with GC-MS, a technology that has been widely used to analyse VOCs emitted by microorganisms and to elucidate their potential function in plant-microbe interactions (Zou et al., 2010; Velázquez-Becerra et al., 2011; Meldau et al., 2013; Naznin et al., 2013; Contreras-Cornejo et al., 2014; Garnica-Vergara et al., 2016; Farag et al., 2017; Nieto-Jacobo et al., 2017; Schenkel et al., 2018). VOCs extraction was performed using a DVB/CAR/PDMS coated fiber that can capture C3-C20 volatiles and semi-volatiles with molecular masses between 40 and 275 Da. A detailed description of the system used to perform these studies is presented in **Figure 1**. As shown in **Supplemental Table 2** and **Figure 5**, SPME GC-MS analyses of VOCs in the headspace of growth chambers containing *A. alternata* or *P. aurantiogriseum* cultures lacking charcoal filters revealed that these microorganisms have different organic volatilomes. Some of the VOCs released by the two fungal phytopathogens have previously been identified among the emissions of plant-growth promoting microorganisms (**Supplemental Table 2**). VIC analyses revealed substantially higher levels of CO and NO in the headspace of growth chambers containing the fungal

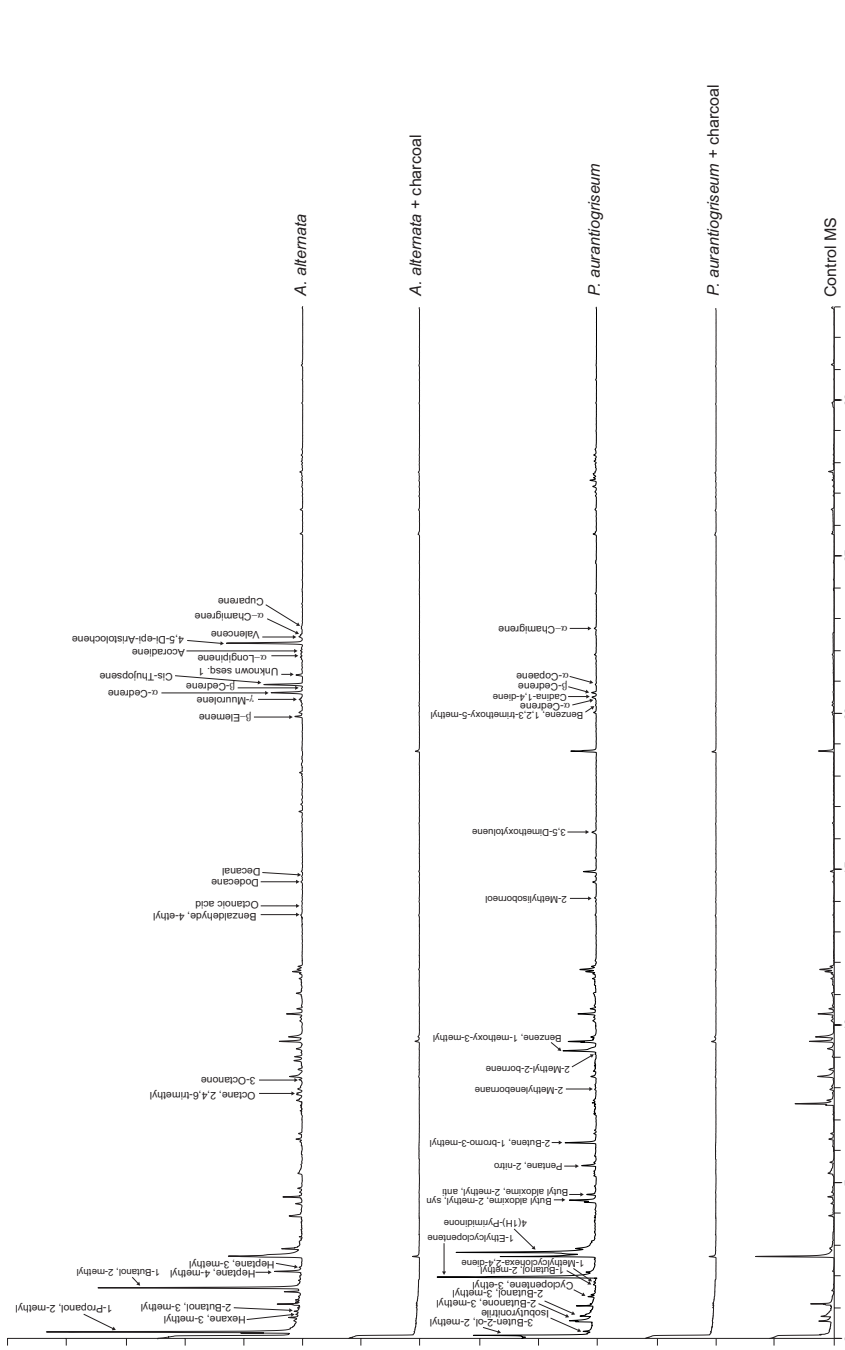

Figure 5: SPME GC-MS chromatograms of VOCs in the headspace of growth boxes containing cultures of *A. alternata* or *P. aurantiogriseum* with or without an upper activated charcoal filter.

cultures than in controls (**Figure 6**). No VOCs were detected in the headspace of growth chambers containing fungal cultures covered with charcoal filters (**Supplemental Table 2**, **Figure 5**), showing that this hydrocarbon material captures all VOCs emitted by *A. alternata* and *P. aurantiogriseum* that can be adsorbed by the DVB/CAR/PDMS coated fiber and detected by GC-MS under the conditions used in this study. In contrast, CO and NO levels in the headspace of growth chambers containing fungal cultures covered with charcoal filters were higher than in controls (**Figure 6**). This shows that the two fungal species emit CO and NO and confirms that the charcoal filter used in this study

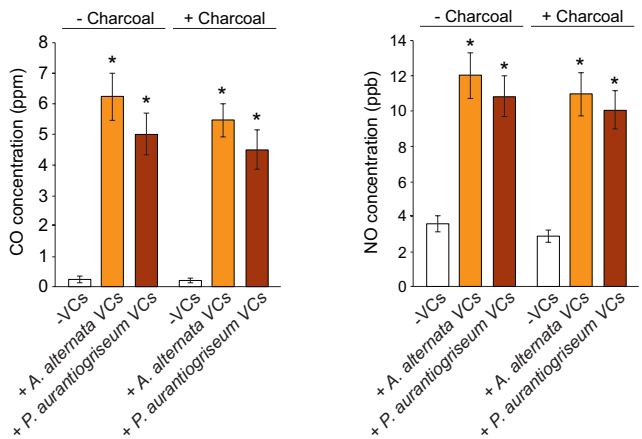

Figure 6: CO and NO contents in the headspace of PVC-sealed growth boxes containing *A. alternata* or *P. aurantiogriseum* cultures with or without charcoal filters. Values represent the means ±SE of four biological replicates obtained from four independent experiments, each biological replicate being four growth boxes. Asterisks indicate significant differences relative to controls (fungal cultures lacking growth boxes) based on Student´s t-test ($p<0.05$).

poorly retains these small VICs.

As expected, plants grown beside fungal cultures not covered with a charcoal filter produced larger rosettes and roots, flowered earlier and developed denser root systems with longer root hairs than control plants **(Figure 7a,b**). Fungal VCs without charcoal filtration also increased photosynthetic activity in the exposed plants (**Figure 8a**) and promoted the accumulation of photosynthetic pigments (**Figure 8a**) and primary photosynthates (i.e. sucrose, glucose, fructose and starch) (**Figure 8b**). Notably, these responses were identical to those of plants grown in the vicinity of fungal cultures covered with a charcoal filter (**Figures 7** and **8**).

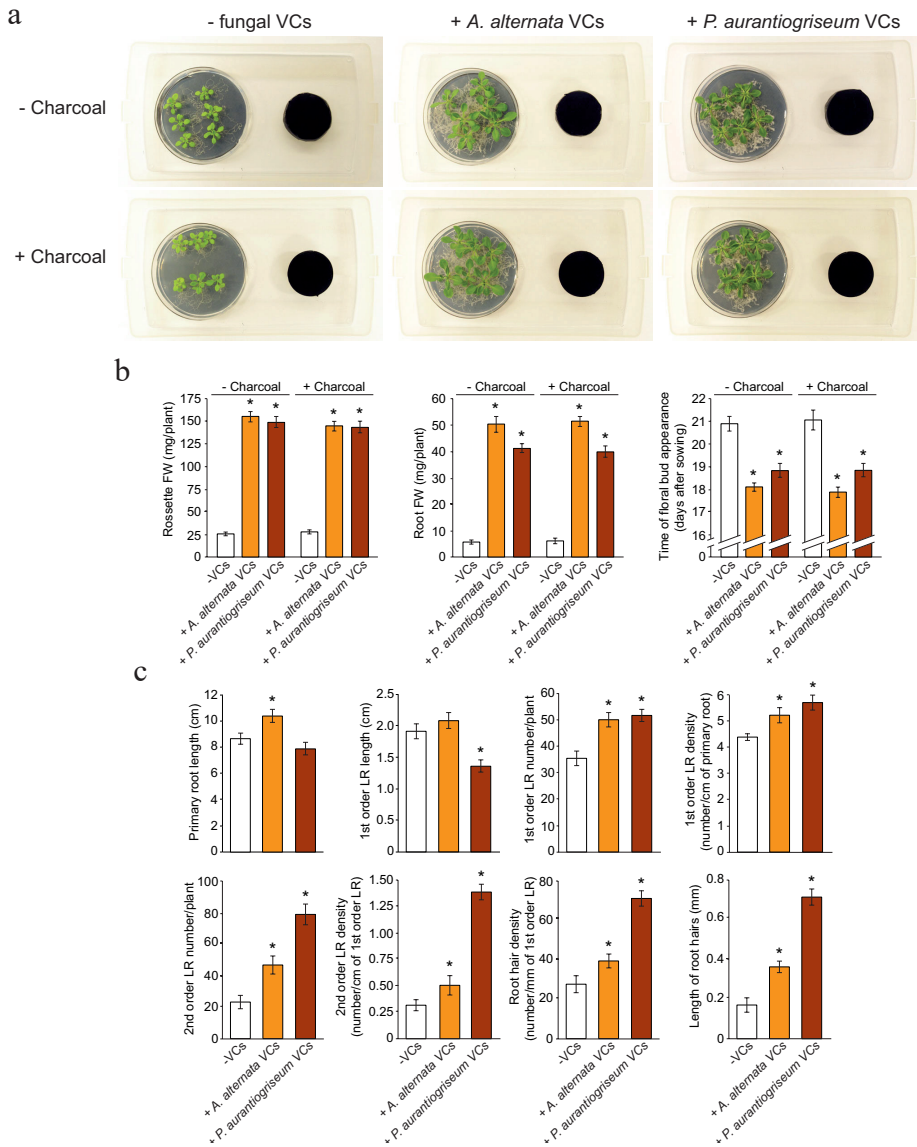

Figure 7: Charcoal-filtered (VOCs-depleted) and non-filtered fungal volatile emissions promote similar growth and root developmental responses in exposed plants. (a) External phenotypes and (b) rosette and root FW and time of floral bud appearance of plants grown with adjacent *A. alternata* or *P. aurantiogriseum* cultures with or without charcoal filter. (c) Root architecture parameters of plants grown with adjacent fungal cultures with charcoal filter. In (a) and (b) plants were grown on horizontal plates, whereas in (c) plants were grown on vertical plates. Values given in (b) and (c) represent the means ± SE of three biological replicates obtained from three independent experiments, each biological replicate being a pool of 12 plants. Asterisks indicate significant differences relative to plants not cultured with adjacent fungal cultures according to Student´s t-test ($p<0.05$).

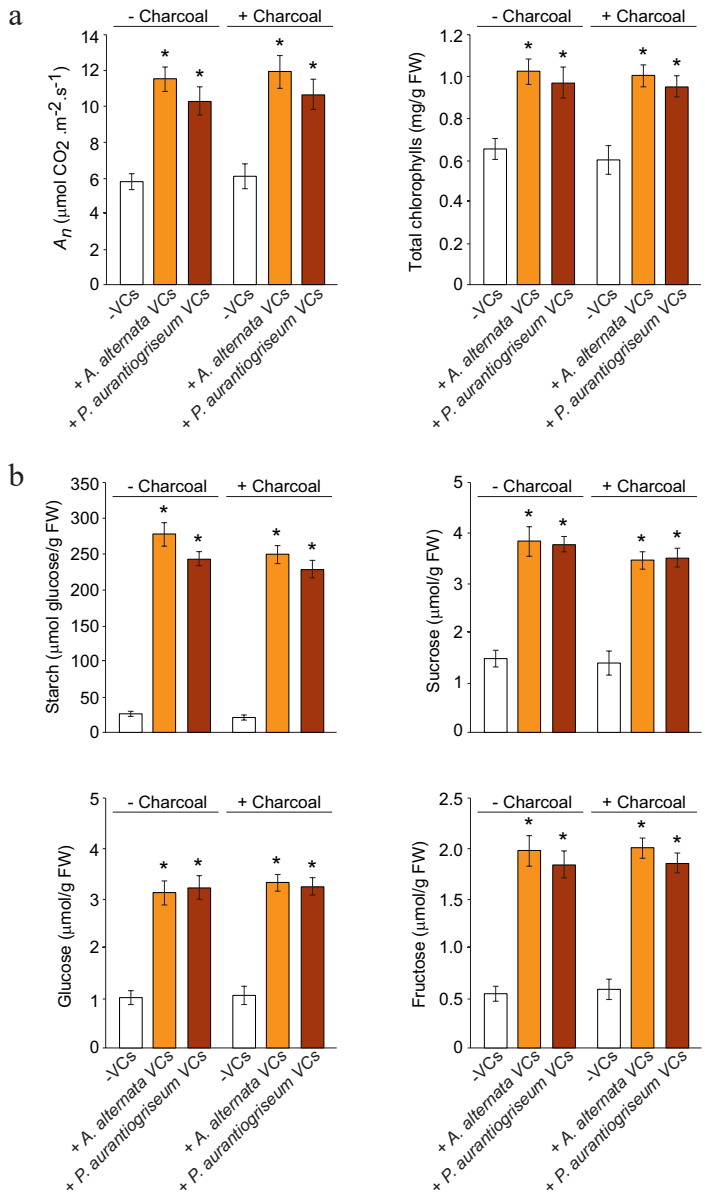

Figure 8: Charcoal-filtered (VOCs-depleted) fungal volatile emissions promote photosynthesis in leaves. (a) Net rates of CO_2 assimilation (*An*) and total chlorophyll content, and (b) photosynthate (starch, sucrose, glucose and fructose) levels in leaves of plants cultured with adjacent *A. alternata* or *P. aurantiogriseum* cultures with or without charcoal filter. Values represent means ± SE of three biological replicates obtained from three independent experiments, each biological replicate being a pool of 12 plants. Asterisks indicate significant differences relative to plants not grown with adjacent fungal cultures according to Student´s t-test ($p<0.05$).

Respiratory CO_2 makes only a minor contribution to the growth and root architecture changes induced by charcoal-filtered fungal VCs

The results presented above would indicate that, in the box-in-box test system used in this study, VICs could play an important role on plant responses to volatiles emitted by *A. alternata* and *P. aurantiogriseum*. We next investigated the contribution of respiratory CO_2 to the changes in plant growth and root development induced by charcoal-filtered fungal VCs. We also investigated whether strong reduction in the O_2 concentration in the headspace of the co-cultivation system could occur that would account for the observed plant´s responses to the presence of adjacent microbial cultures. To this end, we first measured the CO_2 and O_2 concentrations in the headspace of PVC film-sealed boxes containing fungal cultures covered with charcoal filters using the system illustrated in **Figure 1**. To test the CO_2-permeability of the PVC film sealant, sealed boxes with or without fungal cultures were placed in a CO_2-controlled growth cabinet, and the CO_2 levels inside the boxes were monitored while manipulating the CO_2 levels in the cabinet.

As shown in **Figure 9** the CO_2 and O_2 concentrations in the headspace of the sealed boxes before the addition of the *A. alternata* and *P. aurantiogriseum* cultures were ca. 420 ppm and 21 kPa, respectively. The O_2 concentration in the headspace of the sealed boxes did not change significantly upon addition of the fungal cultures (**Figure 9**), but the headspace CO_2 concentration oscillated between ca. 550 ppm and 500 ppm during the day and night periods, respectively (**Figure 9**). This oscillation in the headspace CO_2 concentration can be attributed to the regulation of fungal metabolism by light (Farkas et al., 1990; Tisch and Schmoll, 2010). The CO_2 concentrations inside the sealed boxes rapidly changed to match those inside the growth cabinet when the CO_2 level in the cabinet was increased **(Figure 9** and **Supplemental Figure 2**), showing that the PVC film sealant around the box is highly permeable to CO_2.

We next characterized Arabidopsis plants cultured for one week under 16 h light, 550 ppm CO_2/8 h dark, 500 ppm CO_2 conditions and compared them with plants cultured under the same light/dark cycle with ambient CO_2 levels. As a positive control, we also characterized plants cultured with sustained super-elevated (2000 ppm) CO_2 levels. No differences in shoot fresh weight (FW), root architecture or time of floral bud appearance were detected between plants cultured under ambient CO_2 conditions and plants cultured under 16 h light, 550 ppm CO_2/8 h dark, 500 ppm CO_2 conditions

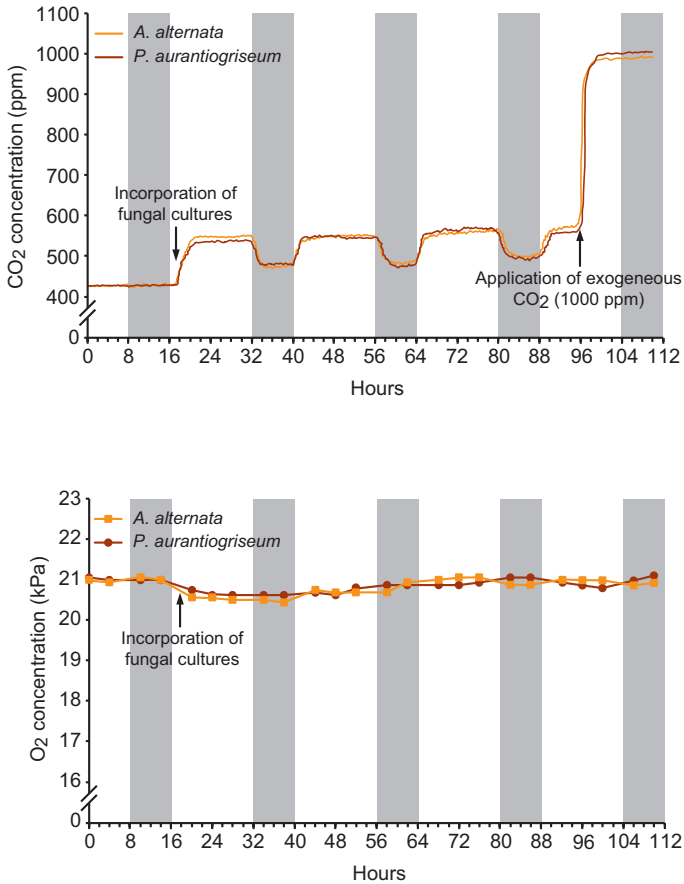

Figure 9: Time-course of CO_2 and O_2 levels in the headspace of PVC-sealed growth boxes containing *A. alternata* or *P. aurantiogriseum* cultures covered with charcoal filters. The sealed boxes were connected to CO_2 and O_2 analysers, and placed in CO_2-controlled growth cabinets with a 16 h light/8 h dark photoperiod (cf. **Figure 1**). At the indicated time the CO_2 concentration in the cabinet was increased to 1000 ppm.

(**Figure 10**). The 2000 ppm CO_2 treatment caused the FW of the plant´s rosettes to increase approximately two-fold (**Figure 10a**), which was substantially lower than the 5-fold increase of FW exhibited by plants cultured with adjacent fungal cultures (cf. **Figure 7b**). The super-elevated CO_2 treatment also promoted early flowering (**Figure 10a**) and the formation of second order LRs and elongation of root hairs (**Figure 10b**). However, unlike treatment with fungal volatiles, the super-elevated CO_2 treatment did not promote the formation of first-order LRs, root hair proliferation, or the formation of brush-like root structures (**Figure 10b**).

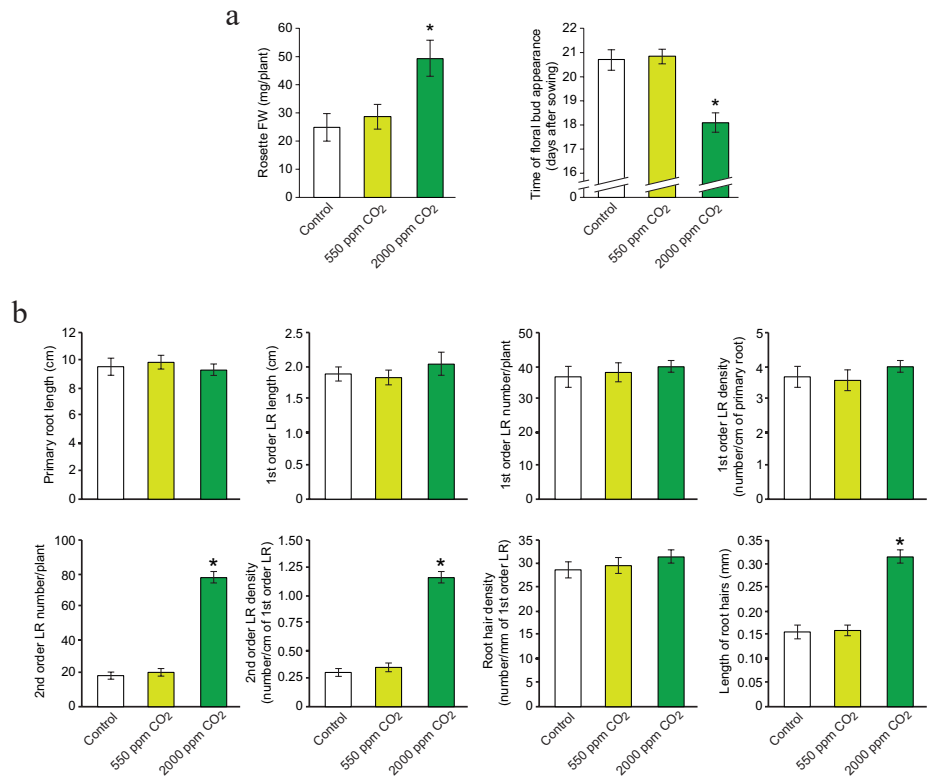

Figure 10: Respiratory CO_2 plays a minor role in growth and root architecture changes induced by charcoal-filtered fungal VCs in Arabidopsis plants grown in a "box-in-box" co-cultivation system. (a) Rosette FW and time of floral bud appearance and (b) root architecture parameters of plants grown under 550 or 2000 ppm CO_2 conditions. In (a) plants were grown on horizontal plates, whereas in (b) plants were grown on vertical plates. Values are means ± SE of three biological replicates obtained from three independent experiments, each biological replicate being a pool of 12 plants. Asterisks indicate significant differences from plants cultured under atmospheric CO_2 conditions according to Student´s t-test ($p<0.05$).

Respiratory CO_2 plays a minor role in the accumulation of exceptionally high starch levels in leaves induced by charcoal-filtered fungal VCs

Short-term exposure to microbial VCs promotes the accumulation of exceptionally high levels of starch in leaves (Ezquer et al., 2010; Li et al., 2011; Sánchez-López et al., 2016b). The contribution of fungal respiratory CO_2 emissions to this phenomenon was investigated by comparing the starch contents in leaves of Arabidopsis plants grown for 16 h under 550 ppm CO_2 conditions to those of plants cultured for 16 h with adjacent

A. alternata cultures covered with a layer of activated charcoal. As positive control, we also characterized plants cultured for 16 h under 2000 ppm CO_2. As shown in **Figure 11,** treatment with 550 ppm and 2000 ppm CO_2 caused a ca. 1.3-fold and 2-fold increases in the leaf starch content, respectively, both of which are much smaller than the ca. 15-fold

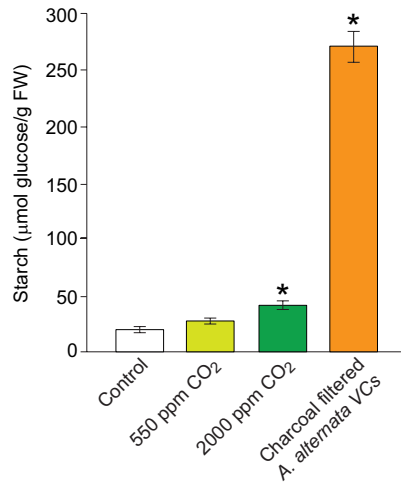

Figure 11: Leaf starch levels in Arabidopsis plants cultured in the absence or presence for 16 h of 550 ppm CO_2, 2000 ppm CO_2 or adjacent *A. alternata* cultures covered with charcoal filters. Values represent means ± SE of three biological replicates obtained from three independent experiments, each biological replicate being a pool of 12 plants. Asterisks indicate significant differences from plants not cultured with exogenously supplied CO_2 or adjacent fungal cultures according to Student´s t-test ($p<0.05$).

increase observed in plants cultured with adjacent fungal cultures (cf. **Figure 8**).

Starch accumulation induced by charcoal-filtered fungal VCs is associated with reductive activation of ADP-glucose pyrophosphorylase, but that induced by super-elevated CO_2 is not

We have shown that short-term exposure to complex mixtures of VICs and VOCs released by *A. alternata* promotes reductive monomerization (activation) of APS1 in leaves (Li et al., 2011). APS1 is the regulatory subunit of ADP-glucose pyrophosphorylase (AGP), which catalyses the first committed step of starch biosynthesis. We therefore proposed that fungal VC-mediated reductive activation of APS1 could at least partly explain the accumulation of high levels of starch in leaves of VCs-exposed plants (Li et al., 2011).

In leaves, APS1 is present as a mixture of 50 kDa active (reduced) monomers

and 100 kDa inactive (oxidized) dimers. To determine whether CO_2- and charcoal-filtered fungal VC-promoted starch accumulation involves APS1 reductive monomerization, we conducted non-reducing APS1 immunoblot analyses of proteins extracted from leaves of plants exposed for one day to 2000 ppm CO_2 or charcoal-filtered VCs emitted by *A. alternata* cultures. As shown in **Figure 12**, exposure of plants to charcoal-filtered fungal

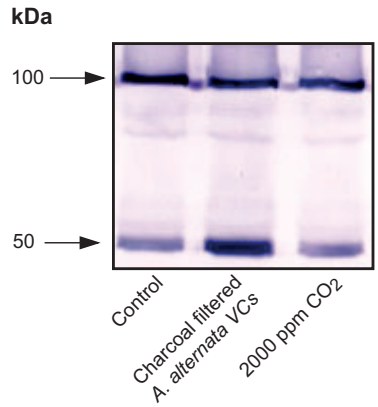

Figure 12: Non-reducing western blot analysis of APS1 in leaves of Arabidopsis plants cultured in the absence or presence for 12 h of charcoal-filtered VCs emitted by adjacent *A. alternata* cultures or 2000 ppm CO_2.

VCs promoted reductive APS1 monomerization. Conversely, exposure of plants to 2000 ppm CO_2 did not alter the redox status of APS1 (**Figure 12**).

Complex mixtures of fungal VCs, charcoal-filtered VCs, super-elevated CO_2 and increased irradiance all induce similar transcriptomic changes in leaves

We finally performed high-throughput transcriptomic analyses of leaves from Arabidopsis plants exposed for 16 h to charcoal-filtered VCs emitted by nearby *A. alternata* cultures, or super-elevated CO_2 levels (2000 ppm CO_2). The sets of genes exhibiting differential expression patterns under these treatments were compared to those previously reported for plants cultured in the absence or in the presence of adjacent *A. alternata* cultures without a covering charcoal filter (cf. Supplemental Table 3 in Sánchez-López et al., 2016b).

As shown in **Supplemental Table 3**, 258 genes were up-regulated and 399 genes were down-regulated when plants were exposed to charcoal-filtered fungal VCs (with a > 3.0-fold difference relative to control; $p < 0.05$). Nearly 50% of the genes that were down-regulated in leaves of plants exposed to charcoal-filtered fungal VCs were

also down-regulated in leaves of plants exposed to fungal VCs without charcoal filtration (**Supplemental Table 3**). Furthermore, 53% of the genes that were up-regulated in leaves of plants exposed to charcoal-filtered fungal VCs were also up-regulated in leaves of plants exposed to fungal VCs not filtered by charcoal (**Supplemental Table 3**). Super-elevated CO_2 treatment induced the up-regulation of 217 genes and down-regulation of 401 genes (with a > 3.0-fold difference relative to control; $p < 0.05$) (**Supplemental Table 4**). Sixty percent of the genes that were down-regulated in leaves of plants treated with 2000 ppm CO_2 were also down-regulated in leaves of plants exposed to fungal VCs without charcoal filtration (**Supplemental Table 4**). Furthermore, 52% of the genes that were up-regulated in leaves of plants exposed to 2000 ppm CO_2 were also up-regulated in leaves of plants exposed to VCs without charcoal filtration (**Supplemental Table 4**).

The most strongly up-regulated gene in leaves of plants exposed to fungal volatiles without charcoal filtration was At1g61800 (Sánchez-López et al., 2016b), which encodes the GPT2 glucose-6-phosphate (G6P)/phosphate translocator that is necessary for dynamic photosynthetic and metabolic acclimation to increased irradiance (Athanasiou et al., 2010; Dyson et al., 2015). Notably, 55% of the genes that were down-regulated in plants exposed to increased irradiance (cf. Supplemental Table 1 in Athanasiou et al., 2010) were also down-regulated in leaves of plants exposed to fungal VCs (**Supplemental Table 5**): 80% of the 20 genes exhibiting the strongest down-regulation in plants exposed to increased irradiance were also down-regulated in leaves exposed to fungal VCs (**Table 1**). Moreover, 25% of the genes that were up-regulated in plants exposed to increased irradiance (cf. Supplemental Table 1 in Athanasiou et al., 2010) were also up-regulated in leaves of plants treated with fungal VCs (**Supplemental Table 5**), 50% of the 20 genes most strongly up-regulated genes in plants exposed to increased irradiance being also up-regulated in leaves exposed to fungal VCs (**Table 1**).

4. DISCUSSION

Features and benefits of the "box-in-box" dual co-cultivation system for studying plant responses to microbial volatile emissions

The sealed split Petri dish-based passive diffusion co-cultivation system has frequently been used to investigate the plant´s response to microbial emissions of volatile compounds. Using tri-partite Petri dishes, Casarrubia et al. (2016) analysed the effect of activated charcoal on growth of Arabidopsis plants cultured in the absence or presence

Table 1: Sets of the 20 most strongly up-regulated and 20 most strongly down-regulated genes in plants exposed to high irradiance (Athanasiou et al., 2010) that are also up- and down-regulated by VICs emitted by *A. alternata***.**

Up-regulated genes	
ID	**Description**
At1g61800	glucose-6-phosphate/phosphate translocator 2, putative mRNA, complete cds
At4g15210	beta-amylase (BMY1) / 1,4-alpha-D-glucan maltohydrolase mRNA, complete cds
At4g25630	fibrillarin 2 (FIB2) mRNA, complete cds
At1g32900	starch synthase, putative mRNA, complete cds
At4g16590	glucosyltransferase-related protein mRNA, complete cds
At2g27840	histone deacetylase-related / HD-related protein mRNA, complete cds
At3g18600	DEAD/DEAH box helicase, putative mRNA, complete cds
At1g06000	UDP-glucoronosyl/UDP-glucosyl transferase family protein mRNA, complete cds
At1g56650	myb family transcription factor (MYB75) mRNA, complete cds
At3g44750	histone deacetylase, putative (HD2A) mRNA, complete cds
Down-regulated genes	
ID	**Description**
At1g74670	gibberellin-responsive protein, putative, complete cds
At2g40610	expansin, putative (EXP8), complete cds
At5g48490	protease inhibitor/seed storage/lipid transfer protein (LTP) family protein, complete cds
At3g15450	expressed protein, complete cds
At1g70290	trehalose-6-phosphate synthase, putative, complete cds
At1g23390	kelch repeat-containing F-box family protein, complete cds
At2g22980	serine carboxypeptidase S10 family protein, complete cds
At2g18700	glycosyl transferase family 20 protein / trehalose-phosphatase family protein, complete cds
At2g33830	dormancy/auxin associated family protein, complete cds
At5g61590	AP2 domain-containing transcription factor family protein mRNA, complete cds
At2g15890	expressed protein mRNA, complete cds
At1g80920	DNAJ heat shock N-terminal domain-containing protein mRNA, complete cds
At5g40890	chloride channel protein (CLC-a) mRNA, complete cds
At1g72150	SEC14 cytosolic factor family protein / phosphoglyceride transfer family protein mRNA, complete cds
At5g24490	30S ribosomal protein, putative mRNA, complete cds
At5g22920	zinc finger (C3HC4-type RING finger) family protein mRNA, complete cds

of adjacent cultures of the endomycorrhizal fungus *Oidiodendron maius.* Irrespective of the inclusion of activated charcoal in one of the three compartments, fungal cultures promoted plant growth of nearby plants. Because CO_2 levels in the headspace of sealed Petri dishes containing microbial cultures can become extremely high as a result of microbial respiration (Kai and Piechulla, 2009) the authors concluded that the observed growth promotion was mainly due to fungal respiratory CO_2 rather than specific fungal

VOC signals (Casarrubia et al., 2016). However, neither the absence of microbial VOCs nor the accumulation of high levels of CO_2 concentrations in the headspace of charcoal-containing Petri dishes was confirmed.

The "box-in-box" system used in this work and our previous studies has a number of advantages over the sealed split Petri dish system when studying plants´ responses to microbial volatile emissions. First, the air diffusion surface of this system is exceedingly larger than that of the sealed Petri dish system (in which air can only diffuse via a slit between the plate and the lid). Second, the sealing wrap used in this experimental setup is highly CO_2- and O_2- permeable PVC, which impedes strong increases in the CO_2/O_2 balance in the headspace of the growth chamber due to respiratory metabolism that would otherwise interfere with the effects of microbial VCs. Third, the system permits easy online monitoring of volatiles in the growth container´s headspace (**Figures 1** and **9**). Fourth, the setup enables the filtration of all VOCs emitted by the microbial cultures, facilitating studies on plant responses to microbial VICs emissions.

Different microbes can release VCs other than CO_2 that promote distinct responses in nearby plants

Results presented here show that diverse microorganisms can release VCs that promote distinct responses in plants. The contribution of VOCs and VICs to plants´ responses to VCs emitted by *A. alternata* and *P. aurantiogriseum* was investigated using a type of charcoal (cf. **Supplemental Figure 1**) that captured all VOCs emitted by these fungal species that can be detected by our SPME GC-MS system (**Supplemental Table 2**). However, the charcoal did not capture small VICs such as CO, NO and CO_2 (**Figures 6** and **9**). Therefore, plants grown in the presence of both fungal cultures with charcoal filters were exposed to VOCs-depleted volatile emissions. The responses of plants to charcoal-filtered VCs emitted by nearby fungal cultures were identical to those of plants exposed to fungal VCs without charcoal filtration (**Figures 7** and **8**). Thus, in our experimental system, microbes can release bioactive VICs and/or VOCs that are either poorly captured by the type of micro-meso-porous charcoal used in this study (**Supplemental Figure 1b**) or not detected by our SPME GC-MS system. Moreover, these VICs and/or uncaptured VOCs appear to be stronger determinants of the plants´ responses to VCs than the fungal VOCs that are detected by our SPME GC-MS system. Some potentially relevant bioactive VICs are CO and NO, whose concentrations in the

headspace of the growth boxes increased in the presence of fungal cultures with charcoal filters (**Figure 6**). The fact that charcoal-filtered *A. alternata* and *P. aurantiogriseum* VCs promoted distinct changes in the leaves and root architecture of exposed plants (**Figure 7**) strongly indicates that the charcoal-filtered volatilomes of the two microorganisms have different action potentials. It is evident that further efforts will be necessary to identify all the bioactive VCs of different microorganisms and characterize their action potentials.

We must emphasize that the data obtained in this study do not imply that microbial VOCs lack bioactivity. In fact, some *A. alternata* and *P. aurantiogriseum* VOCs detected by our SPME GC-MS system (i.e. 2-butanol,3-methyl, 1-butanol,2-methyl, tridecane, 3-octanone, β-elemene, γ-muurolene, cis-thujopsene, acoradiene, valencene, α-chamigrene and α-copaene, cf. **Supplemental Table 2**) are emitted by plant-growth promoting microorganisms. Moreover, some of these compounds are known to be bioactive when exogenously supplied to plants. For example, discrete application of cis-thujopsene massively stimulated LR formation in Arabidopsis (Ditengou et al., 2015), while 2-butanol,3-methyl promoted plant growth and salinity tolerance (Ledger et al., 2016).

Several factors indicate that plant´s responses to charcoal-filtered microbial VCs were not due to enhanced CO_2/O_2 ratio caused by fungal respiration. First, if the enhanced CO_2/O_2 balance were a major determinant of the plant´s response to nearby microbial cultures, one would expect all microbial cultures to induce similar responses in plants. However, charcoal-filtered VCs from *P. aurantiogriseum* and *A. alternata* induced distinct changes in the leaf morphology and root architecture of Arabidopsis plants (**Figures 2** and **7**). Second, plants grown under CO_2 levels equal to those measured in the headspace of sealed chambers containing fungal cultures (ca. 550 ppm) did not promote growth or changes in the root architecture of the plant or accumulation of starch in leaves (**Figures 10** and **11**). Third, super-elevated (2000 ppm) CO_2 caused a 2-fold increase in both leaf starch content and FW of exposed plants, which was substantially lower than the 15-fold increase in leaf starch content and 5-fold increase in FW induced by charcoal-filtered microbial VCs (cf. **Figures 7b, 10a** and **11**). Furthermore, unlike treatment with charcoal-filtered fungal VCs, the super-elevated CO_2 treatment did not promote the formation of first-order LRs, root hair proliferation, or the formation of brush-like root structures (**Figure 10b**). Fourth, charcoal-filtered

microbial VCs promoted reductive activation of the starch biosynthetic AGP enzyme, but super-elevated CO_2 conditions did not (**Figure 12**).

The presence of fungal cultures in the sealed growth chambers increased the headspace CO and NO concentrations (**Figure 6**), which is consistent with the capacity of fungi to emit these VICs (Wharton and Weintraub, 1980; Siegel and Siegel, 1987; Conrath et al., 2004; Schreiber et al., 2012). Exogenous application of CO promotes growth, chlorophyll accumulation, LR formation and root hair elongation (Guo et al., 2008; Xuan et al., 2008; Guo et al., 2009; Kong et al., 2010; Han et al., 2012; Yang et al., 2016). Furthermore, exposure to parts per billion levels of NO promotes growth and chlorophyll accumulation (He et al., 2004). Moreover, NO enhances expression of non-symbiotic hemoglobins (nsHB) (Kuruthukulangarakoola et al., 2017), which is known to promote growth (Hunt et al. 2002; Hebelstrup and Jensen 2008). We observed similar responses in plants exposed to charcoal-filtered fungal VCs **(Figures 7** and **8**, **Supplemental Table 3**) (Sánchez-López et al., 2016a; Sánchez-López et al., 2016b). This suggests that enhancement of growth and photosynthesis and promotion of early flowering and changes in the root architecture of plants exposed to charcoal-filtered fungal VCs could be at least partly due to fungal CO and NO emissions.

Many transcriptional changes occurring in leaves after brief exposure to VCs are probably due to enhanced photosynthetic CO_2 fixation signalling

The transcriptomic changes in leaves of Arabidopsis plants shortly exposed to super-elevated CO_2 and VCs emitted by diverse microorganisms, with and without charcoal filtering, are strikingly similar (**Supplemental Table 3**, **Supplemental Table 4**) (Sánchez-López et al., 2016b). These transcriptomic changes are also very similar to those seen in plants shortly exposed to increased irradiance (**Table 1**, **Supplemental Table 5**). All of these treatments promote photosynthetic CO_2 fixation (**Figure 8a**) (Makino and Mae, 1999; Ainsworth and Rogers, 2007; Athanasiou et al., 2010). We thus propose that many transcriptomic changes in the leaves of plants exposed to super-elevated CO_2, increased irradiance, or microbial VCs indirectly result from signalling of enhanced photosynthetic CO_2 fixation by means of Calvin-Benson cycle (CBC) intermediate(s) or their derivatives. In this respect it should be noted that the production of the CBC intermediate glyceraldehyde 3-phosphate (GAP) is the first point of regulation in the synthesis of isoprenoid compounds derived from the plastidial

methylerythritol 4-phosphate (MEP) pathway, including hormones (Pulido et al., 2012; Pokhilko et al., 2015). Fungal VCs promote the accumulation of high levels of MEP pathway-derived carotenoids and chlorophylls (**Figure 8a**) (Sánchez-López et al., 2016a), which, in turn, further promote photosynthesis. Moreover, fungal VCs promote the accumulation of MEP pathway-derived CKs and the resulting changes in the expression of a significant number of CK-regulated genes (Sánchez-López et al., 2016a; Sánchez-López et al., 2016b). Therefore, as shown schematically in **Figure 13**, we propose that many transcriptional changes occurring in leaves of plants shortly exposed

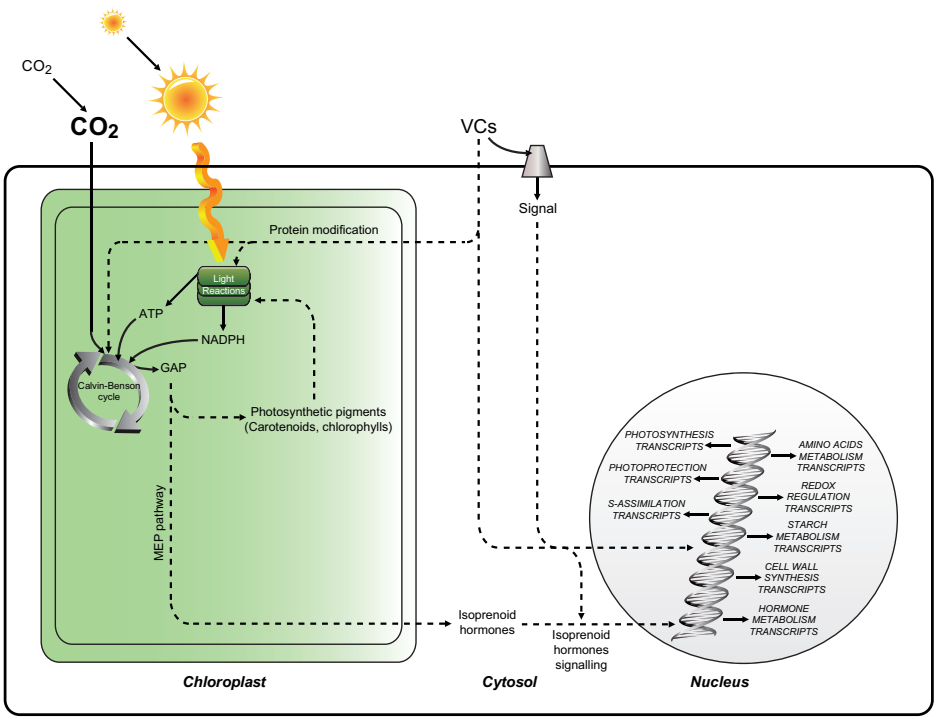

Figure 13: Suggested model for the plant´s transcriptional response to short exposure to fungal VCs, super-elevated CO_2 and increased irradiance. According to this model VCs interact with as yet unidentified plasma membrane receptors to produce signals that rapidly promote changes in gene expression. Alternatively and/or additionally, some VCs (especially small and highly reactive VICs) penetrate the cell and modify photosynthesis- and metabolism-related proteins. Increased irradiance and treatment with super-elevated CO_2 promote photosynthesis. Augmentation of the photosynthetic activity induced by these treatments results in enhanced GAP, which enters the MEP pathway to fuel the production of isoprenoid hormones that initiate a cascade of reactions resulting in highly conserved changes in the expression of genes involved in many different processes.

to microbial VCs, super-elevated CO_2 and increased irradiance are due to signalling involving photosynthetic GAP-derived isoprenoid hormones.

Regulation of some plant responses to fungal VCs is primarily post-transcriptional

The observation of similar transcriptional changes, but distinct developmental and metabolic responses in plants exposed to super-elevated CO_2 levels and VCs emitted by different microorganisms (**Figures 7, 8, 11** and **12, Supplemental Tables 3** and **4**, cf. Supplemental Table 3 in Sánchez-López et al., 2016b) suggests that some responses induced by microbial VCs are regulated, at least in part, by different post-transcriptional mechanisms. This hypothesis is supported by the findings that more than 80% of the proteins that are differentially expressed by fungal VCs are encoded by genes whose expression is not altered by this treatment (Sánchez-López et al., 2016a).

Reversible protein thiol redox regulation through mechanisms such as NO-dependent S-nitrosylation, disulfide bond formation, S-sulfenylation and S-glutathionylation is a fundamental switch mechanism of post-translational regulation of metabolism, growth and development, which allows plants to adjust to ever changing environmental constrains (Buchanan and Balmer, 2005; Hu et al., 2015; Aroca, et al., 2017). The findings that plants exposed to charcoal-filtered microbial VCs, but not to super-elevated CO_2, exhibit reductive activation of the starch biosynthetic enzyme AGP (**Figure 12**) further strengthen the idea that some of the plants´ responses to microbial VCs are post-transcriptionally regulated, and suggest that some of these responses are due to post-translational modifications of the thiol redox proteome. Further investigations will be needed to determine whether global post-translational redox modifications of proteins are involved in plant responses to microbial VCs.

5. SUPPLEMENTAL FIGURES AND TABLES

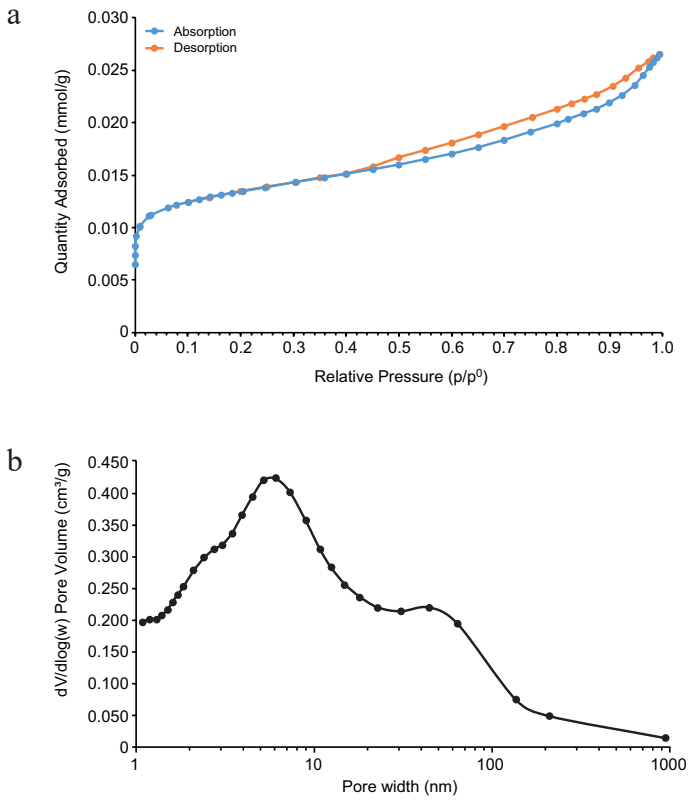

Supplemental Figure 1: Textural characterization of the charcoal used in this study. (a) N_2 adsorption isotherm at −196 ^{o}C of the charcoal, which according to IUPAC classification, is type I(b)–IV(a). The adsorption branch of this xerogel corresponds to type I(b), and the hysteresis loop is characteristic of type-IV(a) isotherms. Type I(b) isotherms are found with materials having pore size distributions over a broader range including wider micropores and possibly narrow mesopores (< ± 2.5 nm). Type IV isotherms are given by mesoporous adsorbents. In the case of a Type IVa isotherm, capillary condensation is accompanied by hysteresis. This occurs when the pore width exceeds a certain critical width, which is dependent on the adsorption system and temperature. The hysteresis loop is H4. The adsorption branch is a composite of Types I and II, the more pronounced uptake at low p/p0 being associated with the filling of micropores. H4 loops are often found in micro-mesoporous carbons. (b) Porosity distribution of Barret, Joyner and Halenda, which predicts that micropores are greater than 0.7 nm. In the porous texture of the coal there are also present mesopores with sizes ranging between 2 and 5 nm.

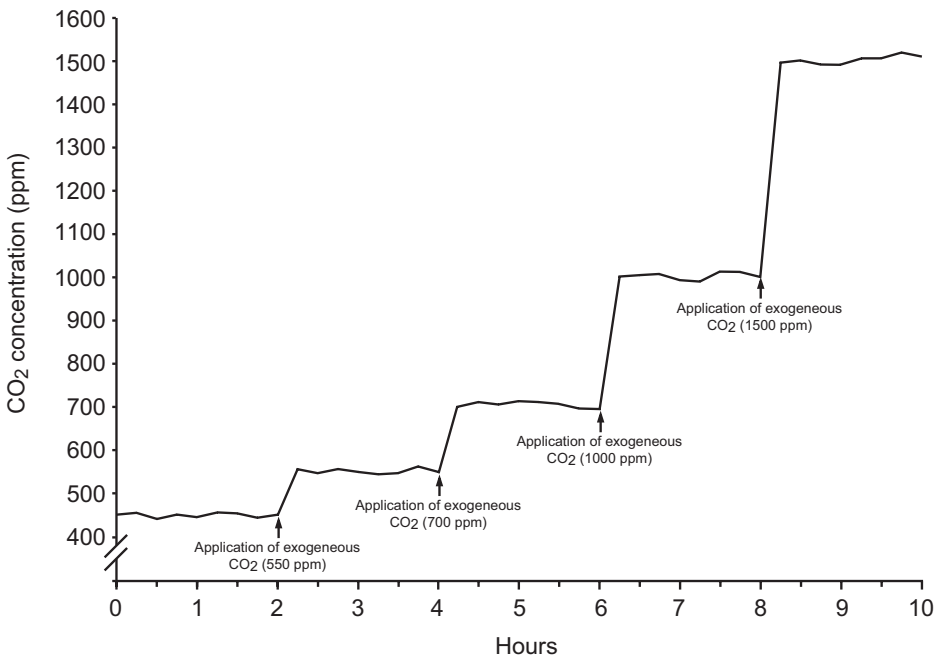

Supplemental Figure 2: Time-course of CO_2 levels in the headspace of PVC-sealed growth boxes placed in a CO_2-controlled growth cabinet in which the CO_2 concentrations were increased stepwise from 550 to 700, 1000 and 1500 ppm. The growth boxes did not contain fungal or plant cultures.

Supplemental Table 1: Textural parameters for the activated charcoal used in this study.

$V_{micro(DR)}$ [a] (cm^3/g)	V_{meso} [b] (cm^3/g)	V_{macro} [c] (cm^3/g)	$a_{BET(N2)}$ (m^2/g)
0.48	0.097	0.115	1109

[a] Micropore volume was deduced by applying the DR.
[b] Deduced by difference between the amount of N_2 adsorbed in the relative pressure range 0.3–0.8.
[c] Deduced by difference between the amount of N_2 adsorbed in the relative pressure range 0.8–1.0.

Supplemental Table 2: VOCs in the headspace of growth boxes containing *A. alternata* and *P. aurantiogriseum* cultures with or without an upper activated charcoal filter. [a] Compounds identified by comparison of RT and mass spectral data to those of authentic compounds. Other compounds were identified by comparing their mass spectral data to spectra from the NIST library and by comparing their linear retention indices (using an n-alkane scale) to literature values. [b]Compounds emitted by *A. alternata* described in Weikl et al. (2016). [c]Compounds previously reported to affect plant growth (Ditengou et al., 2015; Kanchiswamy et al,. 2015). n.d., not detected. Chromatograms are shown in **Figure 5.**

Retention time (min)	Chemical family	*A. alternata*		*P. aurantiogriseum*	
		- Charcoal	+Charcoal	- Charcoal	+ Charcoal
	Alcohol				
2.099		n.d.	n.d.	3-buten-2-ol,2-methyl[a]	n.d.
2.219		1-propanol,2-methyl[a]	n.d.	n.d.	n.d.
2.777		2-butanol,3-methyl[a]	n.d.	2-butanol,3-methyl[a]	n.d.
3.628		1-butanol,2-methyl[a,b]	n.d.	1-butanol,2-methyl[a]	n.d.
	Aldehyde				
16.783		Decanal[a]	n.d.	n.d.	n.d.
	Alkane				
2.680		hexane,3-methyl	n.d.	n.d	n.d
4.156		heptane,4-methyl	n.d.	n.d	n.d
4.284		heptane,3-methyl	n.d.	n.d	n.d
7.532		n.d.	n.d.	pentane,2-nitro-	n.d.
9.810		octane,2,4,6-trimethyl	n.d.	n.d	n.d
16.608		dodecane[a]	n.d.	n.d	n.d
20.003		tridecane[a]	n.d.	n.d	n.d
	Alkene				
3.336		n.d.	n.d.	cyclopentene,3-ethyl	n.d.
3.726		n.d.	n.d.	1-methylcyclohexa-2,4-diene	n.d.
3.970		n.d.	n.d.	1-ethylcyclopentene	n.d.
8.281		n.d.	n.d.	2-butene,1-bromo-3-methyl	n.d.
	Aromatic compound				
10.953		n.d.	n.d.	benzene,1-methoxy-3-methyl[a]	n.d.
15.544		benzaldehyde,4-ethyl	n.d.	n.d	n.d
18.491		n.d	n.d	3,5-dimethoxytoluene	n.d.
22.342		n.d	n.d	benzene,1,2,3-trimethoxy-5-methyl	n.d.
	Carboxilic acid				
15.867		octanoic acid[a]	n.d.	n.d	n.d.

	Ketone			
2.538	n.d.	n.d.	2-butanone,3-methyl	n.d.
4.543	n.d.	n.d.	4(1H)-pyrimidinone[a]	n.d.
10.235	3-octanone[a,c]	n.d.	n.d	n.d.
	Monoterpene			
10.116	n.d.	n.d.	2-methylenebornane	n.d.
11.104	n.d.	n.d.	2-methyl-2-bornene	n.d.
16.089	n.d.	n.d.	2-methylisoborneol[a]	n.d.
	Nitrile			
2.226	n.d.	n.d.	isobutyronitrile	n.d.
	Oxime			
6.433	n.d.	n.d.	butyl aldoxime,2-methyl,syn-	n.d.
6.628	n.d.	n.d.	butyl aldoxime,2-methyl,anti-	n.d.
	Sesquiterpene			
21.894	β-elemene[b,c]	n.d.	n.d.	n.d.
22.377	γ-muurolene[a,c]	n.d.	n.d.	n.d.
22.439	α-cedrene[a,b]	n.d.	α-cedrene[a]	n.d.
22.514	n.d.	n.d.	cadina-1,4-diene[c]	n.d.
22.652	β-cedrene[b]	n.d.	β-cedrene	n.d.
22.909	n.d.	n.d.	α-copaene[c]	n.d.
22.913	cis-thujopsene[a,b]	n.d.	n.d.	n.d.
23.219	unknown sesq. 1	n.d.	n.d.	n.d.
23.791	α-longipinene[a,c]	n.d.	n.d.	n.d.
23.999	acoradiene[b,c]	n.d.	n.d.	n.d.
24.238	4,5-di-epi-aristolochene	n.d.	n.d.	n.d.
24.447	valencene[c]	n.d.	n.d.	n.d.
24.708	α-chamigrene[a,b]	n.d.	α-chamigrene[a]	n.d.
24.763	cuparene[a]	n.d.	n.d.	n.d.

Supplemental Table 3: List of genes whose expression in leaves is altered by charcoal-filtered VCs emitted by *A. alternata*. Genes that are differentially regulated by total *A. alternata* VCs (cf. Supplemental Table 3 in Sánchez-López et al., 2016b) are highlighted in yellow color.

Fold Change	ID	Description
59.14	AT2G24850	ref|Arabidopsis thaliana tyrosine aminotransferase 3 (TAT3), mRNA [NM_128044]
42.09	AT2G41240	ref|Arabidopsis thaliana basic helix-loop-helix protein 100 (BHLH100), mRNA [NM_180018]
35.34	AT2G14560	ref|Arabidopsis thaliana LURP-one-like protein (DUF567) (LURP1), mRNA [NM_127019]
27.3	AT2G39030	ref|Arabidopsis thaliana Acyl-CoA N-acyltransferases (NAT) superfamily protein (NATA1), mRNA [NM_129460]
20.71	AT3G56970	ref|Arabidopsis thaliana basic helix-loop-helix (bHLH) DNA-binding superfamily protein (bHLH38), mRNA [NM_115556]
19.34	AT3G22235	ref|Arabidopsis thaliana cysteine-rich TM module stress tolerance protein mRNA [NM_180292]
18.89	AT3G22240	ref|Arabidopsis thaliana cysteine-rich/transmembrane domain PCC1-like protein mRNA [NM_113122]
18.82	AT3G45140	ref|Arabidopsis thaliana lipoxygenase 2 (LOX2), mRNA [NM_001339198]
17.05	AT2G14247	ref|Arabidopsis thaliana Expressed protein mRNA [NM_201723]
16.45	AT3G56980	ref|Arabidopsis thaliana basic helix-loop-helix (bHLH) DNA-binding superfamily protein (bHLH39), mRNA [NM_115557]
15.78	AT3G44860	ref|Arabidopsis thaliana farnesoic acid carboxyl-O-methyltransferase (FAMT), mRNA [NM_114355]
14.81	AT1G47400	ref|Arabidopsis thaliana hypothetical protein mRNA [NM_103634]
13.64	AT1G47395	ref|Arabidopsis thaliana hypothetical protein mRNA [NM_179449]
13.38	AT1G61120	ref|Arabidopsis thaliana terpene synthase 04 (TPS04), mRNA [NM_104793]
13.06	AT5G44420	ref|Arabidopsis thaliana plant defensin 1.2 (PDF1.2), mRNA [NM_123809]
12.37	AT1G73600	ref|Arabidopsis thaliana S-adenosyl-L-methionine-dependent methyltransferases superfamily protein mRNA [NM_106018]
11.96	AT3G57260	ref|Arabidopsis thaliana beta-1,3-glucanase 2 (BGL2), mRNA [NM_115586]
11.48	AT3G57240	ref|Arabidopsis thaliana beta-1,3-glucanase 3 (BG3), mRNA [NM_115584]
11.27	AT3G22231	ref|Arabidopsis thaliana pathogen and circadian controlled 1 (PCC1), mRNA [NM_113121]
10.64	AT3G26830	ref|Arabidopsis thaliana Cytochrome P450 superfamily protein (PAD3), mRNA [NM_113595]
10.49	AT4G01080	ref|Arabidopsis thaliana TRICHOME BIREFRINGENCE-LIKE 26 (TBL26), mRNA [NM_116338]
10.48	AT1G80130	ref|Arabidopsis thaliana Tetratricopeptide repeat (TPR)-like superfamily protein mRNA [NM_106662]
10.38	AT2G25510	ref|Arabidopsis thaliana transmembrane protein mRNA [NM_001202672]
10.29	AT5G54610	ref|Arabidopsis thaliana ankyrin (ANK), mRNA [NM_124842]
10.02	R65132	tc|AAD15384.1 - Arabidopsis thaliana (Mouse-ear cress), partial (68%) [TC400604]
9.69	AT1G61800	ref|Arabidopsis thaliana glucose-6-phosphate/phosphate translocator 2 (GPT2), mRNA [NM_001334001]
9.18	AT2G43620	ref|Arabidopsis thaliana Chitinase family protein mRNA [NM_129924]
9.13	AT4G23600	ref|Arabidopsis thaliana Tyrosine transaminase family protein (CORI3), mRNA [NM_179099]
8.9	AT2G30766	ref|Arabidopsis thaliana hypothetical protein mRNA [NM_001336300]
8.88	AT1G14880	ref|Arabidopsis thaliana PLANT CADMIUM RESISTANCE 1 (PCR1), mRNA [NM_101357]
8.87	AT4G21840	ref|Arabidopsis thaliana methionine sulfoxide reductase B8 (MSRB8), mRNA [NM_118304]
8.74	AT5G42800	ref|Arabidopsis thaliana dihydroflavonol 4-reductase (DFR), mRNA [NM_123645]
8.69	TA28146_3702	tc|Rep: ER lumen protein retaining receptor - Vitis vinifera (Grape), partial (5%) [TC395123]
8.3	AT4G39950	ref|Arabidopsis thaliana cytochrome P450, family 79, subfamily B, polypeptide 2 (CYP79B2), mRNA [NM_120158]
8.21	EG497537	Unknown

7.94	AT5G44430	ref|Arabidopsis thaliana plant defensin 1.2C (PDF1.2c), mRNA [NM_123810]
7.77	AT3G23120	ref|Arabidopsis thaliana receptor like protein 38 (RLP38), mRNA [NM_113213]
7.72	AT2G27402	ref|Arabidopsis thaliana plastid transcriptionally active protein mRNA [NM_001336115]
7.62	AT4G22870	ref|Arabidopsis thaliana 2-oxoglutarate (2OG) and Fe(II)-dependent oxygenase superfamily protein mRNA [NM_001160794]
7.58	AT2G41090	ref|Arabidopsis thaliana Calcium-binding EF-hand family protein mRNA [NM_129674]
7.32	CB185526	Unknown
7.28	AT1G73010	ref|Arabidopsis thaliana inorganic pyrophosphatase 1 (PS2), mRNA [NM_105959]
7.26	AT2G26400	ref|Arabidopsis thaliana acireductone dioxygenase 3 (ARD3), mRNA [NM_001336065]
7.2	AT3G25180	ref|Arabidopsis thaliana cytochrome P450, family 82, subfamily G, polypeptide 1 (CYP82G1), mRNA [NM_202630]
7.18	AT1G56650	ref|Arabidopsis thaliana production of anthocyanin pigment 1 (PAP1), mRNA [NM_104541]
7.11	CD533642	gb|32O9 Arabidopsis Leaf Senescence Library Arabidopsis thaliana cDNA 3', mRNA sequence [CD533642]
7.07	AT2G30770	ref|Arabidopsis thaliana cytochrome P450 family 71 polypeptide (CYP71A13), mRNA [NM_128630]
7.03	AT1G15520	ref|Arabidopsis thaliana pleiotropic drug resistance 12 (ABCG40), mRNA [NM_001332173]
7.03	AT1G19960	ref|Arabidopsis thaliana transcription factor mRNA [NM_101851]
6.95	AT4G14400	ref|Arabidopsis thaliana ankyrin repeat family protein (ACD6), mRNA [NM_179051]
6.87	AT2G26010	ref|Arabidopsis thaliana plant defensin 1.3 (PDF1.3), mRNA [NM_128160]
6.84	AT1G76960	ref|Arabidopsis thaliana transmembrane protein mRNA [NM_106347]
6.79	AT2G43570	ref|Arabidopsis thaliana chitinase (CHI), mRNA [NM_129919]
6.74	AT5G17220	ref|Arabidopsis thaliana glutathione S-transferase phi 12 (GSTF12), mRNA [NM_121728]
6.66	AT3G24982	ref|Arabidopsis thaliana receptor like protein 40 (RLP40), mRNA [NM_113404]
6.62	AT3G44990	ref|Arabidopsis thaliana xyloglucan endo-transglycosylase-related 8 (XTH31), mRNA [NM_114368]
6.47	AT5G59670	ref|Arabidopsis thaliana Leucine-rich repeat protein kinase family protein mRNA [NM_001345366]
6.46	AT4G21760	ref|Arabidopsis thaliana beta-glucosidase 47 (BGLU47), mRNA [NM_001341512]
6.38	AT2G29350	ref|Arabidopsis thaliana senescence-associated gene 13 (SAG13), mRNA [NM_201829]
6.08	AT4G21830	ref|Arabidopsis thaliana methionine sulfoxide reductase B7 (MSRB7), mRNA [NM_118303]
5.88	AT1G12030	ref|Arabidopsis thaliana phosphoenolpyruvate carboxylase, putative (DUF506) mRNA [NM_101075]
5.86	AT5G03350	ref|Arabidopsis thaliana Legume lectin family protein mRNA [NM_120414]
5.85	AT5G60900	ref|Arabidopsis thaliana receptor-like protein kinase 1 (RLK1), mRNA [NM_001345434]
5.8	AT1G35710	ref|Arabidopsis thaliana kinase family with leucine-rich repeat domain-containing protein mRNA [NM_103273]
5.8	AT5G19240	ref|Arabidopsis thaliana Glycoprotein membrane precursor GPI-anchored mRNA [NM_121929]
5.69	AT1G56430	ref|Arabidopsis thaliana nicotianamine synthase 4 (NAS4), mRNA [NM_104521]
5.69	AT5G54060	ref|Arabidopsis thaliana UDP-glucose:flavonoid 3-o-glucosyltransferase (UF3GT), mRNA [NM_124785]
5.66	AT5G53048	ref|Arabidopsis thaliana other RNA lncRNA [NR_143344]
5.61	AT5G24660	ref|Arabidopsis thaliana response to low sulfur 2 (LSU2), mRNA [NM_122375]
5.55	AT3G27060	ref|Arabidopsis thaliana Ferritin/ribonucleotide reductase-like family protein (TSO2), mRNA [NM_113620]
5.5	AT5G53450	ref|Arabidopsis thaliana OBP3-responsive protein 1 (ORG1), mRNA [NM_001345057]

5.48	AT1G23020	ref|Arabidopsis thaliana ferric reduction oxidase 3 (FRO3), mRNA [NM_001198138]
5.47	AT2G16367	Unknown
5.47	AT1G78370	ref|Arabidopsis thaliana glutathione S-transferase TAU 20 (GSTU20), mRNA [NM_106484]
5.44	AT3G03780	ref|Arabidopsis thaliana methionine synthase 2 (MS2), mRNA [NM_111249]
5.39	AT2G35980	ref|Arabidopsis thaliana Late embryogenesis abundant (LEA) hydroxyproline-rich glycoprotein family (YLS9), mRNA [NM_129157]
5.36	AT1G21525	gb|Arabidopsis thaliana clone 31878 mRNA, complete sequence [AY087114]
5.35	AT1G19250	ref|Arabidopsis thaliana flavin-dependent monooxygenase 1 (FMO1), mRNA [NM_101783]
5.32	AT2G11810	ref|Arabidopsis thaliana monogalactosyldiacylglycerol synthase type C (MGDC), mRNA [NM_001124829]
5.18	AT1G06830	ref|Arabidopsis thaliana Glutaredoxin family protein mRNA [NM_100560]
5.15	AT5G23020	ref|Arabidopsis thaliana 2-isopropylmalate synthase 2 (IMS2), mRNA [NM_122208]
5.09	AT4G39940	ref|Arabidopsis thaliana APS-kinase 2 (AKN2), mRNA [NM_120157]
5.02	AT5G08760	ref|Arabidopsis thaliana transmembrane protein mRNA [NM_001085080]
4.98	AT4G17470	ref|Arabidopsis thaliana alpha/beta-Hydrolases superfamily protein mRNA [NM_001203824]
4.95	AT4G39210	ref|Arabidopsis thaliana Glucose-1-phosphate adenylyltransferase family protein (APL3), mRNA [NM_001342527]
4.95	AT4G15210	ref|Arabidopsis thaliana beta-amylase 5 (BAM5), mRNA [NM_179058]
4.92	AT5G48850	ref|Arabidopsis thaliana Tetratricopeptide repeat (TPR)-like superfamily protein (ATSDI1), mRNA [NM_124262]
4.82	AT1G16410	ref|Arabidopsis thaliana cytochrome p450 79f1 (CYP79F1), mRNA [NM_101507]
4.73	AT5G14200	ref|Arabidopsis thaliana isopropylmalate dehydrogenase 1 (IMD1), mRNA [NM_001036803]
4.65	AT2G46880	ref|Arabidopsis thaliana purple acid phosphatase 14 (PAP14), mRNA [NM_201975]
4.65	AT1G67360	ref|Arabidopsis thaliana Rubber elongation factor protein (REF) mRNA [NM_105404]
4.64	AT4G04610	ref|Arabidopsis thaliana APS reductase 1 (APR1), mRNA [NM_116699]
4.63	AT4G04830	ref|Arabidopsis thaliana methionine sulfoxide reductase B5 (MSRB5), mRNA [NM_001203745]
4.56	AT4G02850	ref|Arabidopsis thaliana phenazine biosynthesis PhzC/PhzF family protein mRNA [NM_116519]
4.48	AT4G28250	ref|Arabidopsis thaliana expansin B3 (EXPB3), mRNA [NM_001341907]
4.46	AT1G73325	ref|Arabidopsis thaliana Kunitz family trypsin and protease inhibitor protein mRNA [NM_105992]
4.44	AT1G06000	ref|Arabidopsis thaliana UDP-Glycosyltransferase superfamily protein mRNA [NM_100480]
4.44	AT1G28480	ref|Arabidopsis thaliana Thioredoxin superfamily protein (GRX480), mRNA [NM_102616]
4.42	AT5G10760	ref|Arabidopsis thaliana Eukaryotic aspartyl protease family protein mRNA [NM_121114]
4.4	AT1G29660	ref|Arabidopsis thaliana GDSL-like Lipase/Acylhydrolase superfamily protein mRNA [NM_102706]
4.35	AT4G03060	gb|Arabidopsis thaliana Col-0 2-oxoglutarate-dependent dioxygenase (AOP2) pseudogene, mRNA sequence [AF418241]
4.32	AT2G43100	ref|Arabidopsis thaliana isopropylmalate isomerase 2 (IPMI2), mRNA [NM_129871]
4.32	AT4G22880	ref|Arabidopsis thaliana leucoanthocyanidin dioxygenase (LDOX), mRNA [NM_001036623]
4.32	AT1G21250	ref|Arabidopsis thaliana cell wall-associated kinase (WAK1), mRNA [NM_101978]
4.29	AT3G25882	ref|Arabidopsis thaliana NIM1-interacting 2 (NIMIN-2), mRNA [NM_148752]
4.28	AT5G05250	ref|Arabidopsis thaliana hypothetical protein mRNA [NM_120607]
4.27	AT1G62560	ref|Arabidopsis thaliana flavin-monooxygenase glucosinolate S-oxygenase 3 (FMO GS-OX3), mRNA [NM_001334038]

4.27	AT3G11340	ref|Arabidopsis thaliana UDP-Glycosyltransferase superfamily protein (UGT76B1), mRNA [NM_111968]
4.27	AT3G22600	ref|Arabidopsis thaliana Bifunctional inhibitor/lipid-transfer protein/seed storage 2S albumin superfamily protein mRNA [NM_113159]
4.26	AT2G46430	ref|Arabidopsis thaliana cyclic nucleotide gated channel 3 (CNGC3), mRNA [NM_130207]
4.22	AT3G49580	ref|Arabidopsis thaliana response to low sulfur 1 (LSU1), mRNA [NM_001203113]
4.17	AT2G26020	ref|Arabidopsis thaliana plant defensin 1.2b (PDF1.2b), mRNA [NM_128161]
4.15	AT4G36010	ref|Arabidopsis thaliana Pathogenesis-related thaumatin superfamily protein mRNA [NM_001036715]
4.13	AT2G38240	ref|Arabidopsis thaliana 2-oxoglutarate (2OG) and Fe(II)-dependent oxygenase superfamily protein mRNA [NM_129381]
4.11	AT1G02450	ref|Arabidopsis thaliana NIM1-interacting 1 (NIMIN1), mRNA [NM_100126]
4.11	AT5G59870	ref|Arabidopsis thaliana histone H2A 6 (HTA6), mRNA [NM_125380]
4.1	AT3G11010	ref|Arabidopsis thaliana receptor like protein 34 (RLP34), mRNA [NM_111938]
4.1	AT1G09200	ref|Arabidopsis thaliana Histone superfamily protein mRNA [NM_100790]
4.1	AT1G68600	ref|Arabidopsis thaliana aluminum activated malate transporter family protein mRNA [NM_105532]
4.09	AT3G44870	ref|Arabidopsis thaliana S-adenosyl-L-methionine-dependent methyltransferases superfamily protein mRNA [NM_114356]
4.07	AT4G25630	ref|Arabidopsis thaliana fibrillarin 2 (FIB2), mRNA [NM_118695]
4.06	AT4G26950	ref|Arabidopsis thaliana senescence regulator (Protein of unknown function, DUF584) mRNA [NM_118829]
4.03	AT4G23130	ref|Arabidopsis thaliana cysteine-rich RLK (RECEPTOR-like protein kinase) 5 (CRK5), mRNA [NM_001341575]
4.03	AT4G14365	ref|Arabidopsis thaliana hypothetical protein (XBAT34), mRNA [NM_117514]
4.02	AT1G01190	ref|Arabidopsis thaliana cytochrome P450, family 78, subfamily A, polypeptide 8 (CYP78A8), mRNA [NM_100001]
4.02	AT5G52760	ref|Arabidopsis thaliana Copper transport protein family mRNA [NM_001345008]
4.01	AT5G45650	ref|Arabidopsis thaliana subtilase family protein mRNA [NM_001344636]
3.99	AT4G39030	ref|Arabidopsis thaliana MATE efflux family protein (EDS5), mRNA [NM_120063]
3.97	AT1G65486	ref|Arabidopsis thaliana transmembrane protein mRNA [NM_001124079]
3.96	AT3G58990	ref|Arabidopsis thaliana isopropylmalate isomerase 1 (IPMI1), mRNA [NM_115761]
3.95	AT5G61000	ref|Arabidopsis thaliana Replication factor-A protein 1-like protein (RPA70D), mRNA [NM_125493]
3.94	AT5G20190	ref|Arabidopsis thaliana Tetratricopeptide repeat (TPR)-like superfamily protein mRNA [NM_122026]
3.94	AT5G44820	ref|Arabidopsis thaliana Nucleotide-diphospho-sugar transferase family protein mRNA [NM_123850]
3.91	AT5G05270	ref|Arabidopsis thaliana Chalcone-flavanone isomerase family protein (CHIL), mRNA [NM_180439]
3.9	AT3G52370	ref|Arabidopsis thaliana FASCICLIN-like arabinogalactan protein 15 precursor (FLA15), mRNA [NM_115097]
3.85	AT3G48080	ref|Arabidopsis thaliana alpha/beta-Hydrolases superfamily protein mRNA [NM_114677]
3.85	AT3G47480	ref|Arabidopsis thaliana Calcium-binding EF-hand family protein mRNA [NM_114616]
3.85	AT5G13740	ref|Arabidopsis thaliana zinc induced facilitator 1 (ZIF1), mRNA [NM_121377]
3.84	AT3G25795	ref|Arabidopsis thaliana other RNA ncRNA [NR_143943]
3.83	AT4G24570	ref|Arabidopsis thaliana dicarboxylate carrier 2 (DIC2), mRNA [NM_118590]
3.83	AT1G64980	ref|Arabidopsis thaliana Nucleotide-diphospho-sugar transferases superfamily protein (CDI), mRNA [NM_001334184]
3.83	AT1G74440	ref|Arabidopsis thaliana ER membrane protein, putative (DUF962) mRNA [NM_106104]
3.8	AT1G18590	ref|Arabidopsis thaliana sulfotransferase 17 (SOT17), mRNA [NM_101717]

3.8	AT2G40435	ref|Arabidopsis thaliana transcription factor SCREAM-like protein mRNA [NM_001336840]
3.79	AT1G43910	ref|Arabidopsis thaliana P-loop containing nucleoside triphosphate hydrolases superfamily protein mRNA [NM_103518]
3.77	AT1G79400	ref|Arabidopsis thaliana cation/H+ exchanger 2 (CHX2), mRNA [NM_106588]
3.77	AT3G52630	ref|Arabidopsis thaliana Nucleic acid-binding, OB-fold-like protein mRNA [NM_115123]
3.77	AT3G54750	ref|Arabidopsis thaliana downstream neighbor of Son mRNA [NM_115332]
3.76	AT5G13320	ref|Arabidopsis thaliana Auxin-responsive GH3 family protein (PBS3), mRNA [NM_001343268]
3.76	NP454661	ref|Arabidopsis thaliana alpha carbonic anhydrase 2 (ACA2), mRNA [NM_001336149]
3.75	AT5G65360	ref|Arabidopsis thaliana Histone superfamily protein mRNA [NM_125934]
3.75	AT5G42530	ref|Arabidopsis thaliana hypothetical protein mRNA [NM_123618]
3.73	AT5G50950	ref|Arabidopsis thaliana FUMARASE 2 (FUM2), mRNA [NM_001344914]
3.72	AT1G56060	ref|Arabidopsis thaliana cysteine-rich/transmembrane domain protein B mRNA [NM_104484]
3.72	BP783345	Unknown
3.7	AT3G49570	ref|Arabidopsis thaliana response to low sulfur 3 (LSU3), mRNA [NM_114817]
3.69	AT4G26960	ref|Arabidopsis thaliana hypothetical protein mRNA [NM_118830]
3.68	AT1G75780	ref|Arabidopsis thaliana tubulin beta-1 chain (TUB1), mRNA [NM_106228]
3.67	AT1G17710	ref|Arabidopsis thaliana Pyridoxal phosphate phosphatase-related protein (PEPC1), mRNA [NM_001084087]
3.67	AT5G10390	ref|Arabidopsis thaliana Histone superfamily protein mRNA [NM_121077]
3.67	AT5G54970	ref|Arabidopsis thaliana hypothetical protein mRNA [NM_124879]
3.65	AT1G24280	ref|Arabidopsis thaliana glucose-6-phosphate dehydrogenase 3 (G6PD3), mRNA [NM_102274]
3.64	AT5G04150	ref|Arabidopsis thaliana basic helix-loop-helix (bHLH) DNA-binding superfamily protein (BHLH101), mRNA [NM_120497]
3.63	AT1G04770	ref|Arabidopsis thaliana Tetratricopeptide repeat (TPR)-like superfamily protein mRNA [NM_100355]
3.62	TA29588_3702	tc|Rep: At2g25510/F13B15.17 - Arabidopsis thaliana (Mouse-ear cress), partial (41%) [TC388653]
3.61	AT1G13470	ref|Arabidopsis thaliana hypothetical protein (DUF1262) mRNA [NM_101217]
3.6	AT5G54490	ref|Arabidopsis thaliana pinoid-binding protein 1 (PBP1), mRNA [NM_124829]
3.58	AT2G26440	ref|Arabidopsis thaliana Plant invertase/pectin methylesterase inhibitor superfamily mRNA [NM_128201]
3.58	AT4G18440	ref|Arabidopsis thaliana L-Aspartase-like family protein mRNA [NM_117957]
3.57	AT3G26960	ref|Arabidopsis thaliana Pollen Ole e 1 allergen and extensin family protein mRNA [NM_113610]
3.57	TC300093	Unknown
3.56	AT1G78570	ref|Arabidopsis thaliana rhamnose biosynthesis 1 (RHM1), mRNA [NM_106504]
3.56	AT3G61920	ref|Arabidopsis thaliana UvrABC system protein C mRNA [NM_116057]
3.55	AT2G45760	ref|Arabidopsis thaliana BON association protein 2 (BAP2), mRNA [NM_130139]
3.54	AT2G18660	ref|Arabidopsis thaliana plant natriuretic peptide A (PNP-A), mRNA [NM_179648]
3.53	T42092	Unknown
3.51	AT5G42650	ref|Arabidopsis thaliana allene oxide synthase (AOS), mRNA [NM_123629]
3.51	AT4G11190	ref|Arabidopsis thaliana Disease resistance-responsive (dirigent-like protein) family protein mRNA [NM_117190]
3.5	AT5G48880	ref|Arabidopsis thaliana peroxisomal 3-keto-acyl-CoA thiolase 2 (KAT5), mRNA [NM_001344808]

3.5	BU917432	ref|Arabidopsis thaliana other RNA snoRNA [NR_139469]
3.47	AT5G23420	ref|Arabidopsis thaliana high-mobility group box 6 (HMGB6), mRNA [NM_001203442]
3.46	AT1G65860	ref|Arabidopsis thaliana flavin-monooxygenase glucosinolate S-oxygenase 1 (FMO GS-OX1), mRNA [NM_105258]
3.46	AT3G46880	ref|Arabidopsis thaliana hypothetical protein mRNA [NM_114555]
3.44	AT4G12880	ref|Arabidopsis thaliana early nodulin-like protein 19 (ENOD19), mRNA [NM_001203782]
3.43	AT2G40750	ref|Arabidopsis thaliana WRKY DNA-binding protein 54 (WRKY54), mRNA [NM_129637]
3.43	AT2G38860	ref|Arabidopsis thaliana Class I glutamine amidotransferase-like superfamily protein (YLS5), mRNA [NM_129443]
3.43	AT2G46440	ref|Arabidopsis thaliana cyclic nucleotide-gated channels (CNGC11), mRNA [NM_001337191]
3.42	AT1G17745	ref|Arabidopsis thaliana D-3-phosphoglycerate dehydrogenase (PGDH), mRNA [NM_001035984]
3.42	AT1G13750	ref|Arabidopsis thaliana Purple acid phosphatases superfamily protein mRNA [NM_101243]
3.39	AT2G41010	ref|Arabidopsis thaliana calmodulin (CAM)-binding protein of 25 kDa (CAMBP25), mRNA [NM_129666]
3.39	AT3G17790	ref|Arabidopsis thaliana purple acid phosphatase 17 (PAP17), mRNA [NM_112660]
3.39	AT3G60540	ref|Arabidopsis thaliana Preprotein translocase Sec, Sec61-beta subunit protein mRNA [NM_202738]
3.39	AT2G35860	ref|Arabidopsis thaliana FASCICLIN-like arabinogalactan protein 16 precursor (FLA16), mRNA [NM_179922]
3.38	AT1G64390	ref|Arabidopsis thaliana glycosyl hydrolase 9C2 (GH9C2), mRNA [NM_105114]
3.37	AT4G14090	ref|Arabidopsis thaliana UDP-Glycosyltransferase superfamily protein mRNA [NM_117485]
3.36	AT5G08640	ref|Arabidopsis thaliana flavonol synthase 1 (FLS1), mRNA [NM_001203337]
3.36	AT3G56400	ref|Arabidopsis thaliana WRKY DNA-binding protein 70 (WRKY70), mRNA [NM_115498]
3.36	AT1G23100	ref|Arabidopsis thaliana GroES-like family protein mRNA [NM_102158]
3.36	AT1G73805	ref|Arabidopsis thaliana Calmodulin binding protein-like protein (SARD1), mRNA [NM_106040]
3.35	AT1G45201	ref|Arabidopsis thaliana triacylglycerol lipase-like 1 (TLL1), mRNA [NM_179441]
3.35	AT4G34200	ref|Arabidopsis thaliana D-3-phosphoglycerate dehydrogenase (EDA9), mRNA [NM_119583]
3.35	AT1G03495	gb|Arabidopsis thaliana HXXXD-type acyl-transferase-like protein (AT1G03495) mRNA, complete cds [NM_100232]
3.34	AT3G29590	ref|Arabidopsis thaliana HXXXD-type acyl-transferase family protein (AT5MAT), mRNA [NM_113880]
3.31	AT4G17770	ref|Arabidopsis thaliana trehalose phosphatase/synthase 5 (TPS5), mRNA [NM_001341241]
3.31	AT3G46320	ref|Arabidopsis thaliana Histone superfamily protein mRNA [NM_180329]
3.31	AT5G44568	ref|Arabidopsis thaliana transmembrane protein mRNA [NM_001085241]
3.3	AT3G22550	ref|Arabidopsis thaliana NAD(P)H-quinone oxidoreductase subunit, putative (DUF581) mRNA [NM_113154]
3.29	AT2G46650	ref|Arabidopsis thaliana cytochrome B5 isoform C (CB5-C), mRNA [NM_130230]
3.29	AT2G39330	ref|Arabidopsis thaliana jacalin-related lectin 23 (JAL23), mRNA [NM_129490]
3.29	AT3G45930	ref|Arabidopsis thaliana Histone superfamily protein mRNA [NM_114462]
3.29	AT1G03820	ref|Arabidopsis thaliana E6-like protein mRNA [NM_100261]
3.28	AT3G14210	ref|Arabidopsis thaliana GDSL-like lipase/acylhydrolase superfamily protein (ESM1), mRNA [NM_001338114]
3.27	AT1G72910	ref|Arabidopsis thaliana Toll-Interleukin-Resistance (TIR) domain-containing protein mRNA [NM_105949]
3.26	AT3G03060	ref|Arabidopsis thaliana P-loop containing nucleoside triphosphate hydrolases superfamily protein mRNA [NM_111176]
3.25	AT3G44750	ref|Arabidopsis thaliana histone deacetylase 3 (HDA3), mRNA [NM_001203083]

3.22	AT5G60730	ref|Arabidopsis thaliana Anion-transporting ATPase mRNA [NM_125466]
3.22	AT5G42020	ref|Arabidopsis thaliana Heat shock protein 70 (Hsp 70) family protein (BIP2), mRNA [NM_123567]
3.22	TA28264_3702	Unknown
3.21	AT2G37040	ref|Arabidopsis thaliana PHE ammonia lyase 1 (PAL1), mRNA [NM_129260]
3.21	AT1G04980	ref|Arabidopsis thaliana PDI-like 2-2 (PDIL2-2), mRNA [NM_100376]
3.21	AT2G23010	ref|Arabidopsis thaliana serine carboxypeptidase-like 9 (SCPL9), mRNA [NM_201788]
3.21	AT4G08300	ref|Arabidopsis thaliana nodulin MtN21 /EamA-like transporter family protein (UMAMIT17), mRNA [NM_116899]
3.21	AT3G60440	ref|Arabidopsis thaliana Phosphoglycerate mutase family protein mRNA [NM_001340043]
3.21	AT5G26690	ref|Arabidopsis thaliana Heavy metal transport/detoxification superfamily protein mRNA [NM_180545]
3.21	TA50968_3702	tc|Rep: Eukaryotic translation initiation factor 4E - Cucumis melo (Muskmelon), partial (11%) [TC394106]
3.2	AT1G66390	ref|Arabidopsis thaliana myb domain protein 90 (MYB90), mRNA [NM_105310]
3.18	AT3G15357	ref|Arabidopsis thaliana phosphopantothenoylcysteine decarboxylase subunit mRNA [NM_112403]
3.18	AT3G44450	ref|Arabidopsis thaliana hypothetical protein mRNA [NM_114313]
3.17	AT5G10400	ref|Arabidopsis thaliana Histone superfamily protein mRNA [NM_121078]
3.16	AT5G28540	ref|Arabidopsis thaliana heat shock protein 70 (Hsp 70) family protein (BIP1), mRNA [NM_122737]
3.16	AT2G28740	ref|Arabidopsis thaliana histone H4 (HIS4), mRNA [NM_128434]
3.15	AT5G03760	ref|Arabidopsis thaliana Nucleotide-diphospho-sugar transferases superfamily protein (ATCSLA09), mRNA [NM_120457]
3.15	AT5G26220	ref|Arabidopsis thaliana ChaC-like family protein mRNA [NM_001343968]
3.14	AT1G11545	ref|Arabidopsis thaliana xyloglucan endotransglucosylase/hydrolase 8 (XTH8), mRNA [NM_101028]
3.13	AT2G28210	ref|Arabidopsis thaliana alpha carbonic anhydrase 2 (ACA2), mRNA [NM_001336148]
3.13	AT3G09870	ref|Arabidopsis thaliana SAUR-like auxin-responsive protein family mRNA [NM_111822]
3.13	AT5G22460	ref|Arabidopsis thaliana alpha/beta-Hydrolases superfamily protein mRNA [NM_122151]
3.12	BP586302	gb|BP586302 RAFL15 Arabidopsis thaliana cDNA clone RAFL15-05-M21 3', mRNA sequence [BP586302]
3.11	AT5G64080	ref|Arabidopsis thaliana Bifunctional inhibitor/lipid-transfer protein/seed storage 2S albumin superfamily protein (XYP1), mRNA [NM_125804]
3.11	AT1G04020	ref|Arabidopsis thaliana breast cancer associated RING 1 (BARD1), mRNA [NM_202029]
3.1	AT1G65890	ref|Arabidopsis thaliana acyl activating enzyme 12 (AAE12), mRNA [NM_105261]
3.1	AT5G46830	ref|Arabidopsis thaliana calcium-binding transcription factor NIG1 (NIG1), mRNA [NM_124054]
3.09	AT5G64550	ref|Arabidopsis thaliana loricrin-like protein mRNA [NM_125851]
3.08	AT5G07690	ref|Arabidopsis thaliana myb domain protein 29 (MYB29), mRNA [NM_120851]
3.08	NP335312	tc|GB|AL590346.1|CAC35882.1 putative protein [Arabidopsis thaliana] [NP335312]
3.07	AT3G27360	ref|Arabidopsis thaliana Histone superfamily protein mRNA [NM_113651]
3.07	AT5G42380	ref|Arabidopsis thaliana calmodulin like 37 (CML37), mRNA [NM_123603]
3.06	AT2G32990	ref|Arabidopsis thaliana glycosyl hydrolase 9B8 (GH9B8), mRNA [NM_128859]
3.05	AT5G25250	ref|Arabidopsis thaliana SPFH/Band 7/PHB domain-containing membrane-associated protein family (FLOT1), mRNA [NM_122434]
3.04	AT1G32900	ref|Arabidopsis thaliana UDP-Glycosyltransferase superfamily protein (GBSS1), mRNA [NM_103023]
3.04	AT1G20510	ref|Arabidopsis thaliana OPC-8:0 CoA ligase1 (OPCL1), mRNA [NM_202143]

3.03	AT1G41830	ref|Arabidopsis thaliana SKU5-similar 6 (SKS6), mRNA [NM_103408]
3.03	TA36353_3702	tc|Rep: At5g42860 - Arabidopsis thaliana (Mouse-ear cress), partial (39%) [TC388419]
3.02	AT4G14680	ref|Arabidopsis thaliana Pseudouridine synthase/archaeosine transglycosylase-like family protein (APS3), mRNA [NM_001340955]
3.02	AT4G23140	ref|Arabidopsis thaliana cysteine-rich RLK (RECEPTOR-like protein kinase) 6 (CRK6), mRNA [NM_179095]
3.01	AT2G16060	ref|Arabidopsis thaliana hemoglobin 1 (HB1), mRNA [NM_127165]
3.01	AT5G61030	ref|Arabidopsis thaliana glycine-rich RNA-binding protein 3 (GR-RBP3), mRNA [NM_125496]
3.01	AT4G23170	ref|Arabidopsis thaliana receptor-like protein kinase-related family protein (EP1), mRNA [NM_118446]
-3.01	AT4G18010	ref|Arabidopsis thaliana myo-inositol polyphosphate 5-phosphatase 2 (IP5PII), mRNA [NM_117911]
-3.01	AT2G03760	ref|Arabidopsis thaliana sulfotransferase 12 (SOT12), mRNA [NM_126423]
-3.01	AT1G21680	ref|Arabidopsis thaliana DPP6 N-terminal domain-like protein mRNA [NM_102017]
-3.01	AT5G45310	ref|Arabidopsis thaliana coiled-coil protein mRNA [NM_123899]
-3.02	AK230465	gb|Arabidopsis thaliana mRNA for hypothetical protein, complete cds, clone: RAFL26-03-H08 [AK230465]
-3.03	AT2G43820	ref|Arabidopsis thaliana UDP-glucosyltransferase 74F2 (UGT74F2), mRNA [NM_129944]
-3.03	AT1G71000	ref|Arabidopsis thaliana Chaperone DnaJ-domain superfamily protein mRNA [NM_001334483]
-3.03	AT2G29480	ref|Arabidopsis thaliana glutathione S-transferase tau 2 (GSTU2), mRNA [NM_128502]
-3.03	AT1G12250	ref|Arabidopsis thaliana Pentapeptide repeat-containing protein mRNA [NM_001084054]
-3.03	AT1G23040	ref|Arabidopsis thaliana hydroxyproline-rich glycoprotein family protein mRNA [NM_001332581]
-3.03	AT2G46220	ref|Arabidopsis thaliana DUF2358 family protein (DUF2358) mRNA [NM_130184]
-3.04	AT5G36910	ref|Arabidopsis thaliana thionin 2.2 (THI2.2), mRNA [NM_123049]
-3.04	AT4G39090	ref|Arabidopsis thaliana Papain family cysteine protease (RD19), mRNA [NM_120069]
-3.04	AT1G76650	ref|Arabidopsis thaliana calmodulin-like 38 (CML38), mRNA [NM_001198484]
-3.04	AT2G25780	ref|Arabidopsis thaliana hypothetical protein (DUF1677) mRNA [NM_128138]
-3.04	AT3G13062	ref|Arabidopsis thaliana Polyketide cyclase/dehydrase and lipid transport superfamily protein mRNA [NM_180243]
-3.04	TC297782	ref|Arabidopsis thaliana other RNA lncRNA [NR_139108]
-3.05	AT1G55850	ref|Arabidopsis thaliana cellulose synthase like E1 (CSLE1), mRNA [NM_104462]
-3.05	AT5G59340	ref|Arabidopsis thaliana WUSCHEL related homeobox 2 (WOX2), mRNA [NM_125325]
-3.05	AT5G39610	ref|Arabidopsis thaliana NAC domain containing protein 6 (NAC6), mRNA [NM_123323]
-3.06	AT1G04280	ref|Arabidopsis thaliana P-loop containing nucleoside triphosphate hydrolases superfamily protein mRNA [NM_001331471]
-3.08	AT1G18270	ref|Arabidopsis thaliana ketose-bisphosphate aldolase class-II family protein mRNA [NM_001198099]
-3.09	AT1G08570	ref|Arabidopsis thaliana atypical CYS HIS rich thioredoxin 4 (ACHT4), mRNA [NM_001123776]
-3.09	AT5G57660	ref|Arabidopsis thaliana CONSTANS-like 5 (COL5), mRNA [NM_125149]
-3.09	AT5G65870	ref|Arabidopsis thaliana phytosulfokine 5 precursor (PSK5), mRNA [NM_125984]
-3.09	CB259684	gb|31-E9537-013-002-M08-T7R MPIZ-ADIS-013 Arabidopsis thaliana cDNA clone MPIZp770M082Q 5-PRIME, mRNA sequence [CB259684]
-3.09	TA29086_3702	Unknown
-3.1	AT4G32480	ref|Arabidopsis thaliana sugar phosphate exchanger, putative (DUF506) mRNA [NM_119400]
-3.11	AT5G63790	ref|Arabidopsis thaliana NAC domain containing protein 102 (NAC102), mRNA [NM_001345612]

-3.11	AT5G65380	ref|Arabidopsis thaliana MATE efflux family protein mRNA [NM_125936]
-3.12	AT4G31870	ref|Arabidopsis thaliana glutathione peroxidase 7 (GPX7), mRNA [NM_001342119]
-3.12	AT3G10910	ref|Arabidopsis thaliana RING/U-box superfamily protein mRNA [NM_111928]
-3.12	AT5G06980	ref|Arabidopsis thaliana hypothetical protein mRNA [NM_001203316]
-3.13	AT1G18020	ref|Arabidopsis thaliana FMN-linked oxidoreductases superfamily protein mRNA [NM_001035985]
-3.13	AT5G17300	ref|Arabidopsis thaliana Homeodomain-like superfamily protein (RVE1), mRNA [NM_121736]
-3.14	AT4G13830	ref|Arabidopsis thaliana DNAJ-like 20 (J20), mRNA [NM_117457]
-3.14	AT1G19660	ref|Arabidopsis thaliana Wound-responsive family protein mRNA [NM_001035991]
-3.14	AT2G38820	ref|Arabidopsis thaliana DNA-directed RNA polymerase subunit beta-beta protein, putative (DUF506) mRNA [NM_001336739]
-3.14	AT4G25690	ref|Arabidopsis thaliana stress response NST1-like protein mRNA [NM_118701]
-3.14	BT025685	ref|Arabidopsis thaliana hypothetical protein mRNA [NM_001334179]
-3.15	AT1G68620	ref|Arabidopsis thaliana alpha/beta-Hydrolases superfamily protein mRNA [NM_105534]
-3.15	AT1G76690	ref|Arabidopsis thaliana 12-oxophytodienoate reductase 2 (OPR2), mRNA [NM_106319]
-3.16	AT5G43450	ref|Arabidopsis thaliana 2-oxoglutarate (2OG) and Fe(II)-dependent oxygenase superfamily protein mRNA [NM_001344483]
-3.16	AT2G29500	ref|Arabidopsis thaliana HSP20-like chaperones superfamily protein mRNA [NM_128504]
-3.16	AT3G16770	ref|Arabidopsis thaliana ethylene-responsive element binding protein (EBP), mRNA [NM_112550]
-3.18	AT5G51970	ref|Arabidopsis thaliana GroES-like zinc-binding alcohol dehydrogenase family protein mRNA [NM_124576]
-3.19	AT4G24050	ref|Arabidopsis thaliana NAD(P)-binding Rossmann-fold superfamily protein mRNA [NM_001341639]
-3.19	AT2G22960	ref|Arabidopsis thaliana alpha/beta-Hydrolases superfamily protein mRNA [NM_001335830]
-3.2	AT3G07350	ref|Arabidopsis thaliana sulfate/thiosulfate import ATP-binding protein, putative (DUF506) mRNA [NM_111614]
-3.22	AT5G08350	ref|Arabidopsis thaliana GRAM domain-containing protein / ABA-responsive protein-like protein mRNA [NM_120919]
-3.22	AT1G20630	ref|Arabidopsis thaliana catalase 1 (CAT1), mRNA [NM_101914]
-3.24	AT3G22370	ref|Arabidopsis thaliana alternative oxidase 1A (AOX1A), mRNA [NM_113135]
-3.26	AT5G64570	ref|Arabidopsis thaliana beta-D-xylosidase 4 (XYL4), mRNA [NM_001345643]
-3.26	AT2G30140	ref|Arabidopsis thaliana UDP-Glycosyltransferase superfamily protein (UGT87A2), mRNA [NM_001084510]
-3.26	AT3G55710	ref|Arabidopsis thaliana UDP-Glycosyltransferase superfamily protein mRNA [NM_115429]
-3.26	AT4G04770	ref|Arabidopsis thaliana ATP binding cassette protein 1 (ABCI8), mRNA [NM_116715]
-3.26	AT3G25190	ref|Arabidopsis thaliana Vacuolar iron transporter (VIT) family protein mRNA [NM_113425]
-3.27	AT3G03480	ref|Arabidopsis thaliana acetyl CoA:(Z)-3-hexen-1-ol acetyltransferase (CHAT), mRNA [NM_111219]
-3.27	AT1G48000	ref|Arabidopsis thaliana myb domain protein 112 (MYB112), mRNA [NM_103696]
-3.27	AT4G25390	ref|Arabidopsis thaliana Protein kinase superfamily protein mRNA [NM_179111]
-3.27	AT5G40690	ref|Arabidopsis thaliana histone-lysine N-methyltransferase trithorax-like protein mRNA [NM_123434]
-3.27	TC312617	tc|Rep: Vacuolar-processing enzyme gamma-isozyme precursor - Arabidopsis thaliana (Mouse-ear cress), partial (23%) [TC400087]
-3.28	AT1G53580	ref|Arabidopsis thaliana glyoxalase II 3 (GLY3), mRNA [NM_202289]
-3.29	AT2G48020	ref|Arabidopsis thaliana Major facilitator superfamily protein mRNA [NM_180152]
-3.3	AT3G02140	ref|Arabidopsis thaliana AFP2 (ABI five-binding protein 2) family protein (TMAC2), mRNA [NM_111081]

-3.31	AT5G65110	ref|Arabidopsis thaliana acyl-CoA oxidase 2 (ACX2), mRNA [NM_001037068]
-3.31	AT3G22200	ref|Arabidopsis thaliana Pyridoxal phosphate (PLP)-dependent transferases superfamily protein (POP2), mRNA [NM_001203018]
-3.31	AT2G29290	ref|Arabidopsis thaliana NAD(P)-binding Rossmann-fold superfamily protein mRNA [NM_128483]
-3.31	AT1G06430	ref|Arabidopsis thaliana FTSH protease 8 (FTSH8), mRNA [NM_100523]
-3.31	AT2G04795	ref|Arabidopsis thaliana hypothetical protein mRNA [NM_126510]
-3.32	AT2G43400	ref|Arabidopsis thaliana electron-transfer flavoprotein:ubiquinone oxidoreductase (ETFQO), mRNA [NM_129901]
-3.32	AT1G09240	ref|Arabidopsis thaliana nicotianamine synthase 3 (NAS3), mRNA [NM_100794]
-3.32	AT1G77210	ref|Arabidopsis thaliana sugar transporter 14 (STP14), mRNA [NM_106370]
-3.32	AT1G03580	gb|Arabidopsis thaliana unknown protein (At1g03580) mRNA, partial cds [AY091013]
-3.33	AT5G39660	ref|Arabidopsis thaliana cycling DOF factor 2 (CDF2), mRNA [NM_180775]
-3.33	AT1G61740	ref|Arabidopsis thaliana Sulfite exporter TauE/SafE family protein mRNA [NM_104856]
-3.35	AT2G28110	ref|Arabidopsis thaliana Exostosin family protein (FRA8), mRNA [NM_179782]
-3.35	AT1G75380	ref|Arabidopsis thaliana bifunctional nuclease in basal defense response 1 (BBD1), mRNA [NM_179560]
-3.35	AT3G62950	ref|Arabidopsis thaliana Thioredoxin superfamily protein mRNA [NM_116160]
-3.35	AT2G22990	ref|Arabidopsis thaliana sinapoylglucose 1 (SNG1), mRNA [NM_127864]
-3.35	AT3G10320	ref|Arabidopsis thaliana Glycosyltransferase family 61 protein mRNA [NM_111867]
-3.37	AT1G64940	ref|Arabidopsis thaliana cytochrome P450, family 87, subfamily A, polypeptide 6 (CYP89A6), mRNA [NM_105168]
-3.38	AT1G64950	ref|Arabidopsis thaliana cytochrome P450, family 89, subfamily A, polypeptide 5 (CYP89A5), mRNA [NM_105169]
-3.39	AT3G29240	ref|Arabidopsis thaliana PPR containing protein (DUF179) mRNA [NM_113848]
-3.4	AT5G49740	ref|Arabidopsis thaliana ferric reduction oxidase 7 (FRO7), mRNA [NM_001344853]
-3.4	AT4G16520	ref|Arabidopsis thaliana Ubiquitin-like superfamily protein (ATG8F), mRNA [NM_179064]
-3.4	AT4G23450	ref|Arabidopsis thaliana RING/U-box superfamily protein (AIRP1), mRNA [NM_001341614]
-3.41	AT5G18170	ref|Arabidopsis thaliana glutamate dehydrogenase 1 (GDH1), mRNA [NM_121822]
-3.41	AT2G13431	gb|Arabidopsis thaliana clone asmbl_5374 unknown mRNA sequence [EF182961]
-3.41	AT5G66480	ref|Arabidopsis thaliana bacteriophage N4 adsorption B protein mRNA [NM_126046]
-3.41	BX822927	gb|Arabidopsis thaliana Full-length cDNA Complete sequence from clone GSLTFB73ZE03 of Flowers and buds of strain col-0 of Arabidopsis thaliar [BX822927]
-3.42	AT4G37610	ref|Arabidopsis thaliana BTB and TAZ domain protein 5 (BT5), mRNA [NM_119924]
-3.43	AT2G32020	ref|Arabidopsis thaliana Acyl-CoA N-acyltransferases (NAT) superfamily protein mRNA [NM_128762]
-3.43	AT2G37750	ref|Arabidopsis thaliana hypothetical protein mRNA [NM_129331]
-3.44	AT5G49730	ref|Arabidopsis thaliana ferric reduction oxidase 6 (FRO6), mRNA [NM_001344852]
-3.44	AT2G30250	ref|Arabidopsis thaliana WRKY DNA-binding protein 25 (WRKY25), mRNA [NM_128578]
-3.45	AT2G37130	ref|Arabidopsis thaliana Peroxidase superfamily protein mRNA [NM_001124989]
-3.45	AT4G31860	ref|Arabidopsis thaliana Protein phosphatase 2C family protein mRNA [NM_202927]
-3.45	AT1G16720	ref|Arabidopsis thaliana high chlorophyll fluorescence phenotype 173 (HCF173), mRNA [NM_001332253]
-3.46	AT3G59930	ref|Arabidopsis thaliana defensin-like protein mRNA [NM_115856]

-3.46	AT2G42870	ref|Arabidopsis thaliana phy rapidly regulated 1 (PAR1), mRNA [NM_129848]
-3.47	AT4G16190	ref|Arabidopsis thaliana Papain family cysteine protease mRNA [NM_117715]
-3.47	AT1G53280	ref|Arabidopsis thaliana Class I glutamine amidotransferase-like superfamily protein (DJ1B), mRNA [NM_104206]
-3.48	AT1G17990	ref|Arabidopsis thaliana FMN-linked oxidoreductases superfamily protein mRNA [NM_001035985]
-3.48	AT3G26220	ref|Arabidopsis thaliana cytochrome P450, family 71, subfamily B, polypeptide 3 (CYP71B3), mRNA [NM_113529]
-3.49	AT4G22920	ref|Arabidopsis thaliana non-yellowing 1 (NYE1), mRNA [NM_001341565]
-3.5	AT2G44130	ref|Arabidopsis thaliana Galactose oxidase/kelch repeat superfamily protein mRNA [NM_129976]
-3.51	AK230421	gb|Arabidopsis thaliana mRNA for hypothetical protein, complete cds, clone: RAFL25-33-B21 [AK230421]
-3.52	AT5G39050	ref|Arabidopsis thaliana HXXXD-type acyl-transferase family protein (PMAT1), mRNA [NM_123267]
-3.53	BU917423	ref|Arabidopsis thaliana RING/U-box protein mRNA [NM_112412]
-3.59	N38085	tc|Rep: Cysteine proteinase - Populus tomentosa (Chinese white poplar), partial (36%) [TC397589]
-3.6	AT1G55920	ref|Arabidopsis thaliana serine acetyltransferase 2;1 (SERAT2;1), mRNA [NM_104470]
-3.6	AT5G64230	ref|Arabidopsis thaliana 1,8-cineole synthase mRNA [NM_125819]
-3.61	AT1G10140	ref|Arabidopsis thaliana Uncharacterized conserved protein UCP031279 mRNA [NM_100888]
-3.61	AV566399	gb|AV566399 Arabidopsis thaliana green siliques Columbia Arabidopsis thaliana cDNA clone SQ242f10F 3', mRNA sequence [AV566399]
-3.63	AT1G13700	ref|Arabidopsis thaliana 6-phosphogluconolactonase 1 (PGL1), mRNA [NM_001332083]
-3.63	AT3G43670	ref|Arabidopsis thaliana Copper amine oxidase family protein mRNA [NM_114235]
-3.63	AT1G20350	ref|Arabidopsis thaliana translocase inner membrane subunit 17-1 (TIM17-1), mRNA [NM_101886]
-3.64	AT2G47180	ref|Arabidopsis thaliana galactinol synthase 1 (GolS1), mRNA [NM_130286]
-3.64	AT2G36950	ref|Arabidopsis thaliana Heavy metal transport/detoxification superfamily protein mRNA [NM_129251]
-3.66	AT2G15890	ref|Arabidopsis thaliana maternal effect embryo arrest 14 (MEE14), mRNA [NM_001084426]
-3.67	AT1G67070	ref|Arabidopsis thaliana Mannose-6-phosphate isomerase, type I (DIN9), mRNA [NM_001334269]
-3.67	AT3G13065	ref|Arabidopsis thaliana STRUBBELIG-receptor family 4 (SRF4), mRNA [NM_112145]
-3.69	AT3G10740	ref|Arabidopsis thaliana alpha-L-arabinofuranosidase 1 (ASD1), mRNA [NM_001337894]
-3.7	AT1G14130	ref|Arabidopsis thaliana 2-oxoglutarate (2OG) and Fe(II)-dependent oxygenase superfamily protein mRNA [NM_101278]
-3.7	AT3G04060	ref|Arabidopsis thaliana NAC domain containing protein 46 (NAC046), mRNA [NM_111277]
-3.71	TC309871	tc|Rep: Conglutin gamma-like protein - Arabidopsis thaliana (Mouse-ear cress), partial (35%) [TC396686]
-3.72	AT5G18130	ref|Arabidopsis thaliana transmembrane protein mRNA [NM_203067]
-3.74	AT1G09420	ref|Arabidopsis thaliana glucose-6-phosphate dehydrogenase 4 (G6PD4), mRNA [NM_001198018]
-3.74	AT1G01240	ref|Arabidopsis thaliana transmembrane protein mRNA [NM_001331263]
-3.75	AT4G20070	ref|Arabidopsis thaliana allantoate amidohydrolase (AAH), mRNA [NM_001341398]
-3.77	AT2G26355	ref|Arabidopsis thaliana other RNA lncRNA [NR_140673]
-3.77	AT4G33660	ref|Arabidopsis thaliana cysteine-rich TM module stress tolerance protein mRNA [NM_119522]
-3.81	TA35940_3702	tc|Rep: Chromosome chr18 scaffold_1, whole genome shotgun sequence - Vitis vinifera (Grape), partial (42%) [TC384450]
-3.84	AT5G66052	ref|Arabidopsis thaliana transmembrane protein mRNA [NM_148167]
-3.84	TA29208_3702	Unknown

-3.85	AT2G40300	ref|Arabidopsis thaliana ferritin 4 (FER4), mRNA [NM_129588]
-3.85	AT4G34138	ref|Arabidopsis thaliana UDP-glucosyl transferase 73B1 (UGT73B1), mRNA [NM_119576]
-3.86	AT3G46080	ref|Arabidopsis thaliana C2H2-type zinc finger family protein mRNA [NM_114477]
-3.86	AT5G55970	ref|Arabidopsis thaliana RING/U-box superfamily protein mRNA [NM_180866]
-3.9	AT5G53970	ref|Arabidopsis thaliana Tyrosine transaminase family protein (TAT7), mRNA [NM_124776]
-3.9	AT2G40420	ref|Arabidopsis thaliana Transmembrane amino acid transporter family protein mRNA [NM_129602]
-3.91	AT5G43580	ref|Arabidopsis thaliana Serine protease inhibitor, potato inhibitor I-type family protein (UPI), mRNA [NM_123724]
-3.92	AT1G58290	ref|Arabidopsis thaliana Glutamyl-tRNA reductase family protein (HEMA1), mRNA [NM_104609]
-3.92	AT5G16960	ref|Arabidopsis thaliana Zinc-binding dehydrogenase family protein mRNA [NM_001343474]
-3.93	AT3G03470	ref|Arabidopsis thaliana cytochrome P450, family 87, subfamily A, polypeptide 9 (CYP89A9), mRNA [NM_111218]
-3.94	AT5G19120	ref|Arabidopsis thaliana Eukaryotic aspartyl protease family protein mRNA [NM_121917]
-3.95	AT5G16970	ref|Arabidopsis thaliana alkenal reductase (AER), mRNA [NM_121703]
-3.96	AT5G18630	ref|Arabidopsis thaliana alpha/beta-Hydrolases superfamily protein mRNA [NM_180517]
-3.96	AT5G02160	ref|Arabidopsis thaliana transmembrane protein mRNA [NM_120294]
-3.97	AT5G28770	ref|Arabidopsis thaliana bZIP transcription factor family protein (BZO2H3), mRNA [NM_001344083]
-3.99	AT5G44973	ref|Arabidopsis thaliana defensin-like protein mRNA [NM_001036935]
-4.01	AT3G14690	ref|Arabidopsis thaliana cytochrome P450, family 72, subfamily A, polypeptide 15 (CYP72A15), mRNA [NM_112330]
-4.01	AT4G32940	ref|Arabidopsis thaliana gamma vacuolar processing enzyme (GAMMA-VPE), mRNA [NM_119448]
-4.03	AT2G36750	ref|Arabidopsis thaliana UDP-glucosyl transferase 73C1 (UGT73C1), mRNA [NM_129230]
-4.03	AT5G65207	ref|Arabidopsis thaliana hypothetical protein mRNA [NM_148161]
-4.04	TA29997_3702	Unknown
-4.06	AT4G24160	ref|Arabidopsis thaliana alpha/beta-Hydrolases superfamily protein mRNA [NM_202876]
-4.08	AT1G63180	ref|Arabidopsis thaliana UDP-D-glucose/UDP-D-galactose 4-epimerase 3 (UGE3), mRNA [NM_104996]
-4.08	AT5G17000	ref|Arabidopsis thaliana Zinc-binding dehydrogenase family protein mRNA [NM_001343476]
-4.1	AT5G16370	ref|Arabidopsis thaliana acyl activating enzyme 5 (AAE5), mRNA [NM_121642]
-4.1	AT1G23390	ref|Arabidopsis thaliana Kelch repeat-containing F-box family protein mRNA [NM_102188]
-4.11	AT1G05340	ref|Arabidopsis thaliana cysteine-rich TM module stress tolerance protein mRNA [NM_100413]
-4.12	AT5G17860	ref|Arabidopsis thaliana calcium exchanger 7 (CAX7), mRNA [NM_121792]
-4.13	AT5G52250	ref|Arabidopsis thaliana Transducin/WD40 repeat-like superfamily protein (RUP1), mRNA [NM_124604]
-4.14	AT5G15850	ref|Arabidopsis thaliana CONSTANS-like 1 (COL1), mRNA [NM_121590]
-4.18	AT2G39400	ref|Arabidopsis thaliana alpha/beta-Hydrolases superfamily protein mRNA [NM_001336772]
-4.19	AT5G64250	ref|Arabidopsis thaliana Aldolase-type TIM barrel family protein mRNA [NM_125821]
-4.19	AT2G17500	ref|Arabidopsis thaliana Auxin efflux carrier family protein mRNA [NM_179633]
-4.19	AT2G27385	ref|Arabidopsis thaliana Pollen Ole e 1 allergen and extensin family protein mRNA [NM_179769]
-4.2	AT1G58180	ref|Arabidopsis thaliana beta carbonic anhydrase 6 (BCA6), mRNA [NM_179492]
-4.2	AT2G25900	ref|Arabidopsis thaliana Zinc finger C-x8-C-x5-C-x3-H type family protein (ATCTH), mRNA [NM_001202675]

-4.21	AT2G28120	ref|Arabidopsis thaliana Major facilitator superfamily protein mRNA [NM_128372]
-4.21	AT5G14120	ref|Arabidopsis thaliana Major facilitator superfamily protein mRNA [NM_121416]
-4.24	AT2G26150	ref|Arabidopsis thaliana heat shock transcription factor A2 (HSFA2), mRNA [NM_001336038]
-4.26	AT5G13330	ref|Arabidopsis thaliana related to AP2 6l (Rap2.6L), mRNA [NM_121336]
-4.26	AT5G17170	ref|Arabidopsis thaliana rubredoxin family protein (ENH1), mRNA [NM_001085129]
-4.28	AT3G15770	ref|Arabidopsis thaliana hypothetical protein mRNA [NM_112447]
-4.28	TA26159_3702	Unknown
-4.3	AT3G50560	ref|Arabidopsis thaliana NAD(P)-binding Rossmann-fold superfamily protein mRNA [NM_114916]
-4.3	AT5G63190	ref|Arabidopsis thaliana MA3 domain-containing protein mRNA [NM_125714]
-4.31	AT3G10020	ref|Arabidopsis thaliana plant/protein mRNA [NM_111837]
-4.33	TA28495_3702	Unknown
-4.36	AT1G76600	ref|Arabidopsis thaliana poly polymerase mRNA [NM_106310]
-4.37	AT3G15620	ref|Arabidopsis thaliana DNA photolyase family protein (UVR3), mRNA [NM_112432]
-4.37	AT3G19390	ref|Arabidopsis thaliana Granulin repeat cysteine protease family protein mRNA [NM_112826]
-4.38	AT1G75490	ref|Arabidopsis thaliana Integrase-type DNA-binding superfamily protein mRNA [NM_106202]
-4.42	AT3G15500	ref|Arabidopsis thaliana NAC domain containing protein 3 (NAC3), mRNA [NM_112418]
-4.43	AT1G77450	ref|Arabidopsis thaliana NAC domain containing protein 32 (NAC032), mRNA [NM_106394]
-4.43	TC313866	tc|Rep: Chaperone protein dnaJ 8, chloroplast precursor - Arabidopsis thaliana (Mouse-ear cress), partial (50%) [TC404503]
-4.45	AT3G14680	ref|Arabidopsis thaliana cytochrome P450, family 72, subfamily A, polypeptide 14 (CYP72A14), mRNA [NM_112329]
-4.46	AT3G22460	ref|Arabidopsis thaliana O-acetylserine (thiol) lyase (OAS-TL) isoform A2 (OASA2), mRNA [NM_113145]
-4.46	AT4G13250	ref|Arabidopsis thaliana NAD(P)-binding Rossmann-fold superfamily protein (NYC1), mRNA [NM_117396]
-4.49	AT1G07890	ref|Arabidopsis thaliana ascorbate peroxidase 1 (APX1), mRNA [NM_100663]
-4.49	AT4G16680	ref|Arabidopsis thaliana P-loop containing nucleoside triphosphate hydrolases superfamily protein mRNA [NM_001341126]
-4.49	AT5G58350	ref|Arabidopsis thaliana with no lysine (K) kinase 4 (WNK4), mRNA [NM_125220]
-4.5	AT1G68190	ref|Arabidopsis thaliana B-box zinc finger family protein (BBX27), mRNA [NM_001334353]
-4.52	AT1G07040	ref|Arabidopsis thaliana plant/protein mRNA [NM_100578]
-4.55	AT5G24120	ref|Arabidopsis thaliana sigma factor E (SIGE), mRNA [NM_001343842]
-4.57	AT1G14870	ref|Arabidopsis thaliana PLANT CADMIUM RESISTANCE 2 (PCR2), mRNA [NM_101356]
-4.6	AT4G26530	ref|Arabidopsis thaliana Aldolase superfamily protein (FBA5), mRNA [NM_001036644]
-4.6	AT1G13300	ref|Arabidopsis thaliana myb-like transcription factor family protein (HRS1), mRNA [NM_101201]
-4.61	AT5G26200	ref|Arabidopsis thaliana Mitochondrial substrate carrier family protein mRNA [NM_122521]
-4.62	AT4G38470	ref|Arabidopsis thaliana ACT-like protein tyrosine kinase family protein (STY46), mRNA [NM_001342498]
-4.63	AT3G46690	ref|Arabidopsis thaliana UDP-Glycosyltransferase superfamily protein mRNA [NM_114536]
-4.63	AT3G13061	ref|Arabidopsis thaliana other RNA lncRNA [NR_141586]
-4.64	AT3G62260	ref|Arabidopsis thaliana Protein phosphatase 2C family protein mRNA [NM_180406]
-4.65	AT1G53100	ref|Arabidopsis thaliana Core-2/i-branching beta-1,6-N-acetylglucosaminyltransferase family protein mRNA [NM_104189]

-4.65	AT2G30600	ref|Arabidopsis thaliana BTB/POZ domain-containing protein mRNA [NM_001202713]
-4.66	AT1G30820	ref|Arabidopsis thaliana CTP synthase family protein mRNA [NM_102819]
-4.66	AT1G79270	ref|Arabidopsis thaliana evolutionarily conserved C-terminal region 8 (ECT8), mRNA [NM_001334878]
-4.66	NP229859	tc|GB|AL391141.1|CAC01711.1 quinone oxidoreductase-like protein [NP229859]
-4.67	AT1G22380	ref|Arabidopsis thaliana UDP-glucosyl transferase 85A3 (UGT85A3), mRNA [NM_102088]
-4.67	AT5G47560	ref|Arabidopsis thaliana tonoplast dicarboxylate transporter (TDT), mRNA [NM_124129]
-4.71	EG427617	gb|AYALO23TFB pooled cDNA populations Arabidopsis thaliana cDNA, mRNA sequence [EG427617]
-4.72	TC295612	ref|Arabidopsis thaliana other RNA ncRNA [NR_143567]
-4.73	AV805941	gb|AV805941 RAFL9 Arabidopsis thaliana cDNA clone RAFL09-44-M15 3', mRNA sequence [AV805941]
-4.74	AT1G32170	ref|Arabidopsis thaliana xyloglucan endotransglucosylase/hydrolase 30 (XTH30), mRNA [NM_102950]
-4.74	AT1G63800	ref|Arabidopsis thaliana ubiquitin-conjugating enzyme 5 (UBC5), mRNA [NM_001334127]
-4.76	AT5G57655	ref|Arabidopsis thaliana xylose isomerase family protein mRNA [NM_180872]
-4.76	AT4G37370	ref|Arabidopsis thaliana cytochrome P450, family 81, subfamily D, polypeptide 8 (CYP81D8), mRNA [NM_119900]
-4.79	DR368472	gb|12826078 CERES-AN65 Arabidopsis thaliana cDNA clone 1361839 5', mRNA sequence [DR368472]
-4.81	AT5G57560	ref|Arabidopsis thaliana Xyloglucan endotransglucosylase/hydrolase family protein (TCH4), mRNA [NM_125137]
-4.82	DR368506	gb|12842501 CERES-AN65 Arabidopsis thaliana cDNA clone 1366811 5', mRNA sequence [DR368506]
-4.84	AT2G39570	ref|Arabidopsis thaliana ACT domain-containing protein (ACR9), mRNA [NM_129515]
-4.85	AT1G35670	ref|Arabidopsis thaliana calcium-dependent protein kinase 2 (CDPK2), mRNA [NM_103271]
-4.86	AT1G80440	ref|Arabidopsis thaliana Galactose oxidase/kelch repeat superfamily protein mRNA [NM_106692]
-4.87	AT4G20860	ref|Arabidopsis thaliana FAD-binding Berberine family protein mRNA [NM_118204]
-4.89	TA30818_3702	Unknown
-4.91	AT4G15530	ref|Arabidopsis thaliana pyruvate orthophosphate dikinase (PPDK), mRNA [NM_001341051]
-4.95	AT3G61900	ref|Arabidopsis thaliana SAUR-like auxin-responsive protein family mRNA [NM_116055]
-4.96	AT2G18050	ref|Arabidopsis thaliana histone H1-3 (HIS1-3), mRNA [NM_179639]
-4.96	AT1G72060	ref|Arabidopsis thaliana serine-type endopeptidase inhibitor mRNA [NM_105864]
-5.01	TA28705_3702	Unknown
-5.05	AT5G50760	ref|Arabidopsis thaliana SAUR-like auxin-responsive protein family mRNA [NM_124454]
-5.08	AT5G38710	ref|Arabidopsis thaliana Methylenetetrahydrofolate reductase family protein mRNA [NM_123232]
-5.09	AT4G24972	ref|Arabidopsis thaliana tapetum determinant 1 (TPD1), mRNA [NM_202883]
-5.1	AT4G34131	ref|Arabidopsis thaliana UDP-glucosyl transferase 73B3 (UGT73B3), mRNA [NM_119574]
-5.1	AT5G51070	ref|Arabidopsis thaliana Clp ATPase (ERD1), mRNA [NM_124486]
-5.11	AT4G34135	ref|Arabidopsis thaliana UDP-glucosyltransferase 73B2 (UGT73B2), mRNA [NM_179161]
-5.12	AT1G70290	ref|Arabidopsis thaliana trehalose-6-phosphatase synthase S8 (TPS8), mRNA [NM_001334443]
-5.15	AT3G14660	ref|Arabidopsis thaliana cytochrome P450, family 72, subfamily A, polypeptide 13 (CYP72A13), mRNA [NM_001338130]
-5.15	AT3G15630	ref|Arabidopsis thaliana plant/protein mRNA [NM_112433]
-5.18	AT5G24490	ref|Arabidopsis thaliana 30S ribosomal protein mRNA [NM_122357]

-5.19	AT1G69490	ref|Arabidopsis thaliana NAC-like, activated by AP3/PI (NAP), mRNA [NM_105616]
-5.21	AT1G18200	ref|Arabidopsis thaliana Rab GTPase-like A1I protein (RABA6b), mRNA [NM_101680]
-5.22	AT1G72680	ref|Arabidopsis thaliana cinnamyl-alcohol dehydrogenase (CAD1), mRNA [NM_105927]
-5.24	AT3G13450	ref|Arabidopsis thaliana Transketolase family protein (DIN4), mRNA [NM_112191]
-5.24	AT3G13750	ref|Arabidopsis thaliana beta galactosidase 1 (BGAL1), mRNA [NM_112225]
-5.25	AT1G60140	ref|Arabidopsis thaliana trehalose phosphate synthase (TPS10), mRNA [NM_001333882]
-5.25	AT3G29035	ref|Arabidopsis thaliana NAC domain containing protein 3 (NAC3), mRNA [NM_113825]
-5.28	AT2G45170	ref|Arabidopsis thaliana AUTOPHAGY 8E (ATG8E), mRNA [NM_180100]
-5.32	AT5G07100	ref|Arabidopsis thaliana WRKY DNA-binding protein 26 (WRKY26), mRNA [NM_120792]
-5.37	AT5G61820	ref|Arabidopsis thaliana stress up-regulated Nod 19 protein mRNA [NM_001345498]
-5.4	AT1G71520	ref|Arabidopsis thaliana Integrase-type DNA-binding superfamily protein mRNA [NM_105820]
-5.4	AT4G12735	ref|Arabidopsis thaliana hypothetical protein mRNA [NM_202810]
-5.41	AT5G49450	ref|Arabidopsis thaliana basic leucine-zipper 1 (bZIP1), mRNA [NM_124322]
-5.46	AT1G71030	ref|Arabidopsis thaliana MYB-like 2 (MYBL2), mRNA [NM_001334485]
-5.48	AT2G47000	ref|Arabidopsis thaliana ATP binding cassette subfamily B4 (ABCB4), mRNA [NM_001337238]
-5.54	AT2G47770	ref|Arabidopsis thaliana TSPO(outer membrane tryptophan-rich sensory protein)-like protein (TSPO), mRNA [NM_130344]
-5.6	AT5G14730	ref|Arabidopsis thaliana hypothetical protein mRNA [NM_121477]
-5.64	AT3G10120	ref|Arabidopsis thaliana hypothetical protein mRNA [NM_111847]
-5.69	AT1G13990	ref|Arabidopsis thaliana plant/protein mRNA [NM_001160863]
-5.69	AT5G51720	ref|Arabidopsis thaliana 2 iron, 2 sulfur cluster binding protein (NEET), mRNA [NM_124551]
-5.7	AT5G56100	ref|Arabidopsis thaliana glycine-rich protein / oleosin mRNA [NM_124992]
-5.71	AT4G24230	ref|Arabidopsis thaliana acyl-CoA-binding domain 3 (ACBP3), mRNA [NM_001084972]
-5.72	AT5G59400	ref|Arabidopsis thaliana PGR5-like A protein mRNA [NM_180889]
-5.75	AT4G39675	ref|Arabidopsis thaliana hypothetical protein mRNA [NM_120128]
-5.76	AT1G21400	ref|Arabidopsis thaliana Thiamin diphosphate-binding fold (THDP-binding) superfamily protein mRNA [NM_001332503]
-5.78	AT5G24800	ref|Arabidopsis thaliana basic leucine zipper 9 (BZIP9), mRNA [NM_122389]
-5.78	AT4G33666	ref|Arabidopsis thaliana hypothetical protein mRNA [NM_119524]
-5.81	AT5G05410	ref|Arabidopsis thaliana DRE-binding protein 2A (DREB2A), mRNA [NM_001036760]
-5.84	AT2G20670	ref|Arabidopsis thaliana sugar phosphate exchanger, putative (DUF506) mRNA [NM_127631]
-5.86	AT1G54100	ref|Arabidopsis thaliana aldehyde dehydrogenase 7B4 (ALDH7B4), mRNA [NM_104287]
-5.86	TA26531_3702	Unknown
-5.89	AT2G15490	ref|Arabidopsis thaliana UDP-glycosyltransferase 73B4 (UGT73B4), mRNA [NM_127109]
-5.91	AT5G63160	ref|Arabidopsis thaliana BTB and TAZ domain protein 1 (BT1), mRNA [NM_001345581]
-5.92	AT2G05380	ref|Arabidopsis thaliana glycine-rich protein 3 short isoform (GRP3S), mRNA [NM_001124801]
-5.94	AT2G29420	ref|Arabidopsis thaliana glutathione S-transferase tau 7 (GSTU7), mRNA [NM_128496]
-5.98	AT5G64190	ref|Arabidopsis thaliana neuronal PAS domain protein mRNA [NM_001345621]

-6	AT5G51440	ref|Arabidopsis thaliana HSP20-like chaperones superfamily protein mRNA [NM_124523]
-6.1	AT5G41080	ref|Arabidopsis thaliana PLC-like phosphodiesterases superfamily protein (GDPD2), mRNA [NM_203136]
-6.11	AT1G05560	ref|Arabidopsis thaliana UDP-glucosyltransferase 75B1 (UGT75B1), mRNA [NM_100435]
-6.13	AT1G15040	ref|Arabidopsis thaliana Class I glutamine amidotransferase-like superfamily protein (GAT1_2.1), mRNA [NM_101374]
-6.14	AT2G31945	ref|Arabidopsis thaliana transmembrane protein mRNA [NM_128753]
-6.18	AT2G15960	ref|Arabidopsis thaliana stress-induced protein mRNA [NM_127155]
-6.19	AT2G37030	ref|Arabidopsis thaliana SAUR-like auxin-responsive protein family mRNA [NM_129259]
-6.2	AT1G02660	ref|Arabidopsis thaliana alpha/beta-Hydrolases superfamily protein mRNA [NM_100146]
-6.22	AT3G57520	ref|Arabidopsis thaliana seed imbibition 2 (SIP2), mRNA [NM_180384]
-6.24	AT1G75750	ref|Arabidopsis thaliana GAST1 protein homolog 1 (GASA1), mRNA [NM_001198478]
-6.26	AT3G45300	ref|Arabidopsis thaliana isovaleryl-CoA-dehydrogenase (IVD), mRNA [NM_114399]
-6.26	AT1G30720	ref|Arabidopsis thaliana FAD-binding Berberine family protein mRNA [NM_102808]
-6.31	AT2G19800	ref|Arabidopsis thaliana myo-inositol oxygenase 2 (MIOX2), mRNA [NM_127538]
-6.39	AT1G42490	Unknown
-6.48	AT2G40000	ref|Arabidopsis thaliana ortholog of sugar beet HS1 PRO-1 2 (HSPRO2), mRNA [NM_129558]
-6.53	AT3G49790	ref|Arabidopsis thaliana Carbohydrate-binding protein mRNA [NM_114839]
-6.57	AT2G17880	ref|Arabidopsis thaliana Chaperone DnaJ-domain superfamily protein mRNA [NM_127342]
-6.62	AT5G07440	ref|Arabidopsis thaliana glutamate dehydrogenase 2 (GDH2), mRNA [NM_001125712]
-6.65	AT4G30670	ref|Arabidopsis thaliana Putative membrane lipoprotein mRNA [NM_119213]
-6.92	AT1G79700	ref|Arabidopsis thaliana Integrase-type DNA-binding superfamily protein (WRI4), mRNA [NM_001334913]
-6.96	AT2G36780	ref|Arabidopsis thaliana UDP-Glycosyltransferase superfamily protein mRNA [NM_129233]
-7.01	AT2G02710	ref|Arabidopsis thaliana PAS/LOV protein B (PLPB), mRNA [NM_179597]
-7.11	AT1G06570	ref|Arabidopsis thaliana 4-hydroxyphenylpyruvate dioxygenase (PDS1), mRNA [NM_100536]
-7.2	AT2G23030	ref|Arabidopsis thaliana SNF1-related protein kinase 2.9 (SNRK2.9), mRNA [NM_127867]
-7.23	AT2G15480	ref|Arabidopsis thaliana UDP-glucosyl transferase 73B5 (UGT73B5), mRNA [NM_127108]
-7.23	TA27461_3702	Unknown
-7.26	AT4G15760	ref|Arabidopsis thaliana monooxygenase 1 (MO1), mRNA [NM_001203809]
-7.31	AT4G36040	ref|Arabidopsis thaliana Chaperone DnaJ-domain superfamily protein (J11), mRNA [NM_119771]
-7.41	AT2G36800	ref|Arabidopsis thaliana don-glucosyltransferase 1 (DOGT1), mRNA [NM_129235]
-7.42	AT5G21170	ref|Arabidopsis thaliana 5'-AMP-activated protein kinase beta-2 subunit protein (AKINBETA1), mRNA [NM_001036841]
-7.45	AT5G66650	ref|Arabidopsis thaliana calcium uniporter (DUF607) mRNA [NM_126063]
-7.6	AT4G33150	ref|Arabidopsis thaliana lysine-ketoglutarate reductase/saccharopine dehydrogenase bifunctional enzyme mRNA [NM_001160811]
-7.65	AT5G54080	ref|Arabidopsis thaliana homogentisate 1,2-dioxygenase (HGO), mRNA [NM_180856]
-7.68	AT5G16980	ref|Arabidopsis thaliana Zinc-binding dehydrogenase family protein mRNA [NM_121704]
-7.7	AT1G23870	ref|Arabidopsis thaliana trehalose-phosphatase/synthase 9 (TPS9), mRNA [NM_102235]
-7.81	AT4G35090	ref|Arabidopsis thaliana catalase 2 (CAT2), mRNA [NM_001342324]

-7.88	AT4G34710	ref|Arabidopsis thaliana arginine decarboxylase 2 (ADC2), mRNA [NM_202955]
-7.94	AT5G22920	ref|Arabidopsis thaliana CHY-type/CTCHY-type/RING-type Zinc finger protein mRNA [NM_122198]
-8.03	AT1G62510	ref|Arabidopsis thaliana Bifunctional inhibitor/lipid-transfer protein/seed storage 2S albumin superfamily protein mRNA [NM_104930]
-8.17	AT1G77760	ref|Arabidopsis thaliana nitrate reductase 1 (NIA1), mRNA [NM_106425]
-8.18	AT1G19530	ref|Arabidopsis thaliana DNA polymerase epsilon catalytic subunit A mRNA [NM_001332396]
-8.25	AT1G28330	ref|Arabidopsis thaliana dormancy-associated protein-like 1 (DYL1), mRNA [NM_179390]
-8.27	AT2G32150	ref|Arabidopsis thaliana Haloacid dehalogenase-like hydrolase (HAD) superfamily protein mRNA [NM_001336371]
-8.45	AT3G14990	ref|Arabidopsis thaliana Class I glutamine amidotransferase-like superfamily protein (DJ1A), mRNA [NM_001035621]
-8.45	AT4G28040	ref|Arabidopsis thaliana nodulin MtN21 /EamA-like transporter family protein (UMAMIT33), mRNA [NM_118943]
-8.56	AT1G66180	ref|Arabidopsis thaliana Eukaryotic aspartyl protease family protein mRNA [NM_105289]
-8.58	AT4G14690	ref|Arabidopsis thaliana Chlorophyll A-B binding family protein (ELIP2), mRNA [NM_117551]
-8.58	AT5G09440	ref|Arabidopsis thaliana EXORDIUM like 4 (EXL4), mRNA [NM_120981]
-8.73	AT2G38400	ref|Arabidopsis thaliana alanine:glyoxylate aminotransferase 3 (AGT3), mRNA [NM_001202772]
-8.81	AT3G24420	ref|Arabidopsis thaliana alpha/beta-Hydrolases superfamily protein mRNA [NM_113349]
-8.88	AT2G23150	ref|Arabidopsis thaliana natural resistance-associated macrophage protein 3 (NRAMP3), mRNA [NM_127879]
-9.15	AT5G54585	ref|Arabidopsis thaliana hypothetical protein mRNA [NM_148130]
-9.25	AT1G76680	ref|Arabidopsis thaliana 12-oxophytodienoate reductase 1 (OPR1), mRNA [NM_202428]
-9.26	AT4G36850	ref|Arabidopsis thaliana PQ-loop repeat family protein / transmembrane family protein mRNA [NM_001342421]
-9.31	AT1G07400	ref|Arabidopsis thaliana HSP20-like chaperones superfamily protein mRNA [NM_100614]
-9.32	TA30874_3702	Unknown
-9.33	AT3G44300	ref|Arabidopsis thaliana nitrilase 2 (NIT2), mRNA [NM_114298]
-9.44	AT5G64260	ref|Arabidopsis thaliana EXORDIUM like 2 (EXL2), mRNA [NM_125822]
-9.74	AT5G66400	ref|Arabidopsis thaliana Dehydrin family protein (RAB18), mRNA [NM_126038]
-9.77	AT3G61060	ref|Arabidopsis thaliana phloem protein 2-A13 (PP2-A13), mRNA [NM_202741]
-10.34	AT1G03090	ref|Arabidopsis thaliana methylcrotonyl-CoA carboxylase alpha chain (MCCA), mRNA [NM_179252]
-10.73	AT4G16690	ref|Arabidopsis thaliana methyl esterase 16 (MES16), mRNA [NM_117770]
-10.84	TC309308	tc|Rep: Chromosome chr19 scaffold_4, whole genome shotgun sequence - Vitis vinifera (Grape), partial (29%) [TC396119]
-11.55	AT2G41380	ref|Arabidopsis thaliana S-adenosyl-L-methionine-dependent methyltransferases superfamily protein mRNA [NM_129701]
-12.28	AT1G66760	ref|Arabidopsis thaliana MATE efflux family protein mRNA [NM_179523]
-12.31	AT1G22500	ref|Arabidopsis thaliana RING/U-box superfamily protein (ATL15), mRNA [NM_102099]
-12.51	AT2G29490	ref|Arabidopsis thaliana glutathione S-transferase TAU 1 (GSTU1), mRNA [NM_128503]
-12.52	AT4G25580	ref|Arabidopsis thaliana CAP160 protein mRNA [NM_001341752]
-12.58	AT1G17170	ref|Arabidopsis thaliana glutathione S-transferase TAU 24 (GSTU24), mRNA [NM_101578]
-12.64	AT1G02610	ref|Arabidopsis thaliana RING/FYVE/PHD zinc finger superfamily protein mRNA [NM_001331347]
-13.3	AT5G20250	ref|Arabidopsis thaliana Raffinose synthase family protein (DIN10), mRNA [NM_001036833]
-13.3	AT3G60140	ref|Arabidopsis thaliana Glycosyl hydrolase superfamily protein (DIN2), mRNA [NM_001340024]

-13.62	TA29020_3702	Unknown
-13.64	AT3G49160	ref|Arabidopsis thaliana pyruvate kinase family protein mRNA [NM_001339402]
-13.65	AT5G14470	ref|Arabidopsis thaliana GHMP kinase family protein mRNA [NM_121451]
-14.27	AT1G80920	ref|Arabidopsis thaliana Chaperone DnaJ-domain superfamily protein (J8), mRNA [NM_106740]
-14.78	AT1G11260	ref|Arabidopsis thaliana sugar transporter 1 (STP1), mRNA [NM_100998]
-14.84	AT5G02020	ref|Arabidopsis thaliana E3 ubiquitin-protein ligase RLIM-like protein (SIS), mRNA [NM_180421]
-15.04	AT3G30775	ref|Arabidopsis thaliana Methylenetetrahydrofolate reductase family protein (ERD5), mRNA [NM_113981]
-15.3	AT3G04000	ref|Arabidopsis thaliana NAD(P)-binding Rossmann-fold superfamily protein mRNA [NM_111271]
-15.36	AT5G56870	ref|Arabidopsis thaliana beta-galactosidase 4 (BGAL4), mRNA [NM_125070]
-15.73	AT4G15610	ref|Arabidopsis thaliana Uncharacterized protein family (UPF0497) mRNA [NM_001341066]
-15.78	AT2G33830	ref|Arabidopsis thaliana Dormancy/auxin associated family protein mRNA [NM_001336474]
-16.41	AT5G06860	ref|Arabidopsis thaliana polygalacturonase inhibiting protein 1 (PGIP1), mRNA [NM_120769]
-16.93	AT5G14180	ref|Arabidopsis thaliana Myzus persicae-induced lipase 1 (MPL1), mRNA [NM_001343319]
-17.15	AT1G09500	ref|Arabidopsis thaliana NAD(P)-binding Rossmann-fold superfamily protein mRNA [NM_100821]
-17.43	AT5G39580	ref|Arabidopsis thaliana Peroxidase superfamily protein mRNA [NM_001036908]
-18.57	AT2G47270	ref|Arabidopsis thaliana transcription factor UPBEAT protein (UPB1), mRNA [NM_130295]
-18.87	AT3G45730	ref|Arabidopsis thaliana hypothetical protein mRNA [NM_114442]
-19.42	AT1G08630	ref|Arabidopsis thaliana threonine aldolase 1 (THA1), mRNA [NM_100736]
-20.29	TC304561	tc|Rep: Xylosidase - Arabidopsis thaliana (Mouse-ear cress), complete [TC384346]
-20.75	AT5G39520	ref|Arabidopsis thaliana hypothetical protein (DUF1997) mRNA [NM_123314]
-20.83	AT2G18700	ref|Arabidopsis thaliana trehalose phosphatase/synthase 11 (TPS11), mRNA [NM_127426]
-20.87	AT2G18193	ref|Arabidopsis thaliana P-loop containing nucleoside triphosphate hydrolases superfamily protein mRNA [NM_179641]
-22.64	AT1G10070	ref|Arabidopsis thaliana branched-chain amino acid transaminase 2 (BCAT-2), mRNA [NM_001035939]
-23.72	AT1G65970	ref|Arabidopsis thaliana thioredoxin-dependent peroxidase 2 (TPX2), mRNA [NM_105269]
-23.82	AT4G27450	ref|Arabidopsis thaliana aluminum induced protein with YGL and LRDR motifs mRNA [NM_118880]
-24.27	AT4G08555	ref|Arabidopsis thaliana hypothetical protein mRNA [NM_179014]
-25.61	BP667596	tc|Rep: Uncharacterized protein At4g35770.3 - Arabidopsis thaliana (Mouse-ear cress), partial (53%) [TC406344]
-27.03	BP660593	Unknown
-27.88	AT1G80160	ref|Arabidopsis thaliana Lactoylglutathione lyase / glyoxalase I family protein (GLYI7), mRNA [NM_001084382]
-28.03	TA25819_3702	Unknown
-30.14	AT4G01870	ref|Arabidopsis thaliana tolB protein-like protein mRNA [NM_001340340]
-30.24	TA29937_3702	Unknown
-30.35	BE039144	tc|Rep: Chromosome chr19 scaffold_4, whole genome shotgun sequence - Vitis vinifera (Grape), partial (59%) [TC393828]
-30.57	AT3G15450	ref|Arabidopsis thaliana aluminum induced protein with YGL and LRDR motifs mRNA [NM_001035625]
-31.15	AT2G34430	ref|Arabidopsis thaliana light-harvesting chlorophyll-protein complex II subunit B1 (LHB1B1), mRNA [NM_128995]
-33.28	AT4G30270	ref|Arabidopsis thaliana xyloglucan endotransglucosylase/hydrolase 24 (XTH24), mRNA [NM_119173]

-35.27	AT1G15380	ref|Arabidopsis thaliana Lactoylglutathione lyase / glyoxalase I family protein (GLYI4), mRNA [NM_001035972]
-35.53	AT1G05680	ref|Arabidopsis thaliana Uridine diphosphate glycosyltransferase 74E2 (UGT74E2), mRNA [NM_100448]
-41.86	TA29646_3702	gb|Arabidopsis thaliana AT4G35770 mRNA, complete cds, clone: RAFL24-21-O03 [AK319042]
-45.78	AT3G28740	ref|Arabidopsis thaliana Cytochrome P450 superfamily protein (CYP81D11), mRNA [NM_113795]
-48.13	AT5G01600	ref|Arabidopsis thaliana ferretin 1 (FER1), mRNA [NM_120238]
-55.33	AT5G49360	ref|Arabidopsis thaliana beta-xylosidase 1 (BXL1), mRNA [NM_124313]
-75.94	AT1G73120	ref|Arabidopsis thaliana F-box/RNI superfamily protein mRNA [NM_105970]
-81.95	AT3G20340	ref|Arabidopsis thaliana protein expression protein mRNA [NM_112925]
-107.47	AT3G47340	ref|Arabidopsis thaliana glutamine-dependent asparagine synthase 1 (ASN1), mRNA [NM_180333]
-305.4	AT4G35770	ref|Arabidopsis thaliana Rhodanese/Cell cycle control phosphatase superfamily protein (SEN1), mRNA [NM_001085028]
-336.01	TA29648_3702	Unknown

Supplemental Table 4: List of genes whose expression is altered by super-elevated CO_2 treatment. Genes that are differentially regulated by *A. alternata* VCs (cf. Supplemental Table 3 in Sánchez-López, et al., 2016b) are highlighted in yellow color.

Fold Change	ID	ProbeID	Description
21.39	AT1G80130	AT1G80130	ref|Arabidopsis thaliana tetratricopeptide repeat domain-containing protein mRNA, complete cds [NM_106662]
13.68	AT2G41240	BHLH100	ref|Arabidopsis thaliana transcription factor bHLH100 mRNA, complete cds [NM_129689]
12.85	AT3G56970	BHLH038	ref|Arabidopsis thaliana transcription factor ORG2 mRNA, complete cds [NM_115556]
11.58	AT2G46880	PAP14	ref|Arabidopsis thaliana purple acid phosphatase 14 mRNA, complete cds [NM_201975]
10.94	AT4G01080	TBL26	ref|Arabidopsis thaliana protein TRICHOME BIREFRINGENCE-LIKE 26 mRNA, complete cds [NM_116338]
10.37	AT3G22240	AT3G22240	ref|Arabidopsis thaliana uncharacterized protein mRNA, complete cds [NM_113122]
9.9	AT3G56980	BHLH039	ref|Arabidopsis thaliana transcription factor ORG3 mRNA, complete cds [NM_115557]
9.88	AT4G22870	AT4G22870	ref|Arabidopsis thaliana leucoanthocyanidin dioxygenase-like protein mRNA, complete cds [NM_001160794]
9.73	AT1G56650	PAP1	ref|Arabidopsis thaliana transcription factor MYB75 mRNA, complete cds [NM_104541]
9.37	AT3G22235	AT3G22235	ref|Arabidopsis thaliana uncharacterized protein mRNA, complete cds [NM_180292]
9.17	AT4G15210	BAM5	ref|Arabidopsis thaliana beta-amylase 5 mRNA, complete cds [NM_117609]
8.95	AT4G39210	APL3	ref|Arabidopsis thaliana glucose-1-phosphate adenylyltransferase large subunit 3 mRNA, complete cds [NM_120081]
8.91	AT5G17220	GSTF12	ref|Arabidopsis thaliana glutathione S-transferase phi 12 mRNA, complete cds [NM_121728]
8.59	AT3G57240	BG3	ref|Arabidopsis thaliana beta-1,3-glucanase 3 mRNA, complete cds [NM_115584]
8.26	R65132	R65132	tc|AAD15384.1 - Arabidopsis thaliana (Mouse-ear cress), partial (68%) [TC400604]
8.25	AT2G27402	AT2G27402	ref|Arabidopsis thaliana uncharacterized protein mRNA, complete cds [NM_201818]
8.19	AT3G22231	PCC1	ref|Arabidopsis thaliana protein PATHOGEN AND CIRCADIAN CONTROLLED 1 mRNA, complete cds [NM_113121]
7.82	AT4G36700	AT4G36700	ref|Arabidopsis thaliana cupin family protein mRNA, complete cds [NM_119834]
7.69	AT3G18000	CPuORF30	ref|Arabidopsis thaliana conserved peptide upstream open reading frame 30 mRNA, complete cds [NM_001125181]
7.66	AT5G54060	UF3GT	ref|Arabidopsis thaliana anthocyanidin 3-O-glucoside 2'''-O-xylosyltransferase mRNA, complete cds [NM_124785]
7.59	AT1G19960	AT1G19960	ref|Arabidopsis thaliana uncharacterized protein mRNA, complete cds [NM_101851]
7.51	AT1G47395	AT1G47395	ref|Arabidopsis thaliana uncharacterized protein mRNA, complete cds [NM_179449]
7.25	AT5G42800	DFR	ref|Arabidopsis thaliana dihydroflavonol-4-reductase mRNA, complete cds [NM_123645]
7.14	AT2G26400	ARD3	ref|Arabidopsis thaliana acireductone dioxygenase 3 mRNA, complete cds [NM_128197]
7.13	CB185526	CB185526	Unknown
6.95	AT1G78370	GSTU20	ref|Arabidopsis thaliana glutathione S-transferase TAU 20 mRNA, complete cds [NM_106484]
6.89	AT4G23600	CORI3	ref|Arabidopsis thaliana cystine lyase CORI3 mRNA, complete cds [NM_179099]
6.86	AT2G14560	LURP1	ref|Arabidopsis thaliana protein LURP1 mRNA, complete cds [NM_127019]
6.62	AT4G17470	AT4G17470	ref|Arabidopsis thaliana putative palmitoyl-protein thioesterase mRNA, complete cds [NM_001203824]
6.48	AT5G03350	AT5G03350	ref|Arabidopsis thaliana lectin-like protein mRNA, complete cds [NM_120414]
6.12	AT4G21760	BGLU47	ref|Arabidopsis thaliana beta-glucosidase 47 mRNA, complete cds [NM_118296]
5.99	AT2G42540	COR15A	ref|Arabidopsis thaliana cold-regulated protein 15a mRNA, complete cds [NM_001202804]
5.85	AT4G22880	LDOX	ref|Arabidopsis thaliana leucoanthocyanidin dioxygenase mRNA, complete cds [NM_118417]
5.8	AT1G61800	GPT2	ref|Arabidopsis thaliana glucose-6-phosphate/phosphate translocator 2 mRNA, complete cds [NM_104862]

5.73	AT1G73325	AT1G73325	ref|Arabidopsis thaliana Kunitz family trypsin and protease inhibitor protein mRNA, complete cds [NM_105992]
5.71	AT3G25795	AK227365	gb|Arabidopsis thaliana mRNA for hypothetical protein, complete cds, clone: RAFL14-04-D19 [AK227365]
5.65	AT1G04040	AT1G04040	ref|Arabidopsis thaliana HAD superfamily, subfamily IIIB acid phosphatase mRNA, complete cds [NM_100285]
5.44	AT3G03780	MS2	ref|Arabidopsis thaliana methionine synthase 2 mRNA, complete cds [NM_111249]
5.44	AT1G23100	AT1G23100	ref|Arabidopsis thaliana GroES-like protein mRNA, complete cds [NM_102158]
5.41	AT3G45140	LOX2	ref|Arabidopsis thaliana lipoxygenase 2 mRNA, complete cds [NM_114383]
5.36	AT1G68600	AT1G68600	ref|Arabidopsis thaliana Aluminum activated malate transporter family protein mRNA, complete cds [NM_105532]
5.33	AT1G62560	FMO GS-OX3	ref|Arabidopsis thaliana flavin-containing monooxygenase FMO GS-OX3 mRNA, complete cds [NM_104934]
5.24	AT1G67360	AT1G67360	ref|Arabidopsis thaliana REF/SRPP-like protein mRNA, complete cds [NM_179525]
5.22	BU917432	BU917432	gb|JKHR01A12 Size-selected small cDNAs of Arabidopsis thaliana Arabidopsis thaliana cDNA clone JKHR01A12, mRNA sequence [E
5.2	AT4G17670	AT4G17670	ref|Arabidopsis thaliana uncharacterized protein mRNA, complete cds [NM_117875]
5.15	AT5G60730	AT5G60730	ref|Arabidopsis thaliana Anion-transporting ATPase mRNA, complete cds [NM_125466]
5.1	AT2G44670	AT2G44670	ref|Arabidopsis thaliana uncharacterized protein mRNA, complete cds [NM_130031]
5.05	AT4G03060	AF418241	gb|Arabidopsis thaliana Col-0 2-oxoglutarate-dependent dioxygenase (AOP2) pseudogene, mRNA sequence [AF418241]
5.04	AT1G66390	MYB90	ref|Arabidopsis thaliana transcription factor MYB90 mRNA, complete cds [NM_105310]
5	AT5G15970	KIN2	ref|Arabidopsis thaliana stress-induced protein KIN2 mRNA, complete cds [NM_121602]
4.99	AT3G44450	AT3G44450	ref|Arabidopsis thaliana uncharacterized protein mRNA, complete cds [NM_114313]
4.94	AT2G41090	AT2G41090	ref|Arabidopsis thaliana calmodulin-like protein 10 mRNA, complete cds [NM_129674]
4.94	AT3G61920	AT3G61920	ref|Arabidopsis thaliana uncharacterized protein mRNA, complete cds [NM_116057]
4.93	AT5G14200	IMD1	ref|Arabidopsis thaliana isopropylmalate dehydrogenase 1 mRNA, complete cds [NM_001036803]
4.87	AT3G25882	NIMIN-2	ref|Arabidopsis thaliana protein NIM1-INTERACTING 2 mRNA, complete cds [NM_148752]
4.82	AT4G16590	CSLA01	ref|Arabidopsis thaliana cellulose synthase-like A01 mRNA, complete cds [NM_117760]
4.78	AT5G20190	AT5G20190	ref|Arabidopsis thaliana tetratricopeptide repeat domain-containing protein mRNA, complete cds [NM_122026]
4.76	AT3G26960	AT3G26960	ref|Arabidopsis thaliana pollen Ole e 1 allergen and extensin family protein mRNA, complete cds [NM_113610]
4.75	AT1G31690	AT1G31690	ref|Arabidopsis thaliana copper amine oxidase family protein mRNA, complete cds [NM_102904]
4.74	AT2G14247	AT2G14247	ref|Arabidopsis thaliana uncharacterized protein mRNA, complete cds [NM_201723]
4.67	AT2G22170	AT2G22170	ref|Arabidopsis thaliana PLAT-plant-stress domain-containing protein mRNA, complete cds [NM_127785]
4.65	AT1G06830	AT1G06830	ref|Arabidopsis thaliana monothiol glutaredoxin-S11 mRNA, complete cds [NM_100560]
4.65	AT4G18440	AT4G18440	ref|Arabidopsis thaliana L-aspartase-like family protein mRNA, complete cds [NM_117957]
4.62	AT4G10270	AT4G10270	ref|Arabidopsis thaliana putative wound-responsive protein mRNA, complete cds [NM_117095]
4.62	AT4G25630	FIB2	ref|Arabidopsis thaliana mediator of RNA polymerase II transcription subunit 36a mRNA, complete cds [NM_118695]
4.6	AT1G47400	AT1G47400	ref|Arabidopsis thaliana uncharacterized protein mRNA, complete cds [NM_103634]
4.55	AT3G28220	AT3G28220	ref|Arabidopsis thaliana TRAF-like family protein mRNA, complete cds [NM_113741]
4.52	AT1G32900	AT1G32900	ref|Arabidopsis thaliana granule-bound starch synthase 1 mRNA, complete cds [NM_103023]
4.52	AT1G18320	AT1G18320	ref|Arabidopsis thaliana mitochondrial import inner membrane translocase subunit TIM22-4 mRNA, complete cds [NM_101690]
4.51	AT5G15960	KIN1	ref|Arabidopsis thaliana cold and ABA inducible protein kin1 mRNA, complete cds [NM_121601]

4.51	AT5G63087	NP1655641	tc|GB|NM_001085318.1|NP_001078787.1 unknown protein;similar to unknown protein [Arabidopsis thaliana] (TAIR:AT5G63063
4.47	AT5G59670	AT5G59670	ref|Arabidopsis thaliana Leucine-rich repeat protein kinase family protein mRNA, complete cds [NM_125359]
4.46	AT3G58990	IPMI1	ref|Arabidopsis thaliana isopropylmalate isomerase 1 mRNA, complete cds [NM_115761]
4.43	AT4G23130	CRK5	ref|Arabidopsis thaliana cysteine-rich receptor-like protein kinase 5 mRNA, complete cds [NM_179094]
4.43	AT1G79400	CHX2	ref|Arabidopsis thaliana cation/H(+) antiporter 2 mRNA, complete cds [NM_106588]
4.41	AT1G56430	NAS4	ref|Arabidopsis thaliana nicotianamine synthase 4 mRNA, complete cds [NM_104521]
4.4	AT2G23010	SCPL9	ref|Arabidopsis thaliana serine carboxypeptidase-like 9 mRNA, complete cds [NM_127866]
4.39	AT1G15150	AT1G15150	ref|Arabidopsis thaliana MATE efflux family protein mRNA, complete cds [NM_101383]
4.37	AT2G43100	IPMI2	ref|Arabidopsis thaliana isopropylmalate isomerase 2 mRNA, complete cds [NM_129871]
4.36	AT5G50950	FUM2	ref|Arabidopsis thaliana fumarate hydratase 2 mRNA, complete cds [NM_124474]
4.29	AT4G02330	ATPMEPCRB	ref|Arabidopsis thaliana Probable pectinesterase/pectinesterase inhibitor 41 mRNA, complete cds [NM_116466]
4.27	AT4G11190	AT4G11190	ref|Arabidopsis thaliana disease resistance-responsive, dirigent domain-containing protein mRNA, complete cds [NM_117190]
4.27	AT1G75040	PR5	ref|Arabidopsis thaliana pathogenesis-related protein 5 mRNA, complete cds [NM_106161]
4.26	AT4G30650	AT4G30650	ref|Arabidopsis thaliana putative low temperature and salt responsive protein mRNA, complete cds [NM_119211]
4.26	AT4G08300	AT4G08300	ref|Arabidopsis thaliana nodulin MtN21 /EamA-like transporter family protein mRNA, complete cds [NM_116899]
4.25	AT5G50800	AT5G50800	ref|Arabidopsis thaliana bidirectional sugar transporter SWEET13 mRNA, complete cds [NM_124458]
4.24	AT1G16410	CYP79F1	ref|Arabidopsis thaliana dihomomethionine N-hydroxylase mRNA, complete cds [NM_101507]
4.24	AT1G64220	TOM7-2	ref|Arabidopsis thaliana mitochondrial import receptor subunit TOM7-2 mRNA, complete cds [NM_105096]
4.18	AT5G13930	TT4	ref|Arabidopsis thaliana chalcone synthase mRNA, complete cds [NM_121396]
4.18	AT3G27060	TSO2	ref|Arabidopsis thaliana ribonucleoside-diphosphate reductase small chain C mRNA, complete cds [NM_113620]
4.17	AT4G39940	AKN2	ref|Arabidopsis thaliana adenosine-5'-phosphosulfate-kinase 2 mRNA, complete cds [NM_120157]
4.17	AT1G64980	AT1G64980	ref|Arabidopsis thaliana putative nucleotide-diphospho-sugar transferase mRNA, complete cds [NM_105172]
4.1	AT3G45930	AT3G45930	ref|Arabidopsis thaliana histone H4 mRNA, complete cds [NM_114462]
4.08	AT2G40750	WRKY54	ref|Arabidopsis thaliana WRKY DNA-binding protein 54 mRNA, complete cds [NM_129637]
4.06	AT1G06000	AT1G06000	ref|Arabidopsis thaliana flavonol-7-O-rhamnosyltransferase mRNA, complete cds [NM_100480]
4.03	AT2G35860	FLA16	ref|Arabidopsis thaliana fasciclin-like arabinogalactan protein 16 mRNA, complete cds [NM_179922]
4.01	AT4G14090	AT4G14090	ref|Arabidopsis thaliana anthocyanin 5-O-glucosyltransferase mRNA, complete cds [NM_117485]
3.99	AT3G44750	HDA3	ref|Arabidopsis thaliana histone deacetylase HDT1 mRNA, complete cds [NM_114344]
3.94	AT5G67370	AT5G67370	ref|Arabidopsis thaliana uncharacterized protein mRNA, complete cds [NM_126137]
3.92	AT4G15440	HPL1	ref|Arabidopsis thaliana hydroperoxide lyase 1 mRNA, complete cds [NM_117633]
3.91	AT5G20740	AT5G20740	ref|Arabidopsis thaliana plant invertase/pectin methylesterase inhibitor domain-containing protein mRNA, complete cds [NM_12
3.9	AT5G23020	IMS2	ref|Arabidopsis thaliana methylthioalkylmalate synthase 3 mRNA, complete cds [NM_122208]
3.85	AT1G29660	AT1G29660	ref|Arabidopsis thaliana GDSL esterase/lipase mRNA, complete cds [NM_102706]
3.83	AT4G12730	FLA2	ref|Arabidopsis thaliana fasciclin-like arabinogalactan protein 2 mRNA, complete cds [NM_117342]
3.82	BP586302	BP586302	gb|BP586302 RAFL15 Arabidopsis thaliana cDNA clone RAFL15-05-M21 3', mRNA sequence [BP586302]
3.8	AT5G08640	FLS1	ref|Arabidopsis thaliana flavonol synthase 1 mRNA, complete cds [NM_001203337]

3.77	AT1G11545	XTH8	ref|Arabidopsis thaliana probable xyloglucan endotransglucosylase/hydrolase protein 8 mRNA, complete cds [NM_101028]
3.76	AT1G73600	CPuORF32	ref|Arabidopsis thaliana conserved peptide upstream open reading frame 32 mRNA, complete cds [NM_001124125]
3.76	AT1G18590	SOT17	ref|Arabidopsis thaliana sulfotransferase 17 mRNA, complete cds [NM_101717]
3.75	BU917428	BU917428	gb|JK04B05 Size-selected small cDNAs of Arabidopsis thaliana Arabidopsis thaliana cDNA clone JK04B05, mRNA sequence [BU917
3.74	AT3G23830	GRP4	ref|Arabidopsis thaliana glycine-rich RNA-binding protein 4 mRNA, complete cds [NM_180298]
3.73	AT3G03060	AT3G03060	ref|Arabidopsis thaliana P-loop containing nucleoside triphosphate hydrolases superfamily protein mRNA, complete cds [NM_111
3.73	AT2G30766	AT2G30766	ref|Arabidopsis thaliana uncharacterized protein mRNA, complete cds [NM_001124947]
3.71	AT1G65860	FMO GS-OX1	ref|Arabidopsis thaliana flavin-containing monooxygenase FMO GS-OX1 mRNA, complete cds [NM_105258]
3.71	AT5G61030	GR-RBP3	ref|Arabidopsis thaliana glycine-rich RNA-binding protein 3 mRNA, complete cds [NM_125496]
3.71	AT4G14400	ACD6	ref|Arabidopsis thaliana protein ACCELERATED CELL DEATH 6 mRNA, complete cds [NM_117519]
3.71	AT3G22550	AT3G22550	ref|Arabidopsis thaliana uncharacterized protein mRNA, complete cds [NM_113154]
3.69	AT5G15120	AT5G15120	ref|Arabidopsis thaliana uncharacterized protein mRNA, complete cds [NM_121516]
3.69	NP226468	NP226468	tc|GB|AB026649.1|BAB01078.1 gene_id:MOJ10.4~unknown protein [NP226468]
3.66	AT3G25700	AT3G25700	ref|Arabidopsis thaliana aspartyl protease family protein mRNA, complete cds [NM_113469]
3.65	AT2G33847	AT2G33847	ref|Arabidopsis thaliana uncharacterized protein mRNA, complete cds [NM_001084533]
3.64	AT1G01580	FRO2	ref|Arabidopsis thaliana ferric reduction oxidase 2 mRNA, complete cds [NM_100040]
3.63	BP783345	BP783345	Unknown
3.62	AT2G07774	AT2G07774	ref|Arabidopsis thaliana uncharacterized protein mRNA, complete cds [NM_147273]
3.6	AT1G80270	PPR596	ref|Arabidopsis thaliana pentatricopeptide repeat-containing protein mRNA, complete cds [NM_001084384]
3.6	AT5G03120	AT5G03120	ref|Arabidopsis thaliana uncharacterized protein mRNA, complete cds [NM_120390]
3.59	AT1G19640	JMT	ref|Arabidopsis thaliana jasmonic acid carboxyl methyltransferase mRNA, complete cds [NM_101820]
3.59	AT3G44860	FAMT	ref|Arabidopsis thaliana farnesoic acid carboxyl-O-methyltransferase mRNA, complete cds [NM_114355]
3.58	AT2G26440	AT2G26440	ref|Arabidopsis thaliana Probable pectinesterase/pectinesterase inhibitor 12 mRNA, complete cds [NM_128201]
3.58	AT3G29590	AT5MAT	ref|Arabidopsis thaliana malonyl-CoA:anthocyanidin 5-O-glucoside-6-O-malonyltransferase mRNA, complete cds [NM_113880]
3.58	AT5G02570	AT5G02570	ref|Arabidopsis thaliana histone H2B mRNA, complete cds [NM_120335]
3.57	AT3G51240	F3H	ref|Arabidopsis thaliana flavanone 3-hydroxylase mRNA, complete cds [NM_114983]
3.56	AT3G52370	FLA15	ref|Arabidopsis thaliana fasciclin-like arabinogalactan protein 15 mRNA, complete cds [NM_115097]
3.56	AT5G22570	WRKY38	ref|Arabidopsis thaliana putative WRKY transcription factor 38 mRNA, complete cds [NM_122163]
3.55	AT2G46650	CB5-C	ref|Arabidopsis thaliana cytochrome B5 isoform C mRNA, complete cds [NM_130230]
3.55	AT2G07815	AT2G07815	ref|Arabidopsis thaliana uncharacterized protein mRNA, complete cds [NM_001124814]
3.54	AT3G17120	AT3G17120	ref|Arabidopsis thaliana uncharacterized protein mRNA, complete cds [NM_202597]
3.54	EG453230	AT1G24270	gb|AYARG52TR pooled cDNA populations Arabidopsis thaliana cDNA, mRNA sequence [EG453230]
3.53	AT4G12030	BAT5	ref|Arabidopsis thaliana probable sodium/metabolite cotransporter BASS5 mRNA, complete cds [NM_117273]
3.51	AT5G12910	AT5G12910	ref|Arabidopsis thaliana histone H3-like 4 mRNA, complete cds [NM_121294]
3.51	AT3G23450	AT3G23450	ref|Arabidopsis thaliana uncharacterized protein mRNA, complete cds [NM_113248]
3.5	AT4G28250	EXPB3	ref|Arabidopsis thaliana expansin B3 mRNA, complete cds [NM_118965]

3.5	AT2G27840	HDT4	ref|Arabidopsis thaliana histone deacetylase HDT4 mRNA, complete cds [NM_128344]
3.49	AT1G66270	BGLU21	ref|Arabidopsis thaliana beta-glucosidase 21 mRNA, complete cds [NM_105298]
3.49	AT4G24265	AT4G24265	ref|Arabidopsis thaliana uncharacterized protein mRNA, complete cds [NM_148370]
3.46	AT2G39030	AT2G39030	ref|Arabidopsis thaliana L-ornithine N5-acetyltransferase NATA1 mRNA, complete cds [NM_129460]
3.46	AT3G52630	AT3G52630	ref|Arabidopsis thaliana Nucleic acid-binding, OB-fold-like protein mRNA, complete cds [NM_115123]
3.46	AT4G02850	AT4G02850	ref|Arabidopsis thaliana phenazine biosynthesis PhzC/PhzF family protein mRNA, complete cds [NM_116519]
3.45	AT1G54040	ESP	ref|Arabidopsis thaliana epithiospecifier protein mRNA, complete cds [NM_180632]
3.44	AT4G04940	AT4G04940	ref|Arabidopsis thaliana transducin/WD40 domain-containing protein mRNA, complete cds [NM_116732]
3.42	AT1G01190	CYP78A8	ref|Arabidopsis thaliana cytochrome P450, family 78, subfamily A, polypeptide 8 mRNA, complete cds [NM_100001]
3.42	AT1G07070	AT1G07070	ref|Arabidopsis thaliana 60S ribosomal protein L35a-1 mRNA, complete cds [NM_100581]
3.39	AT1G04240	SHY2	ref|Arabidopsis thaliana auxin-responsive protein IAA3 mRNA, complete cds [NM_100305]
3.39	AT3G09922	IPS1	ref|Arabidopsis thaliana protein ED BY PHOSPHATE STARVATION1 mRNA, complete cds [NM_180219]
3.34	AT5G61000	RPA70D	ref|Arabidopsis thaliana replication protein A 70 kDa DNA-binding subunit D mRNA, complete cds [NM_125493]
3.34	AT3G46320	AT3G46320	ref|Arabidopsis thaliana histone H4 mRNA, complete cds [NM_180329]
3.34	AT5G45650	AT5G45650	ref|Arabidopsis thaliana subtilase family protein mRNA, complete cds [NM_123933]
3.34	AT5G44565	AT5G44565	ref|Arabidopsis thaliana uncharacterized protein mRNA, complete cds [NM_203153]
3.33	AT1G52040	MBP1	ref|Arabidopsis thaliana myrosinase-binding protein 1 mRNA, complete cds [NM_104085]
3.33	AT4G00360	CYP86A2	ref|Arabidopsis thaliana cytochrome P450 86A2 mRNA, complete cds [NM_116260]
3.33	AT1G74770	AT1G74770	ref|Arabidopsis thaliana zinc ion binding protein mRNA, complete cds [NM_106135]
3.32	AT4G39950	CYP79B2	ref|Arabidopsis thaliana tryptophan N-monooxygenase 1 mRNA, complete cds [NM_120158]
3.3	AT2G16890	AT2G16890	ref|Arabidopsis thaliana UDP-glycosyltransferase 90A1 mRNA, complete cds [NM_127242]
3.3	AT3G10110	MEE67	ref|Arabidopsis thaliana mitochondrial import inner membrane translocase subunit TIM22-1 mRNA, complete cds [NM_111846]
3.3	AT3G23120	RLP38	ref|Arabidopsis thaliana receptor like protein 38 mRNA, complete cds [NM_113213]
3.29	AT1G78020	AT1G78020	ref|Arabidopsis thaliana uncharacterized protein mRNA, complete cds [NM_106451]
3.28	AT1G76790	AT1G76790	ref|Arabidopsis thaliana indole glucosinolate o-methyltransferase 5 mRNA, complete cds [NM_106329]
3.28	AT5G11740	AGP15	ref|Arabidopsis thaliana arabinogalactan protein 15 mRNA, complete cds [NM_121212]
3.26	AT2G37510	AT2G37510	ref|Arabidopsis thaliana RNA recognition motif-containing protein mRNA, complete cds [NM_129306]
3.26	AT5G22460	AT5G22460	ref|Arabidopsis thaliana esterase/lipase/thioesterase family protein mRNA, complete cds [NM_180724]
3.25	AT1G79530	GAPCP-1	ref|Arabidopsis thaliana glyceraldehyde-3-phosphate dehydrogenase GAPCP1 mRNA, complete cds [NM_106601]
3.24	AT4G37400	CYP81F3	ref|Arabidopsis thaliana cytochrome P450, family 81, subfamily F, polypeptide 3 mRNA, complete cds [NM_119903]
3.24	AT4G12880	ENODL19	ref|Arabidopsis thaliana early nodulin-like protein 19 mRNA, complete cds [NM_001203782]
3.24	AT2G33210	HSP60-2	ref|Arabidopsis thaliana heat shock protein 60-2 mRNA, complete cds [NM_179872]
3.23	AT5G05270	AT5G05270	ref|Arabidopsis thaliana Chalcone-flavanone isomerase family protein mRNA, complete cds [NM_180439]
3.23	AT1G24020	MLP423	ref|Arabidopsis thaliana MLP-like protein 423 mRNA, complete cds [NM_102249]
3.23	AT3G19350	MPC	ref|Arabidopsis thaliana maternally expressed PAB C-terminal protein mRNA, complete cds [NM_112822]
3.23	AT2G28740	HIS4	ref|Arabidopsis thaliana histone H4 mRNA, complete cds [NM_128434]

3.21	AT5G11590	TINY2	ref|Arabidopsis thaliana dehydration-responsive element-binding protein 3 mRNA, complete cds [NM_121197]
3.21	AT1G45010	AT1G45010	ref|Arabidopsis thaliana TRAM, LAG1 and CLN8 (TLC) lipid-sensing domain containing protein mRNA, complete cds [NM_103581]
3.2	AT1G45201	TLL1	ref|Arabidopsis thaliana triacylglycerol lipase-like 1 mRNA, complete cds [NM_179441]
3.2	AT1G23410	AT1G23410	ref|Arabidopsis thaliana 40S ribosomal protein S27a-1 mRNA, complete cds [NM_102190]
3.19	AT5G10390	AT5G10390	ref|Arabidopsis thaliana histone H3 mRNA, complete cds [NM_121077]
3.18	AT1G56150	AT1G56150	ref|Arabidopsis thaliana SAUR-like auxin-responsive protein mRNA, complete cds [NM_104494]
3.18	AT5G14330	AT5G14330	ref|Arabidopsis thaliana uncharacterized protein mRNA, complete cds [NM_121437]
3.17	AT4G04750	AT4G04750	ref|Arabidopsis thaliana sugar transporter ERD6-like 14 mRNA, complete cds [NM_116713]
3.17	AT2G46430	CNGC3	ref|Arabidopsis thaliana cyclic nucleotide gated channel 3 mRNA, complete cds [NM_130207]
3.17	AT1G03820	AT1G03820	ref|Arabidopsis thaliana uncharacterized protein mRNA, complete cds [NM_100261]
3.16	AT1G41830	SKS6	ref|Arabidopsis thaliana SKU5 similar 6 mRNA, complete cds [NM_103408]
3.15	AT1G19940	GH9B5	ref|Arabidopsis thaliana glycosyl hydrolase 9B5 mRNA, complete cds [NM_101849]
3.15	AT1G03495	AT1G03495	ref|Arabidopsis thaliana coumaroyl-CoA:anthocyanidin 3-O-glucoside-6-O-coumaroyltransferase 2 mRNA, complete cds [NM_100
3.15	AT2G31230	ERF15	ref|Arabidopsis thaliana ethylene-responsive transcription factor 15 mRNA, complete cds [NM_179831]
3.15	AT5G05365	AT5G05365	ref|Arabidopsis thaliana Heavy metal transport/detoxification superfamily protein mRNA, complete cds [NM_001085064]
3.14	AT4G28780	AT4G28780	ref|Arabidopsis thaliana GDSL esterase/lipase mRNA, complete cds [NM_119022]
3.13	AT5G25830	GATA12	ref|Arabidopsis thaliana GATA transcription factor 12 mRNA, complete cds [NM_122484]
3.13	AT5G44568	AT5G44568	ref|Arabidopsis thaliana uncharacterized protein mRNA, complete cds [NM_001085241]
3.12	AT1G24070	CSLA10	ref|Arabidopsis thaliana cellulose synthase-like A10 mRNA, complete cds [NM_102254]
3.12	AT2G11810	MGDC	ref|Arabidopsis thaliana Monogalactosyldiacylglycerol synthase 3 mRNA, complete cds [NM_001124829]
3.12	AT1G02450	NIMIN1	ref|Arabidopsis thaliana protein NIM1-INTERACTING 1 mRNA, complete cds [NM_100126]
3.12	AT1G61580	RPL3B	ref|Arabidopsis thaliana 60S ribosomal protein L3-2 mRNA, complete cds [NM_104840]
3.11	AT1G74440	AT1G74440	ref|Arabidopsis thaliana uncharacterized protein mRNA, complete cds [NM_106104]
3.11	AY334555	AY334555	gb|Arabidopsis thaliana At4-2 mRNA, complete sequence [AY334555]
3.09	AT2G15000	AT2G15000	ref|Arabidopsis thaliana uncharacterized protein mRNA, complete cds [NM_001084423]
3.08	AT1G52400	BGLU18	ref|Arabidopsis thaliana beta glucosidase 18 mRNA, complete cds [NM_104118]
3.07	AT2G18328	RL4	ref|Arabidopsis thaliana protein RADIALIS-like 4 mRNA, complete cds [NM_001084443]
3.06	AT1G23020	FRO3	ref|Arabidopsis thaliana ferric reduction oxidase 3 mRNA, complete cds [NM_102150]
3.06	AT3G17830	AT3G17830	ref|Arabidopsis thaliana molecular chaperone Hsp40/DnaJ family protein mRNA, complete cds [NM_112664]
3.06	AT1G65486	AT1G65486	ref|Arabidopsis thaliana uncharacterized protein mRNA, complete cds [NM_001124079]
3.06	AT3G15357	AT3G15357	ref|Arabidopsis thaliana uncharacterized protein mRNA, complete cds [NM_112403]
3.04	AT1G30530	UGT78D1	ref|Arabidopsis thaliana UDP-glucosyl transferase 78D1 mRNA, complete cds [NM_102790]
3.04	AT5G23420	HMGB6	ref|Arabidopsis thaliana high-mobility group B6 protein mRNA, complete cds [NM_122249]
3.03	AT1G45191	AT1G45191	ref|Arabidopsis thaliana beta-glucosidase 1 mRNA, complete cds [NM_179440]
3.03	AT5G64080	AT5G64080	ref|Arabidopsis thaliana Non-specific lipid-transfer protein-like protein mRNA, complete cds [NM_125804]
3.03	AT4G12600	AT4G12600	ref|Arabidopsis thaliana ribosomal protein L7Ae/L30e/S12e/Gadd45 family protein mRNA, complete cds [NM_117330]

3.03	AT2G40435	AT2G40435	ref|Arabidopsis thaliana uncharacterized protein mRNA, complete cds [NM_129604]
3.03	AT5G41460	AT5G41460	ref|Arabidopsis thaliana uncharacterized protein mRNA, complete cds [NM_123510]
3.01	AT1G09200	AT1G09200	ref|Arabidopsis thaliana histone H3 mRNA, complete cds [NM_100790]
-3.01	AT5G65870	PSK5	ref|Arabidopsis thaliana putative phytosulfokines 5 precursor mRNA, complete cds [NM_125984]
-3.01	AT2G38820	AT2G38820	ref|Arabidopsis thaliana uncharacterized protein mRNA, complete cds [NM_201907]
-3.02	AT3G03480	CHAT	ref|Arabidopsis thaliana acetyl CoA:(Z)-3-hexen-1-ol acetyltransferase mRNA, complete cds [NM_111219]
-3.02	AT4G13830	J20	ref|Arabidopsis thaliana chaperone protein dnaJ 20 mRNA, complete cds [NM_179045]
-3.02	AT1G30720	AT1G30720	ref|Arabidopsis thaliana FAD-binding Berberine family protein mRNA, complete cds [NM_102808]
-3.02	AT1G02470	AT1G02470	ref|Arabidopsis thaliana SRPBCC ligand-binding domain-containing protein mRNA, complete cds [NM_100128]
-3.03	AT3G10985	SAG20	ref|Arabidopsis thaliana senescence associated protein 20 mRNA, complete cds [NM_202550]
-3.04	AT1G68320	MYB62	ref|Arabidopsis thaliana R2R3-MYB transcription family mRNA, complete cds [NM_105503]
-3.05	AT3G26200	CYP71B22	ref|Arabidopsis thaliana cytochrome P450 71B22 mRNA, complete cds [NM_113527]
-3.06	AT1G63800	UBC5	ref|Arabidopsis thaliana ubiquitin-conjugating enzyme E2 5 mRNA, complete cds [NM_105055]
-3.07	AT5G18670	BMY3	ref|Arabidopsis thaliana putative beta-amylase BMY3 mRNA, complete cds [NM_121872]
-3.07	AT3G13450	DIN4	ref|Arabidopsis thaliana branched chain alpha-keto acid dehydrogenase E1 beta mRNA, complete cds [NM_112191]
-3.07	AT3G09580	AT3G09580	ref|Arabidopsis thaliana FAD/NAD(P)-binding oxidoreductase family protein mRNA, complete cds [NM_111792]
-3.07	AT5G13370	AT5G13370	ref|Arabidopsis thaliana auxin-responsive GH3 family protein mRNA, complete cds [NM_121340]
-3.07	AT5G44572	AT5G44572	ref|Arabidopsis thaliana uncharacterized protein mRNA, complete cds [NM_001085242]
-3.08	AT1G62380	ACO2	ref|Arabidopsis thaliana 1-aminocyclopropane-1-carboxylate oxidase 2 mRNA, complete cds [NM_104918]
-3.08	AT5G10250	DOT3	ref|Arabidopsis thaliana putative BTB/POZ domain-containing protein DOT3 mRNA, complete cds [NM_121063]
-3.08	AT2G27385	AT2G27385	ref|Arabidopsis thaliana pollen Ole e 1 allergen and extensin family protein mRNA, complete cds [NM_179769]
-3.09	AT2G38400	AGT3	ref|Arabidopsis thaliana alanine:glyoxylate aminotransferase 3 mRNA, complete cds [NM_001202772]
-3.09	AT2G36320	AT2G36320	ref|Arabidopsis thaliana zinc finger A20 and AN1 domain-containing stress-associated protein 4 mRNA, complete cds [NM_12918
-3.09	AT4G20070	AAH	ref|Arabidopsis thaliana allantoate amidohydrolase mRNA, complete cds [NM_118126]
-3.09	AT3G60300	AT3G60300	ref|Arabidopsis thaliana RWD domain-containing protein mRNA, complete cds [NM_115894]
-3.09	AT2G37750	AT2G37750	ref|Arabidopsis thaliana uncharacterized protein mRNA, complete cds [NM_129331]
-3.1	AT1G80840	WRKY40	ref|Arabidopsis thaliana putative WRKY transcription factor 40 mRNA, complete cds [NM_106732]
-3.12	AT2G37760	AT2G37760	ref|Arabidopsis thaliana aldo-keto reductase family 4 member C8 mRNA, complete cds [NM_201898]
-3.12	AT1G58180	BCA6	ref|Arabidopsis thaliana beta carbonic anhydrase 6 mRNA, complete cds [NM_179492]
-3.12	AT4G19880	AT4G19880	ref|Arabidopsis thaliana Glutathione S-transferase family protein mRNA, complete cds [NM_118108]
-3.12	AT3G61430	PIP1A	ref|Arabidopsis thaliana aquaporin PIP1-1 mRNA, complete cds [NM_001084854]
-3.12	AT5G58570	AT5G58570	ref|Arabidopsis thaliana uncharacterized protein mRNA, complete cds [NM_125244]
-3.13	AT3G15500	NAC3	ref|Arabidopsis thaliana ATAF-like NAC-domain transcription factor mRNA, complete cds [NM_112418]
-3.13	AT4G32940	GAMMA-VPE	ref|Arabidopsis thaliana vacuolar-processing enzyme gamma mRNA, complete cds [NM_119448]
-3.13	AT4G27410	RD26	ref|Arabidopsis thaliana NAC transcription factor RD26 mRNA, complete cds [NM_001084983]
-3.14	AT3G22370	AOX1A	ref|Arabidopsis thaliana alternative oxidase 1A mRNA, complete cds [NM_113135]

-3.14	AT5G62020	HSFB2A	ref|Arabidopsis thaliana heat stress transcription factor B-2a mRNA, complete cds [NM_125595]
-3.15	AT1G67810	SUFE2	ref|Arabidopsis thaliana sulfur E2 mRNA, complete cds [NM_105449]
-3.16	AT1G01720	ATAF1	ref|Arabidopsis thaliana putative transcriptional activator with NAC domain mRNA, complete cds [NM_100054]
-3.16	AT2G24100	AT2G24100	ref|Arabidopsis thaliana uncharacterized protein mRNA, complete cds [NM_127972]
-3.16	AT4G25170	AT4G25170	ref|Arabidopsis thaliana uncharacterized protein mRNA, complete cds [NM_001160795]
-3.17	AT5G14740	CA2	ref|Arabidopsis thaliana carbonic anhydrase 2 mRNA, complete cds [NM_001036806]
-3.17	AT2G28110	FRA8	ref|Arabidopsis thaliana probable glucuronoxylan glucuronosyltransferase IRX7 mRNA, complete cds [NM_179782]
-3.17	AT1G58370	RXF12	ref|Arabidopsis thaliana xylanase 1 mRNA, complete cds [NM_104617]
-3.17	AT4G35420	DRL1	ref|Arabidopsis thaliana dihydroflavonol 4-reductase-like1 mRNA, complete cds [NM_119708]
-3.17	AT5G43570	AT5G43570	ref|Arabidopsis thaliana PR-6 proteinase inhibitor family protein mRNA, complete cds [NM_123723]
-3.17	AT5G18600	AT5G18600	ref|Arabidopsis thaliana monothiol glutaredoxin-S2 mRNA, complete cds [NM_121865]
-3.17	AT3G29240	AT3G29240	ref|Arabidopsis thaliana uncharacterized protein mRNA, complete cds [NM_180317]
-3.18	AT4G15670	AT4G15670	ref|Arabidopsis thaliana monothiol glutaredoxin-S7 mRNA, complete cds [NM_117658]
-3.18	AT5G57910	AT5G57910	ref|Arabidopsis thaliana uncharacterized protein mRNA, complete cds [NM_125176]
-3.19	AT4G39090	RD19	ref|Arabidopsis thaliana cysteine proteinase RD19a mRNA, complete cds [NM_120069]
-3.2	AT2G39980	AT2G39980	ref|Arabidopsis thaliana HXXXD-type acyl-transferase-like protein mRNA, complete cds [NM_129556]
-3.2	AT3G25790	AT3G25790	ref|Arabidopsis thaliana myb-like transcription factor family protein mRNA, complete cds [NM_113478]
-3.2	AT3G06420	ATG8H	ref|Arabidopsis thaliana autophagy-related protein 8h mRNA, complete cds [NM_111517]
-3.22	AT1G11080	scpl31	ref|Arabidopsis thaliana serine carboxypeptidase-like 31 mRNA, complete cds [NM_001198028]
-3.22	AT2G17500	AT2G17500	ref|Arabidopsis thaliana auxin efflux carrier family protein mRNA, complete cds [NM_179633]
-3.22	AT5G21940	AT5G21940	ref|Arabidopsis thaliana uncharacterized protein mRNA, complete cds [NM_147877]
-3.23	AT5G18630	AT5G18630	ref|Arabidopsis thaliana putative class 3 lipase mRNA, complete cds [NM_121868]
-3.23	AT2G41230	AT2G41230	ref|Arabidopsis thaliana uncharacterized protein mRNA, complete cds [NM_180017]
-3.24	AT3G30775	ERD5	ref|Arabidopsis thaliana proline dehydrogenase 1 mRNA, complete cds [NM_113981]
-3.24	AT1G03230	AT1G03230	ref|Arabidopsis thaliana aspartyl protease-like protein mRNA, complete cds [NM_100205]
-3.25	AT5G48490	AT5G48490	ref|Arabidopsis thaliana bifunctional inhibitor/lipid-transfer protein/seed storage 2S albumin superfamily protein mRNA, complet [NM_124225]
-3.25	AT1G02850	BGLU11	ref|Arabidopsis thaliana beta glucosidase 11 mRNA, complete cds [NM_202017]
-3.25	AT2G26740	SEH	ref|Arabidopsis thaliana soluble epoxide hydrolase mRNA, complete cds [NM_128231]
-3.25	AT5G04340	ZAT6	ref|Arabidopsis thaliana zinc finger protein ZAT6 mRNA, complete cds [NM_120516]
-3.25	AT2G16340	AT2G16340	ref|Arabidopsis thaliana uncharacterized protein mRNA, complete cds [NM_127188]
-3.26	AT1G76690	OPR2	ref|Arabidopsis thaliana 12-oxophytodienoate reductase 2 mRNA, complete cds [NM_106319]
-3.26	AT1G28260	AT1G28260	ref|Arabidopsis thaliana Telomerase activating protein Est1 mRNA, complete cds [NM_102591]
-3.26	AT3G19615	AT3G19615	ref|Arabidopsis thaliana uncharacterized protein mRNA, complete cds [NM_001084720]
-3.26	AT1G16720	HCF173	ref|Arabidopsis thaliana high chlorophyll fluorescence phenotype 173 protein mRNA, complete cds [NM_101533]
-3.27	AT2G36950	AT2G36950	ref|Arabidopsis thaliana heavy-metal-associated domain-containing protein mRNA, complete cds [NM_129251]

-3.27	AT2G36895	AT2G36895	ref|Arabidopsis thaliana uncharacterized protein mRNA, complete cds [NM_179941]
-3.28	AT2G38170	CAX1	ref|Arabidopsis thaliana vacuolar cation/proton exchanger 1 mRNA, complete cds [NM_201901]
-3.28	AT1G70780	AT1G70780	ref|Arabidopsis thaliana uncharacterized protein mRNA, complete cds [NM_105746]
-3.29	AT2G22960	AT2G22960	ref|Arabidopsis thaliana putative serine carboxypeptidase-like 52 mRNA, complete cds [NM_127861]
-3.29	AT5G66480	AT5G66480	ref|Arabidopsis thaliana uncharacterized protein mRNA, complete cds [NM_126046]
-3.3	AT2G04795	AT2G04795	ref|Arabidopsis thaliana uncharacterized protein mRNA, complete cds [NM_126510]
-3.31	AT3G01500	CA1	ref|Arabidopsis thaliana carbonic anhydrase 1 mRNA, complete cds [NM_111016]
-3.32	AT3G55710	AT3G55710	ref|Arabidopsis thaliana UDP-glycosyltransferase 76F2 mRNA, complete cds [NM_115429]
-3.33	AT1G21400	AT1G21400	ref|Arabidopsis thaliana thiamin diphosphate-binding fold protein mRNA, complete cds [NM_101992]
-3.34	AT1G73920	AT1G73920	ref|Arabidopsis thaliana alpha/beta-hydrolase domain-containing protein mRNA, complete cds [NM_179552]
-3.34	AT1G27290	AT1G27290	ref|Arabidopsis thaliana uncharacterized protein mRNA, complete cds [NM_001084133]
-3.35	AT2G03760	SOT12	ref|Arabidopsis thaliana sulphotransferase 12 mRNA, complete cds [NM_126423]
-3.35	AT1G78830	AT1G78830	ref|Arabidopsis thaliana curculin-like (mannose-binding) lectin-like protein mRNA, complete cds [NM_106531]
-3.35	AT2G25090	CIPK16	ref|Arabidopsis thaliana SNF1-related kinase mRNA, complete cds [NM_128066]
-3.36	AT5G61410	RPE	ref|Arabidopsis thaliana D-ribulose-5-phosphate-3-epimerase mRNA, complete cds [NM_125534]
-3.36	AT5G64750	abr-01	ref|Arabidopsis thaliana ethylene-responsive transcription factor ABR1 mRNA, complete cds [NM_125871]
-3.36	AT2G47560	AT2G47560	ref|Arabidopsis thaliana RING-H2 finger protein ATL64 mRNA, complete cds [NM_130324]
-3.36	AT5G58770	AT5G58770	ref|Arabidopsis thaliana dehydrodolichyl diphosphate synthase 2 mRNA, complete cds [NM_125264]
-3.37	AT1G75380	BBD1	ref|Arabidopsis thaliana bifunctional nuclease 1 mRNA, complete cds [NM_179559]
-3.37	AT2G30140	AT2G30140	ref|Arabidopsis thaliana UDP-glycosyltransferase 87A2 mRNA, complete cds [NM_128569]
-3.37	AT3G52480	AT3G52480	ref|Arabidopsis thaliana uncharacterized protein mRNA, complete cds [NM_115108]
-3.38	AT4G04770	ABC1	ref|Arabidopsis thaliana ATP binding cassette protein 1 mRNA, complete cds [NM_116715]
-3.39	AT5G64250	AT5G64250	ref|Arabidopsis thaliana Aldolase-type TIM barrel family protein mRNA, complete cds [NM_125821]
-3.4	AT3G15760	AT3G15760	ref|Arabidopsis thaliana uncharacterized protein mRNA, complete cds [NM_112446]
-3.41	AT3G49160	AT3G49160	ref|Arabidopsis thaliana pyruvate kinase-like protein mRNA, complete cds [NM_114775]
-3.41	AT5G57560	TCH4	ref|Arabidopsis thaliana xyloglucan endotransglucosylase/hydrolase protein 22 mRNA, complete cds [NM_125137]
-3.41	AT1G30820	AT1G30820	ref|Arabidopsis thaliana CTP synthase-like protein mRNA, complete cds [NM_102819]
-3.43	AT1G12780	UGE1	ref|Arabidopsis thaliana bifunctional UDP-glucose 4-epimerase and UDP-xylose 4-epimerase 1 mRNA, complete cds [NM_101148]
-3.43	AT3G10120	AT3G10120	ref|Arabidopsis thaliana uncharacterized protein mRNA, complete cds [NM_111847]
-3.44	AT4G15700	AT4G15700	ref|Arabidopsis thaliana monothiol glutaredoxin-S3 mRNA, complete cds [NM_117661]
-3.45	AT3G11930	AT3G11930	ref|Arabidopsis thaliana universal stress protein-like protein mRNA, complete cds [NM_180231]
-3.45	AT5G06865	PGIP1	gb|Arabidopsis thaliana clone 108218 mRNA sequence [DQ108691]
-3.46	AT1G52100	AT1G52100	ref|Arabidopsis thaliana jacalin-like lectin domain-containing protein mRNA, complete cds [NM_001198273]
-3.46	AT4G35440	CLC-E	ref|Arabidopsis thaliana chloride channel protein CLC-e mRNA, complete cds [NM_119709]
-3.46	AT2G46220	AT2G46220	ref|Arabidopsis thaliana uncharacterized protein mRNA, complete cds [NM_130184]
-3.47	AT5G51970	AT5G51970	ref|Arabidopsis thaliana putative sorbitol dehydrogenase mRNA, complete cds [NM_124576]

-3.47	AT5G63790	NAC102	ref|Arabidopsis thaliana NAC domain-containing protein 102 mRNA, complete cds [NM_125774]
-3.47	AT4G02380	SAG21	ref|Arabidopsis thaliana senescence-associated protein SAG21 mRNA, complete cds [NM_116471]
-3.48	AT1G13700	PGL1	ref|Arabidopsis thaliana 6-phosphogluconolactonase 1 mRNA, complete cds [NM_101239]
-3.48	AT3G57760	AT3G57760	ref|Arabidopsis thaliana protein kinase family protein mRNA, complete cds [NM_001035802]
-3.51	AT4G18010	5PTASE2	ref|Arabidopsis thaliana Type I inositol-1,4,5-trisphosphate 5-phosphatase 2 mRNA, complete cds [NM_179071]
-3.51	AT5G62520	SRO5	ref|Arabidopsis thaliana probable inactive poly [ADP-ribose] polymerase SRO5 mRNA, complete cds [NM_203252]
-3.51	AT4G06746	RAP2.9	ref|Arabidopsis thaliana ethylene-responsive transcription factor RAP2-9 mRNA, complete cds [NM_179009]
-3.51	TC314163	TC405990	tc|Rep: Formate dehydrogenase - Arabidopsis thaliana (Mouse-ear cress), partial (18%) [TC405990]
-3.52	AT3G46600	AT3G46600	ref|Arabidopsis thaliana scarecrow-like protein 30 mRNA, complete cds [NM_114527]
-3.53	AT3G26220	CYP71B3	ref|Arabidopsis thaliana cytochrome P450 71B3 mRNA, complete cds [NM_113529]
-3.55	AT5G39080	AT5G39080	ref|Arabidopsis thaliana HXXXD-type acyl-transferase-like protein mRNA, complete cds [NM_123270]
-3.55	AT5G59820	RHL41	ref|Arabidopsis thaliana high light responsive zinc finger protein ZAT12 mRNA, complete cds [NM_125374]
-3.56	AT5G28770	BZO2H3	ref|Arabidopsis thaliana basic leucine zipper 63 mRNA, complete cds [NM_001036885]
-3.56	AT1G66180	AT1G66180	ref|Arabidopsis thaliana aspartyl protease family protein mRNA, complete cds [NM_105289]
-3.57	AT3G44300	NIT2	ref|Arabidopsis thaliana nitrilase 2 mRNA, complete cds [NM_114298]
-3.57	AT2G41100	TCH3	ref|Arabidopsis thaliana calmodulin-like protein 4 mRNA, complete cds [NM_001202794]
-3.57	TA35940_3702	TA35940_3702	tc|Rep: Chromosome chr18 scaffold_1, whole genome shotgun sequence - Vitis vinifera (Grape), partial (42%) [TC384450]
-3.58	AT3G01970	WRKY45	ref|Arabidopsis thaliana WRKY DNA-binding protein 45 mRNA, complete cds [NM_111063]
-3.59	AT1G20630	CAT1	ref|Arabidopsis thaliana catalase 1 mRNA, complete cds [NM_101914]
-3.59	AT3G04010	AT3G04010	ref|Arabidopsis thaliana O-glycosyl hydrolases family 17 protein mRNA, complete cds [NM_111272]
-3.6	AT2G32150	AT2G32150	ref|Arabidopsis thaliana haloacid dehalogenase-like hydrolase domain-containing protein mRNA, complete cds [NM_128774]
-3.61	AT1G69530	EXPA1	ref|Arabidopsis thaliana expansin A1 mRNA, complete cds [NM_001124101]
-3.61	AT1G20350	TIM17-1	ref|Arabidopsis thaliana translocase inner membrane subunit 17-1 mRNA, complete cds [NM_101886]
-3.62	AT4G24230	ACBP3	ref|Arabidopsis thaliana acyl-CoA-binding domain 3 mRNA, complete cds [NM_001084972]
-3.62	AT4G34710	ADC2	ref|Arabidopsis thaliana arginine decarboxylase 2 mRNA, complete cds [NM_119637]
-3.62	AT4G24050	AT4G24050	ref|Arabidopsis thaliana NAD(P)-binding Rossmann-fold superfamily protein mRNA, complete cds [NM_118537]
-3.64	AT4G20860	AT4G20860	ref|Arabidopsis thaliana FAD-binding Berberine family protein mRNA, complete cds [NM_118204]
-3.64	AT3G53140	LUT1	ref|Arabidopsis thaliana carotene epsilon-monooxygenase mRNA, complete cds [NM_115173]
-3.64	AT1G49500	AT1G49500	ref|Arabidopsis thaliana uncharacterized protein mRNA, complete cds [NM_103838]
-3.64	AT2G27830	AT2G27830	ref|Arabidopsis thaliana uncharacterized protein mRNA, complete cds [NM_128343]
-3.65	AT5G17860	CAX7	ref|Arabidopsis thaliana calcium exchanger 7 mRNA, complete cds [NM_121792]
-3.66	AT5G65110	ACX2	ref|Arabidopsis thaliana acyl-coenzyme A oxidase 2 mRNA, complete cds [NM_001037068]
-3.66	AT1G23310	GGT1	ref|Arabidopsis thaliana glutamate:glyoxylate aminotransferase mRNA, complete cds [NM_001036006]
-3.67	AT5G06570	AT5G06570	ref|Arabidopsis thaliana probable carboxylesterase 15 mRNA, complete cds [NM_120740]
-3.68	AT1G64720	CP5	ref|Arabidopsis thaliana membrane related protein CP5 mRNA, complete cds [NM_105147]
-3.68	AT5G59340	WOX2	ref|Arabidopsis thaliana WUSCHEL-related homeobox 2 mRNA, complete cds [NM_125325]

-3.68	AT3G53230	AT3G53230	ref|Arabidopsis thaliana cell division control protein 48-B mRNA, complete cds [NM_115183]
-3.68	AT4G33660	AT4G33660	ref|Arabidopsis thaliana uncharacterized protein mRNA, complete cds [NM_119522]
-3.7	AT2G05380	GRP3S	ref|Arabidopsis thaliana glycine-rich protein 3 short isoform mRNA, complete cds [NM_001124801]
-3.71	AT5G43450	AT5G43450	ref|Arabidopsis thaliana 1-aminocyclopropane-1-carboxylate oxidase-like protein mRNA, complete cds [NM_123711]
-3.71	AT1G26800	AT1G26800	ref|Arabidopsis thaliana RING/U-box domain-containing protein mRNA, complete cds [NM_102444]
-3.73	AT3G50560	AT3G50560	ref|Arabidopsis thaliana Rossmann-fold NAD(P)-binding domain-containing protein mRNA, complete cds [NM_114916]
-3.74	AT5G66650	AT5G66650	ref|Arabidopsis thaliana uncharacterized protein mRNA, complete cds [NM_126063]
-3.75	AT4G17245	AT4G17245	ref|Arabidopsis thaliana RING/U-box domain-containing protein mRNA, complete cds [NM_117830]
-3.77	AT5G64570	XYL4	ref|Arabidopsis thaliana beta-D-xylosidase 4 mRNA, complete cds [NM_125853]
-3.8	AT1G69260	AFP1	ref|Arabidopsis thaliana ABI five binding protein mRNA, complete cds [NM_105593]
-3.81	AT3G03470	CYP89A9	ref|Arabidopsis thaliana cytochrome P450, family 87, subfamily A, polypeptide 9 mRNA, complete cds [NM_111218]
-3.81	AT5G59510	RTFL5	ref|Arabidopsis thaliana protein rotundifolia like 5 mRNA, complete cds [NM_125343]
-3.83	AT1G08570	ACHT4	ref|Arabidopsis thaliana atypical CYS HIS rich thioredoxin 4 mRNA, complete cds [NM_001123776]
-3.83	AT4G34138	UGT73B1	ref|Arabidopsis thaliana UDP-glucosyl transferase 73B1 mRNA, complete cds [NM_119576]
-3.84	AT1G03220	LTP4	ref|Arabidopsis thaliana aspartyl protease-like protein mRNA, complete cds [NM_100204]
-3.85	AT5G59310	AT4G24160	ref|Arabidopsis thaliana non-specific lipid-transfer protein 4 mRNA, complete cds [NM_125322]
-3.85	AT4G24160	AT5G64190	ref|Arabidopsis thaliana lysophosphatidic acid acyltransferase mRNA, complete cds [NM_202876]
-3.85	AT5G64190	LHB1B1	ref|Arabidopsis thaliana uncharacterized protein mRNA, complete cds [NM_125815]
-3.87	AT2G34430	AT4G33150	ref|Arabidopsis thaliana light-harvesting chlorophyll protein complex II subunit B1 mRNA, complete cds [NM_128995]
-3.89	AT4G33150	NAC032	ref|Arabidopsis thaliana lysine-ketoglutarate reductase/saccharopine dehydrogenase bifunctional enzyme mRNA, complete cds [N
-3.89	AT1G77450	AT2G18193	ref|Arabidopsis thaliana NAC domain containing protein 32 mRNA, complete cds [NM_106394]
-3.9	AT2G18193	AT5G02160	ref|Arabidopsis thaliana P-loop containing nucleoside triphosphate hydrolases superfamily protein mRNA, complete cds [NM_175
-3.91	AT5G02160	GSTF3	ref|Arabidopsis thaliana uncharacterized protein mRNA, complete cds [NM_120294]
-3.92	AT2G02930	DREB2C	ref|Arabidopsis thaliana glutathione S-transferase F3 mRNA, complete cds [NM_126346]
-3.93	AT2G40340	AK221828	ref|Arabidopsis thaliana dehydration-responsive element-binding protein 2C mRNA, complete cds [NM_129594]
-3.96	AK221828	AT1G56220	gb|Arabidopsis thaliana mRNA for hypothetical protein, complete cds, clone: RAFL21-96-E04 [AK221828]
-3.99	AT1G56220	AT5G65207	ref|Arabidopsis thaliana dormancy/auxin associated protein mRNA, complete cds [NM_104501]
-4.01	AT5G65207	AT4G15690	ref|Arabidopsis thaliana uncharacterized protein mRNA, complete cds [NM_148161]
-4.02	AT4G15690	AT1G18020	ref|Arabidopsis thaliana monothiol glutaredoxin-S5 mRNA, complete cds [NM_117660]
-4.04	AT1G18020	tic20-IV	ref|Arabidopsis thaliana putative 12-oxophytodienoate reductase-like protein 2B mRNA, complete cds [NM_179352]
-4.06	AT4G03320	AT2G41730	ref|Arabidopsis thaliana translocon at the inner envelope membrane of chloroplasts 20-IV mRNA, complete cds [NM_116570]
-4.06	AT2G41730	IAGLU	ref|Arabidopsis thaliana uncharacterized protein mRNA, complete cds [NM_129737]
-4.08	AT4G15550	GolS1	ref|Arabidopsis thaliana UDP-glucose:indole-3-acetate beta-D-glucosyltransferase mRNA, complete cds [NM_117646]
-4.09	AT2G47180	AT5G47860	ref|Arabidopsis thaliana galactinol synthase 1 mRNA, complete cds [NM_130286]
-4.09	AT5G47860	SERAT2;1	ref|Arabidopsis thaliana uncharacterized protein mRNA, complete cds [NM_124160]
-4.1	AT1G55920	AT1G55920	ref|Arabidopsis thaliana serine acetyltransferase 1 mRNA, complete cds [NM_104470]

-4.1	AT5G63190	AT5G63190	ref|Arabidopsis thaliana MA3 domain-containing protein mRNA, complete cds [NM_125714]
-4.11	AT4G25390	AT4G25390	ref|Arabidopsis thaliana receptor-like serine/threonine-protein kinase mRNA, complete cds [NM_118671]
-4.11	AT3G45730	AT3G45730	ref|Arabidopsis thaliana uncharacterized protein mRNA, complete cds [NM_114442]
-4.12	AT2G25080	GPX1	ref|Arabidopsis thaliana phospholipid hydroperoxide glutathione peroxidase 1 mRNA, complete cds [NM_128065]
-4.13	AT5G14110	AT5G14110	ref|Arabidopsis thaliana uncharacterized protein mRNA, complete cds [NM_121415]
-4.16	AT3G48990	AT3G48990	ref|Arabidopsis thaliana 4-coumarate--CoA ligase-like 10 mRNA, complete cds [NM_114758]
-4.17	AT5G53970	AT5G53970	ref|Arabidopsis thaliana tyrosine aminotransferase mRNA, complete cds [NM_124776]
-4.21	AT2G26980	CIPK3	ref|Arabidopsis thaliana CBL-interacting serine/threonine-protein kinase 3 mRNA, complete cds [NM_001036350]
-4.21	AT2G23030	SNRK2.9	ref|Arabidopsis thaliana serine/threonine-protein kinase SNRK2.9 mRNA, complete cds [NM_127867]
-4.22	AT1G21550	AT1G21550	ref|Arabidopsis thaliana putative calcium-binding protein CML44 mRNA, complete cds [NM_102004]
-4.23	AT1G19660	AT1G19660	ref|Arabidopsis thaliana putative wound-responsive protein mRNA, complete cds [NM_001035991]
-4.24	AT5G20230	BCB	ref|Arabidopsis thaliana blue-copper-binding protein mRNA, complete cds [NM_122030]
-4.25	AT3G06500	AT3G06500	ref|Arabidopsis thaliana protein alkaline/neutral invertase C mRNA, complete cds [NM_111526]
-4.25	AT5G07440	GDH2	ref|Arabidopsis thaliana glutamate dehydrogenase 2 mRNA, complete cds [NM_001125712]
-4.25	AT5G07100	WRKY26	ref|Arabidopsis thaliana WRKY DNA-binding protein 26 mRNA, complete cds [NM_203017]
-4.26	AT1G71000	AT1G71000	ref|Arabidopsis thaliana chaperone DnaJ-domain containing protein mRNA, complete cds [NM_105769]
-4.26	AT2G28120	AT2G28120	ref|Arabidopsis thaliana major facilitator protein mRNA, complete cds [NM_128372]
-4.27	AT2G17880	AT2G17880	ref|Arabidopsis thaliana DNAJ heat shock N-terminal domain-containing protein mRNA, complete cds [NM_127342]
-4.28	AT2G47730	GSTF8	ref|Arabidopsis thaliana glutathione S-transferase phi 8 mRNA, complete cds [NM_180148]
-4.32	AT1G53280	AT1G53280	ref|Arabidopsis thaliana DJ1-like protein B mRNA, complete cds [NM_104206]
-4.35	AT5G14780	FDH	ref|Arabidopsis thaliana formate dehydrogenase mRNA, complete cds [NM_121482]
-4.38	AT1G66570	SUC7	ref|Arabidopsis thaliana putative sucrose transport protein SUC7 mRNA, complete cds [NM_001036165]
-4.38	AT4G25580	AT4G25580	ref|Arabidopsis thaliana CAP160 protein mRNA, complete cds [NM_118690]
-4.4	AT5G49740	FRO7	ref|Arabidopsis thaliana ferric reduction oxidase 7 mRNA, complete cds [NM_124352]
-4.4	AT3G62260	AT3G62260	ref|Arabidopsis thaliana putative protein phosphatase 2C 49 mRNA, complete cds [NM_116091]
-4.41	BU917423	BU917423	Unknown
-4.44	AT4G26530	AT4G26530	ref|Arabidopsis thaliana fructose-bisphosphate aldolase 5 mRNA, complete cds [NM_001036644]
-4.44	AT1G33110	AT1G33110	ref|Arabidopsis thaliana MATE efflux family protein mRNA, complete cds [NM_103045]
-4.45	AT3G22460	OASA2	ref|Arabidopsis thaliana O-acetylserine (thiol) lyase (OAS-TL) isoform A2 mRNA, complete cds [NM_113145]
-4.45	AT2G15960	AT2G15960	ref|Arabidopsis thaliana uncharacterized protein mRNA, complete cds [NM_127155]
-4.45	AT3G20395	AT3G20395	ref|Arabidopsis thaliana RING-finger domain-containing protein mRNA, complete cds [NM_001084725]
-4.46	AT5G49730	FRO6	ref|Arabidopsis thaliana ferric reduction oxidase 6 mRNA, complete cds [NM_124351]
-4.46	AT1G79700	AT1G79700	ref|Arabidopsis thaliana AP2-like ethylene-responsive transcription factor WRI4 mRNA, complete cds [NM_001084380]
-4.46	AT5G51070	ERD1	ref|Arabidopsis thaliana chaperone protein ClpD mRNA, complete cds [NM_124486]
-4.46	AT3G15630	AT3G15630	ref|Arabidopsis thaliana uncharacterized protein mRNA, complete cds [NM_112433]
-4.48	AT5G24490	AT5G24490	ref|Arabidopsis thaliana putative 30S ribosomal protein mRNA, complete cds [NM_122357]

-4.48	AT1G73750	AT1G73750	ref|Arabidopsis thaliana uncharacterized protein mRNA, complete cds [NM_106034]
-4.49	AT5G56100	AT5G56100	ref|Arabidopsis thaliana glycine-rich protein / oleosin mRNA, complete cds [NM_124992]
-4.49	AT4G38470	AT4G38470	ref|Arabidopsis thaliana ACT-like protein tyrosine kinase family protein mRNA, complete cds [NM_120008]
-4.5	AT2G25900	ATCTH	ref|Arabidopsis thaliana putative Cys3His zinc finger protein ATCTH mRNA, complete cds [NM_128150]
-4.51	AT1G01240	AT1G01240	ref|Arabidopsis thaliana uncharacterized protein mRNA, complete cds [NM_202007]
-4.54	AT5G16970	AER	ref|Arabidopsis thaliana 2-alkenal reductase mRNA, complete cds [NM_121703]
-4.56	AT5G57655	AT5G57655	ref|Arabidopsis thaliana xylose isomerase mRNA, complete cds [NM_180872]
-4.56	AT3G46080	AT3G46080	ref|Arabidopsis thaliana zinc finger protein ZAT8 mRNA, complete cds [NM_114477]
-4.57	AT5G16980	AT5G16980	ref|Arabidopsis thaliana zinc-binding dehydrogenase family protein mRNA, complete cds [NM_121704]
-4.57	AT1G15415	AT1G15415	ref|Arabidopsis thaliana phosphatase 2A B'gamma subunit mRNA, complete cds [NM_101411]
-4.58	AT3G15770	AT3G15770	ref|Arabidopsis thaliana uncharacterized protein mRNA, complete cds [NM_001035628]
-4.6	AT1G05340	AT1G05340	ref|Arabidopsis thaliana uncharacterized protein mRNA, complete cds [NM_100413]
-4.62	AT2G24550	AT2G24550	ref|Arabidopsis thaliana uncharacterized protein mRNA, complete cds [NM_128016]
-4.62	CF652575	TA32560_3702	tc|Rep: Beta-glucosidase - Arabidopsis thaliana (Mouse-ear cress), partial (29%) [TC395229]
-4.63	AT3G61060	PP2-A13	ref|Arabidopsis thaliana phloem protein 2-A13 mRNA, complete cds [NM_202741]
-4.66	AT5G44973	AT5G44973	ref|Arabidopsis thaliana defensin-like protein 285 mRNA, complete cds [NM_001036935]
-4.66	AT5G64260	EXL2	ref|Arabidopsis thaliana protein EXORDIUM like 2 mRNA, complete cds [NM_125822]
-4.67	AT1G63180	UGE3	ref|Arabidopsis thaliana UDP-glucose 4-epimerase mRNA, complete cds [NM_104996]
-4.69	AT4G13250	NYC1	ref|Arabidopsis thaliana probable chlorophyll(ide) b reductase NYC1 mRNA, complete cds [NM_117396]
-4.72	AT3G49620	DIN11	ref|Arabidopsis thaliana 2-oxoacid-dependent dioxygenase-like protein DIN11 mRNA, complete cds [NM_114822]
-4.72	NP229859	NP229859	tc|GB|AL391141.1|CAC01711.1 quinone oxidoreductase-like protein [NP229859]
-4.73	AT5G13330	Rap2.6L	ref|Arabidopsis thaliana ethylene-responsive transcription factor ERF113 mRNA, complete cds [NM_121336]
-4.74	AT3G14660	CYP72A13	ref|Arabidopsis thaliana cytochrome P450, family 72, subfamily A, polypeptide 13 mRNA, complete cds [NM_112327]
-4.74	AT3G16770	EBP	ref|Arabidopsis thaliana ethylene-responsive transcription factor RAP2-3 mRNA, complete cds [NM_112550]
-4.74	AT5G14120	AT5G14120	ref|Arabidopsis thaliana major facilitator protein mRNA, complete cds [NM_121416]
-4.75	AT3G10740	ASD1	ref|Arabidopsis thaliana bifunctional alpha-l-arabinofuranosidase/beta-d-xylosidase mRNA, complete cds [NM_111911]
-4.75	AT5G49480	CP1	ref|Arabidopsis thaliana Ca2+-binding protein 1 mRNA, complete cds [NM_124325]
-4.77	AT4G12735	AT4G12735	ref|Arabidopsis thaliana uncharacterized protein mRNA, complete cds [NM_202810]
-4.82	AT2G45170	ATG8E	ref|Arabidopsis thaliana autophagy-related protein 8e mRNA, complete cds [NM_180100]
-4.82	AT2G22990	SNG1	ref|Arabidopsis thaliana sinapoylglucose:malate sinapoyltransferase mRNA, complete cds [NM_127864]
-4.85	AT2G39400	AT2G39400	ref|Arabidopsis thaliana alpha/beta-Hydrolases superfamily protein mRNA, complete cds [NM_129497]
-4.85	AT5G48180	NSP5	ref|Arabidopsis thaliana nitrile specifier protein 5 mRNA, complete cds [NM_124193]
-4.85	AT5G15850	COL1	ref|Arabidopsis thaliana zinc finger protein CONSTANS-LIKE 1 mRNA, complete cds [NM_121590]
-4.86	AT3G14630	CYP72A9	ref|Arabidopsis thaliana cytochrome P450, family 72, subfamily A, polypeptide 9 mRNA, complete cds [NM_112324]
-4.87	AT1G37130	NIA2	ref|Arabidopsis thaliana nitrate reductase [NADH] 2 mRNA, complete cds [NM_103364]
-4.87	AT3G46660	UGT76E12	ref|Arabidopsis thaliana UDP-glucosyl transferase 76E12 mRNA, complete cds [NM_114533]

-4.92	AT1G23390	AT1G23390	ref|Arabidopsis thaliana F-box/kelch-repeat protein mRNA, complete cds [NM_102188]
-4.95	AT1G72900	AT1G72900	ref|Arabidopsis thaliana Toll-Interleukin-Resistance domain-containing protein mRNA, complete cds [NM_105948]
-4.95	TC309308	TC396119	tc|Rep: Chromosome chr19 scaffold_4, whole genome shotgun sequence - Vitis vinifera (Grape), partial (29%) [TC396119]
-4.98	AT1G07890	APX1	ref|Arabidopsis thaliana L-ascorbate peroxidase 1 mRNA, complete cds [NM_001123772]
-5	AT5G22920	AT5G22920	ref|Arabidopsis thaliana ring finger and CHY zinc finger domain-containing protein 1 mRNA, complete cds [NM_122198]
-5.04	AT5G52640	HSP90.1	ref|Arabidopsis thaliana heat shock protein 90.1 mRNA, complete cds [NM_124642]
-5.05	AT3G28210	PMZ	ref|Arabidopsis thaliana zinc finger (AN1-like) family protein mRNA, complete cds [NM_113740]
-5.09	AT5G54080	HGO	ref|Arabidopsis thaliana homogentisate 1,2-dioxygenase mRNA, complete cds [NM_180856]
-5.1	AT2G20670	AT2G20670	ref|Arabidopsis thaliana uncharacterized protein mRNA, complete cds [NM_127631]
-5.14	AT1G70290	TPS8	ref|Arabidopsis thaliana putative alpha,alpha-trehalose-phosphate synthase [UDP-forming] 8 mRNA, complete cds [NM_105697]
-5.14	AT1G72680	CAD1	ref|Arabidopsis thaliana cinnamyl-alcohol dehydrogenase mRNA, complete cds [NM_105927]
-5.14	AT2G23150	NRAMP3	ref|Arabidopsis thaliana metal transporter Nramp3 mRNA, complete cds [NM_127879]
-5.18	AT1G22890	AT1G22890	ref|Arabidopsis thaliana uncharacterized protein mRNA, complete cds [NM_102136]
-5.2	AT5G39050	AT5G39050	ref|Arabidopsis thaliana phenolic glucoside malonyltransferase 1 mRNA, complete cds [NM_123267]
-5.29	AT2G31945	AT2G31945	ref|Arabidopsis thaliana uncharacterized protein mRNA, complete cds [NM_128753]
-5.31	AT1G60140	TPS10	ref|Arabidopsis thaliana putative alpha,alpha-trehalose-phosphate synthase [UDP-forming] 10 mRNA, complete cds [NM_104705
-5.33	AT4G36040	AT4G36040	ref|Arabidopsis thaliana chaperone protein dnaJ 11 mRNA, complete cds [NM_119771]
-5.33	AT1G68190	AT1G68190	ref|Arabidopsis thaliana putative zinc finger protein mRNA, complete cds [NM_105490]
-5.33	AT4G16680	AT4G16680	ref|Arabidopsis thaliana putative RNA helicase mRNA, complete cds [NM_117769]
-5.34	AT5G21170	AKINBETA1	ref|Arabidopsis thaliana SNF1-related protein kinase regulatory subunit beta-1 mRNA, complete cds [NM_001036841]
-5.34	AT2G41380	AT2G41380	ref|Arabidopsis thaliana S-adenosyl-L-methionine-dependent methyltransferase-like protein mRNA, complete cds [NM_129701]
-5.35	AT5G24800	BZIP9	ref|Arabidopsis thaliana basic leucine zipper 9 mRNA, complete cds [NM_122389]
-5.35	AT1G69490	NAP	ref|Arabidopsis thaliana NAC transcription factor protein family mRNA, complete cds [NM_105616]
-5.37	AT4G37370	CYP81D8	ref|Arabidopsis thaliana cytochrome P450, family 81, subfamily D, polypeptide 8 mRNA, complete cds [NM_119900]
-5.39	AT4G36850	AT4G36850	ref|Arabidopsis thaliana PQ-loop repeat family protein / transmembrane family protein mRNA, complete cds [NM_119849]
-5.4	AT1G22400	UGT85A1	ref|Arabidopsis thaliana UDP-glycosyltransferase 85A1 mRNA, complete cds [NM_102089]
-5.41	AT5G26200	AT5G26200	ref|Arabidopsis thaliana mitochondrial substrate carrier family protein mRNA, complete cds [NM_122521]
-5.42	AT1G15040	AT1G15040	ref|Arabidopsis thaliana putative glutamine amidotransferase mRNA, complete cds [NM_101374]
-5.46	AT5G54165	AT5G54165	ref|Arabidopsis thaliana uncharacterized protein mRNA, complete cds [NM_001125962]
-5.48	BP660593	BP660593	Unknown
-5.49	AT1G10070	BCAT-2	ref|Arabidopsis thaliana branched-chain-amino-acid aminotransferase 2 mRNA, complete cds [NM_001035939]
-5.53	TA32559_3702	TA32559_3702	tc|Rep: AT3g60140/T2O9_120 - Arabidopsis thaliana (Mouse-ear cress), partial (9%) [TC397325]
-5.55	AT1G54100	ALDH7B4	ref|Arabidopsis thaliana aldehyde dehydrogenase 7B4 mRNA, complete cds [NM_104287]
-5.55	AT3G13750	BGAL1	ref|Arabidopsis thaliana beta galactosidase 1 mRNA, complete cds [NM_112225]
-5.61	AT3G12580	HSP70	ref|Arabidopsis thaliana heat shock protein 70-4 mRNA, complete cds [NM_112093]
-5.63	AT2G37130	AT2G37130	ref|Arabidopsis thaliana peroxidase mRNA, complete cds [NM_001124989]

-5.64	AT5G47560	TDT	ref|Arabidopsis thaliana tonoplast dicarboxylate transporter mRNA, complete cds [NM_124129]
-5.67	AT1G03090	MCCA	ref|Arabidopsis thaliana methylcrotonoyl-CoA carboxylase subunit alpha mRNA, complete cds [NM_179252]
-5.71	AT4G30270	XTH24	ref|Arabidopsis thaliana xyloglucan endotransglucosylase/hydrolase protein 24 mRNA, complete cds [NM_119173]
-5.75	AT2G37770	AT2G37770	ref|Arabidopsis thaliana aldo-keto reductase family 4 member C9 mRNA, complete cds [NM_001036428]
-5.81	AT2G26150	HSFA2	ref|Arabidopsis thaliana heat stress transcription factor A-2 mRNA, complete cds [NM_001124916]
-5.81	AT2G29420	GSTU7	ref|Arabidopsis thaliana glutathione S-transferase tau 7 mRNA, complete cds [NM_128496]
-5.82	AT4G17840	AT4G17840	ref|Arabidopsis thaliana uncharacterized protein mRNA, complete cds [NM_117893]
-5.86	AT1G06570	PDS1	ref|Arabidopsis thaliana 4-hydroxyphenylpyruvate dioxygenase mRNA, complete cds [NM_100536]
-5.87	AT5G25130	CYP71B12	ref|Arabidopsis thaliana cytochrome P450 71B12 mRNA, complete cds [NM_122422]
-5.89	AT5G06860	PGIP1	ref|Arabidopsis thaliana polygalacturonase inhibitor 1 mRNA, complete cds [NM_120769]
-5.9	AT1G52690	AT1G52690	ref|Arabidopsis thaliana Late embryogenesis abundant protein (LEA) family protein mRNA, complete cds [NM_202280]
-5.91	AT5G17170	ENH1	ref|Arabidopsis thaliana protein ENHANCER OF SOS3-1 mRNA, complete cds [NM_001085129]
-5.99	AT3G29035	NAC3	ref|Arabidopsis thaliana NAC domain-containing protein 3 mRNA, complete cds [NM_113825]
-6.02	AT2G43820	UGT74F2	ref|Arabidopsis thaliana UDP-glucosyltransferase 74F2 mRNA, complete cds [NM_129944]
-6.05	AT2G47770	TSPO	ref|Arabidopsis thaliana tryptophan-rich sensory protein-like protein mRNA, complete cds [NM_130344]
-6.09	AT1G02610	AT1G02610	ref|Arabidopsis thaliana RING/FYVE/PHD zinc finger-containing protein mRNA, complete cds [NM_100141]
-6.12	AT3G07350	AT3G07350	ref|Arabidopsis thaliana uncharacterized protein mRNA, complete cds [NM_111614]
-6.16	AT5G39610	NAC6	ref|Arabidopsis thaliana NAC-domain transcription factor mRNA, complete cds [NM_123323]
-6.18	AT4G24972	TPD1	ref|Arabidopsis thaliana protein TAPETUM DETERMINANT 1 mRNA, complete cds [NM_202883]
-6.22	AT1G13990	AT1G13990	ref|Arabidopsis thaliana uncharacterized protein mRNA, complete cds [NM_001160863]
-6.23	AT1G75490	AT1G75490	ref|Arabidopsis thaliana dehydration-responsive element-binding protein 2D mRNA, complete cds [NM_106202]
-6.25	AT1G22500	AT1G22500	ref|Arabidopsis thaliana putative C3HC4-type RING zinc finger protein mRNA, complete cds [NM_102099]
-6.27	AT5G61820	AT5G61820	ref|Arabidopsis thaliana uncharacterized protein mRNA, complete cds [NM_125576]
-6.28	AT5G63160	BT1	ref|Arabidopsis thaliana BTB and TAZ domain protein 1 mRNA, complete cds [NM_125711]
-6.29	AT4G15610	AT4G15610	ref|Arabidopsis thaliana uncharacterized protein mRNA, complete cds [NM_117652]
-6.31	AT5G14730	AT5G14730	ref|Arabidopsis thaliana uncharacterized protein mRNA, complete cds [NM_121477]
-6.34	AT5G59400	AT5G59400	ref|Arabidopsis thaliana uncharacterized protein mRNA, complete cds [NM_125331]
-6.36	AT2G02710	PLPB	ref|Arabidopsis thaliana PAS/LOV protein B mRNA, complete cds [NM_201672]
-6.46	AT5G33355	AT5G33355	ref|Arabidopsis thaliana defensin-like protein mRNA, complete cds [NM_147989]
-6.49	AT2G29490	GSTU1	ref|Arabidopsis thaliana glutathione S-transferase tau 1 mRNA, complete cds [NM_128503]
-6.49	AT3G10020	AT3G10020	ref|Arabidopsis thaliana uncharacterized protein mRNA, complete cds [NM_111837]
-6.51	AT3G48360	BT2	ref|Arabidopsis thaliana TAC1-mediated telomerase activation pathway protein BT2 mRNA, complete cds [NM_114697]
-6.52	AT5G64230	AT5G64230	ref|Arabidopsis thaliana uncharacterized protein mRNA, complete cds [NM_125819]
-6.54	AT3G59930	AT3G59930	ref|Arabidopsis thaliana defensin-like protein 206 mRNA, complete cds [NM_115856]
-6.56	TC309871	TC396686	tc|Rep: Conglutin gamma-like protein - Arabidopsis thaliana (Mouse-ear cress), partial (35%) [TC396686]
-6.63	AT1G02820	AT1G02820	ref|Arabidopsis thaliana late embryogenesis abundant 3-like protein mRNA, complete cds [NM_100163]

-6.65	AT4G34131	UGT73B3	ref|Arabidopsis thaliana UDP-glucosyl transferase 73B3 mRNA, complete cds [NM_119574]
-6.7	AT4G34135	UGT73B2	ref|Arabidopsis thaliana UDP-glucosyltransferase 73B2 mRNA, complete cds [NM_179161]
-6.73	AT3G14990	AT3G14990	ref|Arabidopsis thaliana protein DJ-1-like A mRNA, complete cds [NM_001035621]
-6.74	BP667596	BP667596	tc|Rep: Uncharacterized protein At4g35770.3 - Arabidopsis thaliana (Mouse-ear cress), partial (53%) [TC406344]
-6.79	AT1G62510	AT1G62510	ref|Arabidopsis thaliana bifunctional inhibitor/lipid-transfer protein/seed storage 2S albumin-like protein mRNA, complete cds [N
-6.88	AT1G10585	AT1G10585	ref|Arabidopsis thaliana basic helix-loop-helix domain-containing protein mRNA, complete cds [NM_100934]
-6.98	AT5G51720	AT5G51720	ref|Arabidopsis thaliana CDGSH iron-sulfur domain-containing protein NEET mRNA, complete cds [NM_124551]
-7.01	AT4G39675	AT4G39675	ref|Arabidopsis thaliana uncharacterized protein mRNA, complete cds [NM_120128]
-7.03	AT5G05410	DREB2A	ref|Arabidopsis thaliana dehydration-responsive element-binding protein 2A mRNA, complete cds [NM_120623]
-7.04	AT4G37610	BT5	ref|Arabidopsis thaliana BTB and TAZ domain protein 5 mRNA, complete cds [NM_119924]
-7.1	AT5G49450	bZIP1	ref|Arabidopsis thaliana basic leucine-zipper 1 mRNA, complete cds [NM_124322]
-7.14	AT1G23870	TPS9	ref|Arabidopsis thaliana putative alpha,alpha-trehalose-phosphate synthase [UDP-forming] 9 mRNA, complete cds [NM_102235]
-7.17	AT1G71030	MYBL2	ref|Arabidopsis thaliana putative myb family transcription factor mRNA, complete cds [NM_105772]
-7.22	AT3G49790	AT3G49790	ref|Arabidopsis thaliana Carbohydrate-binding protein mRNA, complete cds [NM_114839]
-7.25	AT5G39520	AT5G39520	ref|Arabidopsis thaliana uncharacterized protein mRNA, complete cds [NM_123314]
-7.29	AT1G19530	AT1G19530	ref|Arabidopsis thaliana uncharacterized protein mRNA, complete cds [NM_101811]
-7.32	AT2G15490	UGT73B4	ref|Arabidopsis thaliana UDP-glycosyltransferase 73B4 mRNA, complete cds [NM_127109]
-7.46	AT1G28330	DYL1	ref|Arabidopsis thaliana dormancy-associated protein-like 1 mRNA, complete cds [NM_001160906]
-7.65	AT5G19120	AT5G19120	ref|Arabidopsis thaliana aspartyl protease family protein mRNA, complete cds [NM_121917]
-7.66	AT5G52570	BETA-OHASE 2	ref|Arabidopsis thaliana beta-carotene hydroxylase 2 mRNA, complete cds [NM_124636]
-7.85	AT1G72060	AT1G72060	ref|Arabidopsis thaliana serine-type endopeptidase inhibitor mRNA, complete cds [NM_105864]
-7.86	AT1G08630	THA1	ref|Arabidopsis thaliana threonine aldolase mRNA, complete cds [NM_100736]
-7.95	AT1G71520	AT1G71520	ref|Arabidopsis thaliana ERF/AP2 transcription factor family protein DREB A-5 mRNA, complete cds [NM_105820]
-7.98	AT2G36750	UGT73C1	ref|Arabidopsis thaliana UDP-glucosyl transferase 73C1 mRNA, complete cds [NM_129230]
-8.03	AT3G45300	IVD	ref|Arabidopsis thaliana isovaleryl-CoA-dehydrogenase mRNA, complete cds [NM_114399]
-8.48	AT1G66760	AT1G66760	ref|Arabidopsis thaliana MATE efflux family protein mRNA, complete cds [NM_179523]
-8.61	AT1G43160	RAP2.6	ref|Arabidopsis thaliana ethylene-responsive transcription factor RAP2-6 mRNA, complete cds [NM_103468]
-8.64	AT2G15480	UGT73B5	ref|Arabidopsis thaliana UDP-glucosyl transferase 73B5 mRNA, complete cds [NM_127108]
-8.71	AT1G15380	AT1G15380	ref|Arabidopsis thaliana Lactoylglutathione lyase / glyoxalase I family protein mRNA, complete cds [NM_101407]
-8.71	AT2G29480	GSTU2	ref|Arabidopsis thaliana glutathione S-transferase tau 2 mRNA, complete cds [NM_128502]
-8.75	AT1G05560	UGT75B1	ref|Arabidopsis thaliana UDP-glucosyltransferase 75B1 mRNA, complete cds [NM_100435]
-8.76	AT1G11260	STP1	ref|Arabidopsis thaliana sugar transporter 1 mRNA, complete cds [NM_100998]
-8.85	AT1G15010	AT1G15010	ref|Arabidopsis thaliana uncharacterized protein mRNA, complete cds [NM_101370]
-9.32	AT1G77760	NIA1	ref|Arabidopsis thaliana nitrate reductase [NADH] 1 mRNA, complete cds [NM_106425]
-9.76	AT2G40000	HSPRO2	ref|Arabidopsis thaliana HS1 PRO-1 2-like protein mRNA, complete cds [NM_129558]
-9.94	AT2G36800	DOGT1	ref|Arabidopsis thaliana UDP-glycosyltransferase 73C5 mRNA, complete cds [NM_129235]

-10.1	AT1G76600	AT1G76600	ref|Arabidopsis thaliana uncharacterized protein mRNA, complete cds [NM_106310]
-10.12	AT4G35090	CAT2	ref|Arabidopsis thaliana catalase 2 mRNA, complete cds [NM_119675]
-10.19	AT4G15760	MO1	ref|Arabidopsis thaliana monooxygenase 1 mRNA, complete cds [NM_001203809]
-10.72	AT5G20250	DIN10	ref|Arabidopsis thaliana putative galactinol--sucrose galactosyltransferase 6 mRNA, complete cds [NM_001036833]
-10.8	AT1G76680	OPR1	ref|Arabidopsis thaliana 12-oxophytodienoate reductase 1 mRNA, complete cds [NM_106318]
-11.01	AT5G51440	AT5G51440	ref|Arabidopsis thaliana heat shock protein 23.5 mRNA, complete cds [NM_124523]
-11.06	AT1G80440	AT1G80440	ref|Arabidopsis thaliana F-box/kelch-repeat protein mRNA, complete cds [NM_106692]
-11.13	AT1G65970	TPX2	ref|Arabidopsis thaliana thioredoxin-dependent peroxidase 2 mRNA, complete cds [NM_105269]
-11.18	AT4G16690	MES16	ref|Arabidopsis thaliana methyl esterase 16 mRNA, complete cds [NM_117770]
-11.56	AT4G33666	AT4G33666	ref|Arabidopsis thaliana uncharacterized protein mRNA, complete cds [NM_119524]
-11.92	AT2G47270	AT2G47270	ref|Arabidopsis thaliana transcription factor UPBEAT1 mRNA, complete cds [NM_130295]
-12.02	AT5G54585	AT5G54585	ref|Arabidopsis thaliana uncharacterized protein mRNA, complete cds [NM_148130]
-12.03	AT1G80920	J8	ref|Arabidopsis thaliana chaperone protein dnaJ 8 mRNA, complete cds [NM_106740]
-12.2	AT2G36780	AT2G36780	ref|Arabidopsis thaliana UDP-glucosyl transferase 73C3 mRNA, complete cds [NM_129233]
-12.35	AT5G22140	AT5G22140	ref|Arabidopsis thaliana FAD/NAD(P)-binding oxidoreductase family protein mRNA, complete cds [NM_147895]
-12.43	AT5G16960	AT5G16960	ref|Arabidopsis thaliana zinc-binding dehydrogenase family protein mRNA, complete cds [NM_121702]
-13.14	AT3G04000	AT3G04000	ref|Arabidopsis thaliana aldehyde reductase mRNA, complete cds [NM_111271]
-13.43	AT1G17170	GSTU24	ref|Arabidopsis thaliana glutathione S-transferase TAU 24 mRNA, complete cds [NM_101578]
-14.23	AT1G07400	AT1G07400	ref|Arabidopsis thaliana class I heat shock protein mRNA, complete cds [NM_100614]
-14.85	AT5G66400	RAB18	ref|Arabidopsis thaliana dehydrin Rab18 mRNA, complete cds [NM_126038]
-14.87	AT1G80160	AT1G80160	ref|Arabidopsis thaliana GLYOXYLASE I 7 mRNA, complete cds [NM_001084382]
-15.89	AT4G27450	AT4G27450	ref|Arabidopsis thaliana aluminum induced protein with YGL and LRDR motifs mRNA, complete cds [NM_118880]
-16.14	AT2G33830	AT2G33830	ref|Arabidopsis thaliana dormancy/auxin associated protein mRNA, complete cds [NM_179889]
-16.16	AT2G18700	TPS11	ref|Arabidopsis thaliana putative alpha,alpha-trehalose-phosphate synthase [UDP-forming] 11 mRNA, complete cds [NM_127426
-16.54	TC304561	TC384346	tc|Rep: Xylosidase - Arabidopsis thaliana (Mouse-ear cress), complete [TC384346]
-16.74	AT1G09500	AT1G09500	ref|Arabidopsis thaliana alcohol dehydrogenase-like protein mRNA, complete cds [NM_001035935]
-17.51	AT5G14180	MPL1	ref|Arabidopsis thaliana Myzus persicae-induced lipase 1 mRNA, complete cds [NM_121422]
-17.67	AT5G02020	AT5G02020	ref|Arabidopsis thaliana uncharacterized protein mRNA, complete cds [NM_180421]
-17.72	AT5G56870	BGAL4	ref|Arabidopsis thaliana beta-galactosidase 4 mRNA, complete cds [NM_125070]
-19.16	AT5G14470	AT5G14470	ref|Arabidopsis thaliana GHMP kinase family protein mRNA, complete cds [NM_121451]
-19.62	AT2G05540	AT2G05540	ref|Arabidopsis thaliana glycine-rich protein mRNA, complete cds [NM_126577]
-20.85	AT3G24420	AT3G24420	ref|Arabidopsis thaliana hydrolase, alpha/beta fold family protein mRNA, complete cds [NM_113349]
-22.75	AT4G08555	AT4G08555	ref|Arabidopsis thaliana uncharacterized protein mRNA, complete cds [NM_179014]
-23	AT3G28740	CYP81D1	ref|Arabidopsis thaliana cytochrome P450 CYP81D11 mRNA, complete cds [NM_113795]
-24.7	AT3G60140	DIN2	ref|Arabidopsis thaliana beta-glucosidase 30 mRNA, complete cds [NM_115877]
-25.49	AT5G01600	FER1	ref|Arabidopsis thaliana ferritin 1 mRNA, complete cds [NM_120238]

-31.28	AT1G73120	AT1G73120	ref|Arabidopsis thaliana uncharacterized protein mRNA, complete cds [NM_105970]
-34.59	AT3G20340	AT3G20340	ref|Arabidopsis thaliana paraquat downregulated protein mRNA, complete cds [NM_112925]
-41.4	AT3G15450	AT3G15450	ref|Arabidopsis thaliana aluminum induced protein with YGL and LRDR motif mRNA, complete cds [NM_001035625]
-41.54	AT1G05680	UGT74E2	ref|Arabidopsis thaliana Uridine diphosphate glycosyltransferase 74E2 mRNA, complete cds [NM_100448]
-41.68	AT5G49360	BXL1	ref|Arabidopsis thaliana bifunctional {beta}-D-xylosidase/{alpha}-L-arabinofuranosidase mRNA, complete cds [NM_124313]
-41.95	AT4G01870	AT4G01870	ref|Arabidopsis thaliana tolB-related protein mRNA, complete cds [NM_116417]
-42.02	BE039144	BE039144	tc|Rep: Chromosome chr19 scaffold_4, whole genome shotgun sequence - Vitis vinifera (Grape), partial (59%) [TC393828]
-48.66	AT3G47340	ASN1	ref|Arabidopsis thaliana asparagine synthetase [glutamine-hydrolyzing] mRNA, complete cds [NM_180333]
-111.32	AT4G35770	SEN1	ref|Arabidopsis thaliana senescence-associated protein DIN1 mRNA, complete cds [NM_119743]

Supplemental Table 5: List of genes whose expression is altered by high irradiance treatment (Athanasiou et al., 2010). Genes that are differentially regulated by *A. alternata* VCs (cf. Supplemental Table 3 in Sánchez-López, et al., 2016) are highlighted in yellow color.

Representative Public ID	Gene Title	Fold change
At1g74670	gibberellin-responsive protein, putative	-22.4
At2g40610	expansin, putative (EXP8)	-16.2
At5g48490	protease inhibitor/seed storage/lipid transfer protein (LTP) family protein	-15.4
At3g15450	expressed protein	-12.1
At1g70290	trehalose-6-phosphate synthase, putative	-10.4
At1g23390	kelch repeat-containing F-box family protein	-10.2
At2g25900	zinc finger (CCCH-type) family protein	-9.8
At2g22980	serine carboxypeptidase S10 family protein	-9.6
At2g18700	glycosyl transferase family 20 protein / trehalose-phosphatase family protein	-9.5
At2g33830	dormancy/auxin associated family protein	-9.2
At5g59080	expressed protein	-9.2
At5g61590	AP2 domain-containing transcription factor family protein	-9
At5g02760	protein phosphatase 2C family protein / PP2C family protein	-8.8
At2g15890	expressed protein	-8.6
At1g80920	DNAJ heat shock N-terminal domain-containing protein	-8.5
At5g40890	chloride channel protein (CLC-a)	-8.3
At1g72150	SEC14 cytosolic factor family protein / phosphoglyceride transfer family protein	-8
At5g24490	30S ribosomal protein, putative	-8
At5g22920	zinc finger (C3HC4-type RING finger) family protein	-8
At4g24800	MA3 domain-containing protein	-7.8
At1g18620	expressed protein	-7.7
At2g44740	cyclin family protein	-7.4
At4g30690	translation initiation factor 3 (IF-3) family protein	-7
At3g19850	phototropic-responsive NPH3 family protein	-6.9
At3g13750	beta-galactosidase, putative / lactase, putative	-6.7
At1g63800	ubiquitin-conjugating enzyme 5 (UBC5)	-6.6
At3g62550	universal stress protein (USP) family protein	-6.5
At5g35790	glucose-6-phosphate 1-dehydrogenase / G6PD (APG1)	-6.5
At1g19660	wound-responsive family protein /// wound-responsive protein-related	-6.4
At1g80440	kelch repeat-containing F-box family protein	-6.3
At1g52200	expressed protein	-6.3
At5g16030	expressed protein	-6.3
At1g25230	purple acid phosphatase family protein	-6.1
At4g33666	L-galactose dehydrogenase (L-GalDH) /// expressed protein	-6.1
At3g53800	armadillo/beta-catenin repeat family protein	-6.1
At4g20260	DREPP plasma membrane polypeptide family protein	-6.1
At1g08980	amidase family protein	-5.9
At1g11260	glucose transporter (STP1)	-5.8
At1g15740	leucine-rich repeat family protein	-5.8
At3g26510	octicosapeptide/Phox/Bem1p (PB1) domain-containing protein	-5.6
At1g56220	dormancy/auxin associated family protein	-5.6
At5g03350	legume lectin family protein	-5.6
At5g63190	MA3 domain-containing protein	-5.4
At2g32100	ovate protein-related	-5.4
At1g68190	zinc finger (B-box type) family protein	-5.3
At5g18600	glutaredoxin family protein	-5.3
At4g27450	expressed protein	-5.3
At5g60680	expressed protein	-5.1
At1g13260	DNA-binding protein RAV1 (RAV1)	-5.1
At1g02300	cathepsin B-like cysteine protease, putative	-5.1
At4g39090	cysteine proteinase RD19a (RD19A) / thiol protease	-5

At5g14120	nodulin family protein	-5
At3g61060	F-box family protein / lectin-related	-4.9
At2g27050	ethylene-insensitive3-like1 (EIL1)	-4.8
At1g13650	expressed protein	-4.7
At3g47160	expressed protein	-4.6
At2g15960	expressed protein	-4.4
At4g04330	expressed protein	-4.4
At4g27440	protochlorophyllide reductase B, chloroplast / PCR B / NADPH-protochlorophyllide oxidoreductase B (PORB)	-4.4
At4g14270	expressed protein	-4.4
At3g51840	short-chain acyl-CoA oxidase	-4.4
At3g28860	multidrug resistance P-glycoprotein, putative	-4.4
At4g26530	fructose-bisphosphate aldolase, putative	-4.3
At5g49730	ferric reductase-like transmembrane component family protein /// ferric reductase-like transmembrane component family protein	-4.3
At1g12780	UDP-glucose 4-epimerase / UDP-galactose 4-epimerase / Galactowaldenase	-4.3
At4g01026	expressed protein	-4.2
At1g54820	protein kinase family protein	-4.2
At5g02160	expressed protein	-4.1
At2g39400	hydrolase, alpha/beta fold family protein	-4
At4g05070	expressed protein	-4
At4g32340	expressed protein	-4
At1g71030	myb family transcription factor	-4
At1g01240	expressed protein	-4
At5g02020	expressed protein	-4
At2g18300	basic helix-loop-helix (bHLH) family protein	-4
At1g29395	stress-responsive protein, putative	-4
At2g46220	expressed protein	-3.9
At1g17990	12-oxophytodienoate reductase, putative /// 12-oxophytodienoate reductase, putative	-3.9
At5g44680	methyladenine glycosylase family protein	-3.9
At5g44530	subtilase family protein	-3.9
At3g18080	glycosyl hydrolase family 1 protein	-3.9
At3g26170	cytochrome P450 71B20, putative (CYP71B2) /// cytochrome P450 71B19, putative (CYP71B19)	-3.9
At3g59940	autophagy 4b (APG4b) /// kelch repeat-containing F-box family protein	-3.8
At1g11530	thioredoxin family protein	-3.8
At1g09750	chloroplast nucleoid DNA-binding protein-related	-3.8
At2g30510	signal transducer of phototropic response (RPT2)	-3.8
At4g03510	zinc finger (C3HC4-type RING finger) family protein (RMA1)	-3.8
At5g06690	thioredoxin family protein	-3.7
At5g62360	invertase/pectin methylesterase inhibitor family protein	-3.7
At2g40750	WRKY family transcription factor	-3.7
At2g02710	PAC motif-containing protein	-3.6
At3g26740	light responsive protein-related	-3.6
At4g36040	DNAJ heat shock N-terminal domain-containing protein (J11)	-3.6
At1g49500	expressed protein	-3.6
At4g28240	wound-responsive protein-related /// NADH dehydrogenase-related	-3.6
At1g33240	trihelix DNA-binding protein, putative	-3.6
At5g05690	cytochrome P450 90A1 (CYP90A1) (CYP90) (CPD)	-3.6
At4g39510	cytochrome P450 family protein	-3.6
At2g34620	mitochondrial transcription termination factor-related / mTERF-related	-3.6
At2g22990	sinapoylglucose:malate sinapoyltransferase (SNG1)	-3.5
At2g29290	tropinone reductase, putative / tropine dehydrogenase, putative	-3.5

At1g32540	zinc finger protein, putative	-3.5
At5g63800	glycosyl hydrolase family 35 protein	-3.5
At2g27830	expressed protein	-3.5
At5g10860	CBS domain-containing protein	-3.5
At1g13210	haloacid dehalogenase-like hydrolase family protein	-3.5
At5g62630	expressed protein	-3.5
At1g27290	expressed protein	-3.4
At5g28020	cysteine synthase, putative / O-acetylserine (thiol)-lyase, putative / O-acetylserine sulfhydrylase, putative	-3.4
At2g46330	arabinogalactan-protein (AGP16)	-3.4
At5g24470	pseudo-response regulator 5 (APRR5)	-3.4
At1g21500	expressed protein	-3.4
At4g16520	autophagy 8f (APG8f)	-3.4
At4g39640	gamma-glutamyltranspeptidase family protein	-3.4
At1g25275	expressed protein	-3.4
At5g47040	Lon protease homolog 1, mitochondrial (LON)	-3.3
At1g19770	purine permease-related	-3.3
At1g80460	glycerol kinase, putative	-3.3
At3g52840	beta-galactosidase, putative / lactase, putative	-3.3
At5g25280	serine-rich protein-related	-3.3
At3g26280	cytochrome P450 family protein	-3.3
At3g56360	expressed protein	-3.3
At5g04490	phosphatidate cytidylyltransferase family protein	-3.3
At1g68520	zinc finger (B-box type) family protein	-3.3
At2g37490	expressed protein	-3.3
At1g54130	RelA/SpoT protein, putative (RSH3)	-3.3
At1g30250	expressed protein	-3.3
At5g16150	hexose transporter, putative	-3.3
At4g29190	zinc finger (CCCH-type) family protein	-3.3
At1g52190	proton-dependent oligopeptide transport (POT) family protein	-3.3
At4g34220	leucine-rich repeat transmembrane protein kinase, putative	-3.2
At1g73480	hydrolase, alpha/beta fold family protein	-3.2
At1g09350	galactinol synthase, putative	-3.2
At4g19860	lecithin:cholesterol acyltransferase family protein / LACT family protein	-3.2
At5g08520	myb family transcription factor	-3.2
At1g63690	protease-associated (PA) domain-containing protein	-3.2
At4g19170	9-cis-epoxycarotenoid dioxygenase, putative / neoxanthin cleavage enzyme, putative / carotenoid cleavage dioxygenase, putative	-3.1
At3g50270	transferase family protein	-3.1
At2g41870	remorin family protein	-3.1
At1g74840	myb family transcription factor	-3.1
At3g16520	UDP-glucoronosyl/UDP-glucosyl transferase family protein	-3.1
At2g30930	expressed protein	-3.1
At1g08930	early-responsive to dehydration stress protein (ERD6) / sugar transporter family protein	-3.1
At5g40450	expressed protein	-3
At1g75460	ATP-dependent protease La (LON) domain-containing protein	-3
At5g22270	expressed protein	-3
At2g43010	phytochrome-interacting factor 4 (PIF4) / basic helix-loop-helix protein 9 (bHLH9) / short under red-light 2 (SRL2)	-3
At3g27690	chlorophyll A-B binding protein (LHCB2:4)	-3
At5g65730	xyloglucan:xyloglucosyl transferase, putative / xyloglucan endotransglycosylase, putative / endo-xyloglucan transferase, putative	-3
At1g69850	nitrate transporter (NTL1)	-3

At4g23820	glycoside hydrolase family 28 protein / polygalacturonase (pectinase) family protein	-3
At3g14050	RelA/SpoT protein, putative (RSH2)	-3
At1g48300	expressed protein	-3
At5g19140	auxin/aluminum-responsive protein, putative	-3
At5g03230	expressed protein	-3
At3g50500	protein kinase, putative	-3
At1g72160	SEC14 cytosolic factor family protein / phosphoglyceride transfer family protein	-3
At1g24070	glycosyl transferase family 2 protein	3
At4g25700	beta-carotene hydroxylase	3
At4g29510	protein arginine N-methyltransferase, putative	3
At4g32720	RNA recognition motif (RRM)-containing protein	3
At1g31860	histidine biosynthesis bifunctional protein (HISIE)	3
At3g03920	Gar1 RNA-binding region family protein	3
At1g09240	nicotianamine synthase, putative	3
At5g06110	DNAJ heat shock N-terminal domain-containing protein / cell division protein-related	3
At4g27570	glycosyltransferase family protein /// glycosyltransferase family protein	3
At2g23340	AP2 domain-containing transcription factor, putative	3
At3g23810	adenosylhomocysteinase, putative / S-adenosyl-L-homocysteine hydrolase, putative / AdoHcyase, putative	3.1
At3g44990	xyloglucan:xyloglucosyl transferase, putative / xyloglucan endotransglycosylase, putative / endo-xyloglucan transferase, putative	3.1
At5g14050	transducin family protein / WD-40 repeat family protein	3.1
At2g18230	inorganic pyrophosphatase (soluble) (PPA) / pyrophosphate phospho-hydrolase / PPase	3.1
At1g61570	mitochondrial import inner membrane translocase (TIM13)	3.1
At4g39950	cytochrome P450 79B2, putative (CYP79B2)	3.1
At3g56070	peptidyl-prolyl cis-trans isomerase, putative / cyclophilin, putative / rotamase, putative	3.1
At1g31970	DEAD/DEAH box helicase, putative	3.1
At5g14520	pescadillo-related	3.1
At3g51240	naringenin 3-dioxygenase / flavanone 3-hydroxylase (F3H)	3.2
At1g67360	rubber elongation factor (REF) family protein	3.2
At1g80750	60S ribosomal protein L7 (RPL7A)	3.2
At1g17100	SOUL heme-binding family protein	3.2
At3g58070	zinc finger (C2H2 type) family protein	3.2
At5g65860	ankyrin repeat family protein	3.2
At1g26770	expansin, putative (EXP10)	3.2
At5g55915	nucleolar protein, putative	3.2
At3g16810	pumilio/Puf RNA-binding domain-containing protein	3.3
At2g44860	60S ribosomal protein L24, putative	3.3
At2g28600	expressed protein	3.3
At3g03770	leucine-rich repeat transmembrane protein kinase, putative	3.3
At1g55900	NLI interacting factor (NIF) family protein	3.3
At2g37250	adenylate kinase family protein	3.3
At1g07890	L-ascorbate peroxidase 1, cytosolic (APX1)	3.3
At3g16780	60S ribosomal protein L19 (RPL19B)	3.4
At5g08180	ribosomal protein L7Ae/L30e/S12e/Gadd45 family protein	3.4
At3g13940	expressed protein	3.4
At1g55210	disease resistance response protein-related/ dirigent protein-related	3.5
At5g64680	expressed protein	3.5
At1g15100	zinc finger (C3HC4-type RING finger) family protein	3.5
At1g25260	acidic ribosomal protein P0-related	3.5
At1g63780	brix domain-containing protein	3.5
At3g23620	brix domain-containing protein	3.6
At3g57490	40S ribosomal protein S2 (RPS2D)	3.6

At3g23990	chaperonin (CPN60) (HSP60)	3.7
At3g17790	acid phosphatase type 5 (ACP5)	3.7
At3g21890	zinc finger (B-box type) family protein	3.7
At2g38210	stress-responsive protein, putative /// ethylene-responsive protein, putative	3.7
At1g15425	expressed protein	3.7
At5g09590	heat shock protein 70 / HSP70 (HSC70-5)	3.8
At3g57000	nucleolar essential protein-related	3.8
At1g63810	nucleolar RNA-associated family protein / Nrap family protein	3.8
At3g08590	2,3-biphosphoglycerate-independent phosphoglycerate mutase, putative / phosphoglyceromutase, putative	3.8
At1g15440	transducin family protein / WD-40 repeat family protein	3.9
At1g31660	bystin family	3.9
At4g01560	brix domain-containing protein	3.9
At5g15550	transducin family protein / WD-40 repeat family protein	3.9
At3g22310	DEAD box RNA helicase, putative /// DEAD box RNA helicase, putative (RH9)	4
At4g37910	heat shock protein 70, mitochondrial, putative / HSP70, mitochondrial, putative	4
At2g36630	expressed protein	4
At3g57150	dyskerin, putative / nucleolar protein NAP57, putative	4.1
At3g05060	SAR DNA-binding protein, putative	4.1
At5g61770	brix domain-containing protein	4.1
At1g19640	S-adenosyl-L-methionine:jasmonic acid carboxyl methyltransferase (JMT)	4.2
At4g20170	expressed protein /// expressed protein	4.3
At4g34710	arginine decarboxylase 2 (SPE2)	4.3
At1g60850	DNA-directed RNA polymerase, putative	4.4
At3g56090	ferritin, putative	4.4
At1g29940	DNA-directed RNA polymerase family protein	4.4
At5g02050	mitochondrial glycoprotein family protein / MAM33 family protein	4.5
At2g40360	transducin family protein / WD-40 repeat family protein	4.6
At1g56110	nucleolar protein Nop56, putative	4.6
At5g01600	ferritin 1 (FER1)	4.6
At1g52930	brix domain-containing protein	4.6
At1g57590	pectinacetylesterase, putative	4.7
At4g15770	60S ribosome subunit biogenesis protein, putative	4.9
At2g03760	steroid sulfotransferase, putative	5
At1g80270	DNA-binding protein, putative	5.1
At3g14720	mitogen-activated protein kinase, putative / MAPK, putative (MPK19)	5.2
At4g33030	UDP-sulfoquinovose synthase / sulfite:UDP-glucose sulfotransferase / sulfolipid biosynthesis protein (SQD1)	5.4
At4g01080	expressed protein	5.5
At3g06530	BAP28-related	5.5
At1g02820	late embryogenesis abundant 3 family protein / LEA3 family protein	5.6
At3g13230	expressed protein	5.7
At2g47990	transducin family protein / WD-40 repeat family protein	5.9
At5g42760	O-methyltransferase N-terminus domain-containing protein	6
At3g44750	histone deacetylase, putative (HD2A)	6.1
At4g34590	bZIP transcription factor family protein	6.1
At1g56650	myb family transcription factor (MYB75)	6.2
At1g06000	UDP-glucoronosyl/UDP-glucosyl transferase family protein	6.4
At3g18600	DEAD/DEAH box helicase, putative	6.7
At2g27840	histone deacetylase-related / HD-related	6.8
At3g14395	expressed protein	6.8
At5g58770	dehydrodolichyl diphosphate synthase, putative / DEDOL-PP synthase, putative	6.9
At2g34260	transducin family protein / WD-40 repeat family protein	7.2

At3g10530	transducin family protein / WD-40 repeat family protein	7.2
At4g16590	glucosyltransferase-related	7.6
At1g32900	starch synthase, putative	8
At4g25630	fibrillarin 2 (FIB2)	9
At2g27420	cysteine proteinase, putative	9.2
At5g49480	sodium-inducible calcium-binding protein (ACP1) / sodium-responsive calcium-binding protein (ACP1)	9.7
At1g64780	ammonium transporter 1, member 2 (AMT1.2)	10
At4g15210	beta-amylase (BMY1) / 1,4-alpha-D-glucan maltohydrolase	13.7
At1g61800	glucose-6-phosphate/phosphate translocator, putative	34

upna
Universidad Pública de Navarra
Nafarroako Unibertsitate Publikoa

CAPÍTULO 2

Volatile emissions from fungal phytopathogens modulate plant root metabolism and architecture through mechanisms involving cyanide scavenging and hormone- and ROS- mediated proteome resetting

upna
Universidad Pública de Navarra
Nafarroako Unibertsitate Publikoa

1. INTRODUCTION

The root system represents an important interface through which plants interact with the environment. It provides anchorage, facilitates the acquisition of water and mineral nutrients from the soil and allows the establishment of biotic relationships with the rhizosphere (van Dam and Bouwmeester, 2016). In response to environmental changes, roots reorganize their metabolism and architecture in order to improve fitness and cope with and survive these changes (López-Bucio et al., 2003; Yang et al., 2008; Krapp et al., 2011; Gargallo-Garriga et al., 2014; Bouguyon et al., 2016). These adjustments result from the integration of environmental cues leading to shifts in phytohormone signaling and gene expression. Physiological and genetic studies have provided strong evidence that auxin is a master regulator of root system architecture (RSA) (Boerjan et al., 1995; Casimiro et al., 2001; Saini et al., 2013). Other phytohormones such as ethylene and cytokinins (CK) interact with auxin to trigger cascades of events leading to root morphogenesis (Pitts et al., 1998; Stepanova et al., 2005; Ivanchenko et al., 2008; Strader et al., 2010; Lewis et al., 2011; Schaller et al., 2015; Liu et al., 2017). In addition to phytohormones, reactive oxygen species (ROS) play important roles in RSA adjustment to varying environmental conditions (Foreman et al., 2003; Passardi et al., 2006; Tsukagoshi et al., 2010; Sundaravelpandian et al., 2013; Manzano et al., 2014).

In soil, microorganisms communicate with plants by exchanging chemical signals throughout the rhizosphere. Such interactions are important for plant productivity (De-la-Peña and Loyola-Vargas, 2014). In the precolonization phase, before direct contact with plants occurs, beneficial bacteria and fungi emit diffusible substances (e.g. carbohydrates, proteins, fatty acids, flavonols, organic acids, amino acids and hormones) that cause massive lateral root (LR) formation and enhanced root hair (RH) growth, thus improving the root´s capacity to explore for water and minerals and predisposing plants to fungal colonization and infection (López-Bucio et al., 2007; Contreras-Cornejo et al., 2009; Felten et al., 2009; Verbon and Liberman, 2016). These microorganisms also emit a large number of volatile compounds (VCs) with molecular masses of less than 300 Da that promote growth and photosynthesis, and modulate RSA in both host and non-host plants (Ryu et al., 2003; Zhang et al., 2008; Splivallo et al., 2009; Gutiérrez-Luna et al., 2010; Delaplace et al., 2015; Ditengou et al., 2015; Garnica-Vergara et al., 2016; Cordovez et al., 2018). Recent studies have shown that this capacity is not restricted to beneficial microbes; it also extends to phytopathogens and microbes that do not

normally interact mutualistically with plants (Sánchez-López et al., 2016b; Cordovez et al., 2017; García-Gómez et al., 2019; Moisan et al., 2019).

RSA modulation by microbial VCs has frequently been associated with lipophilic carbon-based compounds, which are known as volatile organic compounds (VOCs) (Zhang et al., 2007; Splivallo et al., 2009; Gutiérrez-Luna et al., 2010; Bitas et al., 2015; Delaplace et al., 2015; Ditengou et al., 2015; Garnica-Vergara et al., 2016; Cordovez et al., 2018). In addition to VOCs, microorganisms also release a limited number of volatile inorganic compounds (VICs) with molecular masses of less than 45 Da such as hydrogen sulfide, molecular hydrogen, nitric oxide (NO), nitrogen dioxide, nitrous oxide and carbon monoxide (CO) (Engel et al., 1972; Wharton and Weintraub, 1980; Siegel and Siegel, 1987; Nandi and Sengupta, 1998; Conrath et al., 2004; Shatalin et al., 2011). These compounds can act as signaling molecules that promote growth and modulate RSA when applied individually and at low concentrations (Correa-Aragunde et al., 2004; Cao et al., 2007; Guo et al., 2009; Fernández-Marcos et al., 2011; Dooley et al., 2013; Lin et al., 2014; Takahashi et al. 2014, Zhu et al., 2016). There is evidence that VIC emissions from growth-promoting rhizobacteria promote changes in the RSA of their host plants (Creus et al., 2005; Molina-Favero et al., 2008).

Using a "box-in-box" co-cultivation system in which plants are grown in the vicinity of microbial cultures covered with charcoal filters, we have recently provided evidence that VCs with molecular masses of less than 40 Da are major determinants of plant responses to microbial volatile emissions (García-Gómez et al., 2019). VOCs-depleted (NO and CO-containing) volatile emissions from *Penicillium aurantiogriseum* (a fungal phytopathogen that can be found in the rhizosphere [Bodini et al., 2011; Gharaei-Fathabad et al., 2014; Kłapeć et al., 2018]) inhibit primary root (PR) and LR growth, stimulate the de novo LR formation, and promote extensive proliferation and elongation of RHs leading to the formation of peculiar "brush-like" structures at the root tip and the development of a "cotton-like" external root phenotype (García-Gómez et al., 2019). These changes in RSA resemble those occurring in plants treated with exogenous auxins (Casimiro et al., 2001), CO (Guo et al., 2008; Guo et al., 2009), NO (Pagnussat et al., 2002; Correa-Aragunde et al., 2004; Fernández-Marcos et al., 2011) and diffusible substances emitted by beneficial microorganisms (López-Bucio et al., 2007; Splivallo et al., 2009; Ditengou et al., 2015; Garnica-Vergara et al., 2016).

To date, the majority of studies on the root response to complex mixtures

of microbial VCs have been conducted using beneficial microorganisms and focused mainly on analyses of reporters for auxin-inducible gene expression, RSA adjustments in ethylene and auxin transport/signaling mutants, transcriptome changes in roots of VC-exposed plants and identification of bioactive microbial VOCs (Zhang et al., 2007; Felten et al., 2009; Splivallo et al., 2009; Bailly et al., 2014; Ditengou et al., 2015; Garnica-Vergara et al., 2016; Cordovez et al., 2018; Camarena-Pozos et al., 2019). These studies have shown that RSA modulation promoted by microbial VCs is associated with changes in the root transcriptome, and involves processes wherein auxin and ethylene play important roles. Recent studies have provided evidence that this type of RSA modulation is associated with ROS production (Ditengou et al., 2015) and post-translational thiol-redox proteome changes (Ameztoy et al., 2019).

Post-transcriptional events such as the regulation of translation and protein stability result in weak correlations between the transcriptomic and proteomic responses of plants to environmental cues. Although there has been a considerable increase in our knowledge in recent years regarding the importance of post-transcriptionally regulated root morphogenetic adjustments to changing environmental conditions (Floris et al., 2009; Lan et al., 2012; Žd'árská et al., 2013), nothing is known about root proteome reprogramming following exposure to microbial VCs. Plants use metabolic pathways as a source of energy and signaling molecules to drive extensive defense programs and promote developmental changes in response to pathogens (Bolton, 2009; Rojas et al., 2014). However, the metabolic and developmental adjustments made by roots in response to compounds (particularly VCs) emitted by microbial phytopathogens remain largely unknown. To obtain insights into the mechanisms involved in the response of roots to VCs emitted by microbes, we performed comprehensive proteomic, metabolic and developmental analyses of Arabidopsis plants exposed to VOCs-depleted volatile emissions from *P. aurantiogriseum* cultures. We also characterized the response to VOCs-depleted fungal VCs in mutants with altered hormone and ROS status. Our findings show that VCs emitted by the fungal phytopathogen *P. aurantiogriseum* modulate plant root metabolism and architecture through complex mechanisms that involve cyanide scavenging and proteome resetting mediated by hormones and ROS. Some of these mechanisms differ from those involved in the response to VCs emitted by beneficial microorganisms.

2. MATERIALS AND METHODS

Plant and microbial cultures, growth conditions and sampling

The experiments were carried out using *Arabidopsis thaliana* L. (Heynh) WT plants (ecotype Col-0), the *aux1-T* auxin influx carrier mutant (N657534) (Fischer et al., 2006), the *etr1-3* ethylene receptor mutant (N3070) (Hua and Meyerowitz, 1998), the *eir1* ethylene insensitive and auxin efflux carrier mutant (N8058) (Luschnig et al., 1998), the *ahk2/3, ahk2/4* and *ahk3/4* CK signaling mutants (Riefler et al., 2006), the *rhd2* mutant which is impaired in a plasma membrane NADPH oxidase (Foreman et al., 2003), the *cas-c1* mutant which is impaired in the mitochondrial β-cyanoalanine synthase (N522479) (García et al., 2010), the auxin- and ethylene-inducible *DR5:GUS* reporter (N16703) (Ulmasov et al., 1997; Stepanova et al., 2005) and the CK *ARR5:GUS* reporter (D'Agostino et al., 2000). Unless otherwise indicated the plants were cultured in Petri dishes (92 x 16mm, Ref. 82.1472.001, Sarstedt) containing sucrose-free half-strength solid Murashige and Skoog (MS) (Phytotechlab M519) medium in growth chambers providing 'long day' 16 h light (90 µmol photons sec^{-1} m^{-2}), 22 ºC /8 h dark, 18 ºC cycles. *P. aurantiogriseum* was cultured in small Petri dishes (35 x 10mm, Sarstedt, Ref. 82.1135.500) containing solid MS medium supplemented with 90 mM sucrose. Effects of microbial VCs on plants were investigated using the "box-in-box" co-cultivation system as described in (García-Gómez et al., 2019). Briefly, plant cultures 14 days after sowing and fungal cultures in unlidded Petri dishes with a top layer of charcoal filters that adsorb VCs with molecular masses of more than 40 Da were placed in sterile plastic boxes (200 x 150 x 50 mm IT200N Instrument Trays; AW Gregory, UK) sealed with polyvinyl chloride plastic wrap. As negative controls, Petri dishes containing plants were cultured in sealed boxes together with Petri dishes each containing sterile microbial culture media and a charcoal filter. After the incubation time indicated for each experiment, roots were harvested, immediately freeze-clamped and ground to a fine powder in liquid nitrogen with a pestle and mortar.

Determination of gas exchange rates and photosynthetic parameters

Gas exchange rates were determined as described by Sánchez-López et al. (2016b) using a LI-COR 6400 gas exchange portable photosynthesis system (LI-COR, Lincoln, NE, USA). Net rates of CO_2 assimilation (A_n) and stomatal conductance (g_s) were calculated as described by von Caemmerer and Farquhar (1981). Water use efficiency (WUE_i) was

calculated as the ratio of A_n to gs as described by Flexas et al. (2016).

Root morphological analysis

Ten days after sowing plants cultured on vertical square Petri dishes (10 x 10 x 2 cm, Sarstedt, Ref. 82.9923.422) were placed in sealed plastic boxes containing fungal cultures covered with charcoal filters. After 6 days of co-cultivation in vertical position, the numbers and lengths of the plants´ roots and RHs were measured using an MVX10 stereomicroscope (Olympus, Japan). Photomicrographs were captured with a DP72 video camera (Olympus, Japan) and the Cell D package (Olympus, Japan). RHs were measured in a region of 5 mm from the LR tips.

ROS staining

ROS were semi-quantitatively detected in rosettes essentially as described by Nguyen et al. (2017). Briefly, O_2^- was detected by staining roots for 15 min with 0.05% nitro blue tetrazolium (NBT) (w/v) in 50 mM potassium phosphate, pH 7.0, and H_2O_2 by staining for 5 h with 0.1% 3,3′-diaminobenzidine in 10 mM potassium phosphate, pH 7.0.

GUS expression analysis

Expression of the GUS reporter gene was monitored using the histochemical staining assay described by Jefferson et al. (1987).

Analytical procedures

The amino acids contents were determined from frozen powder samples (see above) as described by Loiret et al. (2009). To determine the levels of CKs, aliquots of the frozen powders were lyophilized and CKs were quantified according to the method described in Novák et al. (2008). HCN contents in roots and ethylene produced and released by roots were measured as described by García et al. (2010). Levels of UDP-glucose and TCA intermediates were measured as described by Ghaffari et al. (2016). Fe and Zn levels were measured as indicated in Eggert and von Wirén (2013).

Proteomic analysis

High-throughput, isobaric labeling-based differential proteomic analyses were conducted essentially as described in Sánchez-López et al. (2016a) for Arabidopsis leaves but with

the following modifications. For protein sample preparation, samples were prepared by grinding 200 mg of root material into a fine powder under liquid nitrogen using a pre-cooled mortar and pestle. The tryptic peptides were labeled using a iTRAQ-4 plex Isobaric Mass Tagging Kit (SCIEX, Foster City, CA, USA). Search engines were configured to match potential peptide candidates with a mass error tolerance of 25 ppm and fragment ion tolerance of 0.02Da, allowing for up to two missed tryptic cleavage sites and a maximum isotope error (13C) of 1, and also allowing for fixed MMTS modification of cysteine and variable oxidation of methionine, pyroglutamic acid from glutamine or glutamic acid at the peptide N-terminus, acetylation of the protein N-terminus and modification of lysine and peptide N-terminus with iTRAQ 4-plex reagents. Statistical significance was measured using q-values (FDR). The cut-off for identifying differentially regulated proteins was established at a FDR ≤ 2.7% and log2 ratios (+VC treatment vs. –VC treatment) of either > 0.4 (for proteins whose expression is up-regulated by fungal VCs) and < -0.4 (for proteins whose expression is down-regulated by VCs).

Statistical analysis

Unless otherwise indicated, data presented here are means (± SE) obtained from 3-4 independent experiments, with 3-5 replicates for each experiment. The significance of differences between plants not exposed to VCs, and plants exposed to *P. aurantiogriseum* VCs was statistically evaluated with Student´s t-test using the SPSS package. Differences were considered significant if $P<0.05$.

3. RESULTS

Fungal VCs promote changes in the root proteome and metabolome of exposed plants

We carried out high-throughput, isobaric labeling-based differential proteomic analysis of roots of Arabidopsis plants cultured in the absence, or presence for three days, of VOCs-depleted (VICs-containing) emissions of adjacent cultures of *P. aurantiogriseum* covered with charcoal filters that adsorb VCs with molecular masses of more than 40 Da. As shown in **Supplemental Table 1**, 178 out of the 2988 proteins identified in this study were proteins of known functions that were differentially expressed in response to VOCs-depleted fungal VCs. Among them, 49 were up-regulated and 129

were down-regulated (**Supplemental Table 1**). We compared the sets of proteins that were differentially expressed in leaves exposed to fungal VCs (Sánchez-López et al., 2016a) with those of fungal VC-exposed roots (this work). We found that only 8% of the proteins that were differentially expressed in response to fungal VCs in roots were also differentially expressed in VC-exposed leaves (**Supplemental Table 1**). Using the broad categories outlined by the MapMan tool (https://mapman.gabipd.org/) (Thimm et al., 2004), the 178 differentially expressed proteins (DEPs) with known functions were assembled into 23 functional groups (**Figure 1**). The general trend indicates that RSA and root metabolic changes in plants treated with VOCs-depleted fungal VCs are associated with DEPs that fit into the following groups:

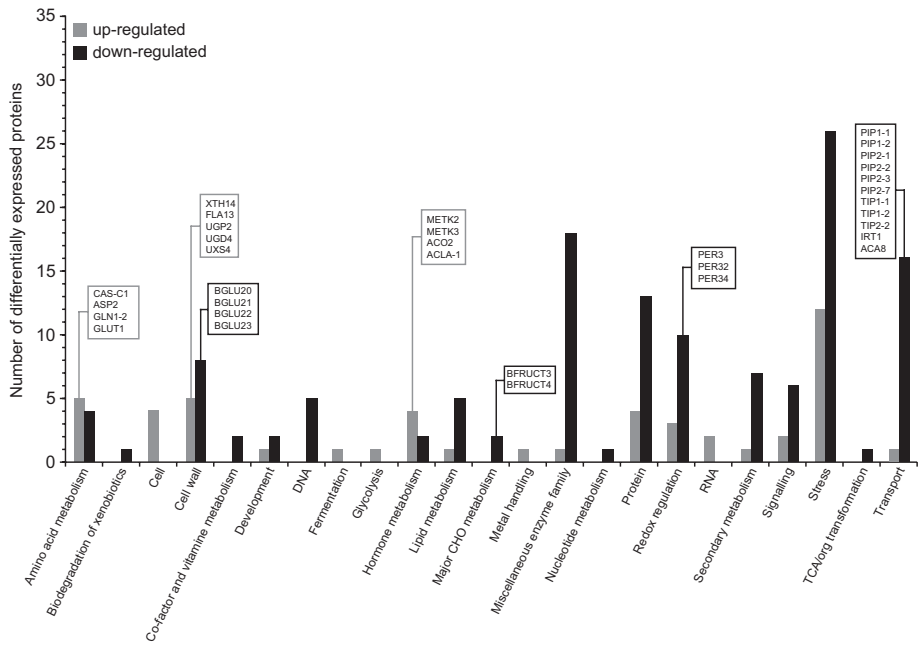

Figure 1: Functional categorization of DEPs in roots of plants cultured in the presence of VOCs-depleted VCs emitted by *P. aurantiogriseum*. Proteins that were significantly down- or up-regulated following VC exposure were sorted according to the putative functional categories assigned by MapMan software. The numbers of up- and down-regulated proteins in each categorical group are indicated by gray and black bars, respectively. Proteins discussed here are boxed.

Transport

Fungal volatile emissions down-regulated the expression of plasma membrane and vacuolar aquaporins (e.g. PIP1-1, PIP1-2, PIP2-1, PIP2-2, PIP2-3, PIP2-7, TIP1-1, TIP1-

2 and TIP2-2) involved in processes such as water transport (Maurel et al., 2015) and hydrogen peroxide (H_2O_2) transport and detoxification (Bienert et al., 2007; Dynowski et al., 2008; Rodrigues et al., 2017) (**Supplemental Table 1, Figure 1**). Exposure to fungal VCs also reduced the expression of ACA8, a plasma membrane calcium pump that regulates cytosolic calcium concentration and signaling in response to environmental changes (Costa et al., 2017; Yang et al., 2017) and that of IRT1, (**Supplemental Table 1**, **Figure 1**), a metal ion carrier protein that mediates the entry of Fe and Zn into roots (Korshunova et al., 1999; Rogers et al., 2000; Varotto et al., 2002). Consistent with this finding, leaves of VC-exposed plants had lower levels of Fe and Zn than controls (166 ± 9.4 and 96.5 ± 4 μg g^{-1} dry weight (DW) of Fe in leaves of VC-treated and non-treated plants, respectively, and 128 ± 18.2 and 86.3 ± 2.3 μg g^{-1} DW fo Zn in leaves of VC-treated and non-treated plants, respectively).

Major carbohydrate metabolism

Exposure to VOCs-depleted fungal VCs diminished the expression of the two vacuolar invertases of Arabidopsis (**Supplemental Table 1, Figure 1**), BFRUCT3 and BFRUCT4, the latter being an important determinant of root length in Arabidopsis (Sergeeva et al., 2006; Leskow et al., 2016).

Redox metabolism

Exposure to charcoal-filtered fungal VCs down-regulated the expression of various extracellular peroxidases (e.g. PER3, PER32 and PER34) (**Supplemental Table 1, Figure 1**). Some of them (e.g. PER34) are important determinants of root and RH growth (Passardi et al., 2006; Manzano et al., 2017).

Cell wall metabolism

VOCs-depleted fungal VCs down-regulated the expression of cell wall breakdown enzymes (e.g. BGLU20-23), and stimulated the expression of enzymes involved in the synthesis of precursors for cell wall biosynthesis (e.g. UGP2, UGD4 and UXS4) (**Supplemental Table 1, Figure 1**). In agreement with this observation, roots of fungal VC-exposed plants accumulated higher levels of cell wall precursor molecules than controls (81.1 ± 15.2 and 10.9 ± 3.2 nmol g^{-1} dry weight (DW) of UDP-glucose in roots of VC-treated and non-treated plants, respectively, and 107 ± 8.8 and 46.6 ± 8.7 nmol

g^{-1} DW glucuronic acid in roots of VC-treated and non-treated plants, respectively). VCs also up-regulated the expression of enzymes involved in cell wall expansion such as arabinogalactan proteins and xyloglucan endotransglucosylases (e.g. XTH14, FLA6 and FLA13) (**Supplemental Table 1**).

Amino acid metabolism

Charcoal-filtered fungal VCs increased the expression of enzymes involved in nitrogen assimilation (e.g. GLUT1), the conversion of cytosolic citrate to Gln (e.g. ASP2 and GLN1-2) and the conversion of cytosolic Met and mitochondrial Cys to Asp and Asn (e.g. METK2, METK3, ACO2 and CAS-C1) (**Supplemental Table 1, Figure 1**). Accordingly, levels of α-ketoglutarate, Glu, Gln, Asp and Asn in roots of VC-treated plants were higher than in controls (**Table 1**). Levels of citrate and other TCA metabolic intermediates acting as precursors for amino acid biosynthesis (e.g. cis- and trans-aconitate, citrate, α-ketoglutarate, malate, and succinate) were higher in VC-exposed roots than in controls (**Table 1**).

Hormone metabolism

VOCs-depleted fungal VCs increased the expression of ACLA-1, an enzyme that participates directly in the conversion of cytosolic citrate into the acetyl-CoA necessary for the synthesis of mevalonate (MVA)-derived isoprenoids (Fatland et al., 2005). Fungal VCs also increased the expression of ethylene biosynthetic enzymes such as METK2, METK3 and ACO2 (**Supplemental Table 1, Figure 1**); the latter catalyzes the rate-limiting step of ethylene biosynthesis in many processes in response to environmental changes and is an important determinant in plant-microbe interactions (Barry et al., 1996; Nascimento et al., 2018).

Down-regulation of water and iron transport systems in response to VOCs-depleted fungal VCs is associated with enhanced intrinsic photosynthetic water use efficiency

Fe participates in electron transfer reactions starting from the photochemical water splitting occurring during photosynthesis. Down-regulation of the expression of aquaporins and IRT1in roots and of Fe contents in leaves in response to VOCs-depleted fungal VCs suggested enhancement of photosynthetic efficiency thus reducing the water and Fe demands of leaves. To test this hypothesis we measured the WUE_i by analyzing

Table 1: Metabolites contents in roots of plants cultured in solid MS medium in the absence or presence of adjacent cultures of *P. aurantiogriseum* covered with VOC-adsorbing charcoal filters for one week. Values represent the mean ± SE of determinations in 3 independent experiments. Asterisks indicate significant differences, according to Student´s t-test (P<0.05), between VC-treated and non-treated plants.

		-VCs (nmol/g DW)	**+VCs (nmol/g DW)**
TCA compounds	Cis-Aconitate	8.7 ± 2.0	20.5 ± 1.6*
	Citrate	962 ± 138	1,409 ± 130*
	Malate	1,011 ± 125	1,897 ± 279*
	α-ketoglutarate	40.5 ± 11.7	118.1 ± 4.8*
	Succinate	121.1 ± 14.7	271.4 ± 21.5*
	Trans-Aconitate	5.1 ± 2.2	20.0 ± 1.7*
Amino acids	Asp	14,540 ± 1,262	18,158 ± 722*
	Glu	23,474 ± 1,250	34,459 ± 942*
	Ser	40,058 ± 1,835	15,532 ± 371*
	Asn	163,959 ± 5,315	195,804 ± 2,941*
	Gly	7,002 ± 358	5,641 ± 329*
	Gln	38,920 ± 1,689	62,034 ± 1,408*
	His	5,241 ± 297	5,144 ± 197
	Thr	16,750 ± 883	15,277 ± 345
	Ala	53,608 ± 3,614	129,404 ± 3,263*
	Arg	8,401 ± 469	7,098 ± 1,049
	GABA	16,172 ± 373	23,221 ± 689*
	Pro	13,227 ± 404	14,306 ± 279
	Tyr	9,926 ± 449	9,848 ± 252
	Val	4,983 ± 938	5,563 ± 139
	Met	2,465 ± 215	2,100 ± 109
	Ile	4,474 ± 290	3,668 ± 128
	Leu	4,095 ± 283	3,769 ± 279
	Lys	1,889 ± 171	1,687 ± 211
	Phe	3,723 ± 279	2,894 ± 117

An and *gs* at varying intercellular CO_2 concentrations (*Ci*) in plants cultured in the absence, or presence for three days, of adjacent cultures of *P. aurantiogriseum* covered with charcoal filters. These analyses revealed that plants exposed to fungal VCs had higher *An* and similar *gs* (and thus higher WUE*i*) values than controls at all *Ci* levels (**Figure 2**). This indicates that enhancement of photosynthetic activity by fungal VCs is due not to and increased rate of passage of CO_2 entering through the stomata, but to improved photosynthetic efficiency.

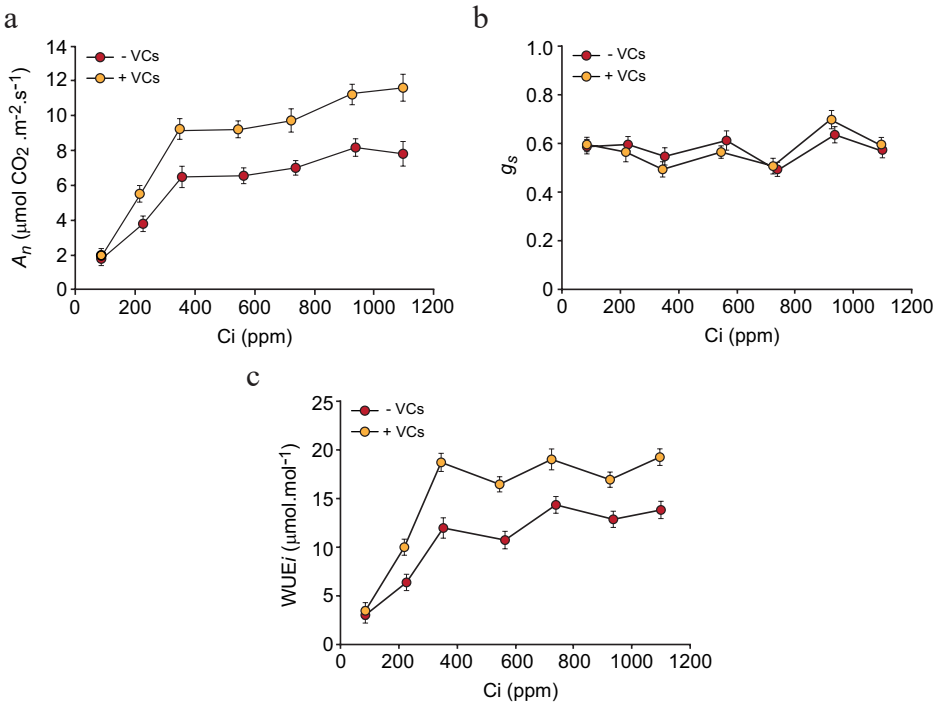

Figure 2: *P. aurantiogriseum* VCs enhance photosynthetic water use efficiency. Curves of (a) net CO_2 assimilation rate (*An*), (b) Gs versus intercellular CO_2 concentration (*Ci*) and (c) WUE*i* in leaves of plants cultured in the absence or continuous presence of adjacent cultures of *P. aurantiogriseum* covered with VOC-adsorbing charcoal filters for three days. Treatment with VCs began 28 days after seeds were sown.

VOCs-depleted fungal VCs enhance CK, auxin and ethylene signaling in roots

CKs negatively regulate IRT1 expression (Séguéla et al., 2008) and up-regulate the expression of ethylene biosynthetic enzymes (e.g. METK2, METK3 and ACO2) (Žd'árská et al., 2013; Brenner and Schmülling, 2015). On the other hand ethylene up-regulates the expression of ACO2 and CAS-C1 (Maruyama et al., 2001; van

Zhong and Burns, 2003) whereas auxin down-regulates the expression of aquaporins (Nemhauser et al., 2006; Péret et al., 2012). Down-regulation of IRT1 and aquaporins, and up-regulation of METK2, METK3, ACO2 and CAS-C1 promoted by fungal VCs suggested that these VCs enhance CK, ethylene and auxin signaling. This inference was corroborated by characterization of plants harboring the CK-inducible *ARR5:GUS* CK marker and the auxin- and ethylene-inducible *DR5:GUS* marker. As shown in **Figure 3**,

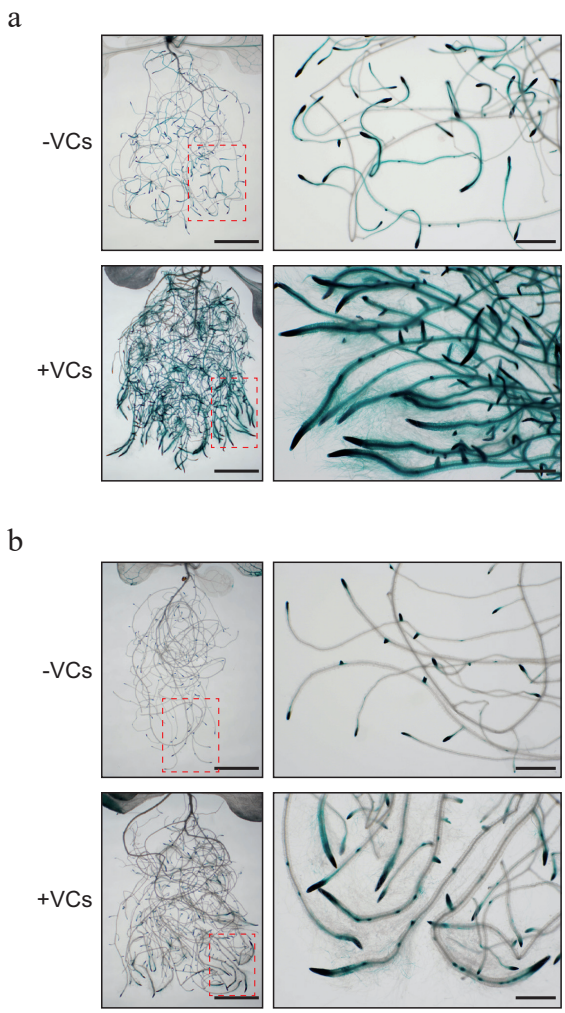

Figure 3: VOCs-depleted fungal VCs enhance CK- and auxin-responsive gene expression in roots. GUS activity in roots of plants harboring (a) the CK *ARR5:GUS* reporter and (b) the auxin and ethylene *DR5:GUS* reporter, cultured in the absence or presence of adjacent cultures of *P. aurantiogriseum* covered with VOC-adsorbing charcoal filters for one week. Scale bars: left panels: 5 mm; right panels: 1 mm.

ARR5:GUS and *DR5:GUS* plants grown with adjacent fungal cultures showed greater GUS expression in vascular tissues, root tips, LR primordia and RHs than controls. Furthermore, ethylene production in roots of plants treated with VOCs-depleted fungal VCs was substantially higher than in controls (**Figure 4**). Moreover, CK content analyses revealed that treatment with fungal VCs causes a significant increase in the total content of both MVA- and 2-C-methyl-D-erythritol 4-phosphate (MEP)-derived CKs. The most strongly accumulated CK forms were the free bases of the biologically active cis-zeatin (cZ) and isopentenyladenine (iP), their ribosides (cZR and iPR respectively), their precursors (cZRMP and iPRMP, respectively) and the precursor and transport forms of tZ (tZR and tZRMP, respectively) (**Table 2, Supplemental Figure 1**).

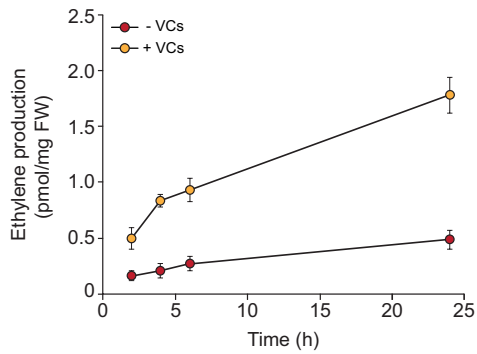

Figure 4: VOCs-depleted fungal VCs enhance ethylene production in roots. Time-course of ethylene accumulation in sealed vials containing roots of WT plants cultured in the absence or presence of adjacent cultures of *P. aurantiogriseum*. Values are means ± SE for three biological replicates obtained from three independent experiments.

Growth and developmental responses to fungal VCs in auxin, ethylene and CK signaling mutants

To address the roles of auxin, ethylene and CKs in RSA changes induced by VOCs-depleted fungal VCs we assessed root development in the *aux1-T* auxin influx carrier mutant, the *etr1-3* ethylene receptor mutant, the *eir1* ethylene insensitive and auxin efflux carrier mutant and the *ahk2/3, ahk2/4* and *ahk3/4* CK signaling mutants cultured in the absence, or presence for one week, of adjacent cultures of *P. aurantiogriseum* covered with VOC-adsorbing charcoal filters. As shown in **Figure 5b** and **6b,** fungal VCs promoted similar to WT enhancements of root growth (on a fresh weight basis) in these mutants. However, the stimulatory effect on rosette growth was weaker in the

Table 2: CK content (pmol g^{-1} DW) in roots of plants cultured in solid MS medium in the absence or presence of adjacent cultures of *P. aurantiogriseum* covered with VOC-adsorbing charcoal filters for 3 days. Values represent the mean ± SE of determinations in 3 independent experiments. Asterisks indicate significant differences, according to Student´s t-test (P<0.05), between VC-treated and non-treated plants.

		MEP pathway (plastid) derived CKs		MVA pathway (cytosol) derived CKs		
		-VCs	+VCs		-VCs	+VCs
Precursors	iPRMP	41.5 ± 4.8	243 ± 34*			
	tZRMP	83.1 ± 8.3	252 ± 64*	cZRMP	88.7 ± 7.3	145.9 ± 8.5*
	DHZMP	0.49 ± 0.09	0.65 ± 0.17			
	∑ (%)	125	621		88.7	145.9
Transport forms	iPR	11.6 ± 0.4	51.3 ± 6.6*			
	tZR	31.7 ± 5.3	68.9 ± 15.2*	cZR	47.2 ± 1.3	57.3 ± 1.7*
	DHZR	3.55 ± 0.16	3.39 ± 0.19			
	∑ (%)	46.9	123.6		47.2	57.3
Active forms	iP	34.9 ± 1.9	76.9 ± 10.0*			
	tZ	69.5 ± 6.6	53.3 ± 9.1	cZ	26.0 ± 1.3	53.2 ± 1.5*
	DZ	0.76 ± 0.13	0.77 ± 0.16			
	∑ (%)	105	131		26.0	53.2
Glycosylated (inactive) forms	iP7G	128 ± 5	138 ± 3			
	tZ7G	238 ± 15	88.9 ± 3.5*			
	DHZ7G	33.9 ± 1.9	11.7 ± 0.2*			
	iP9G	31.4 ± 0.9	46.5 ± 1.2*	cZ9G	60.9 ± 2.6	52.8 ± 4.2
	tZ9G	373 ± 20	172 ± 13*			
	DHZ9G	24.8 ± 2.5	10.9 ± 1.0*			
	tZROG	6.89 ± 0.34	5.91 ± 0.27	cZROG	42.7 ± 2.6	21.2 ± 0.8*
	∑ (%)	837	473		103	74.1
TOTAL	∑ (%)	1,114	1,350		265	330

aux1-T, eir1, etr1-3 and ahk2/3 mutants than in WT plants. These findings indicate that auxin, ethylene and CKs are important determinants of shoot growth responses to VOCs-depleted fungal VCs.

In keeping with García-Gómez et al. (2019), VOCs-depleted fungal VCs shortened the PR and LRs, and increased the number of elongated LRs in WT plants (**Figure 5c**). As in WT plants, fungal VCs increased the number of elongated LRs in *aux1-T, eir1, etr1-3* and CK signaling mutants. However, fungal VCs did not shorten the LRs in these mutants (**Figure 5c, Figure 6c**). Furthermore, unlike in WT plants and CK signaling mutants, fungal VCs did not shorten the PRs in *aux1-T, eir1* and *etr1-3* mutants (**Figure 5a,c, Figure 6c**).

Under non-induced conditions, roots of CK signaling mutants produced RHs whose numbers and sizes were comparable to those of WT roots (**Figure 6c**). *aux1-T, eir1* and *etr1-3* mutants produced fewer and shorter RHs than WT plants (**Figure 5c**), observations consistent with those of Pitts et al. (1998). As in WT plants, auxin, ethylene

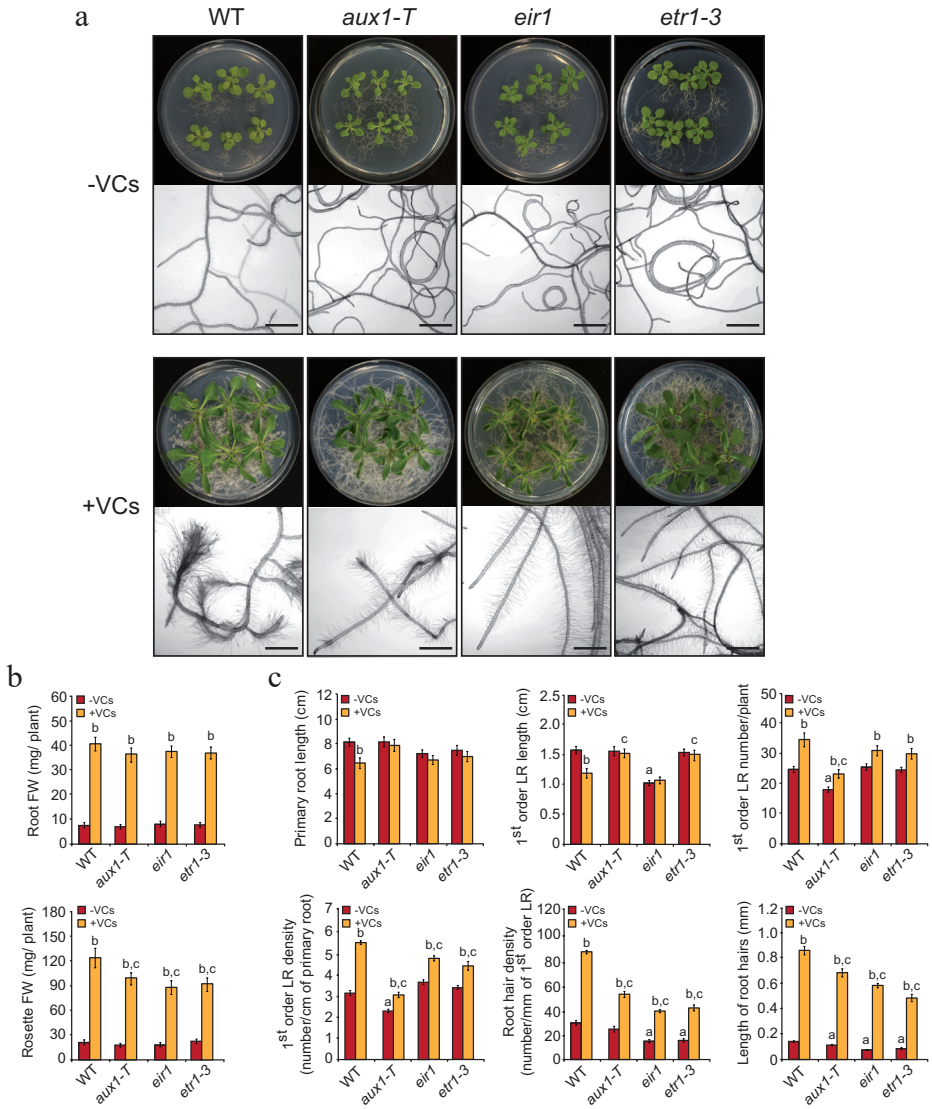

Figure 5: Changes in RSA promoted by VOCs-depleted fungal VCs involve enhanced auxin and ethylene signaling (a) external phenotypes, (b) root and rosette FW and (c) root architecture parameters of WT, *aux1-T, eir1* and *etr1-3* plants cultured in the absence or continuous presence of VOCs-depleted VCs emitted by adjacent *P. aurantiogriseum* cultures. Values in panels (b) and (c) are means ± SE for three biological replicates (each a pool of 12 plants) obtained from four independent experiments. Letters "a", "b" and "c" indicate significant differences, according to Student´s t-test ($P<0.05$), between: "a" WT plants and mutants cultured without fungal VC treatment, "b" VC-treated and non-treated plants, and "c" VC-treated WT and mutant plants. RH number and length data were obtained from a pool of 6 first order LRs per plant. Scale bars in "a", 2 mm. Plants providing data shown in (a) and (b) were grown on horizontal plates whereas those providing data in (c) were grown on vertical plates.

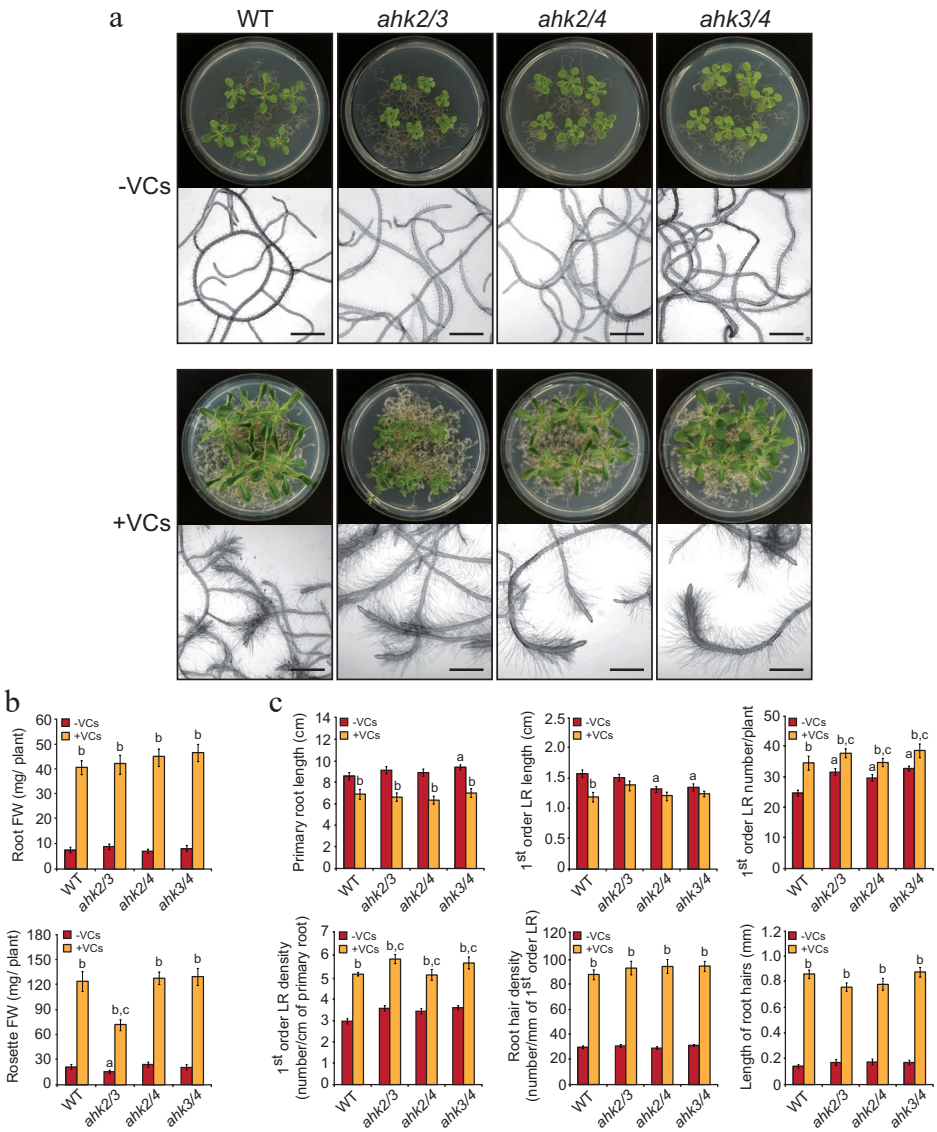

Figure 6: (a) external phenotypes, (b) rosette and root FW and (c) root architecture parameters of WT, *ahk2/3, ahk2/4* and *ahk3/4* plants cultured in the absence or continuous presence of VOCs-depleted VCs emitted by adjacent *P. aurantiogriseum* cultures for one week. Values in panels (b) and (c) are means ± SE for three biological replicates (each a pool of 12 plants) obtained from four independent experiments. Letters "a", "b" and "c" indicate significant differences, according to Student´s t-test ($P<0.05$), between: "a" WT plants and mutants cultured without fungal VC treatment, "b" VC-treated and non-treated plants, and "c" VC-treated WT and mutant plants. RH number and length data were obtained from a pool of 6 first order LRs per plant. Plants providing data shown in (a) and (b) were grown on horizontal plates, whereas those providing data in (c) were grown on vertical plates. Scale bars in "a", 2 mm.

and CK mutants developed new RHs and elongated them in response to fungal VCs, although the stimulatory effect in auxin and ethylene mutants was weaker than that in WT plants and CK signaling mutants (**Figure 5a,c, Figure 6c**). Unlike in WT and CK mutants, fungal VCs did not promote the development of a "cotton-like" external root phenotype caused by the formation of "brush-like" structures at the root tips in *aux1-T, eir1* and *etr1-3* mutants (**Figure 5a,c, Figure 6a**).

RSA adjustment promoted by VOCs-depleted fungal VCs is associated with enhanced ROS content in roots and RHs

Root and RH growth is associated with ROS accumulation (Foreman et al., 2003; Tsukagoshi et al., 2010; Manzano et al., 2014), which in turn is determined by cytosolic calcium concentration (Foreman et al., 2003; Drerup et al., 2013; Dubiella et al., 2013). VOCs-depleted fungal VCs promoted down-regulation of the expressions of calcium pumps, aquaporins and apoplastic peroxidases in roots (cf. **Supplemental Table 1, Figure 1**) suggesting enhanced ROS content. This was corroborated by specific superoxide anion (O_2^-) and H_2O_2 staining analyses, which revealed higher levels of O_2^- and H_2O_2 in roots and RHs of fungal VC-treated plants than in controls (**Figure 7**).

The possible involvement of ROS accumulation in the fungal VC-promoted RSA changes was investigated by characterizing the root and RH growth response of WT plants to the NADPH oxidase inhibitor diphenyleneiodium (DPI) (Cross and Jones, 1986). We also characterized the response of plants to ascorbic acid, which is known to modulate root architecture through antioxidant action (Olmos et al., 2006). Furthermore, we characterized the response of *rhd2* plants to VOCs-depleted fungal VCs. These plants lack an NADPH oxidase that contributes to ROS production in roots, and have shorter roots and RHs than WT plants (Foreman et al., 2003). As shown in **Figure 8** and **9**, enhancement of RH growth promoted by VOCs-depleted fungal VCs was weaker in DPI- and ascorbic acid-treated plants than in controls. As in WT plants, VOCs-depleted fungal VCs promoted root and rosette growth in *rhd2* plants (**Figure 10a,b**). As expected, in the absence of fungal VCs *rhd2* roots showed only a few short malformed RHs (**Figure 10a**) that accumulated low levels of O_2^- (**Figure 10**). Notably, unlike WT plants, this mutant was unresponsive in terms of O_2^- accumulation in RHs (**Supplemental Figure 2**), RH growth stimulation (**Figure 10a,c**) and PR and LR shortening promoted by fungal VCs (**Figure 10c**).

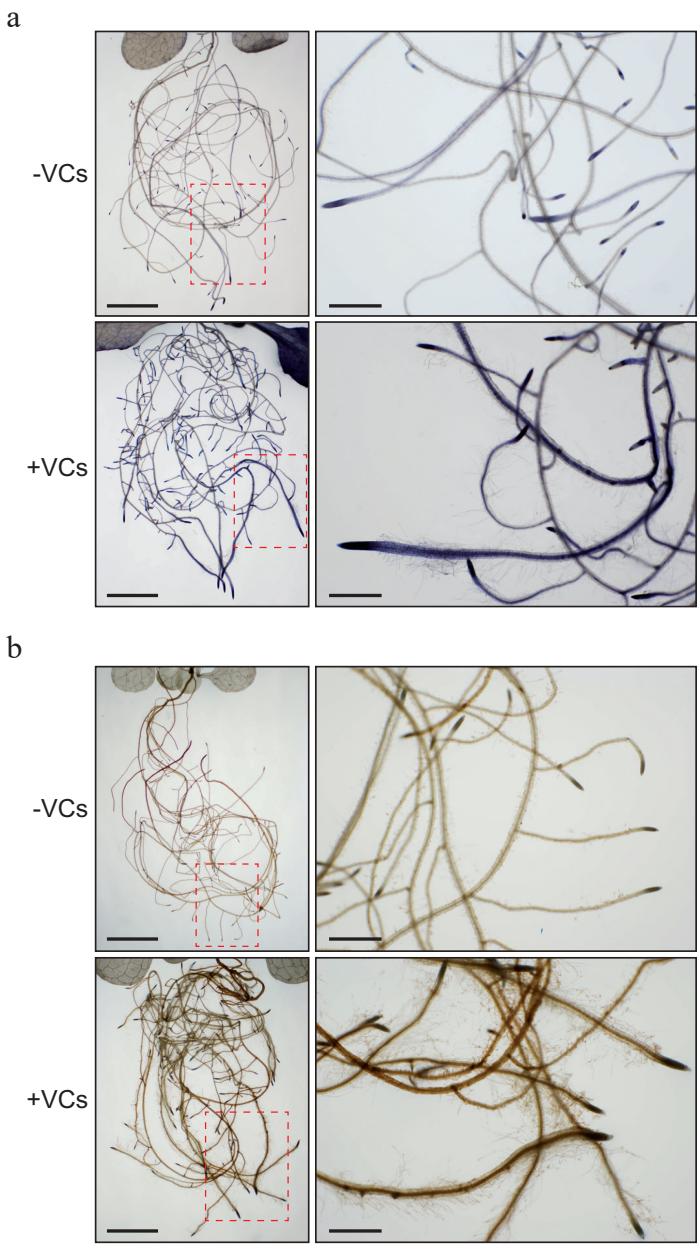

Figure 7: VOCs-depleted fungal VCs promote ROS accumulation in roots. (a) NBT staining of O_2- and (b) 3,3′-diaminobenzidine staining of H_2O_2 in roots of WT plants cultured in the absence or presence of adjacent cultures of *P. aurantiogriseum* with charcoal filters for one week. Scale bars: left panels, 5 mm; right panels, 1 mm.

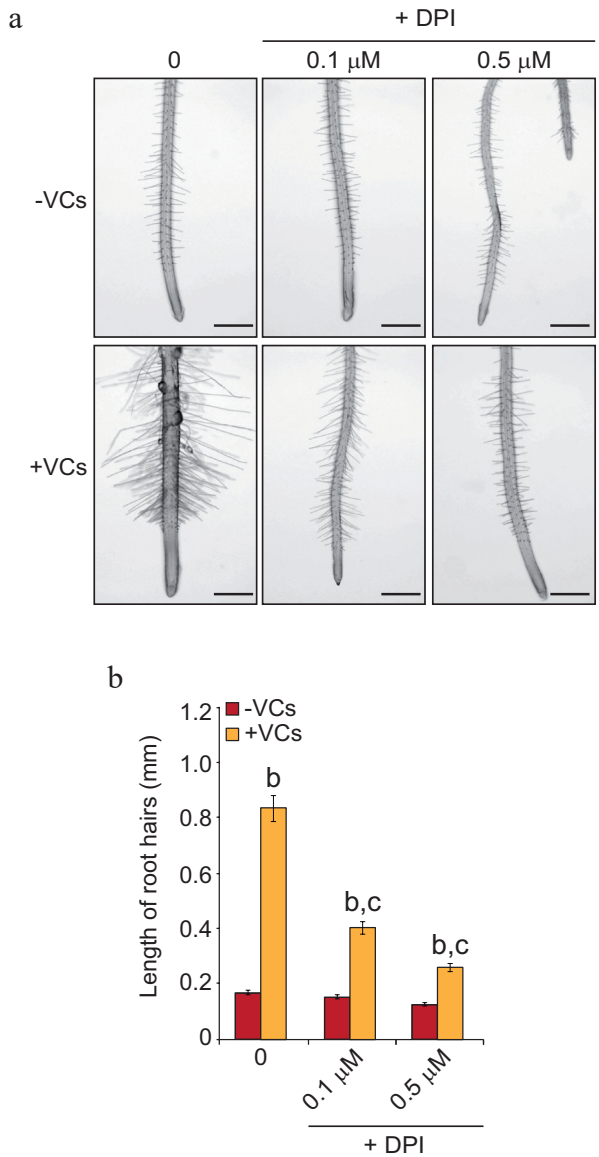

Figure 8: DPI treatment inhibits the fungal VC-promoted elongation of RHs. (a) Photographs of roots and (b) RH lengths of WT plants cultured in the absence or continuous presence of VOCs-depleted VCs emitted by adjacent *P. aurantiogriseum* cultures for one week, with or without DPI supplementation. Values in panel (b) are means ± SE for three biological replicates (each a pool of 12 plants) obtained from four independent experiments. Letter "b" and "c" indicate significant differences, according to Student´s t-test ($P<0.05$), between: "b" VC-treated and non-treated plants, and "c" VC-treated plants without DPI treatment and VC-treated plants with DPI treatment. RH length data were obtained from a pool of 6 first order LRs per plant. Plants were grown on vertical plates. Scale bars in "a", 500µm.

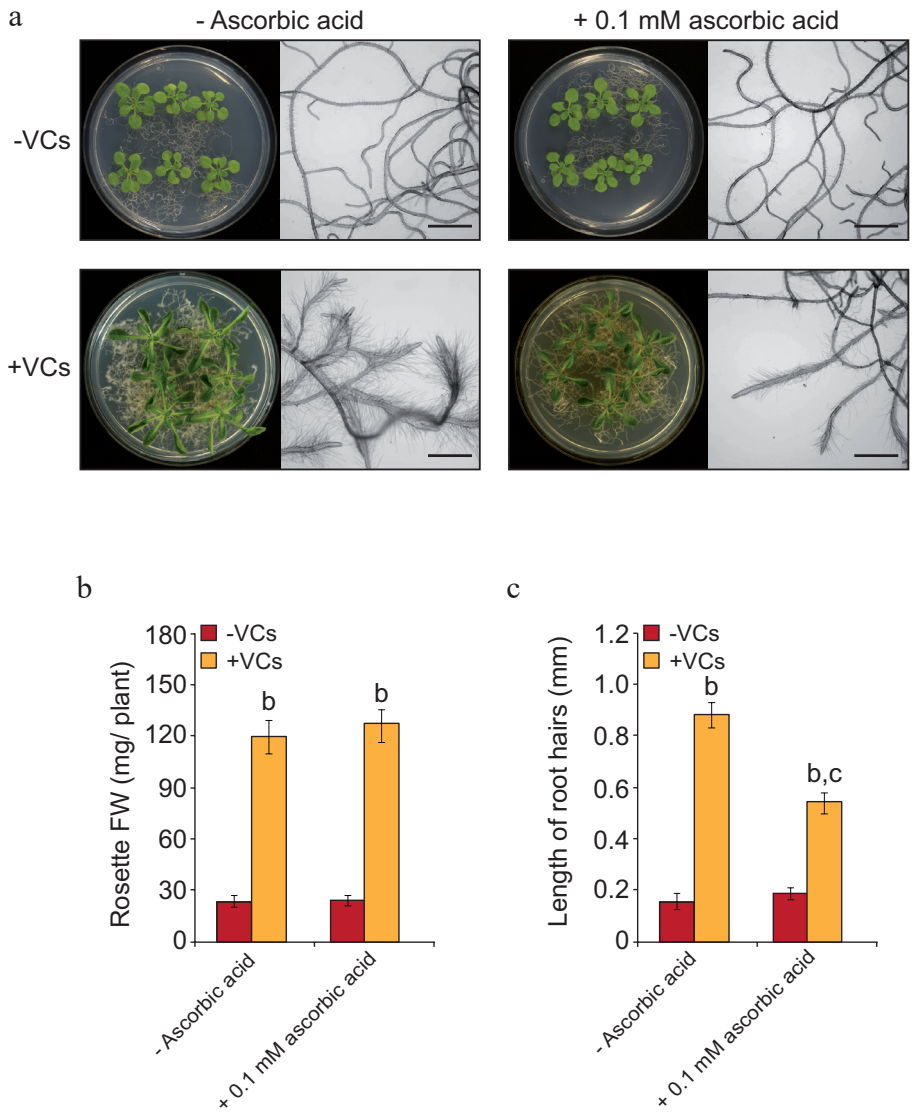

Figure 9: Ascorbic acid treatment inhibits the fungal VC-promoted elongation of RHs. (a) External phenotypes, (b) rosette FW and (c) RH length of WT plants cultured in solid MS medium with or without 0,1 mM ascorbic acid supplementation. Values in panels (b) and (c) are means ± SE for three biological replicates (each a pool of 12 plants) obtained from four independent experiments. Letters "b" and "c" indicate significant differences, according to Student´s t-test ($P<0.05$), between: "b" VC-treated and non-treated plants, and "c" VC-treated plants without ascorbic acid treatment and VC-treated plants with ascorbic acid treatment. RH length data were obtained from a pool of 6 first order LRs per plant. Plants were grown on vertical plates. Scale bars in "a", 2 mm.

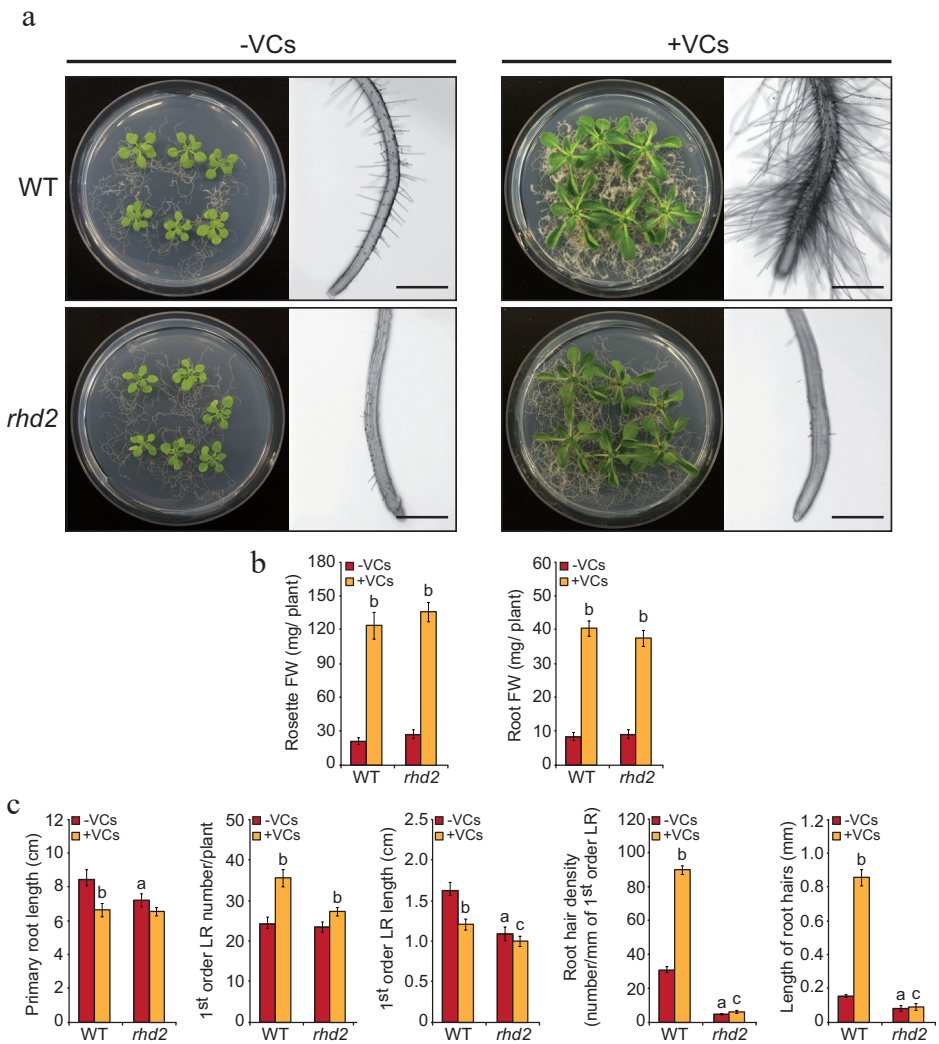

Figure 10: RSA adjustment promoted by VOCs-depleted fungal VCs is a ROS dependent process. (a) External phenotypes, (b) rosette and root FW, (c) root architecture parameters of WT and *rhd2* plants cultured in the absence or continuous presence of VOCs-depleted VCs emitted by adjacent *P. aurantiogriseum* cultures. Values in panels (b) and (c) are means ± SE for three biological replicates (each a pool of 12 plants) obtained from four independent experiments. Letters "a", "b" and "c" indicate significant differences, according to Student´s t-test (P<0.05), between: "a" WT and *rhd2* plants cultured without fungal VC treatment, "b" VC-treated and non-treated plants, and "c" VC-treated WT and *rhd2* plants. RH number and length data were obtained from a pool of 6 first order LRs per plant. Plants providing data shown in (a) and (b) were grown on horizontal plates, whereas those providing data in (c) were grown on vertical plates. Scale bars in "a", 500 µm.

CAS-C1 is an important mediator of root responses to VOCs-depleted fungal VCs

Cyanide (HCN) is a toxic compound produced mainly by 1-aminocyclopropane-1-carboxylate oxidase (ACO) in the last step of the ethylene biosynthetic pathway. Mitochondrial β-cyanoalanine synthase (CAS-C1) participates in HCN detoxification (García et al., 2010; Arenas-Alfonseca et al., 2018). CAS-C1 null *cas-c1* mutants accumulate more HCN and produce fewer and shorter RHs than WT plants (García et al., 2010, Arenas-Alfonseca et al., 2018). It has therefore been suggested that CAS-C1 is essential in order to maintain low HCN levels and allow for proper RH development (García et al., 2010). In addition, *cas-c1* RHs accumulate lower levels of ROS than WT RHs (García et al., 2010; Arenas-Alfonseca et al., 2018). Fungal VC-promoted expression of ethylene biosynthetic enzymes (e.g. METK2, METK3 and ACO2) and CAS-C1 (cf. **Supplemental Table 1, Figure 1**) suggested that up-regulation of CAS-C1 could play a role in the elongation process promoted by fungal VCs by removing the HCN generated by ACO2. To test this hypothesis we measured HCN levels in roots of WT plants cultured in the absence or presence of adjacent fungal cultures covered with charcoal filters. We also characterized the RSA and ROS accumulation responses of *cas-c1* mutants to VOCs-depleted fungal VCs.

Fungal VCs caused a ca. 3-fold increase in HCN contents in roots (15.5 ± 5.9 and 42.3 ± 6.2 nmol g^{-1} FW in non-treated and VC-treated plants, respectively). As in WT plants, VOCs-depleted fungal VCs promoted root and rosette growth in *cas-c1* plants (**Figure 11a,b**). In keeping with findings by García et al. (2010), *cas-c1* roots not treated with fungal VCs exhibited only a few short malformed RHs (**Figure 11a**) and accumulated low levels of O_2^- in the RHs (**Supplemental Figure 2**). Notably, unlike WT plants, this mutant did not exhibit O_2^- accumulation in RHs (**Supplemental Figure 2**), RH growth stimulation (**Figure 11a,c**) and LR shortening in response to exposure to fungal VCs (**Figure 11c**).

4. DISCUSSION

Fungal VCs promote changes in the root proteome that affect metabolic processes involved in growth and development

This is the first study reporting a high-throughput, isobaric labeling-based analysis of the changes in the roots proteome in response to microbial emissions, particularly VCs. Using a 2DE approach, Kwon et al. (2016) reported changes in the expression of 17

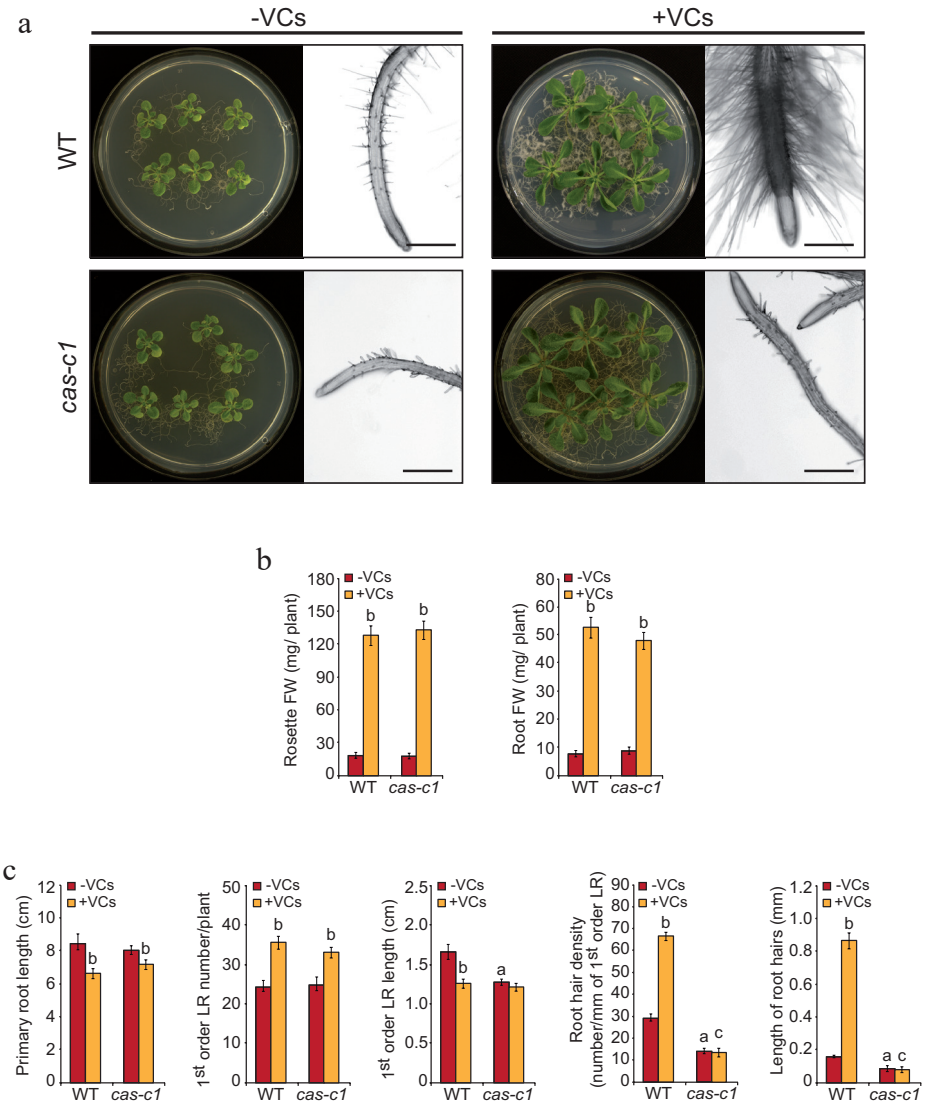

Figure 11: CAS-C1 is an important mediator of the root response to VOCs-depleted fungal VCs. (a) External phenotypes, (b) rosette and root FW, (c) root architecture parameters of WT and *cas-c1* plants cultured in the absence or continuous presence of VOCs-depleted VCs emitted by adjacent *P. aurantiogriseum* cultures for one week. Values in panels (b) and (c) are means ± SE for three biological replicates (each a pool of 12 plants) obtained from four independent experiments. Letters "a", "b" and "c" indicate significant differences, according to Student´s t-test ($P<0.05$), between: "a" WT and *cas-c1* plants cultured without fungal VC treatment, "b" VC-treated and non-treated plants, and "c" VC-treated WT and cas-c1 plants. RH number and length data were obtained from a pool of 6 first order LRs per plant. Plants providing data shown in (a) and (b) were grown on horizontal plates, whereas those providing data in (c) were grown on vertical plates. Scale bars in "a", 500 µm

proteins in roots of Arabidopsis plants after inoculation with the plant-growth promoting rhizobacterium *Paenibacillus polymyxa* E681; none of them were identified in our study. This indicates that the strategies of proteome adaptation to inoculation with beneficial bacteria and treatment with VCs emitted by a fungal phytopathogen differ greatly. That only 8% of the proteins that were differentially expressed by fungal VCs in roots were also differentially expressed in VC-exposed leaves (**Supplemental Table 1**) strongly indicates that strategies for acclimation to fungal VCs are quite distinct in tissues below and above ground.

Our data strongly indicate that root growth and developmental changes promoted by VCs from fungal phytopathogens is largely due to metabolic reorganization partly caused by proteome resetting. ATP-citrate lyase (ACL) is a cytosolic enzyme that catalyzes the conversion of citrate to acetyl-CoA and oxalacetate and is required for normal growth and development (Fatland et al., 2005). Changes in ACLA expression are associated with alterations in the levels of cytosolic acetyl-CoA-derived metabolites including MVA-derived isoprenoids some of which (e.g. CKs) are important mediators in the growth and developmental responses to environmental changes. For this reason, it has been suggested that ACLA is an important determinant of MVA-derived isoprenoid synthesis growth and development (Fatland et al., 2005). VOCs-depleted fungal VCs enhanced ACLA-1 expression (**Supplemental Table 1, Figure 1**) and levels of MVA-derived CKs (e.g. cZ, cZR and cZRMP) (**Table 2**). It is therefore conceivable that the accumulation of MVA-derived CKs promoted by fungal VCs is due, at least in part, to augmented ACLA-1 expression as schematically illustrated in **Figure 12**. The high levels of MEP-derived CKs (**Table 2**) occurring in fungal VC-exposed roots could be explained by the transport of dimethylallyl diphosphate from the cytosolic MVA pathway into plastids (Kasahara et al., 2004) (**Figure 12**).

VOCs-depleted fungal VCs reduced the expression of aquaporins and the IRT1 metal ion transporter in roots (**Figure 1, Supplemental Table 1**), and this was associated with reduced Fe and Zn levels in leaves. Because CKs down-regulate IRT1 expression (Séguéla et al., 2008), it is tempting to speculate that fungal VC-promoted reduction in the metal ion content of roots is primarily due to reduced IRT1 expression caused by the enhancement of CK levels (**Table 2**) and signaling (**Figure 3a**). One possible explanation for the fungal VC-promoted down-regulation of expression of IRT1 and aquaporins is that fungal VCs greatly enhance the photosynthetic efficiency

thus reducing the water and Fe demands of leaves. In line with this presumption, plants exposed to fungal VCs had higher WUE*i* than controls (**Figure 2**). Our findings are consistent with the idea that root iron acquisition is under long-distance regulation by photosynthesis (Vert et al., 2003).

Amino acid metabolism plays an important role in regulating root growth and development (Mo et al., 2006; Muñoz-Bertomeu et al., 2009; Pelagio-Flores et al., 2011; Frémont et al., 2013). Fungal VCs promoted the accumulation of the long-distance nitrogen transport amino acids Glu, Asn and Gln (**Table 1**). This metabolic change was associated with enhanced expression of plastidial Glu synthase 1 (GLUT1) and enzymes involved in the conversion of cytosolic citrate to Glu and Gln (e.g. ASP2 and GLN1-2) and the conversion of cytosolic Met and mitochondrial Cys to cytosolic Asp, Asn, Glu and Gln (e.g. METK2, METK3, ACO2 and CAS-C1) (**Supplemental Table 1, Figure 1**). CKs up-regulate METK2, METK3 and ACO2 expression (Žd'árská et al., 2013; Brenner and Schmülling, 2015), which suggests that fungal VC-promoted augmentation of Asp, Asn, Glu and Gln contents in roots is due, at least in part, to enhanced METK2, METK3 and ACO2 expression caused by the increase in CK levels. Fungal VCs also led to the accumulation of citrate and other TCA intermediates (**Table 1**). This metabolic change was not associated with altered expression of TCA cycle enzymes or other proteins involved in mitochondrial respiration. Overall, the findings indicate that the stimulatory effect of fungal VCs on Glu, Gln, Asp and Asn contents and growth is due, at least in part, to activation of amino acid metabolism through mechanisms involving post-translational activation of mitochondrial respiration enzymes and CK-mediated transcriptional and/or translational up-regulation of the expression of enzymes involved in the conversion of cytosolic Met and mitochondrially synthesized citrate and Cys into cytosolic Glu, Gln, Asp and Asn as schematically illustrated in **Figure 12.**

VOCs-depleted fungal VCs down-regulated the expression of cell wall breakdown enzymes, and stimulated the expression of enzymes involved in the synthesis of precursors for cell wall biosynthesis (**Supplemental Table 1, Figure 1**). Consistently, fungal VCs enhanced the intracellular levels of the cell wall polysaccharides precursors glucuronic acid and UDP-glucose in roots. In Arabidopsis, mutants impaired in enzymes involved in the synthesis of cell wall polysaccharides show reduced growth and defects in LR and RH development (Favery et al., 2001; Diet et al., 2006; Handford et al., 2012). It is therefore conceivable that the root growth and RSA changes promoted by fungal

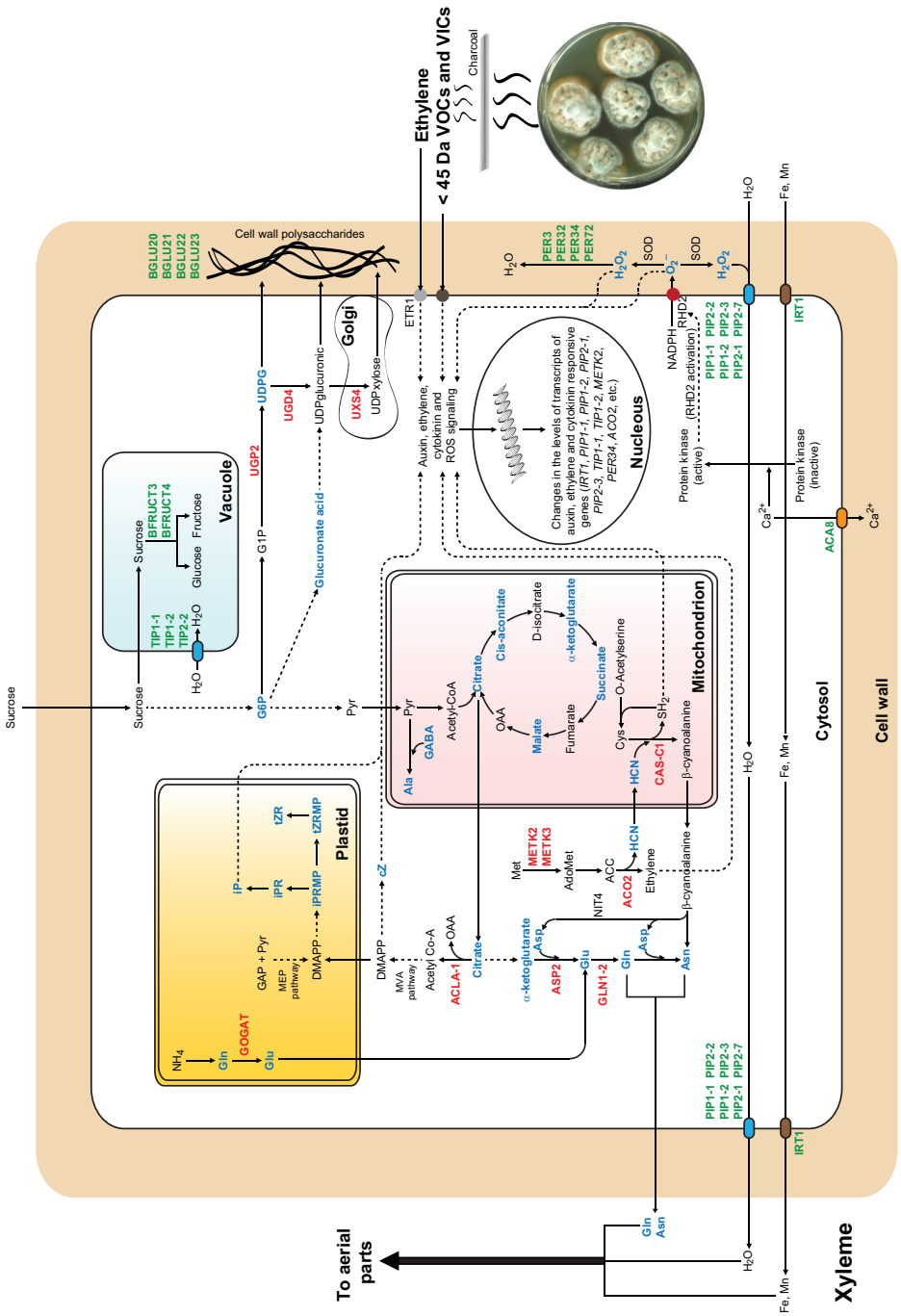

VCs are at least partly due to enhanced expression of cell wall biosynthetic enzymes and down-regulation of cell wall degradation enzymes, as illustrated in **Figure 12.**

BFRUCT4 is a vacuolar invertase that has been suggested as being in the conversion of sucrose to fructose and glucose leading to osmotic water uptake and a subsequent increase in turgor as a driving force for root elongation (Sergeeva et al., 2006). Consistent with this hypothesis, plants lacking BFRUCT4 have shorter roots than WT plants (Sergeeva et al., 2006; Leskow et al., 2016). VOCs-depleted fungal VCs down-regulated the expression of BFRUCT4 (**Supplemental Table 1, Figure 1**) and shortened PR and LRs (**Figure 5**). This finding indicates that root shortening in response to fungal VCs is due, at least to some extent, to down-regulation of BFRUCT4 expression.

Promotion of root shortening by VOCs-depleted fungal VCs involves enhanced auxin, ethylene and CK signaling

Ethylene, auxin and CK inhibit root growth (Riefler et al., 2006; Stepanova et al., 2007; Swarup et al., 2007; Street et al., 2015). VOCs-depleted fungal VCs shortened PR, but not LR, in the *ahk2/3, ahk2/4* and *ahk3/4* CK signaling mutants (**Figure 6c**). Furthermore, fungal VCs did not shorten PR and LRs in the *aux1-T, eir1* and *etr1-3* mutants (**Figure**

Figure 12: Suggested model for regulation of root proteomic and metabolic responses to VOC-depleted fungal VCs. Mixtures of VOC-depleted fungal VCs (VICs and/or VOCs with molecular masses of less than 40 Da) up-regulate the expression of ACLA-1, which regulates the metabolic flux from mitochondrially synthesized citrate to MVA-derived isoprenoids such as CKs. The resulting enhanced CK content down-regulates the expression of IRT1, thus restricting the uptake and subsequent transport of Fe to the aerial part of the plant. CKs up-regulate the expression of enzymes involved in the conversion of cytosolic Met to ethylene and HCN (METK2, METK and ACO2) the latter being converted to Asp, Glu and the long-distance nitrogen transport amino acids Asn and Gln by means of the ethylene-induced CAS-C1, ASP2 and GLN1-2. The resulting enhanced ethylene level promotes root shortening and RH formation and elongation. Fungal VCs down-regulate the expression of aquaporins through enhanced auxin signaling action, thus reducing H_2O and H_2O_2 uptake by root cells. Fungal VCs also down-regulate ACA8 calcium pump expression. Activation of plasma membrane NADPH oxidases by the resulting high cytoplasmic calcium concentrations, and down-regulation of aquaporins and apoplastic peroxidases (e.g. PER3, PER32, PER34 and PER72) by fungal VCs leads to apoplastic oxidative burst due to the accumulation H_2O_2 and O_2-, which promotes root and RH growth and RH elongation. Fungal VCs down-regulate the expression of vacuolar invertases (e.g. BFRUCT 3 and 4), thus limiting glucose and fructose production from sucrose. This, and the reduction of water uptake due to down-regulation of aquaporin expression, leads to a reduction in turgor as a driving force for root elongation. Enzymatic activities that are up-regulated by VOC-depleted fungal VCs are highlighted with red letters, whereas enzymatic activities and pathways that are down-regulated by VCs are highlighted with green letters. Multistep enzymatic reactions and signaling cascades are depicted with dashed arrows. Metabolites whose levels are higher in roots exposed to fungal VCs than in controls are highlighted in blue. DMAPP: dimethylallyl diphosphate.

5a,c). It can therefore be concluded that fungal VC-promoted RSA changes related to PR length are largely CK-independent, whereas those related to LR length involve CK and canonical auxin and ethylene signaling pathways. Root elongation is due mainly to an increase in the volume of cells along the growing zone, which is caused by water entering the cell via aquaporins (Hukin et al., 2002). Aquaporin genes are repressed by auxin (Nemhauser et al., 2006; Péret et al., 2012). VOCs-depleted fungal VCs enhanced auxin signaling (**Figure 3b**) and down-regulated the expression of aquaporins (**Supplemental Table 1, Figure 1**). It is thus conceivable that the PR and LR shortening that results from exposure to fungal VCs is due, at least in part, to enhanced auxin signaling, which in turn limits water uptake as a consequence of the down-regulation of the expression of aquaporins (**Figure 12**).

VOCs-depleted fungal VCs enhanced ethylene and active CK synthesis and signaling (**Table 3, Figures 3** and **5**) and the expression of ethylene biosynthetic enzymes (e.g. METK2, METK3 and ACO2) (**Supplemental Table 1, Figure 1**). CKs up-regulate the expression of enzymes involved in the synthesis of ethylene (Žd'árská et al., 2013; Brenner and Schmülling, 2015), which is known to exert a negative effect on LR growth (Stepanova et al., 2005). It is thus likely that the fungal VC-promoted LR shortening is due, at least in part, to enhanced CK signaling, which in turn limits LR growth through enhanced ethylene action (**Figure 12**).

Promotion of LR formation and RH proliferation and elongation by VOCs-depleted fungal VCs involves auxin, ethylene and CK signaling independent mechanisms

Auxin, ethylene and CKs are important determinants of LR formation (Pitts et al., 1998; Riefler et al., 2006; Ivanchenko et al., 2008; Negi et al., 2008; Werner et al., 2010; Chang et al., 2013). Moreover, auxin and ethylene serve as key mediators of RH formation and elongation (Pitts et al., 1998). VOCs-depleted VCs emitted by *P. aurantiogriseum* increased LR number in auxin, ethylene and CK signaling mutants (**Figures 5a,c** and **6c**), and strongly promoted RH formation and elongation in these mutants (**Figures 5a,c** and **6c**). These findings suggest the operation of important auxin, ethylene and CK signaling independent mechanisms in the promotion of LR formation and proliferation and elongation of RHs by fungal VCs. It is worth to note that the stimulatory effect of fungal VCs on RH formation and elongation was stronger in WT plants than in auxin and ethylene mutants (**Figure 5c**). In the presence of fungal VCs,

these mutants failed to form "brush-like" structures at the root tips (**Figure 5a**). It thus appears that the promotion of the "cotton-like" external root phenotype by fungal VCs caused by the strong proliferation and elongation of RHs at the root tips is auxin- and ethylene- dependent.

LR shortening and RH formation and elongation promoted by VOCs-depleted fungal VCs are ROS-dependent processes

ROS accumulation in the apoplast, mediated through the activity of redox metabolism-related enzymes (e.g. NADPH oxidases and peroxidases), plays an important role in root and RH growth and development (Foreman et al., 2003; Passardi et al., 2006; Montiel et al., 2012; Manzano et al., 2017). Plasma membrane aquaporins are capable of transporting H_2O_2 (Bienert et al., 2007; Dynowski et al., 2008; Rodrigues et al., 2017) and thus may act as determinants of apoplastic ROS content (Grondin et al., 2015). Here we found that VOCs-depleted fungal VCs enhanced ROS levels in roots and RHs (**Figure 7, Supplemental Figure 2**). Fungal VCs also down-regulated the expression of plasma membrane aquaporins and redox metabolism-related enzymes **(Supplemental Table 1, Figure 1**), some of which (e.g. PER34) are directly involved in root growth and RH formation and development (Passardi et al., 2006; Manzano et al., 2017). Furthermore, VOCs-depleted fungal VCs reduced the expression of ACA8, a calcium pump that determines the concentration of the cytosolic calcium that regulates NADPH oxidase activity through calcium-dependent protein kinases (Drerup et al., 2013; Dubiella et al., 2013; Costa et al., 2017; Yang et al., 2017). We also found that the NADPH oxidase inhibitor DPI and the antioxidant ascorbic acid prevent the RH elongation promoted by *P. aurantiogriseum* VCs (**Figures 8** and **9**) and that *rhd2* plants lacking a root-expressed NADPH oxidase do not show O_2^- accumulation in RHs (**Supplemental Figure 2**), RH growth stimulation (**Figure 10a,c**) and LR shortening in response to fungal VCs (**Figure 10c**). Overall the data provide evidence that an apoplastic oxidative burst due to down-regulation of plasma membrane aquaporins and apoplastic peroxidases, and activation of NADPH oxidases by calcium-dependent protein kinases, are major determinants of the root´s response to VOCs-depleted fungal VCs (**Figure 12**).

ROS may function as a downstream component in auxin-mediated signal transduction (Ma et al., 2014; Mangano et al., 2017). As auxin down-regulates aquaporin gene expression (Nemhauser et al., 2006; Péret et al., 2012) and fungal VCs

enhance auxin signaling (**Figure 3b**), it is conceivable that the fungal VC-promoted root response caused by an apoplastic oxidative burst is due, at least in part, to down-regulation of expression of plasma membrane aquaporins caused by enhanced auxin signaling (**Figure 12**).

CAS-C1 mediates the root response to VOCs-depleted fungal VCs through mechanisms other than the maintenance of low HCN levels

Synthesis of ethylene results in the production of HCN, which is a potent toxin that inhibits heme-containing enzymes such as cytochrome c oxidase and peroxidases. To prevent self-poisoning, plants maintain an endogenous HCN detoxification pathway involving CAS-C1, which catalyzes the addition of HCN to Cys to produce H_2S and β-cyanoalanine, the latter being transported from mitochondria to the cytosol where it is converted to Asp or Asn by β-cyanoalanine nitrilase (NIT4) (Piotrowski et al., 2001) (**Figure 12**). CAS-C1 null mutants accumulate 40-60% more HCN and produce fewer and shorter RHs than WT plants (García et al., 2010; Arenas-Alfonseca et al., 2018). Thus, it has been suggested that CAS-C1 is essential in maintaining HCN at low levels that allow proper RH development (García et al., 2010).

VOCs-depleted fungal VCs enhanced the expression of ethylene biosynthetic enzymes (e.g. METK2, METK3 and ACO2) and CAS-C1 (**Supplemental Table 1, Figure 1**). This finding suggests that CAS-C1 may play a role in the fungal VC-promoted RH elongation and activation of mitochondrial respiration by removing the HCN generated by ACO2. We found that fungal VCs do not promote RH elongation in *cas-c1* plants (**Figure 11**), which supports the idea that CAS-C1 is an important mediator of the RH response to fungal VCs and indicates that no other HCN scavenging system can replace CAS-C1 in promoting RH elongation in response to fungal VC exposure. However, fungal VCs caused a ca. 3-fold increase in HCN contents in the roots of WT plants. This finding strongly indicates that (a) roots of WT plants exposed to fungal VCs are capable of accumulating high levels of HCN without inhibiting mitochondrial respiration and RH formation and elongation, and (b) CAS-C1 operates in the fungal VC-promoted RH formation and elongation through mechanisms other than maintaining low levels of HCN.

In Arabidopsis, enhanced flux from HCN to Asn and Asp by the ectopic expression of β-cyanoalanine nitrilase promotes RH elongation (O'Leary et al., 2014).

One possible explanation for the fungal VC-promoted RH formation and elongation could therefore involve the conversion of HCN produced by ACO2 to cytosolic Asp, Asn, Glu and Gln through the coupled reactions of CAS-C1, NIT4, ASP2 and GLN1-2 as schematically illustrated in **Figure 12**. Lack of CAS-C1 prevents not only the scavenging of HCN molecules produced in the last step of the ethylene biosynthetic pathway but also the formation of ROS by hitherto unknown mechanisms (Arenas-Alfonseca et al., 2018). Here we found that *cas-c1* plants are unresponsive in terms of O_2^- accumulation in RHs (**Supplemental Figure 2**). Therefore, another possible explanation for the RH formation and elongation promoted by fungal VCs could involve the enhancement of ROS production and signaling by as yet to be identified CAS-C1 dependent mechanisms. At low concentrations H_2S can act as a signaling molecule that promotes growth and RSA changes (Chen et al., 2011; Lisjak et al., 2013; Mei et al., 2017). Therefore, a third explanation for the fungal VC-promoted RH changes could involve the enhancement of CAS-C1-mediated H_2S production.

Concluding and additional remarks

This is to our knowledge the first comprehensive study on the response of roots to VCs emitted by a fungal phytopathogen. Our results show for the first time that microbial VCs can modulate root architecture through mechanisms involving HCN scavenging. Our findings also show that VCs from a fungal phytopathogen can modulate root metabolism and architecture through complex mechanisms involving proteome changes mediated by CK, ethylene, auxin and ROS. Our data contrast with previous reports showing that complex mixtures of VCs or discrete (individual) VOCs emitted by beneficial microorganisms exert a null or minor effect on LR formation and RH formation and elongation in auxin and ethylene signaling mutants (Splivallo et al., 2009, Contreras-Cornejo et al., 2015; Garnica-Vergara et al., 2016). Furthermore, our results differ from those of studies showing that complex mixtures of VCs emitted by the symbiotic fungus *Trichoderma atroviride* inhibit PR growth in ethylene signaling mutants (Contreras-Cornejo et al., 2015). In addition, our findings contrast with reports showing that VCs from beneficial rhizobacteria and rhizofungi enhance IRT1 expression (Zhang et al., 2009; Zamioudis et al., 2013; Martínez-Medina et al., 2017). It thus appears that the mechanisms involved in RSA and metabolic adjustments to VCs emitted by beneficial and by pathogenic microorganisms are different. Clearly, further

experiments are necessary in order to test this hypothesis.

5. SUPPLEMENTAL FIGURES AND TABLES

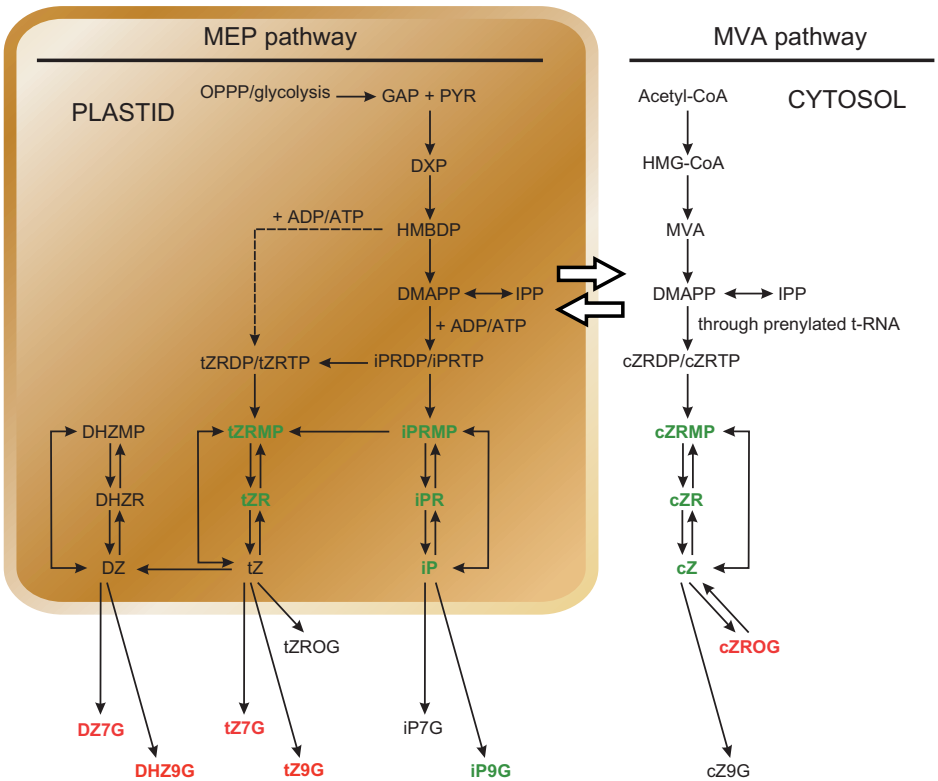

Supplemental Figure 1: VCs emitted by *P. aurantiogriseum* promote augmentation of the levels of CKs in roots. Scheme representing pathways of CK biosynthesis through the plastidic MEP and cytosolic MVA pathways is shown. Metabolites whose levels are higher in roots exposed to fungal VCs-exposed than in controls are highlighted in green, and metabolites whose levels are lower in roots exposed to fungal VCs-exposed than in controls are highlighted in red. Data from Table 3. Multistep reactions are depicted with hollow arrows.

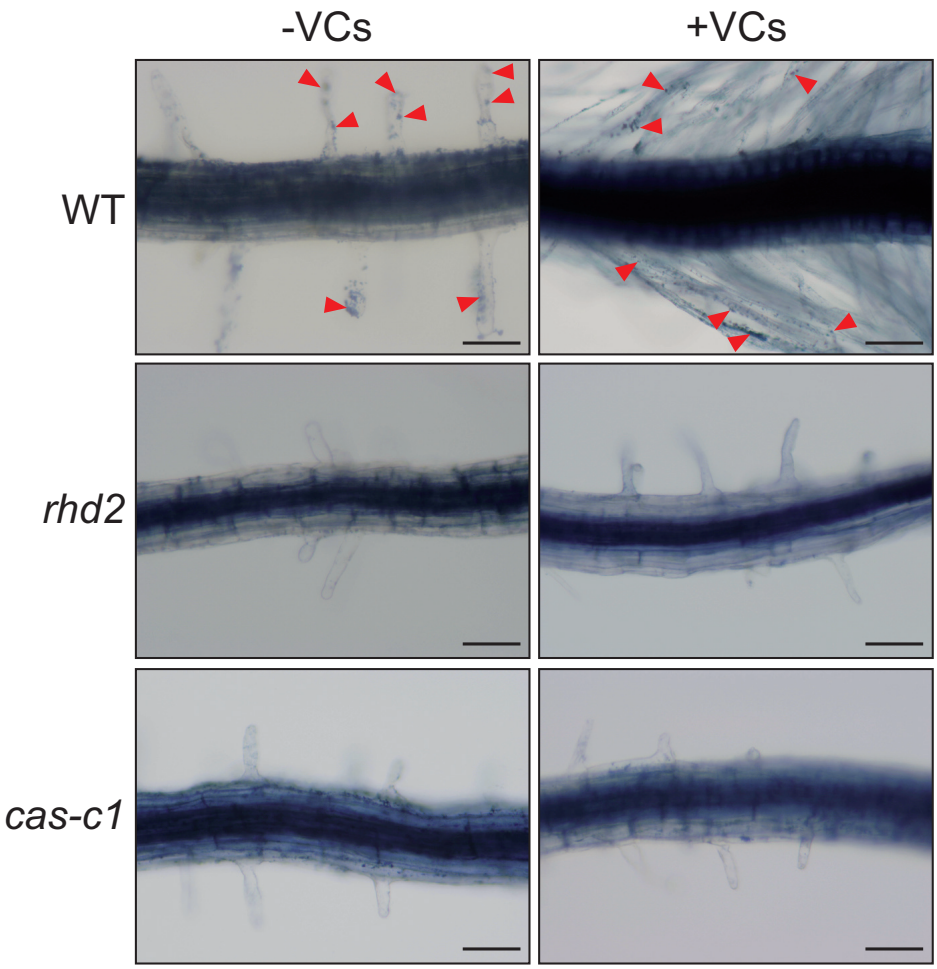

Supplemental Figure 2: VOCs-depleted fungal VCs promote O_2^- accumulation in WT RHs but not in *rhd2* and *cas-c1* RHs. NBT staining of O2- in RHs of WT, *rhd2* and *cas-c1* plants cultured in the absence or presence of adjacent cultures of *P. aurantiogriseum* with charcoal filters for one week. Red arrowheads indicate diformazan precipitates formed by NBT reduction by O_2^-. Scale bars 200 μm.

Supplemental Table 1: list of proteins whose expression is differentially regulated by VOCs-depleted VCs of *P. aurantigrioseum*. DEPs are classified according to their functions. DEPs that are discussed in the main text are highlighted in yellow.

Accesión number	Protein ID	Fold change (log2)	qValue (FDR)	Subcellular location	Description
Amino acid metabolism					
AT3G04520	Q9FPH3	1.497	0,019	Cytosol	Q9FPH3|THA2_ARATH Probable low-specificity L-threonine aldolase 2 OS=Arabidopsis thaliana GN=THA2 PE=1 SV=1
AT1G66200	Q8LCE1	0.968	0,011	Cytosol	Q8LCE1|GLN1-2_ARATH Glutamine synthetase cytosolic isozyme 1-2 OS=Arabidopsis thaliana GN=GLN1-2 PE=1 SV=2
AT5G53460	Q9LV03	0.626	0,014	Plastid	Q9LV03|GLUT1_ARATH Glutamate synthase 1 [NADH], chloroplastic OS=Arabidopsis thaliana GN=GLUT1 PE=1 SV=2
AT3G61440	Q9S757	0.52	0,025	Mitochondrion	Q9S757|CAS-C1_ARATH Bifunctional L-3-cyanoalanine synthase/cysteine synthase C1, mitochondrial OS=Arabidopsis thaliana GN=CAS-C1 PE=1 SV=1
AT5G19550	P46645	0.419	0,05	Cytosol	P46645|AAT2_ARATH Aspartate aminotransferase, cytoplasmic isozyme 1 OS=Arabidopsis thaliana GN=ASP2 PE=1 SV=2
AT2G43910	Q0WP12	-0.558	0,015	Cytosol	Q0WP12-2|HOL1_ARATH Isoform 2 of Thiocyanate methyltransferase 1 OS=Arabidopsis thaliana GN=HOL1
AT1G23310	Q9LR30	-0.873	0,013	Peroxisome	Q9LR30|GGT1_ARATH Glutamate--glyoxylate aminotransferase 1 OS=Arabidopsis thaliana GN=GGAT1 PE=1 SV=1
AT3G45300	Q9SWG0	-0.942	0,002	Mitochondrion	Q9SWG0|IVD_ARATH Isovaleryl-CoA dehydrogenase, mitochondrial OS=Arabidopsis thaliana GN=IVD PE=1 SV=2
AT4G29840	Q9S7B5	-2.352	0,013	Plastid	Q9S7B5|THRC1_ARATH Threonine synthase 1, chloroplastic OS=Arabidopsis thaliana GN=TS1 PE=1 SV=1
Biodegradation of xenobiotics					
AT1G53580	Q9C8L4	-0.633	0,02	Mitochondrion	Q9C8L4|ETHE1_ARATH Persulfide dioxygenase ETHE1 homolog, mitochondrial OS=Arabidopsis thaliana GN=GLY3 PE=1 SV=3
Cell					
AT5G39510	Q9SEL6	1.218	0,048	ER, Golgi	Q9SEL6|VTI11_ARATH Vesicle transport v-SNARE 11 OS=Arabidopsis thaliana GN=VTI11 PE=1 SV=2
AT1G52360	Q9C827	0.843	0,024	Golgi	Q9C827|COB22_ARATH Coatomer subunit beta'-2 OS=Arabidopsis thaliana GN=At1g52360 PE=1 SV=1
AT4G34870	Q42406	0.609	0,005	Golgi	Q42406|CP18D_ARATH Peptidyl-prolyl cis-trans isomerase CYP18-4 OS=Arabidopsis thaliana GN=CYP18-4 PE=1 SV=1
AT1G35720	Q9SYT0	0.502	0,008	Apoplast	Q9SYT0|ANXD1_ARATH Annexin D1 OS=Arabidopsis thaliana GN=ANN1 PE=1 SV=1
Cell Wall					
AT4G25820	Q9ZSU4	1.857	0,044	Extracellular	Q9ZSU4|XTH14_ARATH Xyloglucan endotransglucosylase/hydrolase protein 14 OS=Arabidopsis thaliana GN=XTH14 PE=1 SV=1
AT5G44130	Q9FFH6	0.941	0,045	Plasma membrane	Q9FFH6|FLA13_ARATH Fasciclin-like arabinogalactan protein 13 OS=Arabidopsis thaliana GN=FLA13 PE=1 SV=1
AT2G47650	Q8S8T4	0.711	0,003	Golgi	Q8S8T4|UXS4_ARATH UDP-glucuronic acid decarboxylase 4 OS=Arabidopsis thaliana GN=UXS4 PE=2 SV=1
AT5G39320	Q9FM01	0.705	0,004	Cytosol	Q9FM01|UGDH4_ARATH UDP-glucose 6-dehydrogenase 4 OS=Arabidopsis thaliana GN=UGD4 PE=1 SV=1
AT3G03250	Q9M9P3	0.414	0,05	Cytosol	Q9M9P3|UGPA2_ARATH UTP--glucose-1-phosphate uridylyltransferase 2 OS=Arabidopsis thaliana GN=UGP2 PE=1 SV=1
AT3G10740	Q9SG80	-0.621	0,022	Apoplast	Q9SG80|ASD1_ARATH Alpha-L-arabinofuranosidase 1 OS=Arabidopsis thaliana GN=ASD1 PE=1 SV=1
AT1G66280	Q9C8Y9	-0.674	0,014	ER	Q9C8Y9|BGL22_ARATH Beta-glucosidase 22 OS=Arabidopsis thaliana GN=BGLU22 PE=1 SV=1
AT5G06860	Q9M5J9	-0.744	0,005	Golgi, cell wall	Q9M5J9|PGIP1_ARATH Polygalacturonase inhibitor 1 OS=Arabidopsis thaliana GN=PGIP1 PE=1 SV=1
AT3G09260	Q9SR37	-0.857	0,006	ER	Q9SR37|BGL23_ARATH Beta-glucosidase 23 OS=Arabidopsis thaliana GN=BGLU23 PE=1 SV=1
AT5G58090	Q93Z08	-0.934	0,034	Plasma membrane	Q93Z08|E136_ARATH Glucan endo-1,3-beta-glucosidase 6 OS=Arabidopsis thaliana GN=At5g58090 PE=1 SV=2
AT1G66270	Q9C525	-1.312	0,013	ER	Q9C525|BGL21_ARATH Beta-glucosidase 21 OS=Arabidopsis thaliana GN=BGLU21 PE=1 SV=1
AT5G04970	Q9FF77	-1.689	0,005	Cell wall	Q9FF77|PME47_ARATH Probable pectinesterase/pectinesterase inhibitor 47 OS=Arabidopsis thaliana GN=PME47 PE=2 SV=1
AT1G75940	Q84WV2	-1.834	0,005	ER	Q84WV2|BGL20_ARATH Beta-glucosidase 20 OS=Arabidopsis thaliana GN=BGLU20 PE=2 SV=1
Co-factor and vitamine metabolism					
AT3G14990	Q9FPF0	-1.147	0,001	Golgi	Q9FPF0|DJ1A_ARATH Protein DJ-1 homolog A OS=Arabidopsis thaliana GN=DJ1A PE=1 SV=1
AT5G50960	Q8H1Q2	-1.605	0,008	Cytosol	Q8H1Q2|NBP35_ARATH Cytosolic Fe-S cluster assembly factor NBP35 OS=Arabidopsis thaliana GN=NBP35 PE=1 SV=1
Development					
AT3G03340	A0A1I9LRM4	1.555	0,013	Nucleus	A0A1I9LRM4|A0A1I9LRM4_ARATH LUC7 related protein OS=Arabidopsis thaliana GN=UNE6 PE=4 SV=1
AT2G23810	Q8S8Q6	-0.97	0,016	Plasma membrane	Q8S8Q6|TET8_ARATH Tetraspanin-8 OS=Arabidopsis thaliana GN=TET8 PE=2 SV=1
AT4G37070	O23179	-1.076	0,001	Plasma membrane	O23179|PLP1_ARATH Patatin-like protein 1 OS=Arabidopsis thaliana GN=PLP1 PE=1 SV=2

DNA					
AT3G54560	O23628	-0.68	0,014	Nucleus	O23628|H2AV1_ARATH Histone H2A variant 1 OS=Arabidopsis thaliana GN=H2AV PE=1 SV=1
AT3G15950	Q9LSB4	-0.691	0,001	ER	Q9LSB4|NAI2_ARATH TSA1-like protein OS=Arabidopsis thaliana GN=NAI2 PE=1 SV=1
At1g07660	P59259	-0.845	0,001	Nucleus	P59259|H4_ARATH Histone H4 OS=Arabidopsis thaliana GN=At1g07660 PE=1 SV=2
AT1G08880	O04848	-1.149	0,017	Nucleus	O04848|H2AXA_ARATH Probable histone H2AXa OS=Arabidopsis thaliana GN=At1g08880 PE=1 SV=1
AT5G28740	Q9LKU3	-1.356	0,031	Nucleus	Q9LKU3|Q9LKU3_ARATH Tetratricopeptide repeat (TPR)-like superfamily protein OS=Arabidopsis thaliana GN=T32B20.g PE=4 SV=1
Fermentation					
AT1G77120	P06525	1.312	0,001	Cytosol	P06525|ADH1_ARATH Alcohol dehydrogenase class-P OS=Arabidopsis thaliana GN=ADH1 PE=1 SV=2
Glycolysis					
AT2G29560	Q9ZW34	2.122	0,027	Cytosol	Q9ZW34|ENO3_ARATH Cytosolic enolase 3 OS=Arabidopsis thaliana GN=ENO3 PE=1 SV=1
Hormone metabolism					
AT1G62380	Q41931	1.025	0,002	Golgi	Q41931|ACCO2_ARATH 1-aminocyclopropane-1-carboxylate oxidase 2 OS=Arabidopsis thaliana GN=ACO2 PE=1 SV=2
AT4G01850	P17562	0.896	0,014	Cytosol	P17562|METK2_ARATH S-adenosylmethionine synthase 2 OS=Arabidopsis thaliana GN=SAM2 PE=1 SV=1
AT1G10670	Q9SGY2	0.598	0,05	Cytosol	Q9SGY2|ACLA1_ARATH ATP-citrate synthase alpha chain protein 1 OS=Arabidopsis thaliana GN=ACLA-1 PE=1 SV=1
AT2G36880	Q9SJL8	0.435	0,049	Cytosol	Q9SJL8|METK3_ARATH S-adenosylmethionine synthase 3 OS=Arabidopsis thaliana GN=METK3 PE=1 SV=1
AT3G44320	P46010	-0.776	0,027	Cytosol	P46010|NRL3_ARATH Nitrilase 3 OS=Arabidopsis thaliana GN=NIT3 PE=1 SV=1
AT3G44310	P32961	-1.114	0,003	Cytosol	P32961|NRL1_ARATH Nitrilase 1 OS=Arabidopsis thaliana GN=NIT1 PE=1 SV=2
Lipid metabolism					
AT1G65290	O80800	1.298	0,021	Mitochondrion	O80800|ACPM2_ARATH Acyl carrier protein 2, mitochondrial OS=Arabidopsis thaliana GN=MTACP2 PE=1 SV=1
AT2G33150	Q56WD9	-0.539	0,024	Peroxisome	Q56WD9|THIK2_ARATH 3-ketoacyl-CoA thiolase 2, peroxisomal OS=Arabidopsis thaliana GN=PED1 PE=1 SV=2
AT1G45201	A0A1P8AVY3	-0.62	0,023	Golgi	A0A1P8AVY3|A0A1P8AVY3_ARATH Triacylglycerol lipase-like 1 OS=Arabidopsis thaliana GN=TLL1 PE=4 SV=1
AT5G48880	Q570C8	-0.699	0,044	Peroxisome	Q570C8|THIK5_ARATH 3-ketoacyl-CoA thiolase 5, peroxisomal OS=Arabidopsis thaliana GN=KAT5 PE=1 SV=2
AT3G51840	Q96329	-1.185	0,001	Peroxisome	Q96329|ACOX4_ARATH Acyl-coenzyme A oxidase 4, peroxisomal OS=Arabidopsis thaliana GN=ACX4 PE=1 SV=1
AT4G16155	F4JLP5	-2.272	0,018	Plastid	F4JLP5|PLPD2_ARATH Dihydrolipoyl dehydrogenase 2, chloroplastic OS=Arabidopsis thaliana GN=LPD2 PE=2 SV=2
Major CHO metabolism					
AT1G62660	Q43348	-0.577	0,018	Vacuole	Q43348|INVA3_ARATH Acid beta-fructofuranosidase 3, vacuolar OS=Arabidopsis thaliana GN=BFRUCT3 PE=2 SV=1
AT1G12240	Q39041	-0.56	0,016	Vacuole	Q39041|INVA4_ARATH Acid beta-fructofuranosidase 4, vacuolar OS=Arabidopsis thaliana GN=BFRUCT4 PE=1 SV=2
Metal handling.binding					
AT3G56240	A0A1I9LNC0	0.678	0,004	Peroxisome	A0A1I9LNC0|A0A1I9LNC0_ARATH Copper chaperone OS=Arabidopsis thaliana GN=CCH PE=4 SV=1
Miscellaneous enzyme family					
AT4G16260	Q8VZJ2	1.053	0,001	Extracellular	Q8VZJ2|BGNEM_ARATH Probable glucan endo-1,3-beta-glucosidase At4g16260 OS=Arabidopsis thaliana GN=At4g16260 PE=1 SV=1
AT4G13180	Q9SVQ9	-0.578	0,039	Plastid	Q9SVQ9|Q9SVQ9_ARATH AT4g13180/F17N18_70 OS=Arabidopsis thaliana GN=At4g13180 PE=1 SV=1
AT3G16420	O04314	-0.702	0,001	Cytosol	O04314|JAL30_ARATH PYK10-binding protein 1 OS=Arabidopsis thaliana GN=PBP1 PE=1 SV=1
AT1G78850	Q9ZVA4	-0.717	0,002	Extracellular	Q9ZVA4|EP1L3_ARATH EP1-like glycoprotein 3 OS=Arabidopsis thaliana GN=At1g78850 PE=1 SV=1
AT3G26720	P94078	-0.718	0,003	Extracellular	P94078|MANA1_ARATH Alpha-mannosidase At3g26720 OS=Arabidopsis thaliana GN=At3g26720 PE=1 SV=1
AT3G16410	O04316	-0.727	0,001	Cytosol	O04316|JAL29_ARATH Nitrile-specifier protein 4 OS=Arabidopsis thaliana GN=NSP4 PE=2 SV=1
AT3G16400	Q9SDM9	-0.782	0,023	Cytosol	Q9SDM9|JAL28_ARATH Nitrile-specifier protein 1 OS=Arabidopsis thaliana GN=NSP1 PE=1 SV=2
AT5G66920	Q8LPS9	-0.783	0,036	Extracellular	Q8LPS9|Q8LPS9_ARATH At5g66920/MUD21_18 OS=Arabidopsis thaliana GN=sks17 PE=2 SV=1
AT3G29250	F4J2Z7	-0.84	0,011	Extracellular	F4J2Z7|SDR4_ARATH Short-chain dehydrogenase reductase 4 OS=Arabidopsis thaliana GN=SDR4 PE=2 SV=1
AT4G34138	Q8VZE9	-0.902	0,011	Plasma membrane	Q8VZE9|U73B1_ARATH UDP-glycosyltransferase 73B1 OS=Arabidopsis thaliana GN=UGT73B1 PE=2 SV=1

AT4G21580	O65423	-0.918	0,003	Cytosol	O65423 | O65423_ARATH AT4g21580/F18E5_200 OS=Arabidopsis thaliana GN=F18E5_200 PE=2 SV=1	
AT2G24180	O65787	-0.939	0,021	ER	O65787 | C71B6_ARATH Cytochrome P450 71B6 OS=Arabidopsis thaliana GN=CYP71B6 PE=2 SV=1	
AT4G12510	Q9S7U3	-1.086	0,001	Extracellular	Q9S7U3 | Q9S7U3_ARATH At4g12520 OS=Arabidopsis thaliana GN=At4g12510 PE=2 SV=1	
AT3G03980	Q9SQR4	-1.167	0,028	Plastid	Q9SQR4 | ADRC3_ARATH NADPH-dependent aldehyde reductase-like protein, chloroplastic OS=Arabidopsis thaliana GN=At3g03980 PE=3 SV=1	
AT2G44790	O80517	-1.195	0,006	Plasma membrane	O80517 | BCB2_ARATH Uclacyanin-2 OS=Arabidopsis thaliana GN=At2g44790 PE=1 SV=1	
AT4G09750	Q9SZ91	-1.321	0,001	Mitochondrion	Q9SZ91 | Q9SZ91_ARATH NAD(P)-binding Rossmann-fold superfamily protein OS=Arabidopsis thaliana GN=At4g09750 PE=2 SV=1	
AT1G10290	Q9SE83	-1.383	0,023	Golgi	Q9SE83 | DRP2A_ARATH Dynamin-2A OS=Arabidopsis thaliana GN=DRP2A PE=1 SV=2	
AT2G42250	O48532	-1.544	0,011	ER	O48532 | O48532_ARATH Cytochrome P450, family 712, subfamily A, polypeptide 1 OS=Arabidopsis thaliana GN=CYP712A1 PE=3 SV=1	
AT5G46900	Q39100	-2.265	0,001	Extracellular	Q39100 | Q39100_ARATH Bifunctional inhibitor/lipid-transfer protein/seed storage 2S albumin superfamily protein OS=Arabidopsis thaliana GN=extA PE=2 SV=1	
Nucleotide metabolism						
AT4G29630	Q9S847	-1.196	0,02	Cytosol	Q9S847 | CDA3_ARATH Cytidine deaminase 3 OS=Arabidopsis thaliana GN=CDA3 PE=2 SV=1	
Protein						
AT2G30050	O64740	0,9	0,016	Cytosol	O64740 | SC13B_ARATH Protein transport protein SEC13 homolog B OS=Arabidopsis thaliana GN=SEC13B PE=1 SV=1	
AT4G31700	O48549	0.859	0,013	Cytosol	O48549 | RS61_ARATH 40S ribosomal protein S6-1 OS=Arabidopsis thaliana GN=RPS6A PE=1 SV=2	
AT5G47700	Q8LEQ0	0.836	0,046	Cytosol	Q8LEQ0 | RLA13_ARATH 60S acidic ribosomal protein P1-3 OS=Arabidopsis thaliana GN=RPP1C PE=1 SV=2	
AT3G07110	Q9SFU1	0.683	0,014	Cytosol	Q9SFU1 | R13A1_ARATH 60S ribosomal protein L13a-1 OS=Arabidopsis thaliana GN=RPL13AA PE=2 SV=1	
AT1G47128	P43297	-0.649	0,007	Extracellular	P43297 | RD21A_ARATH Cysteine proteinase RD21A OS=Arabidopsis thaliana GN=RD21A PE=1 SV=1	
AT1G03230	Q9ZV55	-0.696	0,005	Extracellular	Q9ZV55 | Q9ZV55_ARATH Eukaryotic aspartyl protease family protein OS=Arabidopsis thaliana GN=At1g03230 PE=2 SV=1	
AT4G20110	Q8L7E3	-0.744	0,027	Vacuole	Q8L7E3 | VSR7_ARATH Vacuolar-sorting receptor 7 OS=Arabidopsis thaliana GN=VSR7 PE=2 SV=2	
AT5G59090	Q8L7D2	-0.802	0,005	Extracellular	Q8L7D2 | SBT4C_ARATH Subtilisin-like protease SBT4.12 OS=Arabidopsis thaliana GN=SBT4.12 PE=2 SV=1	
AT3G50500	Q39192	-0.941	0,038	Cytosol	Q39192 | SRK2D_ARATH Serine/threonine-protein kinase SRK2D OS=Arabidopsis thaliana GN=SRK2D PE=1 SV=1	
AT1G04850	Q9MAT3	-1	0,029	Nucleus	Q9MAT3 | Q9MAT3_ARATH F13M7.16 protein OS=Arabidopsis thaliana GN=At1g04850 PE=2 SV=1	
AT1G11910	O65390	-1.016	0,005	Vacuole	O65390 | APA1_ARATH Aspartic proteinase A1 OS=Arabidopsis thaliana GN=APA1 PE=1 SV=1	
AT1G02305	Q93VC9	-1.023	0,001	Extracellular	Q93VC9 | CATB2_ARATH Cathepsin B-like protease 2 OS=Arabidopsis thaliana GN=CATHB2 PE=2 SV=1	
AT1G03220	Q9ZVS4	-1.158	0,001	Extracellular	Q9ZVS4 | Q9ZVS4_ARATH Eukaryotic aspartyl protease family protein OS=Arabidopsis thaliana GN=At1g03220 PE=2 SV=1	
AT1G14570	Q94JZ8	-1.517	0,019	Nucleus	Q94JZ8 | PUX7_ARATH Plant UBX domain-containing protein 7 OS=Arabidopsis thaliana GN=PUX7 PE=1 SV=1	
AT4G16190	Q9SUL1	-1.659	0,004	Vacuole	Q9SUL1 | RD19C_ARATH Probable cysteine protease RD19C OS=Arabidopsis thaliana GN=RD19C PE=2 SV=1	
AT5G14950	Q9LFR0	-2.042	0,029	Golgi	Q9LFR0 | GMAN2_ARATH Alpha-mannosidase 2 OS=Arabidopsis thaliana GN=GMII PE=1 SV=1	
AT1G30690	Q94C59	-2.067	0,001	Cytosol	Q94C59 | PATL4_ARATH Patellin-4 OS=Arabidopsis thaliana GN=PATL4 PE=1 SV=2	
Redox regulation						
AT2G16060	O24520	1.896	0,001	Cytosol	O24520 | HBL1_ARATH Non-symbiotic hemoglobin 1 OS=Arabidopsis thaliana GN=AHB1 PE=1 SV=1	
AT4G25100	P21276	0.888	0,004	Plastid	P21276 | SODF1_ARATH Superoxide dismutase [Fe] 1, chloroplastic OS=Arabidopsis thaliana GN=FSD1 PE=1 SV=4	
AT1G78370	Q8L7C9	0.829	0,021	Peroxisome	Q8L7C9 | GSTUK_ARATH Glutathione S-transferase U20 OS=Arabidopsis thaliana GN=GSTU20 PE=1 SV=1	
AT3G32980	Q9LHB9	-0.454	0,047	Extracellular	Q9LHB9 | PER32_ARATH Peroxidase 32 OS=Arabidopsis thaliana GN=PER32 PE=1 SV=3	
AT1G05260	O23044	-0.539	0,024	Extracellular	O23044 | PER3_ARATH Peroxidase 3 OS=Arabidopsis thaliana GN=PER3 PE=2 SV=1	
AT3G52880	Q9LFA3	-0.622	0,006	Peroxisome	Q9LFA3 | MDAR1_ARATH Monodehydroascorbate reductase 1, peroxisomal OS=Arabidopsis thaliana GN=MDAR1 PE=1 SV=1	
AT1G78380	Q9ZRW8	-0.8	0,001	Cytosol	Q9ZRW8 | GSTU_ARATH Glutathione S-transferase U19 OS=Arabidopsis thaliana GN=GSTU19 PE=1 SV=1	
AT5G28840	Q93VR3	-0.826	0,004	Cytosol	Q93VR3 | GME_ARATH GDP-mannose 3,5-epimerase OS=Arabidopsis thaliana GN=At5g28840 PE=1 SV=1	
AT3G49120	Q9SMU8	-1.009	0,001	Extracellular	Q9SMU8 | PER34_ARATH Peroxidase 34 OS=Arabidopsis thaliana GN=PER34 PE=1 SV=1	
AT2G28190	O78310	-1.105	0,009	Plastid	O78310 | SODC2_ARATH Superoxide dismutase [Cu-Zn] 2, chloroplastic OS=Arabidopsis thaliana GN=CSD2 PE=1 SV=2	
AT1G10370	Q9FUS8	-1.403	0,001	Cytosol	Q9FUS8 | GSTU17_ARATH Glutathione S-transferase U17 OS=Arabidopsis thaliana GN=GSTU17 PE=2 SV=1	
AT1G17170	Q9SHH6	-1.551	0,005	Cytosol	Q9SHH6 | GSTU24_ARATH Glutathione S-transferase U24 OS=Arabidopsis thaliana GN=GSTU24 PE=2 SV=1	
AT1G08830	P24704	-1.988	0,003	Cytosol	P24704 | SODC1_ARATH Superoxide dismutase [Cu-Zn] 1 OS=Arabidopsis thaliana GN=CSD1 PE=1 SV=2	
RNA						
AT2G02470	Q8S8M9	1.301	0,04	Nucleus	Q8S8M9 | ALF16_ARATH PHD finger protein ALFIN-LIKE 6 OS=Arabidopsis thaliana GN=AL6 PE=1 SV=1	
[illegible]	[illegible]	[illegible]	[illegible]	[illegible]	[illegible]	

Secondary metabolism						
AT4G34050	O49499	0.509	0,035	Cytosol	O49499|CAMT4_ARATH Caffeoyl-CoA O-methyltransferase 1 OS=Arabidopsis thaliana GN=CCOAOMT1 PE=1 SV=1
AT1G74020	P94111	-0.717	0,023	Vacuole	P94111|SSL12_ARATH Protein STRICTOSIDINE SYNTHASE-LIKE 12 OS=Arabidopsis thaliana GN=SSL12 PE=2 SV=2
AT3G09220	Q9SR40	-0.757	0,007	Extracellular	Q9SR40|LAC7_ARATH Laccase-7 OS=Arabidopsis thaliana GN=LAC7 PE=2 SV=1
AT1G06000	Q9LNE6	-0.837	0,002	Cytosol	Q9LNE6|U89C1_ARATH UDP-glycosyltransferase 89C1 OS=Arabidopsis thaliana GN=UGT89C1 PE=2 SV=1
AT3G51240	Q9S818	-0.854	0,016	Cytosol	Q9S818|FL3H_ARATH Naringenin,2-oxoglutarate 3-dioxygenase OS=Arabidopsis thaliana GN=F3H PE=1 SV=1
AT1G51470	Q3ECS3	-0.937	0,001	Extracellular	Q3ECS3|BGL35_ARATH Myrosinase 5 OS=Arabidopsis thaliana GN=TGG5 PE=1 SV=1
AT5G13930	P13114	-0.98	0,001	ER	P13114|CHS3_ARATH Chalcone synthase OS=Arabidopsis thaliana GN=CHS PE=1 SV=1
AT3G55120	P41088	-1.4	0,001	ER	P41088|CFI1_ARATH Chalcone--flavonone isomerase 1 OS=Arabidopsis thaliana GN=CHI1 PE=1 SV=2
Signalling					
AT3G05490	Q9MA62	1.387	0,024	Extracellular	Q9MA62|RLF22_ARATH Protein RALF-like 22 OS=Arabidopsis thaliana GN=RALFL22 PE=3 SV=1
AT4G33240	Q0WUR5	1.201	0,046	Golgi	Q0WUR5|FAB1A_ARATH 1-phosphatidylinositol-3-phosphate 5-kinase FAB1A OS=Arabidopsis thaliana GN=FAB1A PE=2 SV=1
AT1G51840	F4IB68	-0.769	0,05	Extracellular	F4IB68|F4IB68_ARATH Kinase-like protein OS=Arabidopsis thaliana GN=At1g51840 PE=4 SV=2
AT5G16590	Q9FMD7	-0.94	0,039	Plasma membrane	Q9FMD7|Y5659_ARATH Probable inactive receptor kinase At5g16590 OS=Arabidopsis thaliana GN=At5g16590 PE=1 SV=1
AT4G20260	Q96262	-1.209	0,008	Plasma membrane	Q96262|PCAP1_ARATH Plasma membrane-associated cation-binding protein 1 OS=Arabidopsis thaliana GN=PCAP1 PE=1 SV=1
AT3G16570	Q9LUS7	-1.534	0,008	Extracellular	Q9LUS7|RLF23_ARATH Rapid alkalinization factor 23 OS=Arabidopsis thaliana GN=RALF23 PE=1 SV=1
AT1G51820	C0LGG3	-1.657	0,007	Plasma membrane	C0LGG3|Y5182_ARATH Probable LRR receptor-like serine/threonine-protein kinase At1g51820 OS=Arabidopsis thaliana GN=At1g51820 PE=2 SV=1
AT5G41940	Q67YN2	-2.047	0,03	Mitochondrion	Q67YN2|Q67YN2_ARATH GTPase activator protein of Rab-like small GTPases-like protein OS=Arabidopsis thaliana GN=MJC20.4 PE=2 SV=1
Stress					
AT4G33720	O81888	2.748	0,001	Extracellular	O81888|O81888_ARATH AT4g33720 OS=Arabidopsis thaliana GN=T16L1.210 PE=2 SV=1
AT4G08780	Q9LDA4	1.605	0,002	Extracellular	Q9LDA4|PER38_ARATH Peroxidase 38 OS=Arabidopsis thaliana GN=PER38 PE=3 SV=1
AT5G38940	Q9FMA8	1.497	0,013	Extracellular	Q9FMA8|GL111_ARATH Germin-like protein subfamily 1 member 11 OS=Arabidopsis thaliana GN=At5g38940 PE=2 SV=1
AT4G02520	P46422	1.431	0,001	Cytosol	P46422|GSTF2_ARATH Glutathione S-transferase F2 OS=Arabidopsis thaliana GN=GSTF2 PE=1 SV=3
AT4G08770	Q9LDN9	1.427	0,002	Extracellular	Q9LDN9|PER37_ARATH Peroxidase 37 OS=Arabidopsis thaliana GN=PER37 PE=2 SV=1
AT2G43590	O24658	1.383	0,024	Extracellular	O24658|CHI59_ARATH Endochitinase At2g43590 OS=Arabidopsis thaliana GN=At2g43590 PE=2 SV=1
AT1G52060	F4IB95	1.145	0,001	Extracellular	F4IB95|AL9_ARATH Jacalin-related lectin 9 OS=Arabidopsis thaliana GN=JAL9 PE=3 SV=1
AT4G26010	Q93V93	1.099	0,002	Extracellular	Q93V93|PER44_ARATH Peroxidase 44 OS=Arabidopsis thaliana GN=PER44 PE=2 SV=1
AT1G05240	P0DI10	1.069	0,012	Extracellular	P0DI10|PER1_ARATH Peroxidase 1 OS=Arabidopsis thaliana GN=PER1 PE=1 SV=1
AT1G52070	Q8GWI7	0.88	0,001	Extracellular	Q8GWI7|JAL10_ARATH Jacalin-related lectin 10 OS=Arabidopsis thaliana GN=JAL10 PE=2 SV=1
AT3G12500	P19171	0.697	0,02	Extracellular	P19171|CHIB_ARATH Basic endochitinase B OS=Arabidopsis thaliana GN=CHI-B PE=1 SV=3
AT3G04720	P43082	0.672	0,023	Extracellular	P43082|HEVL_ARATH Hevein-like preproprotein OS=Arabidopsis thaliana GN=HEL PE=1 SV=1
AT2G39310	O80950	-0.499	0,023	Plasma membrane	O80950|JAL22_ARATH Jacalin-related lectin 22 OS=Arabidopsis thaliana GN=JAL22 PE=1 SV=1
At1g33590	F4HR88	-0.51	0,043	Extracellular	A0A1P8AWX3|A0A1P8AWX3_ARATH Leucine-rich repeat (LRR) family protein OS=Arabidopsis thaliana GN=At1g33590 PE=4 SV=1
AT3G16460	O04310	-0.533	0,006	Cytosol	O04310|JAL34_ARATH Jacalin-related lectin 34 OS=Arabidopsis thaliana GN=JAL34 PE=1 SV=1
AT3G12580	Q9LHA8	-0.613	0,039	Cytosol	Q9LHA8|MD37C_ARATH Probable mediator of RNA polymerase II transcription subunit 37c OS=Arabidopsis thaliana GN=MED37C PE=1 SV=1
AT4G19880	Q8H121	-0.623	0,007	Plastid	Q8H121|Q8H121_ARATH Glutathione S-transferase family protein OS=Arabidopsis thaliana GN=At4g19880 PE=1 SV=1
AT1G30360	Q9C8G5	-0.635	0,007	Plasma membrane	Q9C8G5|CSCL1_ARATH CSC1-like protein ERD4 OS=Arabidopsis thaliana GN=ERD4 PE=2 SV=1
AT2G02390	Q92VQ3	-0.639	0,026	Cytosol	Q92VQ3|GSTZ1_ARATH Glutathione S-transferase Z1 OS=Arabidopsis thaliana GN=GSTZ1 PE=1 SV=1
AT3G16470	O04309	-0.654	0,003	Cytosol	O04309|JAL35_ARATH Jacalin-related lectin 35 OS=Arabidopsis thaliana GN=JAL35 PE=1 SV=1
AT2G01520	Q9ZVF3	-0.71	0,002	Cytosol	Q9ZVF3|ML328_ARATH MLP-like protein 328 OS=Arabidopsis thaliana GN=MLP328 PE=2 SV=1
AT1G20440	P31168	-0.712	0,037	Nucleus	P31168|COR47_ARATH Dehydrin COR47 OS=Arabidopsis thaliana GN=COR47 PE=1 SV=2
AT4G23670	Q9SUR0	-0.723	0,007	Cytosol	Q9SUR0|Q9SUR0_ARATH AT4G23670 protein OS=Arabidopsis thaliana GN=At4g23670 PE=2 SV=1
AT1G76690	Q8GYB8	-0.76	0,005	Cytosol	Q8GYB8|OPR2_ARATH 12-oxophytodienoate reductase 2 OS=Arabidopsis thaliana GN=OPR2 PE=1 SV=2
AT1G18970	P92995	-0.874	0,013	Extracellular	P92995|GLT1_ARATH Germin-like protein subfamily T member 1 OS=Arabidopsis thaliana GN=GLP1 PE=2 SV=2
AT1G70850	Q9SSK7	-0.88	0,001	Cytosol	Q9SSK7|MLP34_ARATH MLP-like protein 34 OS=Arabidopsis thaliana GN=MLP34 PE=2 SV=1
AT3G16450	O04311	-0.927	0,004	Cytosol	O04311|JAL33_ARATH Jacalin-related lectin 33 OS=Arabidopsis thaliana GN=JAL33 PE=1 SV=1

AT2G01530	Q9ZVF2	-0.965	0,043	Cytosol	Q9ZVF2|ML329_ARATH MLP-like protein 329 OS=Arabidopsis thaliana GN=MLP329 PE=2 SV=1
AT1G17860	Q9LMU2	-1.029	0,001	Extracellular	Q9LMU2|KTI2_ARATH Kunitz trypsin inhibitor 2 OS=Arabidopsis thaliana GN=KTI2 PE=2 SV=1
AT3G01420	Q9SGH6	-1.067	0,001	Cytosol	Q9SGH6|DOX1_ARATH Alpha-dioxygenase 1 OS=Arabidopsis thaliana GN=DOX1 PE=1 SV=1
AT4G23680	Q9SUQ9	-1.068	0,016	Cytosol	Q9SUQ9|Q9SUQ9_ARATH AT4g23680/F9D16_150 OS=Arabidopsis thaliana GN=At4g23680 PE=2 SV=1
AT1G09560	P94014	-1.098	0,01	Extracellular	P94014|GL21_ARATH Germin-like protein subfamily 2 member 1 OS=Arabidopsis thaliana GN=GLP4 PE=2 SV=2
AT4G14060	O23267	-1.117	0,029	Cytosol	O23267|O23267_ARATH AT4g14060/dl3070w OS=Arabidopsis thaliana GN=dl3070w PE=2 SV=1
AT1G73260	Q8RXD5	-1.361	0,001	Extracellular	Q8RXD5|KTI1_ARATH Kunitz trypsin inhibitor 1 OS=Arabidopsis thaliana GN=KTI1 PE=2 SV=1
AT5G20970	F4K6X6	-1.492	0,02	Cytosol	F4K6X6|F4K6X6_ARATH HSP20-like chaperones superfamily protein OS=Arabidopsis thaliana GN=At5g20970 PE=3 SV=1
AT1G52100	Q5XF82	-1.703	0,008	Cytosol	Q5XF82|JAL11_ARATH Jacalin-related lectin 11 OS=Arabidopsis thaliana GN=JAL11 PE=2 SV=1
TCA/org transformation					
AT2G13560	Q9SIU0	-0.797	0,036	Mitochondrion	Q9SIU0|MAO1_ARATH NAD-dependent malic enzyme 1, mitochondrial OS=Arabidopsis thaliana GN=NAD-ME1 PE=1 SV=1
Transport					
AT5G43350	Q8VYM2	0.884	0,004	Plasma membrane	Q8VYM2|PHT11_ARATH Inorganic phosphate transporter 1-1 OS=Arabidopsis thaliana GN=PHT1-1 PE=1 SV=2
AT1G78900	O23654	-0.398	0,043	Golgi, vacuole	O23654|VATA_ARATH V-type proton ATPase catalytic subunit A OS=Arabidopsis thaliana GN=VHA-A PE=1 SV=1
AT5G57110	Q9LF79	-0.549	0,038	Plasma membrane	Q9LF79|ACA8_ARATH Calcium-transporting ATPase 8, plasma membrane-type OS=Arabidopsis thaliana GN=ACA8 PE=1 SV=1
AT1G72150	Q56WK6	-0.762	0,004	Plasma membrane	Q56WK6|PATL1_ARATH Patellin-1 OS=Arabidopsis thaliana GN=PATL1 PE=1 SV=2
AT2G37170	P43287	-0.842	0,006	Plasma membrane	P43287|PIP22_ARATH Aquaporin PIP2-2 OS=Arabidopsis thaliana GN=PIP2-2 PE=1 SV=2
AT3G26520	Q41963	-0.943	0,02	Vacuole	Q41963|TIP12_ARATH Aquaporin TIP1-2 OS=Arabidopsis thaliana GN=TIP1-2 PE=1 SV=2
AT5G58070	Q9FGT8	-1.003	0,002	ER	Q9FGT8|TIL_ARATH Temperature-induced lipocalin-1 OS=Arabidopsis thaliana GN=TIL PE=1 SV=1
AT2G36830	P25818	-1.132	0,005	Vacuole	P25818|TIP11_ARATH Aquaporin TIP1-1 OS=Arabidopsis thaliana GN=TIP1-1 PE=1 SV=1
AT4G25640	F4JTB3	-1.207	0,048	Vacuole	F4JTB3|DTX35_ARATH Protein DETOXIFICATION 35 OS=Arabidopsis thaliana GN=DTX35 PE=1 SV=1
AT4G19690	Q38856	-1.264	0,02	Plasma membrane	Q38856|IRT1_ARATH Fe(2+) transport protein 1 OS=Arabidopsis thaliana GN=IRT1 PE=1 SV=2
AT4G35100	P93004	-1.399	0,01	Plasma membrane	P93004|PIP27_ARATH Aquaporin PIP2-7 OS=Arabidopsis thaliana GN=PIP2-7 PE=1 SV=2
AT1G61800	Q94B38	-1.454	0,023	Plastid	Q94B38|GPT2_ARATH Glucose-6-phosphate/phosphate translocator 2, chloroplastic OS=Arabidopsis thaliana GN=GPT2 PE=2 SV=2
AT3G61430	P61837	-1.465	0,008	Plasma membrane	P61837|PIP11_ARATH Aquaporin PIP1-1 OS=Arabidopsis thaliana GN=PIP1-1 PE=1 SV=1
AT4G17340	Q41975	-1.606	0,05	Vacuole	Q41975|TIP22_ARATH Probable aquaporin TIP2-2 OS=Arabidopsis thaliana GN=TIP2-2 PE=1 SV=2
AT3G53420	P43286	-1.74	0,003	Plasma membrane	P43286|PIP21_ARATH Aquaporin PIP2-1 OS=Arabidopsis thaliana GN=PIP2-1 PE=1 SV=1
AT2G45960	Q06611	-1.747	0,002	Plasma membrane	Q06611|PIP12_ARATH Aquaporin PIP1-2 OS=Arabidopsis thaliana GN=PIP1-2 PE=1 SV=1
AT2G37180	P30302	-2.091	0,001	Plasma membrane	P30302|PIP23_ARATH Aquaporin PIP2-3 OS=Arabidopsis thaliana GN=PIP2-3 PE=1 SV=1

upna
Universidad Pública de Navarra
Nafarroako Unibertsitate Publikoa

CONCLUSIONES

upna
Universidad Pública de Navarra
Nafarroako Unibertsitate Publikoa

upna
Universidad Pública de Navarra
Nafarroako Unibertsitate Publikoa

1) Las plantas responden de modo diferente a los VCs emitidos por distintos microorganismos.

2) VICs y VOCs de tamaño molecular inferior a 45 Da son determinantes importantes de la respuesta de las plantas a VCs emitidos por hongos fitopatógenos.

3) El CO_2 respiratorio juega un papel minoritario en la respuesta de la planta a VCs emitidos por hongos fitopatógenos.

4) Los cambios altamente conservados que ocurren en el transcriptoma de plantas expuestas a VCs fúngicos son debidos a la señalización del aumento de la fotosíntesis.

5) La respuesta de las plantas a VCs fúngicos está regulada en gran medida a nivel post-transcripcional.

6) Los VCs de *P. aurantiogriseum* fomentan cambios en la arquitectura y en el metabolismo de la raíz causados a su vez por cambios en el proteoma.

7) Las auxinas, las CKs, el etileno y los ROS juegan un papel importante en los cambios de la arquitectura de la raíz inducidos por la exposición a VCs de *P. aurantiogriseum.*

8) CAS-C1 juega un papel fundamental en los cambios de la arquitectura de la raíz inducidos por VCs de *P. aurantiogriseum* a través de mecanismos no relacionados con el mantenimiento de los niveles intracelulares de cianuro.

upna
Universidad Pública de Navarra
Nafarroako Unibertsitate Publikoa

REFERENCIAS

upna
Universidad Pública de Navarra
Nafarroako Unibertsitate Publikoa

upna
Universidad Pública de Navarra
Nafarroako Unibertsitate Publikoa

Adie BAT, Pérez-Pérez J, Pérez-Pérez MM, Godoy M, Sánchez-Serrano JJ, Schmelz EA, Solano R (2007) ABA is an essential signal for plant resistance to pathogens affecting JA biosynthesis and the activation of defenses in Arabidopsis. Plant Cell **19**: 1665–1681

Ainsworth EA, Rogers A (2007) The response of photosynthesis and stomatal conductance to rising [CO_2]: mechanisms and environmental interactions. Plant Cell Environ **3**: 258–270

Alonso JM, Hirayama T, Roman G, Nourizadeh S, Ecker JR (1999) EIN2, a bifunctional transducer of ethylene and stress responses in Arabidopsis. Science **25**: 2148–2152

Ameztoy K, Baslam M, Sánchez-López ÁM, Muñoz FJ, Bahaji A, Almagro G, García-Gómez P, Baroja-Fernández E, De Diego N, Humplík JF, et al (2019) Plant responses to fungal volatiles involve global posttranslational thiol redox proteome changes that affect photosynthesis. Plant Cell Environ **42**: 2627–2644

Apel K, Hirt H (2004) Reactive oxygen species: metabolism, oxidative stress, and signal transduction. Annu Rev Plant Biol **55**: 373–399

Arenas-Alfonseca L, Gotor C, Romero LC, García I (2018) β-cyanoalanine synthase action in root hair elongation is exerted at early steps of the root hair elongation pathway and is independent of direct cyanide inactivation of NADPH oxidase. Plant Cell Physiol **59**: 1072–1083

Aroca A, Benito JM, Gotor C, Romero LC (2017) Persulfidation proteome reveals the regulation of protein function by hydrogen sulfide in diverse biological processes in Arabidopsis. J Exp Bot **68**: 4915–4927

Asada K (2006) Production and scavenging of reactive oxygen species in chloroplasts and their functions. Plant Physiol **141**: 391–396

Athanasiou K, Dyson BC, Webster RE, Johnson GN (2010) Dynamic acclimation of photosynthesis increases plant fitness in changing environments. Plant Physiol **152**: 366–373

Bahaji A, Li J, Sánchez-López ÁM, Baroja-Fernández E, Muñoz FJ, Ovecka M, Almagro G, Montero M, Ezquer I, Etxeberria E, et al (2014a) Starch biosynthesis, its regulation and biotechnological approaches to improve crop yields. Biotechnol Adv **32**: 87–106

Bahaji A, Baroja-Fernández E, Sánchez-López ÁM, Muñoz FJ, Li J, Almagro G, Montero M, Pujol P, Galarza R, Kaneko K, et al (2014b) HPLC-MS/MS analyses show that the near-starchless *aps1* and *pgm* leaves accumulate wild type levels of ADPglucose: further evidence for the occurrence of important ADPglucose biosynthetic pathway(s) alternative to the pPGI-pPGM-AGP pathway. PLoS One **10**(3):e0121181

doi: 10.1371/journal.pone.0104997

Bailly A, Groenhagen U, Schulz S, Geisler M, Eberl L, Weisskopf L (2014) The inter-kingdom volatile signal indole promotes root development by interfering with auxin signalling. Plant J **80**: 758–771

Bao Y, Aggarwal P, Robbins NE, Sturrock CJ, Thompson MC, Tan HQ, Tham C, Duan L, Rodriguez PL, Vernoux T, et al (2014) Plant roots use a patterning mechanism to position lateral root branches toward available water. Proc Natl Acad Sci U S A **111**: 9319–9324

Barry CS, Blume B, Bouzayen M, Cooper W, Hamilton AJ, Grierson D (1996) Differential expression of the 1-aminocyclopropane-1-carboxylate oxidase gene family of tomato. Plant J **9**: 525–535

Baxter A, Mittler R, Suzuki N (2014) ROS as key players in plant stress signalling. J Exp Bot **65**: 1229–1240

Beck E, Wagner BM (1994) Quantification of the daily cytokinin transport from the root to the shoot of *Urtica dioica L*. Bot Acta **107**: 342–348

Bellini C, Pacurar DI, Perrone I (2014) Adventitious roots and lateral roots: similarities and differences. Annu Rev Plant Biol **65**: 639–666

Bennett MJ, Marchant A, Green HG, May ST, Ward SP, Millner PA, Walker AR, Schulz B, Feldmann KA (1996) Arabidopsis AUX1 gene: a permease-like regulator of root gravitropism. Science **273**: 948–950

Bhattacharyya PN, Jha DK (2012) Plant growth-promoting rhizobacteria (PGPR): emergence in agriculture. World J Microbiol Biotechnol **28**: 1327–1350

Bienert GP, Møller ALB, Kristiansen KA, Schulz A, Møller IM, Schjoerring JK, Jahn TP (2007) Specific aquaporins facilitate the diffusion of hydrogen peroxide across membranes. J Biol Chem **282**: 1183–1192

Bishopp A, Help H, Helariutta Y (2009) Cytokinin signaling during root development. Int Rev Cell Mol Biol **276**: 1–48

Bitas V, McCartney N, Li N, Demers J, Kim JE, Kim HS, Brown KM, Kang S (2015) *Fusarium oxysporum* volatiles enhance plant growth via affecting auxin transport and signaling. Front Microbiol doi: 10.3389/fmicb.2015.01248

Blilou I, Xu J, Wildwater M, Willemsen V, Paponov I, Friml J, Heidstra R, Aida M, Palme K, Scheres B (2005) The PIN auxin efflux facilitator network controls growth and patterning in Arabidopsis roots. Nature **433**: 39–44

Blom D, Fabbri C, Eberl L, Weisskopf L (2011) Volatile-mediated killing of

Arabidopsis thaliana by bacteria is mainly due to hydrogen cyanide. Appl Environ Microbiol **77**: 1000–1008

Boccara M, Mills CE, Zeier J, Anzi C, Lamb C, Poole RK, Delledonne M (2005) Flavohaemoglobin HmpX from *Erwinia chrysanthemi* confers nitrosative stress tolerance and affects the plant hypersensitive reaction by intercepting nitric oxide produced by the host. Plant J **43**: 226–237

Bodini SF, Cicalini AR, Santori F (2011) Rhizosphere dynamics during phytoremediation of olive mill wastewater. Bioresour Technol **102**: 4383–4389

Boerjan W, Cervera M-T, Delarue M, Beeckman T, Dewitte W, Bellini C, Caboche M, van Onckelen H, van Monatgu M, Inze D (1995) *Superroot*, a recessive mutation in Arabidopsis, confers auxin overproduction. Plant Cell **7**: 1405–1419

Bolton MD (2009) Primary metabolism and plant defense-fuel for the fire. Mol Plant-Microbe Interact **22**: 487–497

Bolwell GP, Daudi A (2009) Reactive oxygen species in plant–pathogen interactions. In: del Río LA, Puppo A, eds. Reactive oxygen species in plant signaling . Berlin, Heidelberg: Springer-Verlag, 113–133

Bouguyon E, Perrine-Walker F, Pervent M, Rochette J, Cuesta C, Benkova E, Martinière A, Bach L, Krouk G, Gojon A, et al (2016) Nitrate controls root development through post-transcriptional regulation of the NRT1.1/NPF6.3 transporter/sensor. Plant Physiol **172**: 1237–1248

Brenner WG, Schmülling T (2015) Summarizing and exploring data of a decade of cytokinin-related transcriptomics. Front Plant Sci **6**: 29

Buchanan BB, Balmer Y (2005) Redox regulation: a broadening horizon. Ann Rev Plant Biol **56**: 187–220

Camarena-Pozos DA, Flores-Núñez VM, López MG, López-Bucio J, Partida-Martínez LP (2019) Smells from the desert: microbial volatiles that affect plant growth and development of native and non-native plant species. Plant Cell Environ **42**: 1368–1380

Cao ZY, Xuan W, Liu ZY, Li XN, Zhao N, Xu P, Wang Z, Guan RZ, Shen WB (2007) Carbon monoxide promotes lateral root formation in rapeseed. J Integr Plant Biol **49**: 1070–1079

Casarrubia S, Sapienza S, Fritz H, Daghino S, Rosenkranz M, Schnitzler JP, Martin F, Perotto S, Martino E (2016) Ecologically different fungi affect Arabidopsis development: contribution of soluble and volatile compounds. PLoS One Dec 14;11(12):e0168236. doi: 10.1371/journal.pone.0168236

Casimiro I, Marchant A, Bhalerao RP, Beeckman T, Dhooge S, Swarup R, Graham N, Inze D, Sandberg G, Casero PJ, et al (2001) Auxin transport promotes Arabidopsis lateral root initiation. Plant Cell **13**: 843–852

Cassán F, Perrig D, Sgroy V, Masciarelli O, Penna C, Luna V (2009) *Azospirillum brasilense* Az39 and *Bradyrhizobium japonicum* E109, inoculated singly or in combination, promote seed germination and earlyseedling growth in corn (*Zea mays L.*) and soybean (*Glycine max L.*). Eur J Soil Biol **45**: 28–35

Chamam A, Sanguin H, Bellvert F, Meiffren G, Comte G, Wisniewski-Dyé F, Bertrand C, Prigent-Combaret C (2013) Plant secondary metabolite profiling evidences strain-dependent effect in the *Azospirillum-Oryza sativa* association. Phytochemistry **87**: 65–77

Chang L, Ramireddy E, Schmülling T (2013) Lateral root formation and growth of Arabidopsis is redundantly regulated by cytokinin metabolism and signalling genes. J Exp Bot **64**: 5021–5032

Chen J, Wu FH, Wang WH, Zheng CJ, Lin GH, Dong XJ, He JX, Pei ZM, Zheng HL (2011) Hydrogen sulphide enhances photosynthesis through promoting chloroplast biogenesis, photosynthetic enzyme expression, and thiol redox modification in *Spinacia oleracea* seedlings. J Exp Bot **62**: 4481–4493

Combes-Meynet E, Pothier JF, Moënne-Loccoz Y, Prigent-Combaret C (2011). The Pseudomonas secondary metabolite 2,4-diacetylphloroglucinol is a signal inducing rhizoplane expression of Azospirillum genes involved in plant-growth promotion. Mol Plant Microbe Interact **24**: 271–284

Conrath U, Amoroso G, Köhle H, Sültemeyer DF (2004) Non-invasive online detection of nitric oxide from plants and some other organisms by mass spectrometry. Plant J **38**: 1015–1022

Contesto C, Desbrosses G, Lefoulon C, Bena G, Borel F, Galland M, Gamet L, Varoquaux F, Touraine B (2008) Effects of rhizobacterial ACC deaminase activity on Arabidopsis indicate that ethylene mediates local root responses to plant growth-promoting rhizobacteria. Plant Sci **175**: 178–189

Contreras-Cornejo HA, López-Bucio JS, Méndez-Bravo A, Macías-Rodríguez L, Ramos-Vega M, Guevara-García ÁA, López-Bucio J (2015) Mitogen-activated protein kinase 6 and ethylene and auxin signaling pathways are involved in Arabidopsis root-system architecture alterations by *Trichoderma atroviride*. Mol Plant-Microbe Interact **28**: 701–710

Contreras-Cornejo HA, Macías-Rodríguez L, Cortés-Penagos C, López-Bucio J (2009) *Trichoderma virens*, a plant beneficial fungus, enhances biomass production and promotes lateral root growth through an auxin-dependent mechanism in Arabidopsis.

Plant Physiol **149**: 1579–1592

Contreras-Cornejo HA, Macías-Rodríguez L, Herrera-Estrella A, López-Bucio J (2014) The 4-phosphopantetheinyl transferase of *Trichoderma virens* plays a role in plant protection against *Botrytis cinerea* through volatile organic compound emission. Plant Soil **379**: 261–274

Cordovez V, Mommer L, Moisan K, Lucas-Barbosa D, Pierik R, Mumm R, Carrion VJ, Raaijmakers JM (2017) Plant phenotypic and transcriptional changes induced by volatiles rom the fungal root pathogen *Rhizoctonia solani*. Front Plant Sci **8**: doi: 10.3389/fpls.2017.01262

Cordovez V, Schop S, Hordjik K, de Boulois HD, Coppens F, Hanssen I, Raaijmakers JM, Carrión VJ (2018) Priming of plant growth promotion by volatiles of root-associated *Microbacterium* spp. Appl Environ Microbiol **84**: pii:e01865-18

Correa-Aragunde N, Graziano M, Lamattina L (2004) Nitric oxide plays a central role in determining lateral root development in tomato. Planta **218**: 900–905

Costa A, Luoni L, Marrano CA, Hashimoto K, Köster P, Giacometti S, De Michelis MI, Kudla J, Bonza MC (2017) Ca^{2+}-dependent phosphoregulation of the plasma membrane Ca^{2+}-ATPase ACA8 modulates stimulus-induced calcium signatures. J Exp Bot **68**: 3215–3230

Creus CM, Graziano M, Casanovas EM, Pereyra MA, Simontacchi M, Puntarulo S, Barassi CA, Lamattina L (2005) Nitric oxide is involved in the *Azospirillum brasilense*-induced lateral root formation in tomato. Planta **221**: 297–303

Cross AR, Jones OTG (1986) The effect of the inhibitor diphenylene iodonium on the superoxide-generating system of neutrophils. Specific labelling of a component polypeptide of the oxidase. Biochem J **237**: 111–116

D'Agostino IB, Deruère J, Kieber JJ (2000) Characterization of the response of the Arabidopsis response regulator gene family to cytokinin. Plant Physiol **124**: 1706–1717

De-la-Peña C, Loyola-Vargas VM (2014) Biotic interactions in the rhizosphere: a diverse cooperative enterprise for plant productivity. Plant Physiol **166**: 701–709

Delaplace P, Delory BM, Baudson C, Mendaluk-Saunier de Cazenave M, Spaepen S, Varin S, Brostaux Y, du Jardin P (2015) Influence of rhizobacterial volatiles on the root system architecture and the production and allocation o biomass in the model grass *Brachypodium distachyon* (L.) P. Beauv. BMC Plant Biol doi: 10.1186/s12870-015-0585-3

del Río LA (2011) Peroxisomes as a source of reactive nitrogen species signal molecules. Arch Biochem Biophys **506**: 1–11

del Río LA (2013) Peroxisomes and their key role in cellular signaling and metabolism. Berlin, Heidelberg: Springer-Verlag. ISBN: 978-3-642-00390-5

del Río LA, Corpas FJ, Barroso JB, López-Huertas E, Palma JM (2014) Function of peroxisomes as a cellular source of nitric oxide and other reactive nitrogen species. In: Nasir Khan M, Mobin M, Mohammad F, Corpas FJ, eds. Nitric oxide in plants: metabolism and role in stress physiology . Berlin, Heidelberg: Springer-Verlag, 33–55

del Río LA, Puppo A (2009) Reactive oxygen species in plant signaling . Berlin, Heidelberg: Springer-Verlag.ISBN: 978-3-642-00390-5

del Río LA, Sandalio LM, Corpas FJ, Palma JM, Barroso JB (2006) Reactive oxygen species and reactive nitrogen species in peroxisomes. Production, scavenging, and role in cell signalling. Plant Physiol **141**: 330–335

Diet A, Link B, Seifert GJ, Schellenberg B, Wagner U, Pauly M, Reiter W-D, Ringli C (2006) The Arabidopsis root hair cell wall formation mutant *lrx1* is suppressed by mutations in the *RHM1* gene encoding a UDP-L-rhamnose synthase. Plant Cell **18**: 1630–1641

Ditengou FA, Müller A, Rosenkranz M, Felten J, Lasok H, van Doorn MM, Legué V, Palme K, Schnitzler JP, Polle A (2015) Volatile signalling by sesquiterpenes from ectomycorrhizal fungi reprogrammes root architecture. Nat Commun doi: 10.1038/ncomms7279

Dobbelaere S, Croonenborghs A, Thys A, Vande Broek A, Vanderleyden J (1999) Phytostimulatory effect of *Azospirillum brasilense* wild type and mutant strains altered in IAA production on wheat. Plant Soil **212**: 153–162

Dodd IC, Zinovkina NY, Safronova VI, Belimov AA (2010) Rhizobacterial mediation of plant hormone status. Ann Appl Biol **157**: 361–379

Dong Z, Wu L, Kettlewell B, Caldwell CD, Layzell DB (2003) Hydrogen fertilization of soils - is this a benefit of legumes in rotation? Plant Cell Environ **26**: 1875–1879

Dooley FD, Nair SP, Ward PD (2013) Increased growth and germination success in plants following hydrogen sulfide administration. PLoS ONE **8**: e62048 doi:10.1371/journal.pone.0062048

Drerup MM, Schlücking K, Hashimoto K, Manishankar P, Steinhorst L, Kuchitsu K, Kudla J (2013) The calcineurin B-like calcium sensors CBL1 and CBL9 together with their interacting protein kinase CIPK26 regulate the Arabidopsis NADPH oxidase RBOHF. Mol Plant **6**: 559–569

Dubiella U, Seybold H, Durian G, Komander E, Lassig R, Witte C-P, Schulze WX, Romeis T (2013) Calcium-dependent protein kinase/NADPH oxidase activation circuit is required for rapid defense signal propagation. Proc Natl Acad Sci **110**: 8744–8749

Du Jardin P (2015) Plant biostimulants: Definition, concept, main categories and regulation. Sci Horti **196**: 3–14

Dynowski M, Schaaf G, Loque D, Moran O, Ludewig U (2008) Plant plasma membrane water channels conduct the signalling molecule H_2O_2. Biochem J **414**: 53–61

Dyson BC, Allwood JW, Feil R, Xu YUN, Miller M, Bowsher CG, Goodacre R, Lunn JE, Johnson GN (2015) Acclimation of metabolism to light in *Arabidopsis thaliana*: the glucose 6-phosphate/phosphate translocator GPT2 directs metabolic acclimation. Plant Cell Environ **38**: 1404–1417

Eggert K, von Wirén N (2013) Dynamics and partitioning of the ionome in seeds and germinating seedlings of winter oilseed rape. Metallomics **5**: 1316–1325

Engel RR, Matsen JM, Chapman SS, Schwartz S (1972) Carbon monoxide production from heme compounds by bacteria. J Bacteriol **112**: 1310–1315

Ezquer I, Li J, Ovecka M, Baroja-Fernández E, Muñoz FJ, Montero M, Díaz de Cerio J, Hidalgo M, Sesma MT, Bahaji A, et al (2010) Microbial volatile emissions promote accumulation of exceptionally high levels of starch in leaves in mono- and dicotyledonous plants. Plant Cell Physiol **51**: 1674–1693

Farag MA, Song GC, Park YS, Audrain B, Lee S, Ghigo JM, Kloepper JW, Ryu CM (2017) Biological and chemical strategies for exploring inter- and intra-kingdom communication mediated via bacterial volatile signals. Nat Protoc **12**: 1359–1377

Farkas V, Gresik M, Kolarova N, Sulova Z, Sestak S (1990) Biochemical and physiological changes during photoinduced conidiation and derepression of cellulase synthesis in *Trichoderma*. In *Trichoderma reesei* cellulase: biochemistry, genetics, physiology and application. (eds C.P. Kubicek, D.E. Eveleigh, H. Esterbauer, W. Steiner & E.M. Kubicek-Pranz), pp 139-155. Graham, Cambridge.

Farrar K, Bryant D, Cope-Selby N (2014) Understanding and engineering beneficial plant-microbe interactions: plant growth promotion in energy crops. Plant Biotechnol J **12**: 1193–1206

Fatland BL, Nikolau BJ, Wurtele ES (2005) Reverse genetic characterization of cytosolic acetyl-CoA generation by ATP-citrate lyase in Arabidopsis. Plant Cell **17**: 182–203

Favery B, Ryan E, Foreman J, Linstead P, Boudonck K, Steer M, Shaw P, Dolan L (2001) *KOJAK* encodes a cellulose synthase-like protein required for root hair cell morphogenesis in Arabidopsis. Genes Dev **15**: 79–89

Felten J, Kohler A, Morin E, Bhalerao RP, Palme K, Martin F, Ditengou FA, Legué V (2009) The ectomycorrhizal fungus *Laccaria bicolor* stimulates lateral root formation in poplar and Arabidopsis through auxin transport and signaling. Plant Physiol **151**:

1991–2005

Fernández-Marcos M, Sanz L, Lewis DR, Muday GK, Lorenzo O (2011) Nitric oxide causes root apical meristem defects and growth inhibition while reducing PIN-FORMED 1 (PIN1)-dependent acropetal auxin transport. Proc Natl Acad Sci **108**: 18506–18511

Fischer U, Ikeda Y, Ljung K, Serralbo O, Singh M, Heidstra R, Palme K, Scheres B, Grebe M (2006) Vectorial information for Arabidopsis planar polarity is mediated by combined *AUX1, EIN2*, and *GNOM* activity. Curr Biol **16**: 2143–2149

Flexas J, Díaz-Espejo A, Conesa MA, Coopman RE, Douthe C, Gago J, Gallé A, Galmés J, Medrano H, Ribas-Carbo M, et al (2016) Mesophyll conductance to CO_2 and Rubisco as targets for improving intrinsic water use efficiency in C3 plants. Plant Cell Environ **39**: 965–982

Floris M, Mahgoub H, Lanet E, Robaglia C, Menand B (2009) Post-transcriptional regulation of gene expression in plants during abiotic stress. Int J Mol Sci **10**: 3168–3185

Forde B, Lorenzo H (2001) The nutritional control of root development. Plant Soil **232**: 51–68

Foreman J, Demidchik V, Bothwell JHF, Mylona P, Miedema H, Torres MA, Linstead P, Costa S, Brownlee C, Jones JDG (2003) Reactive oxygen species produced by NADPH oxidase regulate plant cell growth. Nature **422**: 442–446

Frémont N, Riefler M, Stolz A, Schmülling T (2013) The Arabidopsis *TUMOR PRONE5* gene encodes an acetylornithine aminotransferase required for arginine biosynthesis and root meristem maintenance in blue light. Plant Physiol **161**: 1127–1140

García-Gómez P, Almagro G, Sánchez-López ÁM, Bahaji A, Ameztoy K, Ricarte-Bermejo A, Baslam M, Antolín MC, Urdiain A, López-Belchi MD, et al (2019) Volatile compounds other than CO_2 emitted by different microorganisms promote distinct posttranscriptionally regulated responses in plants. Plant Cell Environ **42**: 1729–1746

García I, Castellano JM, Vioque B, Solano R, Gotor C, Romero LC (2010) Mitochondrial β-cyanoalanine synthase is essential for root hair formation in *Arabidopsis thaliana*. Plant Cell **22**: 3268–3279

Gargallo-Garriga A, Sardans J, Pérez-Trujillo M, Rivas-Ubach A, Oravec M, Vecerova K, Urban O, Jentsch A, Kreyling J, Beierkuhnlein C, et al (2014) Opposite metabolic responses of shoots and roots to drought. Sci Rep doi: 10.1038/srep06829

Garnica-Vergara A, Barrera-Ortiz S, Muñoz-Parra E, Raya-González J, Méndez-Bravo A, Macías-Rodríguez L, Ruiz-Herrera LF, López-Bucio J (2016). The volatile 6-pentyle-2H-pyran-2-one from *Trichoderma atroviride* regulates *Arabidopsis thaliana* root morphogenesis via auxin signaling and *ETHYLENE INSENSITIVE 2* functioning.

New Phytol **209**: 1496–1512

Garrido J, Linares-Solano A, Martin-Martinez JM, Molina-Sabio M, Rodríguez-Reinoso F, Torregrosa R (1987) Use of N_2 vs CO_2 in the characterization of activated carbons. Langmuir **3**: 76–81

Geisler M, Murphy AS (2006) The ABC of auxin transport: the role of p-glycoproteins in plant development. FEBS Lett **580**: 1094–1102

Ghaffari MR, Shahinnia F, Usadel B, Junker B, Schreiber F, Sreenivasulu N, Hajirezaei MR (2016) The metabolic signature of biomass formation in barley. Plant Cell Physiol **57**: 1943–1960

Gharaei-Fathabad E, Tajick-Ghanbary MA, Shahrokhi N (2014) Antimicrobial properties of Penicillium species isolated from agricultural soils of northern Iran. Res J Toxins **6**: 1–7

Glick BR (2005) Modulation of plant ethylene levels by the bacterial enzyme ACC deaminase. FEMS Microbiol Lett **251**: 1–7

Groenhagen U, Baumgartner R, Bailly A, Gardiner A, Eberl L, Schulz S, Weisskopf L (2013) Production of bioactive volatiles by different *Burkholderia ambifaria* strains. J Chem Ecol **39**: 892–906

Grondin A, Rodrigues O, Verdoucq L, Merlot S, Leonhardt N, Maurel C (2015) Aquaporins contribute to ABA-triggered stomatal closure through OST1-mediated phosphorylation. Plant Cell **27**: 1945–1954

Gruber BD, Giehl RF, Friedel S, von Wirén N (2013) Plasticity of the Arabidopsis root system under nutrient deficiencies. Plant Physiol **163**: 161–79

Guo K, Kong WW, Yang ZM (2009) Carbon monoxide promotes root hair development in tomato. Plant Cell Environ **32**: 1033–1045

Guo K, Xia K, Yang ZM (2008) Regulation of tomato lateral root development by carbon monoxide and involvement in auxin and nitric oxide. J Exp Bot **59**: 3443–3452

Gutierrez-Luna FM, López-Bucio J, Altamirano-Hernández J, Valencia-Cantero E, Reyes de la Cruz H, Macías-Rodríguez L (2010) Plant growth-promoting rhizobacteria modulate root-system architecture in *Arabidopsis thaliana* through volatile organic compound emission. Symbiosis **51**: 75–83

Hachiya T, Sugiura D, Kojima M, Sato S, Yanagisawa S, Sakakibara H, Terashima I, Noguchi K (2014) High CO_2 triggers preferential root growth of *Arabidopsis thaliana* via two distinct systems under low pH and low N stresses. Plant Cell Physiol **55**: 269–80

Halliwell B, Gutteridge JMC (2007) Free radicals in biology and medicine. Oxford

University Press. ISBN-13: 9780198717478

Han B, Xu S, Xie YJ, Huang JJ, Wang LJ, Yang Z, Zhang CH, Sun Y, Shen WB, Xie GS (2012) *ZmHO-1*, a maize haem oxygenase-1 gene, plays a role in determining lateral root development. Plant Sci **184**: 63–74

Hancock JT (2012) NO synthase? Generation of nitric oxide in plants. Period Biol **114**: 19–24

Handford M, Rodríguez-Furlán C, Marchant L, Segura M, Gómez D, Alvarez-Buylla E, Xiong G-Y, Pauly M, Orellana A (2012) *Arabidopsis thaliana* AtUTr7 encodes a Golgi-localized UDP–glucose/UDP–galactose transporter that affects lateral root emergence. Mol Plant **5**: 1263–1280

He Y, Tang RH, Hao Y, Stevens RD, Cook CW, Ahn SM, Jing L, Yang Z, Chen L, Guo F, et al (2004) Nitric oxide represses the Arabidopsis floral transition. Science **305**: 1968–1971

Hebelstrup KH, Jensen EO (2008) Expression of NO scavenging hemoglobin is involved in the timing of bolting in *Arabidopsis thaliana*. Planta **227**: 917–927

Hendriks JHM, Kolbe A, Gibon Y, Stitt M, Geigenberger P (2003) ADP-glucose pyrophosphorylase is ativated by posttranslational redox-modification in response to light and to sugars in leaves of Arabidopsis and other plant species. Plant Physiol **133**: 838–849

Hirose N, Takei K, Kuroha T, Kamada-Nobusada T, Hayashi H, Sakakibara H (2008) Regulation of cytokinin biosynthesis, compartmentalization and translocation. J Exp Bot **59**: 75–83

Hu J, Huang X, Chen L, Sun X, Lu C, Zhang L, Wang Y, Zuo J (2015) Site-specific nitrosoproteomic identification of endogenously S-nitrosylated proteins in Arabidopsis. Plant Physiol **167**: 1731–1746

Hua J, Meyerowitz EM (1998) Ethylene responses are negatively regulated by a receptor gene family in *Arabidopsis thaliana*. Cell **94**: 261–271

Hukin D, Doering-Saad C, Thomas CR, Pritchard J (2002) Sensitivity of cell hydraulic conductivity to mercury is coincident with symplasmic isolation and expression of plasmalemma aquaporin genes in growing maize roots. Planta **215**: 1047–1056

Hung R, Lee S, Rodriguez-Saona C, Bennett JW (2014) Common gas phase molecules from fungi affect seed germination and plant health in *Arabidopsis thaliana*. AMB Express **4**:53

Hung R, Lee S, Bennett JW (2013) *Arabidopsis thaliana* as a model system for testing the effect of Trichoderma volatile organic compounds. Fungal Ecol **6**: 19–26

Hunt PW, Klok EJ, Trevaskis B, Watts RA, Ellis MH, Peacock WJ, Dennis ES (2002) Increased level of hemoglobin 1 enhances survival of hypoxic stress and promotes early growth in *Arabidopsis thaliana*. Proc Nat Acad Sci U S A **99**: 17197–17202

Huot B, Yao J, Montgomery BL, He SY (2014) Growth–defense tradeoffs in plants: a balancing act to optimize fitness. Mol Plant **7**: 1267–1287

Ivanchenko MG, Muday GK, Dubrovsky JG (2008) Ethylene-auxin interactions regulate lateral root initiation and emergence in *Arabidopsis thaliana*. Plant J **55**: 335–347

Jefferson RA, Kavanagh TA, Bevan MW (1987) GUS fusions: β-glucuronidase as a sensitive and versatile gene fusion marker in higher plants. EMBO J **6**: 3901–3907

Jiang C, Gao X, Liao L, Harberd NP, Fu X (2007) Phosphate starvation root architecture and anthocyanin accumulation responses are modulated by the gibberellin-DELLA signaling pathway in Arabidopsis. Plant Physiol **4**: 1460–1470

Jin CW, Du ST, Zhang YS, Tang C, Lin XY (2009) Atmospheric nitric oxide stimulates plant growth and improves the quality of spinach (*Spinacia oleracea*). Ann Appl Biol **155**: 113–120

Jin Q, Zhu K, Cui W, Xie Y, Han B, Shen W (2013) Hydrogen gas acts as a novel bioactive molecule in enhancing plant tolerance to paraquat-induced oxidative stress via the modulation of heme oxygenase-1 signalling system. Plant Cell Environ **36**: 956–969

Johnson E, Sparks JP, Dzikovski B, Crane BR, Gibson DM, Loria R (2008) Plant-pathogenic Streptomyces species produce nitric oxide synthase-derived nitric oxide in response to host signals. Chem Biol **15**: 43–50

Kai M, Effmert U, Piechulla B (2016) Bacterial-plant-interactions: approaches to unravel the biological function of bacterial volatiles in the rhizosphere. Front Microbiol **7**:108 doi:10.3389/fmicb.2016.00108

Kai M, Piechulla B (2009) Plant growth promotion due to rhizobacterial volatiles-an effect of CO_2? FEBS Lett **583**: 3473–3477

Kanchiswamy CN, Malnoy M, Maffei ME (2015) Chemical diversity of microbial volatiles and their potential for plant growth and productivity. Front Plant Sci **6**: 151 doi:10.3389/fpls.2015.00151

Kang J, Lee Y, Sakakibara H, Martinoia E (2017) Cytokinin Transporters: GO and STOP in Signaling. Trends Plant Sci **6**: 455–461

Kasahara H, Takei K, Ueda N, Hishiyama S, Yamaya T, Kamiya Y, Yamaguchi S, Sakakibara H (2004) Distinct isoprenoid origins of cis- and trans-zeatin biosyntheses in Arabidopsis. J Biol Chem **279**: 14049–14054

Klapeć T, Cholewa G, Cholewa A, Dutkiewicz J, Wójcik-Fatla A (2018) Fungal diversity of root vegetables and soil rhizosphere collected from organic and conventional farms in eastern Poland. Ann Agric Environ Med **25**: 374–381

Korshunova YO, Eide D, Clark WG, Guerinot M Lou, Pakrasi HB (1999) The IRT1 protein from *Arabidopsis thaliana* is a metal transporter with a broad substrate range. Plant Mol Biol **40**: 37–44

Krapp A, Berthomé R, Orsel M, Mercey-Boutet S, Yu A, Castaings L, Elftieh S, Major H, Renou J-P, Daniel-Vedele F (2011) Arabidopsis roots and shoots show distinct temporal adaptation patterns toward nitrogen starvation. Plant Physiol **157**: 1255–1282

Keshishian EA, Rashotte AM (2015) Plant cytokinin signalling. Essays Biochem **58**: 13–27

Kieber JJ, Rothenberg M, Roman G, Feldmann KA, Ecker JR (1993) CTR1, a negative regulator of the ethylene response pathway in Arabidopsis, encodes a member of the raf family of protein kinases. Cell **72**: 427–441

Kong WW, Zhang LP, Guo K, Liu ZP, Yang ZM (2010) Carbon monoxide improves adaptation of Arabidopsis to iron deficiency. Plant Biotech J **8**: 88–99

Kudo T, Kiba T, Sakakibara H (2010) Metabolism and long-distance translocation of cytokinins. J Integr Plant Biol **52**: 53–60

Kuruthukulangarakoola GT, Zhang J, Albert A, Winkler B, Lang H, Buegger F, Gaupels F, Heller W, Michalke B, Sarioglu H, et al (2017) Nitric oxide-fixation by non-symbiotic haemoglobin proteins in *Arabidopsis thaliana* under N-limited conditions. Plant Cell Environ **40**: 36–50

Kwon YS, Lee DY, Rakwal R, Baek SB, Lee JH, Kwak YS, Seo JS, Chung WS, Bae DW, Kim SG (2016) Proteomic analyses of the interaction between plant-growth promoting rhizobacterium *Paenibacillus polymyxa* E681 and *Arabidopsis thaliana*. Proteomics **16**:122–135

Lan P, Li W, Schmidt W (2012) Complementary proteome and transcriptome profiling in phosphate-deficient Arabidopsis roots reveals multiple levels of gene regulation. Mol Cell Proteomics **11**: 1156–1166

Ledger T, Rojas S, Timmermann T, Pinedo I, Poupin MJ, Garrido T, Richter P, Tamayo J, Donoso R (2016) Volatile-mediated effects predominate in *Paraburkholderia phytofirmans* growth promotion and salt stress tolerance of *Arabidopsis thaliana*. Front Microbiol **7**:1838 doi:10.3389/fmicb.2016.01838

Lemfack MC, Gohlke BO, Toguem SMT, Preissner S, Piechulla B, Preissner R (2018) mVOC 2.0: a database of microbial volatiles. Nucleic Acids Res **42**: 1261–1265

Lemfack MC, Nickel J, Dunkel M, Preissner R, Piechulla B (2014) mVOC: a database of microbial volatiles. Nucleic Acids Res **42**: 744–748

Leskow CC, Kamenetzky L, Dominguez PG, Díaz Zirpolo JA, Obata T, Costa H, Martí M, Taboga O, Keurentjes J, Sulpice R, et al (2016) Allelic differences in a vacuolar invertase affect Arabidopsis growth at early plant development. J Exp Bot **67**: 4091–4103

Lewis DR, Negi S, Sukumar P, Muday GK (2011) Ethylene inhibits lateral root development, increases IAA transport and expression of PIN3 and PIN7 auxin efflux carriers. Development **138**: 3485–3495

Li J, Ezquer I, Bahaji A, Montero M, Ovecka M, Baroja-Fernández E, Muñoz FJ, Mérida A, Almagro G, Hidalgo M, et al (2011) Microbial volatile-induced accumulation of exceptionally high levels of starch in Arabidopsis leaves is a process involving NTRC and starch synthase classes III and IV. Mol Plant Microbe Interact **24**: 1165–1178

Lin Y, Zhang W, Qi F, Cui W, Xie Y, Shen W (2014) Hydrogen-rich water regulates cucumber adventitious root development in a heme oxygenase-1/carbon monoxide-dependent manner. J Plant Physiol **171**: 1–8

Lisjak M, Teklic T, Wilson ID, Whiteman M, Hancock JT (2013) Hydrogen sulfide: environmental factor or signalling molecule? Plant Cell Environ **36**: 1607–1616

Liu J, Moore S, Chen C, Lindsey K (2017) Crosstalk complexities between auxin, cytokinin, and ethylene in Arabidopsis root development: from experiments to systems modeling, and back again. Mol Plant **10**: 1480–1496

Ljung K, Hull AK, Celenza J, Yamada M, Estelle M, Normanly J, Sandberg G (2005) Sites and regulation of auxin biosynthesis in Arabidopsis roots. Plant Cell. **17**: 1090–1104

Loiret FG, Grimm B, Hajirezaei MR, Kleiner D, Ortega E (2009) Inoculation of sugarcane with *Pantoea sp*. increases amino acid contents in shoot tissues; serine, alanine, glutamine and asparagine permit concomitantly ammonium excretion and nitrogenase activity of the bacterium. J Plant Physiol **166**: 1152–1161

Lombardo MC, Graziano M, Polacco JC, Lamattina L (2006) Nitric oxide functions as a positive regulator of root hair development. Plant Signal Behav **1**: 28–33

López-Bucio J, Campos-Cuevas JC, Hernández-Calderón E, Velásquez-Becerra C, Farías-Rodríguez R, Macías-Rodríguez LI, Valencia-Cantero E (2007) *Bacillus megaterium* rhizobacteria promote growth and alter root-system architecture through an auxin- and ethylene-independent signaling mechanism in *Arabidopsis thaliana.* Mol Plant-Microbe Interact **20**: 207–212

López-Bucio J, Cruz-Ramírez A, Herrera-Estrella L (2003) The role of nutrient availability in regulating root architecture. Curr Opin Plant Biol **6**: 280–287

López-Bucio J, Hernández-Abreu E, Sánchez-Calderón L, Nieto-Jacobo MF, Simpson J, Herrera-Estrella L (2002) Phosphate availability alters architecture and causes changes in hormone sensitivity in the Arabidopsis root system. Plant Physiol **129**: 244–256

López-Bucio J, Hernández-Abreu E, Sánchez-Calderón L, Pérez-Torres A, Rampey RA, Bartel B, Herrera-Estrella L (2005) An auxin transport independent pathway is involved in phosphate stress-induced root architectural alterations in Arabidopsis. Identification of BIG as a mediator of auxin in pericycle cell activation. Plant Physiol **137**: 681–691

Luschnig C, Gaxiola RA, Grisafi P, Fink GR (1998) EIR1, a root-specific protein involved in auxin transport, is required for gravitropism in *Arabidopsis thaliana*. Genes Dev **12**: 2175–2187

Ma F, Wang L, Li J, Samma MK, Xie Y, Wang R, Wang J, Zhang J, Shen W (2014) Interaction between HY1 and H_2O_2 in auxin-induced lateral root formation in Arabidopsis. Plant Mol Biol **85**: 49–61

Makino A, Mae T (1999) Photosynthesis and plant growth at elevated levels of CO_2. Plant Cell Phys **40**: 999–1006

Malamy JE (2005) Intrinsic and environmental response pathways that regulate root system architecture. Plant Cell Environ **28**: 67–77

Mangano S, Denita-Juarez SP, Choi H-S, Marzol E, Hwang Y, Ranocha P, Velasquez SM, Borassi C, Barberini ML, Aptekmann AA, et al (2017) Molecular link between auxin and ROS-mediated polar growth. Proc Natl Acad Sci **114**: 5289–5294

Manzano C, Pallero-Baena M, Casimiro I, De Rybel B, Orman-Ligeza B, van Isterdael G, Beeckman T, Draye X, Casero P, del Pozo JC (2014) The emerging role of reactive oxygen species signaling during lateral root development. Plant Physiol **165**: 1105–1119

Manzano C, Pallero-Baena M, Silva-Navas J, Navarro Neila S, Casimiro I, Casero P, Garcia-Mina JM, Baigorri R, Rubio L, Fernandez JA, et al (2017) A light-sensitive mutation in Arabidopsis *LEW3* reveals the important role of N-glycosylation in root growth and development. J Exp Bot **68**: 5103–5116

Marino D, Dunand C, Puppo A, Pauly N (2012) A burst of plant NADPH oxidases. Trends Plant Sci **17**: 9–15

Martínez-Medina A, Van Wees SCM, Pieterse CMJ (2017) Airborne signals from *Trichoderma* fungi stimulate iron uptake responses in roots resulting in priming of

jasmonic acid-dependent defences in shoots or *Arabidopsis thaliana* and *Solanum lycopersicum.* Plant Cell Environ **40**: 2691–2705

Maruyama A, Saito K, Ishizawa K (2001) β-Cyanoalanine synthase and cysteine synthase from potato: molecular cloning, biochemical characterization, and spatial and hormonal regulation. Plant Mol Biol **46**: 749–760

Maurel C, Boursiac Y, Luu DT, Santoni V, Shahzad Z, Verdoucq L (2015) Aquaporins in plants. Physiol Rev **95**: 1321–1358

Mei Y, Chen H, Shen W, Shen W, Huang L (2017) Hydrogen peroxide is involved in hydrogen sulfide-induced lateral root formation in tomato seedlings. BMC Plant Biol **17**: 162 doi:1186/12870-017-1110-7

Meldau DG, Meldau S, Hoang LH, Underberg S, Wünsche H, Baldwin IT (2013) Dimethyl disulfide produced by the naturally associated bacterium *Bacillus* sp B55 promotes *Nicotiana attenuata* growth by enhancing sulfur nutrition. Plant Cell **25**: 2731–2747

Mo X, Zhu Q, Li X, Li J, Zeng Q, Rong H, Zhang H, Wu P (2006) The *hpa1* mutant of Arabidopsis reveals a crucial role of histidine homeostasis in root meristem maintenance. Plant Physiol **141**: 1425–1435

Moisan K, Cordovez V, van de Zande EM, Raaijmakers JM, Dicke M, Lucas-Barbosa D (2019) Volatiles of pathogenic and non-pathogenic soil-borne fungi affect plant development and resistance to insects. Oecologia **190**: 589–604

Molina-Favero C, Creus CM, Simontacchi M, Puntarulo S, Lamattina L (2008) Aerobic nitric oxide production by *Azospirillum brasilense* Sp245 and its influence on root architecture in tomato. Mol Plant Microbe Interact **21**: 1001–1009

Montiel J, Nava N, Cárdenas L, Sánchez-López R, Arthikala MK, Santana O, Sánchez F, Quinto C (2012) A *Phaseolus vulgaris* NADPH oxidase gene is required for root infection by rhizobia. Plant Cell Physiol **53**: 1751-1767

Moubayidin L, DiMambro R, Sabatini S (2009) Cytokinin-auxin crosstalk. Trends Plant Sci **14**: 557–562

Muñoz-Bertomeu J, Cascales-Miñana B, Mulet JM, Baroja-Fernández E, Pozueta-Romero J, Kuhn JM, Segura J, Ros R (2009) Plastidial glyceraldehyde-3-phosphate dehydrogenase deficiency leads to altered root development and affects the sugar and amino acid balance in Arabidopsis. Plant Physiol **151**: 541–558

Mur LAJ, Mandon J, Persijn S, Cristescu SM, Moshkov IE, Novikova GV, Hall MA, Harren FJM, Hebelstrup KM, Gupta KJ (2012). Nitric oxide in plants: an assessment of the current state of knowledge. AoB Plants **5**:pls052 doi:10.1093/aobpla/pls052

Nandi R, Sengupta S (1998) Microbial production of hydrogen: an overview. Crit Rev Microbiol **24**: 61–84

Nascimento FX, Rossi MJ, Glick BR (2018) Ethylene and 1-aminocyclopropane-1-carboxylate (ACC) in plant–bacterial interactions. Front Plant Sci **9**: 114

Naznin HA, Kimura M, Miyazawa M, Hyakumachi M (2013) Analysis of volatile organic compounds emitted by plant growth-promoting fungus *Phoma* sp. GS8-3 for growth promotion effects on tobacco. Microbes Environ **28**: 42–49

Negi S, Ivanchenko MG, Muday GK (2008) Ethylene regulates lateral root formation and auxin transport in *Arabidopsis thaliana*. Plant J **55**: 175–187

Nemhauser JL, Hong F, Chory J (2006) Different plant hormones regulate similar processes through largely nonoverlapping transcriptional responses. Cell **126**: 467–475

Nguyen HM, Sako K, Matsui A, Suzuki Y, Mostofa MG, Ha CV, Tanaka M, Tran LSP, Habu Y, Seki M (2017) Ethanol enhances high-salinity stress tolerance by detoxifying reactive oxygen species in *Arabidopsis thaliana* and rice. Front Plant Sci **8**: 1001 doi:10.3389/fpls.2017.01001

Nieto-Jacobo MF, Steyaert JM, Salazar-Badillo FB, Nguyen DV, Rostás M, Braithwaite M, De Souza JT, Jimenez-Bremont JF, Ohkura M, Stewart A, et al (2017) Environmental growth conditions of *Trichoderma* spp. affects indole acetic acid derivatives, volatile organic compounds, and plant growth promotion. Front Plant Sci **8**: 102 doi: 10.3389/fpls.2017.00102

Niu Y, Jin C, Jin G, Zhou Q, Lin X, Tang C, Zhang YS (2011) Auxin modulates the enhanced development of root hairs in *Arabidopsis thaliana* (L.) Heynh. under elevated CO2. Plant Cell Environ **34**: 1304–1317

Novák O, Hauserová E, Amakorová P, Doležal K, Strnad M (2008) Cytokinin profiling in plant tissues using ultra-performance liquid chromatography-electrospray tandem mass spectrometry. Phytochemistry **69**: 2214–2224

O'Brien JA, Daudi A, Butt VS, Bolwell GP (2012) Reactive oxygen species and their role in plant defence and cell wall metabolism. Planta **236**: 765–779

O'Leary B, Preston GM, Sweetlove LJ (2014) Increased β-cyanoalanine nitrilase activity improves cyanide tolerance and assimilation in Arabidopsis. Mol Plant **7**: 231–243

Olmos E, Kiddle G, Pellny TK, Kumar S, Foyer CH (2006) Modulation of plant morphology, root architecture, and cells structure by low vitamin C in *Arabidopsis thaliana*. J Exp Bot **57**: 1645–1655

Orman-Ligueza B, Morris EC, Parizot B, Lavigne T, Babé A, Ligeza A, Klein S,

Sturrock C, Xuan W, Novák O, et al (2018) The xerobranching response represses lateral root formation when roots are not in contact with water. Curr Biol **28**: 3165–3173

Overvoorde P, Fukaki H, Beeckman T (2010) Auxin control of root development. Cold Spring Harb Perspect Biol **2**:a001537 doi: 10.1101/cshperspect.a001537

Pagnussat GC, Simontacchi M, Puntarulo S, Lamattina L (2002) Nitric oxide is required for root organogenesis. Plant Physiol **129**: 954–956

Passardi F, Tognolli M, De Meyer M, Penel C, Dunand C (2006) Two cell wall associated peroxidases from Arabidopsis influence root elongation. Planta **223**: 965–974

Pelagio-Flores R, Ortíz-Castro R, Méndez-Bravo A, Macías-Rodríguez L, López-Bucio J (2011) Serotonin, a tryptophan-derived signal conserved in plants and animals, regulates root system architecture probably acting as a natural auxin inhibitor in *Arabidopsis thaliana*. Plant Cell Physiol **52**: 490–508

Penrose DM, Moffatt BA, Glick BR (2001) Determination of 1-aminocycopropane-1-carboxylic acid (ACC) to assess the effects of ACC deaminase-containing bacteria on roots of canola seedlings. Can J Microbiol **47**: 77–80

Péret B, Li G, Zhao J, Band LR, Voß U, Postaire O, Luu D-T, Da Ines O, Casimiro I, Lucas M, et al (2012) Auxin regulates aquaporin function to facilitate lateral root emergence. Nat Cell Biol 14: 991–998

Pérez-Ruiz JM, Naranjo B, Ojeda V, Guinea M, Cejudo FJ (2017) NTRC-dependent redox balance of 2-Cys peroxiredoxins is needed for optimal function of the photosynthetic apparatus. Proc Natl Acad Sci U S A **114**: 12069–12074

Perrig D, Boiero ML, Masciarelli OA, Penna C, Ruiz OA, Cassán FD, Luna MV (2007) Plant-growth promoting compounds produced by two agronomically important strains of *Azospirillum brasilense*, and implications for inoculant formulation. Appl Microbiol Biotechnol **75**: 1143–1150

Perrot-Rechenmann C, Napier RM (2005) Auxins. Vitam Horm **72**: 203–233

Piechulla B (2017) Considering microbial CO_2 during microbe-plant cocultivation. Plant Physiol **173**: 1529 doi: 10.1104/pp.16.01584

Piechulla B, Lemfack MC, Kai M (2017) Effects of discrete bioactive microbial volatiles on plants and fungi. Plant Cell Environ **40**: 2042–2067

Piotrowski M, Schönfelder S, Weiler EW (2001) The *Arabidopsis thaliana* isogene NIT4 and its orthologs in tobacco encode β-cyano-L-alanine hydratase/nitrilase. J Biol Chem **276**: 2616–2621

Pitts RJ, Cernac A, Estelle M (1998) Auxin and ethylene promote root hair elongation

in Arabidopsis. Plant J **16**: 553–560

Pokhilko A, Bou-Torrent J, Pulido P, Rodríguez-Concepción M, Ebenhöh O (2015) Mathematical modelling of the diurnal regulation of the MEP pathway in Arabidopsis. New Phytol **206**: 1075–1085

Pulido P, Perello C, Rodríguez-Concepcion M (2012) New insights into plant isoprenoid metabolism. Mol Plant **5**: 964–967

Quebedeaux B, Hardy RW (1975) Reproductive growth and dry matter production of *glycine max* (L.) Merr. in response to oxygen concentration. Plant Physiol **55**: 102–107

Rahman A, Hosokawa S, Oono Y, Amakawa T, Goto N, Tsurumi S (2002) Auxin and ethylene response interactions during Arabidopsis root hair development dissected by auxin influx modulators. Plant Physiol **130**: 1908–1917

Ramireddy E, Chang L, Schmülling T (2014) Cytokinin as a mediator for regulating root system architecture in response to environmental cues. Plant Signal Behav **9**(1):e27771

Ramonell KM, Kuang A, Porterfield DM, Crispi ML, Xiao Y, McClure G, Musgrave ME (2001) Influence of atmospheric oxygen on leaf structure and starch deposition in *Arabidopsis thaliana*. Plant Cell Environ **24**: 419–428

Rhoads DM, Umbach AL, Subbaiah CC, Siedow JN (2006). Mitochondrial reactive oxygen species. Contribution to oxidative stress and interorganellar signalling. Plant Physiol **141**: 357–366

Riefler M, Novak O, Strnad M, Schmülling T (2006) Arabidopsis cytokinin receptor mutants reveal functions in shoot growth, leaf senescence, seed size, germination, root development, and cytokinin metabolism. Plant Cell **18**: 40–54

Robbins NE, Dinneny JR (2018) Growth is required for perception of water availability to pattern root branches in plants. Proc Natl Acad Sci U S A **115**: 822–831

Rodrigues O, Reshetnyak G, Grondin A, Saijo Y, Leonhardt N, Maurel C, Verdoucq L (2017) Aquaporins facilitate hydrogen peroxide entry into guard cells to mediate ABA- and pathogen-triggered stomatal closure. Proc Natl Acad Sci U S A**114**: 9200–9205

Rodríguez-Reinoso F, Garrido J, Martín-Martínez JM, Molina-Sabio M, Torregrosa R (1989) The combined use of different approaches in the characterization of microporous carbons. Carbon **27**: 23–32

Rogers EE, Eide DJ, Guerinot M Lou (2000) Altered selectivity in an Arabidopsis metal transporter. Proc Natl Acad Sci U S A **97**: 12356–12360

Rojas CM, Senthil-Kumar M, Tzin V, Mysore KS (2014) Regulation of primary plant metabolism during plant-pathogen interactions and its contribution to plant defense. Front Plant Sci **5**: 17

Ryu CM, Farag MA, Hu CH, Reddy MS, Wei HX, Paré PW, Kloepper JW (2003) Bacterial volatiles promote growth in Arabidopsis. Proc Natl Acad Sci U S A **100**: 4927–4932

Saini S, Sharma I, Kaur N, Pati PK (2013) Auxin: A master regulator in plant root development. Plant Cell Rep **32**: 741–757

Sakakibara H (2006) Cytokinins: activity, biosynthesis, and translocation. Annu Rev Plant Biol **57**: 431–449

Sánchez-Calderón L, López-Bucio J, Chacón-López A, Cruz-Ramírez A, Nieto-Jacobo F, Dubrovsky JG, Herrera-Estrella L (2005) Phosphate starvation induces a determinate developmental program in the roots of *Arabidopsis thaliana*. Plant Cell Physiol **46**:174–84

Sánchez-López ÁM, Bahaji A, De Diego N, Baslam M, Li J, Muñoz FJ, Almagro G, García-Gómez P, Ameztoy K, Ricarte-Bermejo A, et al (2016a) Arabidopsis responds to *Alternaria alternata* volatiles by triggering plastid phosphoglucose isomerase-independent mechanisms. Plant Physiol **172**: 1989–2001

Sánchez-López ÁM, Baslam M, De Diego N, Muñoz FJ, Bahaji A, Almagro G, Ricarte-Bermejo A, García-Gómez P, Li J, Humplík JF, et al (2016b) Volatile compounds emitted by diverse phytopathogenic microorganisms promote plant growth and flowering through cytokinin action. Plant Cell Environ **39**: 2592–2608

Schenkel D, Maciá-Vicente JG, Bissell A, Splivallo R (2018) Fungi indirectly affect plant root architecture by modulating soil volatile organic compounds. Front Microbiol **9**: doi: 10.3389/fmicb.2018.01847

Schaller GE, Bishopp A, Kieber JJ (2015) The yin-yang of hormones: cytokinin and auxin interactions in plant development. Plant Cell **27**: 44–63

Schreiber F, Wunderlin P, Udert KM, Wells GF (2012) Nitric oxide and nitrous oxide turnover in natural and engineered microbial communities: Biological pathways, chemical reactions, and novel technologies. Front Microbiol **3**: 372 doi: https://doi.org/10.3389/fmicb.2012.00372

Schulz S, Dickschat JS (2007) Bacterial volatiles: the smell of small organisms. Nat Prod Rep **24**: 814–842

Séguéla M, Briat J-F, Vert G, Curie C (2008) Cytokinins negatively regulate the root iron uptake machinery in Arabidopsis through a growth-dependent pathway. Plant J **55**: 289–300

Sergeeva LI, Keurentjes JJB, Bentsink L, Vonk J, van der Plas LHW, Koornneef M, Vreugdenhil D (2006) Vacuolar invertase regulates elongation of *Arabidopsis thaliana* roots as revealed by QTL and mutant analysis. Proc Natl Acad Sci U S A **103**: 2994–2999

Shatalin K, Shatalina E, Mironov A, Nudler E (2011) H_2S: a universal defense against antibiotics in bacteria. Science **334**: 986–990

Siegel SM, Siegel BZ (1987) Biogenesis of carbon monoxide: production by fungi and seed plants in the dark. Phytochemistry **26**: 3117–3119

Smyth GK, Speed T (2003) Normalization of cDNA microarray data. Methods **31**: 265–273

Song X, Kristie DN, Reekie EG (2009) Why does elevated CO_2 affect time of flowering? An exploratory study using the photoperiodic flowering mutants of *Arabidopsis thaliana*. New Phytol **181**: 339–346

Splivallo R, Fischer U, Göbel C, Feussner I, Karlovsky P (2009) Truffles regulate plant root morphogenesis via the production of auxin and ethylene. Plant Physiol **150**: 2018–2029

Srivastava LM (2002) Plant growth and development. Hormones and the environment. Oxford: Academic Press

Stepanova AN, Alonso JM (2009) Ethylene signaling and response: where different regulatory modules meet. Curr Opin Plant Biol **12**: 548–555

Stepanova AN, Hoyt JM, Hamilton AA, Alonso JM (2005) A link between ethylene and auxin uncovered by the characterization of two root-specific ethylene-insensitive mutants in Arabidopsis. Plant Cell **17**: 2230–2242

Stepanova AN, Yun J, Likhacheva AV, Alonso JM (2007) Multivel interactions between ethylene and auxin in Arabidopsis roots. Plant Cell **19**: 2169–2185

Strader LC, Chen GL, Bartel B (2010) Ethylene directs auxin to control root cell expansion. Plant J **64**: 874–884

Street IH, Aman S, Zubo Y, Ramzan A, Wang X, Shakeel SN, Kieber JJ, Schaller GE (2015) Ethylene inhibits cell proliferation of the Arabidopsis root meristem. Plant Physio **169**: 338–350

Sundaravelpandian K, Chandrika NNP, Schmidt W (2013) PFT1, a transcriptional mediator complex subunit, controls root hair differentiation through reactive oxygen species (ROS) distribution in Arabidopsis. New Phytol **197**: 151–161

Suzuki N, Miller G, Morales J, Shulaev V, Torres MA, Mittler R (2011) Respiratory

burst oxidases: the engines of ROS signaling. Curr Opin Plant Biol **14**: 691–699

Swarup R, Friml J, Marchant A, Ljung K, Sandberg G, Palme K, Bennett M (2001) Localization of the auxin permease AUX1 suggests two functionally distinct hormone transport pathways operate in the Arabidopsis root apex. Genes Dev **15**: 2648–2653

Swarup R, Perry P, Hagenbeek D, Van Der Straeten D, Beemster GTS, Sandberg G, Bhalerao R, Ljung K, Bennett MJ (2007) Ethylene upregulates auxin biosynthesis in Arabidopsis seedlings to enhance inhibition of root cell elongation. Plant Cell **19**: 2186–2196

Takahashi M, Furuhashi T, Ishikawa N, Horiguchi G, Sakamoto A, Tsukaya H, Morikawa H (2014) Nitrogen dioxide regulates organ growth by controlling cell proliferation and enlargement in Arabidopsis. New Phytol **201**: 1304–1315

Teale WD, Paponov IA, Palme K (2006) Auxin in action: signalling, transport and the control of plant growth and development. Nat Rev Mol Cell Biol **11**: 847–859

Thimm O, Bläsing O, Gibon Y, Nagel A, Meyer S, Krüger P, Selbig J, Müller LA, Rhee SY, Stitt M (2004) MAPMAN: A user-driven tool to display genomics data sets onto diagrams of metabolic pathways and other biological processes. Plant J **37**: 914–939

Thompson M, Gamage D, Hirotsu N, Martin A, Seneweera S (2017) Effects of elevated carbon dioxide on photosynthesis and carbon partitioning: a perspective on root sugar sensing and hormonal crosstalk. Front Physiol **8**: 578 https://doi.org/10.3389/fphys.2017.00578

Thuler DS, Floh EI, Handro W, Barbosa HR (2003) Plant growth regulators and amino acids released by *Azospirillum* sp in chemically defined media. Lett Appl Microbiol **2**: 174–178

Tisch D, Schmoll M (2010) Light regulation of metabolic pathways in fungi. Applied Microbiol Biotech **85**: 1259–1277

Tsukagoshi H, Busch W, Benfey PN (2010) Transcriptional regulation of ROS controls transition from proliferation to differentiation in the root. Cell **143**: 606–616

Ulmasov T, Murfett J, Hagen G, Guilfoyle TJ (1997) Aux/IAA proteins repress expression of reporter genes containing natural and highly active synthetic auxin response elements. Plant Cell **9**: 1963–1971

van Dam NM, Bouwmeester HJ (2016) metabolomics in the rhizosphere: tapping into belowground chemical communication. Trend Plant Sci **21**: 256–265

van Den Dool H, Dec Kratz P (1963) A generalization of the retention index system including linear temperature programmed gas—liquid partition chromatography. J

Chromatogr A **11**: 463–471

Vanneste S, Friml J (2009) Auxin: a trigger for change in plant development. Cell Mar **136**: 1005–1016

van Zhong G, Burns JK (2003) Profiling ethylene-regulated gene expression in *Arabidopsis thaliana* by microarray analysis. Plant Mol Biol **53**: 117–131

Varotto C, Maiwald D, Pesaresi P, Jahns P, Salamini F, Leister D (2002) The metal ion transporter IRT1 is necessary for iron homeostasis and efficient photosynthesis in *Arabidopsis thaliana*. Plant J **31**: 589–599

Velázquez-Becerra C, Macías-Rodríguez LI, López-Bucio J, Altamirano-Hernández J, Flores-Cortez I, Valencia-Cantero E (2011) A volatile organic compound analysis from *Arthrobacter agilis* identifies dimethylhexadecylamine, an amino-containing lipid modulating bacterial growth and Medicago sativa morphogenesis in vitro. Plant Soil **339**: 329–340

Verbon EH, Liberman LM (2016) Beneficial microbes affect endogenous mechanisms controlling root development. Trends Plant Sci **21**: 218–229

Vert GA, Briat JF, Curie C (2003) Dual regulation of the Arabidopsis high-affinity root iron uptake system by local and long-distance signals. Plant Physiol **132**: 796–804

Vieten A, Sauer M, Brewer PB, Friml J (2007) Molecular and cellular aspects of auxin-transport-mediated development. Trends Plant Sci **12**:160–168

von Caemmerer S, Farquhar GD (1981) Some relationships between the biochemistry of photosynthesis and the gas exchange of leaves. Planta **153**: 376–387

Wang M, Liao W (2016) Carbon monoxide as a signaling molecule in plants. Front Plant Sci doi: https://doi.org/10.3389/fpls.2016.00572

Weikl F, Ghirardo A, Schnitzler JP, Pritsch K (2016) Sesquiterpene emissions from *Alternaria alternata* and *Fusarium oxysporum*: effects of age, nutrient availability, and co-cultivation. Sci Rep doi:10.1038/srep22152

Weise T, Kai M, Piechulla B (2013) Bacterial ammonia causes significant plant growth inhibition. PLoS ONE **8**: e63538. doi:10.1371/journal.,pone.0063538

Werner T, Nehnevajova E, Köllmer I, Novák O, Strnad M, Krämer U, Schmülling T (2010) Root-specific reduction of cytokinin causes enhanced root growth, drought tolerance, and leaf mineral enrichment in Arabidopsis and tobacco. Plant Cell **22**: 3905–3920

Wharton DC, Weintraub ST (1980) Identification of nitric oxide and nitrous oxide as products of nitrite reduction by Pseudomonas cytochrome oxidase (nitrite reductase).

Biochem Biophys Res Commun **97**: 236–242

Williamson LC, Ribrioux SP, Fitter AH, Leyser HM (2001) Phosphate availability regulates root system architecture in Arabidopsis. Plant Physiol **126**: 875–82

Wilson ID, Neill SJ, Hancock JT (2008) Nitric oxide synthesis and signaling in plants. Plant Cell Environ **31**: 622–631

Xu Q, Zhou B, Ma C, Xu X, Xu J, Jiang Y, Liu C, Li G, Herbert SJ, Hao L (2010) Salicylic acid-altering Arabidopsis mutants response to NO_2 exposure. Bull Envirol Contam Toxicol **84**: 106–111

Xuan W, Zhu, FY, Xu S, Huang BK, Ling TF, Qi JY, Ye MB, Shen WB (2008) The heme oxygenase/carbon monoxide system is involved in the auxin-induced cucumber adventitious rooting process. Plant Physiol **148**: 881–893

Yang C, Lu X, Ma B, Chen SY, Zhang JS (2015) Ethylene signaling in rice and Arabidopsis: conserved and diverged aspects. Mol Plant **8**: 495–505

Yang DL, Shi Z, Bao Y, Yan J, Yang Z, Yu H, Li Y, Gou M, Wang S, Zou B, et al (2017) Calcium pumps and interacting BON1 protein modulate calcium signature, stomatal closure, and plant immunity. Plant Physiol **175**: 424–437

Yang L, Ji J, Wang H, Harris-Shultz KR, Abd Allah EF, Luo Y, Guan Y, Hu X (2016) Carbon monoxide interacts with auxin and nitric oxide to cope with iron deficiency in Arabidopsis. Front Plant Sci doi: https://doi.org/10.3389/fpls.2016.00112

Yang TJW, Perry PJ, Ciani S, Pandian S, Schmidt W (2008) Manganese deficiency alters the patterning and development of root hairs in Arabidopsis. J Exp Bot **59**: 3453–3464

Zamioudis C, Mastranesti P, Dhonukshe P, Blilou I, Pieterse CMJ (2013) Unraveling root developmental programs initiated by beneficial *Pseudomonas* spp. bacteria. Plant Physiol **162**: 304–318

Žd'árská M, Zatloukalová P, Benítez M, Šedo O, Potěšil D, Novák O, Svačinová J, Pešek B, Malbeck J, Vašíčková J, et al (2013) Proteome analysis in Arabidopsis reveals shoot- and root-specific targets of cytokinin action and differential regulation of hormonal homeostasis. Plant Physiol **161**: 918–930

Zazímalová E, Murphy AS, Yang H, Hoyerová K, Hosek P (2010) Auxin transporters--why so many? Cold Spring Harb Perspect Biol doi: 10.1101/cshperspect.a001552

Zeng J, Zhang M, Sun X (2013) Molecular hydrogen is involved in phytohormone signaling and stress responses in plants. PLoS ONE, **8**: e71038 doi: 10.1371/journal.pone.0071038

Zhang H, Kim MS, Krishnamachari V, Payton P, Sun Y, Grimson M, Farag MA, Ryu CM, Allen R, Melo IS, Paré PW (2007) Rhizobacterial volatile emissions regulate auxin homeostasis and cell expansion in Arabidopsis. Planta **226**: 839–51

Zhang H, Sun Y, Xie X, Kim MS, Dowd SE, Paré PW (2009) A soil bacterium regulates plant acquisition of iron via deficiency-inucible mechanisms. Plant J **58**: 568–577

Zhang H, Xie X, Kim MS, Kornyeyev DA, Holaday S, Paré PW (2008) Soil bacteria augment Arabidopsis photosynthesis by decreasing glucose sensing and abscisic acid levels *in planta*. Plant J **56**: 264–273

Zhao H, Ma T, Wang X, Deng Y, Ma H, Zhang R, Zhao J (2015) OsAUX1 controls lateral root initiation in rice (*Oryza sativa L.*). Plant Cell Environ **38**: 2208–2222

Zhu Y, Liao W, Wang M, Niu L, Xu Q, Jin X (2016) Nitric oxide is required for hydrogen gas-induced adventitious root formation in cucumber. J Plant Physiol **195**: 50–58

Zou C, Li Z, Yu D (2010) *Bacillus megaterium* strain XTBG34 promotes plant growth by producing 2-pentylfuran. J Microbiol **48**: 460–466

APÉNDICE

upna
Universidad Pública de Navarra
Nafarroako Unibertsitate Publikoa

LISTADO DE ABREVIATURAS

ABA	Abscisic acid
ABC	ATP-binding cassette
ACA8	Autoinhibited-Ca2+ ATPase 8
ACLA1	ATP citrate lyase 1
ACO2	Aminocyclopropane-1-carboxylic oxidase 2
ADP	Adenosine diphosphate
AGP	ADP-glucose pyrophosphorylase 1
AHK2	Arabidopsis histidin kinase 2
AHK3	Arabidopsis histidin kinase 3
AHK4	Arabidopsis histidin kinase 4
AK	Adenosine kinase
AMP	Adenosine monophosphate
An	Net CO2 assimilation rate
APS1	Small AGP subunit 1
ARF	Auxin response factor
ARR5	Arabidopsis thaliana response regulator 5
ASP2	Aspartate aminotransferase 2
ATP	Adenosine triphosphate
AUX1	Auxin resistant 1
BFRUCT3	Acid beta-fructofuranosidase 3
BFRUCT4	Acid beta-fructofuranosidase 4
BGLU20	Beta glucosidase 20
BGLU21	Beta glucosidase 21
BGLU22	Beta glucosidase 22
BGLU23	Beta glucosidase 23
BR	Brassinosteroids
CAR	Carboxen
CAS-C1	Cyanoalanine synthase C1
CBC	Calvin-Benson cycle
CHK	Cytokinin histidin kinase
C*i*	Intercellular CO2 concentration
CKs	Cytokinines

CTR1	Constitutive triple response 1
cZ	Cis-zeatine
cZ9G	Cis-zeatine-9-glicoside
cZR	Cis-zeatin riboside
cZRMP	Cis-zeatin riboside monophosphate
cZROG	Cis-zeatine riboside-O-glicoside
DEP	Differentially expressed protein
D(H)Z	Dihidrozeatine
D(H)Z7G	Dihidrozeatine-7-glucoside
D(H)Z9G	Dihidrozeatine-9-glucoside
D(H)ZR	Dihidrozeatine-riboside
D(H)ZRMP	Dihidrozeatin riboside monophosphate
DPI	Diphenyleneiodium
DVB	Divinylbenzene
DW	Dry weight
EIL1	Ethylene-insensitive 3-like 1
EIN3	Ethylene-insensitive 3
EIN4	Ethylene-insensitive 4
EIR1	Ethylene insensitive root 1
ER	Endoplasmatic reticulum
ERF1	Ethylene response factor 1
ERS1	Ethylene response sensor 1
ERS2	Ethylene response sensor 2
ETR1	Ethylene response 1
ETR2	Ethylene response 2
FLA6	Fasciclin-like arabinogalactan 6
FLA13	Fasciclin-like arabinogalactan 13
FW	Fresh weight
G6P	Glucose-6-phosphate
GA	Gibberellins
GAP	Glyceraldehyde 3-phosphate
GC-MS	Gas cromatography mass spectrum
GLN1	Glutamine synthetase 1

GLT1	Glutamate synthase 1
GMP	Guanosine monophosphate
GPT2	Glucose-6-phosphate transporter 2
gs	Stomatal conductance
GSH	Reduced glutathione
GSNO	S-nitrosoglutathione
GSNOR	S-nitrosoglutathione reductase
GUS	β-glucuronidase
HPt	Histidine transference protein
IAA	Indolacetic acid
IGP	Indole-3-glycerol phosphate
iP	Isopentenyladenine
iP7G	Isopentenyladenosine-7-glucoside
iP9G	Isopentenyladenosine-9-glucoside
IPA	Indole-3-piruvic acid
iPR	Isopentenyl riboside
iPRDP	Isopentenyl riboside diphosphate
iPRMP	Isopentenyl riboside monophosphate
iPRTP	Isopentenyl riboside triphosphate
IPT	Isopentenyl transferase
IRT1	Iron-regulated transporter 1
LAX	Like-AUX1
LR	Lateral root
LRP	Lateral root primordium
MAP	Mitogen-activated protein
MEP	Methylerithritol phosphate
METK2	S-Adenosylmethionine synthetase 2
METK3	S-Adenosylmethionine synthetase 3
MMTS	Methyl methanethiosulfonate
MS	Murashige-Skoog
MVA	Mevalonic acid
NADPH	Nicotinamide adenine dinucleotide phosphate
NBT	Nitroblue tetrazolium

NIT4	Nitrilase 4
nsHB	Non-synthetic hemoglobin
NTRC	C-type NADPH dependent thiorredoxin reductase
PDMS	Polydimethylsiloxane
PER3	Peroxidase 3
PER32	Peroxidase 32
PER34	Peroxidase 34
PGI1	Phosphoglucoisomerase 1
PGP	P-glycoprotein
PIN	PIN-formed protein
PIP1	Plasma membrane intrinsic protein 1
PIP2	Plasma membrane intrinsic protein 2
pPGI	Plastidial phosphoglucoisomerase
PR	Primary root
PVC	Polyvinyl chloride
RH	Root hair
RHD2	Root hair defective 2
ROS	Reactive oxygen species
RR	Response regulator
RSA	Root system architecture
SDS-PAGE	Sodium dodecylsulfate polyacrylamide gel electrophoresis
SL	Strigolactones
SPME	Solid phase microextraction
TCA	Tricarboxylic acid
TIP1	Tonoplast intrinsic protein 1
TIP2	Tonoplast intrinsic protein 2
TIR1	Transport inhibitor response 1
tZ	Trans-zeatin
tZ7G	Trans-zeatin-7-glicoside
tZ9G	Trans-zeatin-9-glicoside
tZR	Trans-zeatin-riboside
tZRDP	Trans-zeatin riboside diphosphate
tZRMP	Trans-zeatin riboside monophosphate

tZROG	Trans-zeatin riboside-O-glicoside
tZRTP	Trans-zeatin riboside triphosphate
UDP	Uridine diphosphate
UGD4	UDP-glucose 6-dehydrogenase 4-like
UGP2	UDP-glucose pyrophosphorylase 2
UXS4	UDP-xylose synthase 4
VCs	Volatile compounds
VICs	Volatile inorganic compounds
VOCs	Volatile organic compounds
WT	Wild-type
WUE*i*	Water use efficiency
XTH14	Xyloglucan endotransglucosylase/hydrolase 14

LISTADO DE PUBLICACIONES

1. Sánchez-López ÁM, Baslam M, De Diego N, Muñoz FJ, Bahaji A, Almagro G, Ricarte-Bermejo A, **García-Gómez P**, Li J, Humplík JF, Novák O, Spíchal L, Doležal K, Baroja-Fernández E, Pozueta-Romero J (2016a) Volatile compounds emitted by diverse phytopathogenic microorganisms promote plant growth and flowering through cytokinin action. Plant Cell Environ. doi: 10.1111/pce.12759
2. Sánchez-López ÁM, Bahaji A, De Diego N, Baslam M, Li J, Muñoz FJ, Almagro G, **García-Gómez P**, Ameztoy K, Ricarte-Bermejo A, Novák O, Humplík JF, Spíchal L, Doležal K, Ciordia S, Mena MC, Baroja-Fernández E, Pozueta-Romero J (2016b) Arabidopsis responds to *Alternaria alternata* volatiles by triggering pPGI-independent mechanisms. Plant Physiol. doi:10.1104/pp.16.00945
3. **García-Gómez P**, Almagro G, Sánchez-López ÁM, Bahaji A, Ameztoy K, Ricarte-Bermejo A, Baslam M, Antolín MC, Urdiain A, López-Belchi MD, López-Gómez P, Morán JF, Garrido J, Muñoz FJ, Baroja-Fernández E, Pozueta-Romero J (2019) Volatile compounds other than CO_2 emitted by different microorganisms promote distinct post-transcriptionally regulated responses in plants. Plant Cell Environ. doi: 10.1111/pce.13490
4. Ameztoy K, Baslam M, Sánchez-López ÁM, Muñoz FJ, Bahaji A, Almagro G, **García-Gómez P**, Baroja-Fernández E, De Diego N, Humplík JF, Ugena L, Spíchal L, Doležal K, Kaneko K, Mitsui T, Cejudo FJ, Pozueta-Romero J (2019) Plant responses to fungal volatiles involve global post-translational thiol redox proteome changes that affect photosynthesis. Plant Cell Environ. doi: 10.1111/pce.13601.
5. **García-Gómez P**, Bahaji A, Gámez-Arcas S, Muñoz FJ, Sánchez-López ÁM, Almagro G, Baroja-Fernández E, De Diego N, Ugena L, Spíchal L, Doležal K, Hajirezaei M, Romero L, García I, Pozueta-Romero J (enviado) Volatile emissions from fungal phytopathogens modulate plant root metabolism and architecture through mechanisms involving cyanide scavenging and hormone- and ROS-mediated proteome resetting. Plant Cell Environ

LISTADO DE COMUNICACIONES PRESENTADAS EN CONGRESOS

1. Sánchez-López ÁM, Bahaji A, De Diego N, Baslam M, Li J, Muñoz FJ, Almagro G, **García-Gómez P**, Ameztoy K, Ricarte-Bermejo A, Novák O, Humplík JF, Spíchal L, Doležal K, Ciordia S, Maria del Carmen Mena, Navajas R, Baroja-Fernández E, Pozueta-Romero J. Arabidopsis is capable of responding to volatile phytostimulants emitted by phytopathogenic microorganisms by triggering plastidic phosphoglucose isomerase independent mechanisms. XIII Reunión de Biología Molecular de Plantas. 22-24 junio 2016, Oviedo

2. Sánchez-López ÁM, Baslam M, De Diego N, Muñoz FJ, Bahaji A, Almagro G, Ricarte-Bermejo A, **García-Gómez P**, Li J, Humplík JF, Novák O, Spíchal L, Doležal K, Baroja-Fernández E, Pozueta-Romero J. Volatile compounds emitted by diverse phytopathogenic microorganisms promote plant growth and flowering through cytokinin action: a case of dirty dishes (2016) XIII Reunión de Biología Molecular de Plantas. 22-24 junio 2016, Oviedo
3. Sánchez-López ÁM, Baslam M, De Diego N, Muñoz FJ, Bahaji A, Almagro G, Ricarte-Bermejo A, **García-Gómez P**, Humplík JF, Novák O, Spíchal L, Doležal K, Baroja-Fernández E, Pozueta-Romero J. Volatile compounds emitted by diverse phytopathogenic microorganisms promote plant growth and flowering through cytokinin action. Plant Biology Europe EPSO/FESPB 2016 Congress. 26-30 junio, Praga
4. Sánchez-López ÁM, Bahaji A, De Diego N, Baslam M, Li J, Muñoz FJ, Almagro G, **García-Gómez P**, Ameztoy K, Ricarte-Bermejo A, Ugena L, Novák O, Humplík JF, Spíchal L, Doležal K, Ciordia S, Maria del Carmen Mena, Baroja-Fernández E, Pozueta-Romero J. Arabidopsis respond to volatile compounds emitted by phytopathogenic microorganisms through plastidic phosphoglucose isomerase independent mechanisms. Plant Biology Europe EPSO/FESPB 2016 Congress. 26-30 junio, Praga
5. **García-Gómez P**, Baslam M, Muñoz FJ, Sánchez López ÁM, Bahaji A, Almagro G, De Diego N, Spíchal L, Doležal K, Baroja-Fernández E, Pozueta-Romero J. Volatile compounds emitted by the fungal phytopathogen *Penicillium aurantiogriseum* promote changes in the root architecture of *Arabidopsis thaliana* through auxin action. XXII Reunión de la Sociedad Española de Fisiología vegetal y XV Spanish-Portuguese Congress of Plant Physiology. 26-29 junio 2017, Barcelona
6. Ameztoy K, Baslam M, Sánchez-López ÁM, Muñoz FJ, Bahaji A, Almagro G, **García-Gómez P**, Baroja-Fernández E, De Diego N, Humplík JF, Ugena L, Spíchal L, Dolezal K, Kaneko K, Mitsui T, Cejudo FJ and Pozueta-Romero J. Plant responses to fungal volatiles involve global post-translational thiol redox proteome changes that affect photosynthesis. XXIII Reunión de la Sociedad Española de Fisiología vegetal y XVI Spanish-Portuguese Congress of Plant Physiology. 26-28 junio 2019, Pamplona
7. **García-Gómez P**, Bahaji A, Muñoz FJ, Sánchez-López ÁM, Almagro G, Ameztoy K, Baroja-Fernández E, Baslam M, De Diego N, Ugena L, Spíchal L, Dolezal K, Hajirezai M and Pozueta-Romero J. Volatile organic compounds-depleted microbial emissions modulate plant root architecture and metabolome through proteome resetting, and hormone and ROS signaling. XXIII Reunión de la Sociedad Española

de Fisiología vegetal y XVI Spanish-Portuguese Congress of Plant Physiology. 26-28 junio 2019, Pamplona

8. Gámez-Arcas S, Sánchez-López ÁM, Ricarte-Bermejo A, Baslam M, Baroja-Fernández E, **García-Gómez P**, Muñoz FJ, Bahaji A, Ugena L, Ameztoy K, Almagro G, De Diego N, Spíchal L, Dolezal K and Pozueta-Romero J. Arabidopsis plants lacking plastid phosphoglucose isomerase respond to microbial volatiles through GLUCOSE-6-P/PHOSPHATE TRANSLOCATOR2 action. XXIII Reunión de la Sociedad Española de Fisiología vegetal y XVI Spanish-Portuguese Congress of Plant Physiology. 26-28 junio 2019, Pamplona
9. **García Gómez P**, Bahaji A, Gámez-Arcas S, Muñoz FJ, Sánchez-López ÁM, Almagro G, Baroja-Fernández E, De Diego N, Ugena L, Spíchal L, Doležal K, Hajirezaei M, Romero LC, García I, Pozueta-Romero J. Volatiles from fungal phytopathogens modulate plant root metabolism and architecture through cyanide scavenging, and hormone-and ROS-mediated proteome resetting. Small molecules in plant research: Chemistry and Biology Come Together Symposium. 10-11 diciembre 2019, Valencia

AGRADECIMIENTOS

Hace ya 5 años, me comunicaron una noticia, la concesión de una beca FPI para realizar el Doctorado en Navarra. Ello suponía hacer un sacrificio, dejar a mi familia y amigos en Murcia, pero también una gran oportunidad de poder dedicarme a algo que me gusta y apasiona, la investigación en plantas, y una formación como investigador en un reconocido grupo. Este periodo de formación tristemente se acerca a su fin, y debido a ello, me gustaría expresar mi más sincero agradecimiento a todas las personas e instituciones, que de una forma u otra, me han ayudado a lo largo de este camino y que sin ellos esta tesis no hubiera sido posible.

A Javier Pozueta, mi director, por darme la oportunidad de realizar la tesis doctoral en su grupo y hacer que me sintiera como en casa desde el primer día, y sobre todo, por sus conocimientos, persistencia y motivación que han sido claves para la presentacion de este trabajo.

A Abdellatif Bahaji, por la codirección de este trabajo, por ser un gran compañero de fatigas, y por su guía y consejos tanto para la realización de la tesis como para guiarme en la vida.

A Francisco Muñoz, por su infinita paciencia conmigo, por sus explicaciones tanto de técnicas de laboratorio como de programas informáticos, y por esa alegría (con la dosis necesaria de jocosidad/malicia) que aporta al grupo y que hace que el trabajo sea más agradable.

A Edurne Baroja, por ser como una segunda madre para mí, por todo el cariño que has tenido conmigo desde el primer día que llegué a este grupo.

A mis compañeros del laboratorio. A Ángela, por comportarse como la hermana que siempre está cuando se le necesita, y por compartir tanto buenos como malos momentos, A Samuel, por toda su ayuda, su buen humor, sus famosos “dichos” y los ratos de café en la Mordida. A Goi y a Kinia, por ser unas fantásticas compañeras de laboratorio difícilmente reemplazables. Tampoco puedo olvidarme de antiguos integrantes del

laboratorio (Adriana, Maite, Ohiana, Lydia, Blanca, Curro, Rosa, Ángel...) a los que les doy las gracias por su apoyo a lo largo de estos años.

Al Dr. Karel Doležal (Palacký University of Olomouc, Cezch Republic), por darme la oportunidad de realizar una estancia en Olomouc. A todo su equipo, en especial a Nuria, por su guía, conocimientos y buenos ratos especialmente en congresos. Y a Zoila y Manuel, por haberme hecho más amena dicha estancia.

Al Dr. Mohammed Hajirezai (Institute of Plants Genetics and Crop Research (IPK), Alemania), por acogerme en su grupo de investigación, por el exquisito trato que recibí y por todo lo que me enseñaron él y su equipo.

A todo el personal técnico y de administración del Instituto de Agrobiotecnología, en especial a Víctor, Fernando Zaratiegui y Fernando Armona.

A Inmaculada Farrán, por ser mi tutora de tesis.

A todos los componentes del Instituto de Agrobiotecnología, con especial mención al grupillo de los partidos de voleibol en general y a Javi Buezo en particular.

A todos mis amigos tanto de Murcia como de Pamplona, con mención especial a Álvaro, Mul, Kike, Emi y Rayos por su amistad sincera a lo largo de los años. Y a mis grupos de *Magic* tanto de Pamplona como de Murcia, y a mi equipo de *Heroes of the Storm, Noche en el Nexo,* por hacerme más amena esta estancia de 5 años.

Y por último, a toda mi familia. A Pak, mi hermano y confidente, por nuestras charlas, por su apoyo incondicional, y a mis padres, Pablo y María Dolores, por todo, por haber sido junto con Pak, los grandes pilares de mi vida y los que me habéis hecho ser lo que soy. Mención especial a mi abuelo, Paco, al cual le dedico esta tesis como tributo, pues él, a través de mi padre, me transmitió el cariño hacia el campo en general y las plantas, en particular.

Por haberme hecho esta travesía más grata y más fácil. Gracias a todos!!